NASA Reference Publication 1339

January 1994

Report on Concentrations, Lifetimes, and Trends of CFCs, Halons, and Related Species

Edited by:
J. A. Kaye and S. A. Penkett, Co-Chairs,
and F. M. Ormond

Convening Lead Authors:
P. Fraser, D. Fisher, P. Bloomfield,
S. P. Sander, and M. K. W. Ko

NASA Office of Mission to Planet Earth
Science Division
Washington, D.C.

Table of Contents

Chapter 3: Inferred Lifetimes

Chapter 4: Laboratory Studies of Halocarbon Loss Processes

Chapter 5: Model Calculations of Atmospheric Lifetime

Executive Summary

The atmospheric lifetimes of molecules containing chlorine and bromine are the dominant parameters influencing their ability to promote enhanced ozone destruction in the stratosphere. The purpose of this report is to assess the present state of our knowledge of the lifetimes of halocarbons using two complementary approaches. First, a time series of measurements of gas concentrations is used together with information on their emissions histories and a computational model of atmospheric circulation and chemistry to infer lifetimes through a mass balance approach. Second, an atmospheric chemical-dynamical model is used with detailed information on the chemistry and spectroscopy of the molecules of interest to calculate lifetimes. The lifetimes determined by these two methods are then compared.

In this report, attention will be focused most closely on fully halogenated chlorine- and bromine-containing molecules, primarily the chlorofluorocarbons, and the halons, because of their ability to deliver chlorine and bromine to the stratosphere. Some attention will be given to those molecules containing hydrogen, such as methyl chloroform (CH_3CCl_3), hydrochlorofluorocarbons (HCFCs), methyl chloride (CH_2Cl), and methyl bromide (CH_3Br). These molecules are subject to removal in the troposphere primarily by reaction with OH and by other processes. This summary very briefly enumerates the main conclusions from present understanding of the behavior of halogen-containing source gases. A fuller description of the contents of the report, including a summary representation of measurements and models included, may be found in the report overview which follows this summary.

CFC Abundances

Tropospheric Measurements

- The Atmospheric Lifetime Experiment/Global Atmospheric Gases Experiment (ALE/GAGE) network has provided an extensive set of measurements for CFC-11 (CCl_3F), CFC-12 (CCl_2F_2), CFC-113 ($CF_2ClCFCl_2$), methyl chloroform and carbon tetrachloride (CCl_4) at 4 or 5 surface sites from 41°S to 52°N for more than a decade (for all but CFC-113), from which long-term trends can be derived.
- Concentrations of these and related species are measured by additional networks at surface level which have different temporal and/or spatial coverage than ALE/GAGE as well as smaller sampling frequency. Comparison of these alternative data with those obtained from ALE/GAGE allows for improved determination of measurement accuracy.
- Recent data from the middle to high Northern Hemisphere from several different measurement programs show that the growth rates of CFC-11 and CFC-12 have started to level off, presumably in response to reduced emissions.
- A significant new Northern Hemispheric data set on tropospheric HCFC-22 ($CHClF_2$) based on infrared absorption shows some difference from previous measurements made using *in situ* techniques.
- There is a serious lack of data on the global distributions and trends of other important chlorine- and bromine-containing species, most notably methyl bromide and methyl chloride, along with several other organobromine species.

Calibrations

- Calibration issues continue to limit our understanding of the global atmospheric distributions and trends of these species. In the case of CFC-11 and CFC-12 the calibration uncertainty range between various

laboratories is currently less than 5%, whereas for CFC-113 and CCl_4 it is greater than 20%. For CH_3CCl_3 and HCFC-22, the uncertainty range is on the order of 30%.

Stratospheric Measurements

- Simultaneous measurements have been made in the stratosphere for most of the substances controlled under the Montreal Protocol, along with several others. The individual profiles for many molecules removed by photolysis in the stratosphere correlate well with respect to scale height and allow a check on the lifetimes calculated with atmospheric chemistry models.
- Most data have been collected in balloon flights at mid latitudes in the Northern Hemisphere. Some data are available from polar regions and the tropics, but these are limited. The observed fall-offs show the expected variation with latitude.
- The existing database of stratospheric profiles from space-based measurements is very limited, but will improve in the future due to data from the Upper Atmosphere Research Satellite (UARS) and the Atmospheric Trace Molecule Spectroscopy (ATMOS) instrument.

Production and Emission

- Production of CFC-11 and CFC-12 peaked in 1987 and their estimated emissions have decreased substantially since 1988.
- The major uncertainties in the calculations of current, global emissions for CFC-11 and CFC-12 are the lack of data from companies not reporting to industry panels and estimates of banking times for long-term uses.
- For CFC-11, CFC-12 and CFC-113, reporting companies are estimated to account for 85-90% of total production; higher percentages are believed for most other CFCs and methyl chloroform. At least 95% of the CFC production and emission is believed to take place in the Northern Hemisphere.
- The proportion of emissions of CFC-11 and CFC-12 from non-reporting companies is projected to increase as production is phased out under the Montreal Protocol. In addition, the fraction of total emissions arising from the service bank of CFCs will also increase as new production decreases. Emission levels are therefore likely to fall off less rapidly than production, and the uncertainty in emission relative to production will grow.
- Methyl chloroform emissions increased during the 1980s, partly due to its substitution for restricted substances, including CFC-113 and other volatile organic compounds. There are no industrial estimates for current production of carbon tetrachloride produced for dispersive uses. Somewhat imprecise production and emission data are available for methylene chloride (CH_2Cl_2), trichloroethylene ($CHClCCl_2$) and perchloroethylene (CCl_2CCl_2), which are short-lived compounds whose study may help shed light on global average distributions of tropospheric OH.
- HCFC-22 emissions have increased at approximately 8.5% per year since 1980. This increase is due in part to substitution for restricted CFCs. There are no industrial estimates for other HCFCs since their emissions are significantly lower and presently do not have any agreed-upon criteria for industry reporting.
- Some proportion of methyl chloride emissions may be due to anthropogenic sources (15-30%), probably almost all from biomass burning. The rest of the emissions are from natural sources, primarily the oceans.
- Methyl bromide emissions to the atmosphere have a number of sources. These include a significant natural component, most likely from the oceans, and various anthropogenic sources, such as fumigant use. There is considerable uncertainty about both the anthropogenic and natural emissions of methyl bromide.

Inferred Lifetimes

- The length of the atmospheric measurement record for various halocarbons is as yet short by comparison with their atmospheric lifetimes. The only molecules for which the record can be used with some confidence for determining their lifetimes are probably CFC-11 and methyl chloroform..
- Using the ALE/GAGE data, an optimal inversion analysis and a two-dimensional (2-D) model with parameterized transport, the steady state atmospheric lifetime of CFC-11 is estimated to be 42 years (+7,-5, 68% confidence limits.

- Inference of CFC-11 lifetimes using the ALE/GAGE data with three-dimensional (3-D) models and differing statistical techniques yields contradictory results:
  + A 3-D model from the Max Planck Institut für Meteorologie yields a lifetime of 55.61 years
  + A 3-D model from the Goddard Institute for Space Studies did not converge to a reasonable lifetime unless a systematic correction to CFC abundance was introduced (corresponding to a correction to the total CFC distribution in the model and/or errors in network calibration), in which case a 39 year (+4, -3, 95% confidence limit) lifetime was obtained.
- Using the ALE/GAGE data together with an optimal inversion analysis and a two-dimensional model with parameterized transport, the tropospheric lifetime of CH_3CCl_3 is estimated to be 5.7 years (+0.7, -0.6, 68% confidence limits).. This analysis yields a percentage linear trend in inverse lifetime of 1.0 ± 0.6 % $year^{-1}$, which may correspond to a similar percentage increase in averaged tropospheric OH.
- Inference of CH_3CCl_3 lifetimes using the ALE/GAGE data with the GISS three-dimensional model yielded a lifetime of 5.7-5.9 years assuming an OH increase comparable to that suggested by the ALE/GAGE data. If the ALE/GAGE calibration factor were to drop from 0.80 to 0.70, the best good fit to the measurements obtained using the GISS model, yielded a lifetime of approximately 5 years with no trend.
- The steady state atmospheric lifetime of CFC-12 is estimated to be 122 years (+91,-37, 68% confidence limits) using the ALE/GAGE data, an optimal inversion analysis and a two-dimensional model with parameterized transport. Currently available information does not support the inference of a lifetime for CFC-113, other than to say that it is in excess of 20 years.
- Differences in lifetimes inferred by the two methods (two-dimensional *vs.* three-dimensional models) reflect substantial differences in the models, including in the total burden and in the vertical distribution of the CFCs. These differences are much more important for the longer-lived CFC-11 than they are for the shorter-lived CH_3CCl_3.

Laboratory Studies of Halocarbon Loss Processes

- Improved laboratory data have been obtained from reactions of OH with 14 different halocarbons. The most significant changes were those in reactions with HCFC-141b (CH_3CFCl_2), HCFC-142b (CH_3CF_2Cl), HFC-125 (CHF_2CF_3) and HFC-143a (CH_3CF_3). The largest change in rate constant at atmospheric temperatures is a decrease of about 30% for HCFC-141b.
- New evaluations of reaction rates of $O(^1D)$ with 8 different halocarbons were obtained. Reaction rates of Cl (chlorine) with 18 different halocarbons were measured and the rates of reactions of NO_3 (nitrogen trioxide) with various halocarbons were found to be very slow.
- Absorption cross sections (including temperature dependence) were re-evaluated for CFC-11, CFC-12, CFC-113, CFC-114 ($CClF_2CClF_2$), CFC-115 ($CClF_2CF_3$) and the halons. Hydrolysis rates and Henry's Law constants for methyl chloroform and carbon tetrachloride have been reviewed in the context of recent data.

Model Calculation of Atmospheric Lifetimes

Species primarily removed in the Stratosphere

- Atmospheric lifetimes for the CFCs and halons have been calculated using several multi-dimensional atmospheric models simulating stratospheric photochemistry and transport.
- The calculated steady-state atmospheric lifetimes for CFC-11 are generally consistent with the lifetimes inferred from observations and emission rates based on 95% confidence intervals.
- Simultaneous measurements of the stratospheric concentrations of any two species can be used to estimate the ratio of their lifetimes if enough is known about their local removal processes and a sufficiently broad set of ;measurements is available. This does allow the determination of the ratio of lifetimes for longer-lived CFCs.

Species primarily removed in the Troposphere

- Lifetimes for HCFCs were obtained using model-calculated stratospheric loss and removal by tropospheric OH. Since calculations of tropospheric OH in photochemical models are expected to have significant

uncertainty, the tropospheric OH removal in the models is scaled to similar distributions of methyl chloroform, using the tabulated emissions estimates, the estimated ocean removal rate, the model-calculated stratospheric removal, and knowledge of the OH-induced loss at mid-tropospheric temperatures.

Recommendations

- Long-term *in situ* measurement networks need to be continued with increased speciation. HCFCs, CH_3Cl, CH_3Br and more reactive halocarbon measurements need to be added to existing CFC and halon measurements. Developments in analytical techniques are needed to facilitate these additional measurements.
- Increased attention needs to be given to calibration issues for *in-situ* measurements, especially for CH_3CCl_3, HCFC-22, and bromine-containing molecules.
- Increased use should be made of ground-based spectroscopic measurements, especially for HCFC-22. Laboratory work needed for improvement of accuracy of absorption cross-sections should be conducted.
- Additional balloon and aircraft flights for measurement of multiple species are needed for tropical, mid-latitude, and high-latitude conditions. Continuing flights of the ATMOS instrument are needed, with occultations being made at a variety of latitudes.
- Accurate production and emission information is needed for HCFCs and other CFC replacement compounds; complete worldwide geographic coverage is needed for the production and emission reports for these molecules as well as the CFCs.
- Both natural and anthropogenic components of the source distributions for methyl-halides need to be better understood, particularly for CH_3Br.
- Use of atmospheric chemistry/transport models to examine the consistency between emissions, concentrations, transport and loss processes should be continued. The results from different approaches need to be intercompared and the differences between model results, if any, need to be understood.
- Continuing measurements of ultraviolet absorption cross sections and reaction rates of OH with halocarbons are needed, with the aim of improving measurement accuracy. Particular attention needs to be paid to removing the effects of impurities.
- Continuing application of multidimensional photochemical models for studies of long-lived tracer distribution in the stratosphere is required. Improvements in tropospheric chemistry-transport models are also needed so that better distributions of global OH can be determined from distributions of short-lived halocarbons.

Overview

Atmospheric Lifetimes - Definition

In attempting to understand the effect of industrially produced halogenated hydrocarbon molecules on the Earth's atmosphere, one crucial quantity which must be known is the length of time over which these molecules will have a significant impact. This atmospheric residence time, commonly referred to as the lifetime, represents the average length of time a molecule will stay in the atmosphere from its release to its destruction. The lifetime may also be thought of as the ratio of the total atmospheric burden to its destruction rate or as the inverse of a linear loss coefficient, which to a high degree of approximation is independent of concentration. While in the atmosphere, halogenated hydrocarbons can destroy stratospheric ozone through their photochemical breakdown to chlorine and/or bromine atoms which lead to ozone destruction through catalytic cycles. They can also contribute to global warming through their absorption of infrared radiation (WMO, 1992; IPCC, 1992).

The differential equation for the total molecular burden, B(t) in the atmosphere is related to the lifetime, $\tau(t)$, by the expression

$$\frac{dB(t)}{dt} = E(t) - \frac{B(t)}{\tau(t)} \qquad (1)$$

where E(t) is the emission rate for the molecule into the atmosphere from the Earth's surface.

At steady state $$\frac{dB(t)}{dt} = 0 \text{ and } \tau = \frac{B(t)}{E(t)} \qquad (2)$$

The lifetime is not a quantity which can be simply measured or calculated, however. In principle, the lifetime can be determined in one or two ways. First, it can be inferred in an inverse way using eq. (1) if an accurate series of measurements of B(t) and a record of the emission rates E(t) is available. This is far from trivial however, as eq. (1) is global. To solve the inverse problem one ideally needs to know the total global burden of molecular concentrations and of the emissions. Typically, concentrations are available at only a small number of surface sites and an even smaller number of points in the free troposphere and stratosphere, in which concentrations are also needed if an accurate global burden is to be calculated. In these inverse calculations, only surface observations are used in the comparison of data with models.

The alternative approach to obtaining lifetimes is to calculate them in a forward sense with a photochemical model. In the most straightforward way, a time-dependent photochemical model is used to simulate the evolution of the molecular distribution in the atmosphere by accounting for transport and chemical processes occurring there. The lifetime can be obtained by evaluating the global burdens and integrated global loss rate.

The purpose of this report is to assess how well we can determine the lifetimes of industrially-produced halogenated hydrocarbons. The two approaches described above, inference from concentration and emission data and calculation with atmospheric photochemical models, will be used. Particular attention will be paid to a detailed understanding of how well the components required for these analyses are understood: molecular concentrations and emission rates for the inference procedure; molecular spectroscopy, photochemistry, and atmospheric transport for the calculation procedure. The usefulness and accuracy of the atmospheric models used in the two approaches will also be examined. To help provide some information in this area, several different modeling approaches will be used in both procedures.

This report does not consider the fate of the halocarbon molecules following their breakdown, and does not consider their effectiveness in either the destruction of ozone or in contributing to global warming. For those questions, the reader should refer to other reports such as the assessment reports prepared for the United Nations

Environment Programme (UNEP) and the Intergovernmental Panel on Climate Change (IPCC). (See WMO/UNEP Ozone Assessments, 1986, 1989, 1990, 1991; UNEP/IPCC 1990, 1992; and UNEP/WMO, 1992.)

The range of molecules to be treated in this respect spans the full range of halogenated hydrocarbons, including the fully halogenated molecules, chlorofluorocarbons (CFCs), carbon tetrachloride (CCl_4), and carbon tetrafluoride (CF_4), bromofluorocarbons (halons), hydrogen-containing CFCs (HCFCs) and molecules containing hydrogen, carbon and one type of halogen atom, for example the hydrogenated fluorocarbons (HFCs) and molecules such as methyl chloroform (CH_3CCl_3). For comparison purposes, naturally produced molecules such as methyl chloride (CH_3Cl) and methyl bromide (CH_3Br) will also be included.

In order to provide the most critical test of our current knowledge, effects on lifetime inference and calculation were focused on two molecules - trichlorofluoromethane ($CFCl_3$, or CFC-11) and 1,1,1 trichloroethane (CH_3CCl_3, usually referred to as methyl chloroform). First, these two molecules span a useful set of atmospheric behavior - CFC-11 is lost mainly by photodissociation in the stratosphere, while methyl chloroform is lost mainly by reaction with hydroxyl (OH) in the troposphere. These molecules can then serve as a surrogate for other molecules with similar atmospheric properties. Second, these molecules are particularly well-suited for this analysis in that the industrial production is thought to be especially well understood, there is a good long record of measurements, and the lifetime is believed to be sufficiently short (~50 years for CFC-11 and ~6 years for CH_3CCl_3) that one stands a reasonable chance of being able to infer an accurate lifetime from the available data.

This report is broken up into five sections (beyond this introduction). First, the set of available concentration data for the surface, free troposphere, and the stratosphere is reviewed. Second, estimates of production and emission for these molecules is presented. In both these chapters, data are presented in both tabular and graphical form. The extensive use of tabular data allows for use of these data in subsequent analysis. Third, the results of the inverse inference procedures are presented; methods involving both two-and-three dimensional models are employed. Fourth, data needed in the atmospheric photochemical models are presented. This includes spectroscopic parameters (temperature-dependent absorption cross-sections), chemical reaction rates with OH, $O(^1D)$, and Cl, and a few kinetic and thermodynamic quantities for processes occurring in aqueous solution. Finally, results of atmospheric photochemical model calculations of lifetimes are presented, and the results are intercompared to the inverse inference method to better understand the origin of some of the differences between the model results. A comprehensive summary of the data included in this report sorted by molecule is given in Table 1. The content for individual chapters is summarized below.

Summary of Scope of Report

The plan for this report and the material included were developed by an international group of scientists in the time period from 1991 to mid-1993 when the report was completed. The formal meetings which led up to this report included an organizational meeting in Alexandria, Virginia, USA in February 1991, a science results exchange/discussion meeting in Newport Beach, California, USA in July 1991, and a report preparation workshop in Blakeney, UK in January 1992. A follow-on meeting specifically related to lifetime inference (see Chapter 3) was held in Washington, DC, USA in June 1992. Additional meetings among scientists working on individual parts of the report occurred during this time period as part of the ongoing scientific process. Most of the material in this report is current as of the end of 1991, but modifications of the text of the chapters continued through 1992 and into mid-1993.

It is emphasized (see Future Studies in this Overview) that much of the work covered in this report is rapidly evolving. In particular, continued investigations about calibrations of existing measurement networks are carried out, which could cause many of the concentration numbers in this report to be adjusted. Similarly, investigations in laboratory kinetics and spectroscopy, and developments in atmospheric modeling, could lead to changes in model calculated lifetimes (see Chapter 5). In using this report, the reader should be aware that more up-to-date information affecting some of the quantitative conclusions reached here may be found in the published literature. Readers are encouraged to examine the current literature and/or contact the appropriate investigators before quantitative conclusions from this report are used.

***Table 1:** Summary of Molecular Information**

			Chapter 1: CONC DATA			Chapter 2: PROD/ EMIS	Chapter 3: INFER.		Chapter 4: CHEM DATA			Chapter 5: CALC LIFE/EST. LIFE	
Class	Formula	Abbrev.	Sur	FT	Strat	P/E	I2	I3	S	K	A	Calc. Life	Est. Life
CFCs	CCl_3F	CFC-11	x	x	x	x	x	x	x	x		x	
	CCl_2F_2	CFC-12	x	x	x	x	x		x	x		x	
	$CClF_3$	CFC-13			x	x			x	x			
	CCl_2FCClF_2	CFC-113	x	x	x	x			x	x		x	
	$CClF_2CClF_2$	CFC-114		x	x	x			x	x		x	
	$CClF_2CF_3$	CFC-115		x	x	x			x	x		x	
	C_2F_6	CFC-116			x								
	CCl_4	-------	x	x	x					x	x	x	
	CF_4	-------			x								
	C_2Cl_4	-------	x			x							
CHCs	CH_3CCl_3		x	x	x	x	x	x		x	x	x	
	CH_3Cl		x		x							x	
	$CHCl_3$		x	x						x			
	CH_2Cl_2		x			x				x			
	$CHClCCl_2$		x			x							
	CH_3Br		x			x						x	
HCFCs	$CHFCl_2$	HCFC-21								x			
	$CHClF_2$	HCFC-22	x	x		x				x		x	x
	CH_2FCl	HCFC-31								x			
	$CHCl_2CF_3$	HCFC-123								x			x
	$CHFClCF_3$	HCFC-124								x			x
	CH_2ClCF_3	HCFC-133a								x			
	CH_3CFCl_2	HCFC-141b								x			x
	CH_3CF_2Cl	HCFC-142b								x			x
	$CF_3CF_2CHCl_2$	HCFC-225ca								x			x
	CF_2ClCF_2CHClF	HCFC-225cb								x			x
	$CH_3CF_2CFCl_2$	HCFC-243cc								x			
HFCs	CH_2F_2	HFC-32								x			
	CH_3F	HFC-41								x			
	CHF_2CF_3	HFC-125								x			x
	CHF_2CHF_2	HFC-134								x			
	CH_2FCF_3	HFC-134a								x			x
	CH_2FCHF_2	HFC-143								x			
	CH_3CF_3	HFC-143a								x			
	CH_2FCH_2F	HFC-152								x			
	CH_3CHF_2	HFC-152a								x			x
	CH_3CH_2F	HFC-161								x			
Halons	CBr_2F_2	H-1202							x				
	$CBrClF_2$	H-1211	x		x	x			x	x		x	
	$CBrF_3$	H-1301	x		x	x			x	x		x	
	$C_2F_4Br_2$	H-2402							x				

* Table notes only molecules for which tabular or graphical data are included in the indicated chapter.

Legend: Chapter 1: Sur: Surface Concentration Data; FT: Free Troposphere Data; Strat: Stratospheric Data
Chapter 2: P/E: Production/Emission Data
Chapter 3: I2: Lifetimes Inferred from 2D Model; I3: Lifetimes Inferred from 3D Model
Chapter 4: S: Spectroscopic Data; K: Kinetic Data; A: Aqueous Phase Data
Chapter 5: Calc. Life: Lifetime calculated with 2D Model; Est. Life: Estimated lifetime calculated with 2D Model.

Class: CFCs: Chlorofluorocarbons and fully chlorinated or fluorinated hydrocarbons
CHCs: Chlorinated Hydrocarbons
HCFCs: Hydrogenated Chlorofluorocarbons
HFCs: Hydrogenated Fluorinated Hydrocarbons
Halons: Fully Halogenated Hydrocarbons including Bromine

This section consists of a summary of the information contained in the report broken down by chapter.

1. Molecular Concentrations

Three types of data are included with this chapter: surface level concentrations measured from fixed locations or from aboard ships, free-tropospheric data measured *in situ* from aircraft, and stratospheric vertical profiles measured *in situ* from balloons or remotely from the space shuttle.

Surface data come from a variety of organized networks and more localized single stations. The mapping between measurement location and observing network or organization is given in Table 2; to provide some sense of geographical coverage, stations are arranged in order of decreasing latitude (north to south). The full names of the networks and organizations abbreviated in the text are given in an Appendix of this report.

The list of species measured by the various networks and stations for surface and free-tropospheric data are given in Table 3. This includes species for which graphical and/or tabular data are found in Chapter 1 (CCl_3F, CCl_2F_2, CCl_2FCClF_2, CCl_4, CH_3CCl_3, $CHCl_3$, and HCFC-22) and some additional species which are not dealt with in detail. Chapter 1 includes some discussion of additional species for which no data are presented in tables or figures (other than Table 1.1). These species are not included in Table 3.

A comprehensive list of relatively recent stratospheric profile data for the molecules under consideration is included in Chapter 1. Balloon-borne profiles cover the time period from 1985 to 1990, and were made at low latitudes, mid latitudes, and high latitudes in the Northern Hemisphere. There are also vertical profiles obtained from the Atmospheric Trace Molecule Spectroscopy (ATMOS) instrument at 30°N; these were obtained in April-May 1985 during the Spacelab-3 Space Shuttle mission at approximately 30°N latitude. The set of available stratospheric data is summarized in Table 4, the numbers in the table reflect the number and independent balloon-borne profiles for a given molecule in the indicated latitude region.

2. Emission Rates

In Chapter 2 of this report, estimates of the global emission rates of a variety of molecules are presented. Global emission rates are not measurable quantities, however; they need to be calculated based on a knowledge of molecular production, of their use, and of the characteristic times for molecular emission associated with a given use. Each of these issues is addressed in this chapter. The available data, including the time period of the emission estimates, are summarized in Table 5.

The process of estimating emissions has several steps. Molecular production levels are obtained from surveys carried out by the chemical industry and international organizations. Production from some countries was not included in the industry-sponsored surveys (non-reported emissions), and particular attention is given to assessing what the non-reported produced levels were likely to have been for these molecules. The industry-sponsored surveys also had information on end-use and geographical distribution of sales. Based on some experimental data and industrial experience, a correspondence between constituent end-use and characteristic emission time was derived. It is particularly important to differentiate between those uses of a molecule in which the emission rapidly follows its use, from those in which the molecule is retained for several years following its use. Molecules which are incorporated in various applications and which have not been released into the atmosphere constitute a "bank" from which they will slowly be released. As production of CFCs, halons, and related molecules is phased out due to international agreements such as the modified Montreal Protocol for Substances that Deplete the Ozone Layer, molecular emissions from this service bank will constitute an ever-increasing fraction of the global emissions.

3. Inference Procedures

The surface concentrations of CFC-11 and methyl chloroform measured with the ALE/GAGE Network are used in Chapter 3, together with the emission rates in the inference of molecular lifetimes. Two complementary modeling approaches are used. In one, carried out by the ALE/GAGE team, an ultra-low resolution two-dimensional (2-D) model (typically containing 12 grid boxes) with several adjustable dynamical parameters is used for the lifetime inference. In the other, three-dimensional (3-D) chemistry-transport models are used. Two of the latter models were used - in one study, carried out by Martin Heimann at the Max-Planck-Institut für Meteorologie in Hamburg,

Table 2: *Locations of Atmospheric Measurements Data*

		NETWORKS									
Station	Latitude	ALE/GAGE	NOAA/CMDL	UT	FIAER	OGIST	UCI	MRI	JPL	UEA	SIO
Alaska	71		x								
Ireland	52	x									
Oregon	45	x									
Colorado/PNW	40		x			x					
Hokkaido	40-45			x							
Table Mountain	34								x		
Kitt Peak	32								x		
Mauna Loa	19		x								
Barbados	13	x									
Samoa	-14	x	x								
Cape Point	-34	x				x					
Tasmania	-41				x						
Syowa	-69			x							
South Pole	-90		x			x					
Global Average		x	x	x		x	x				
Aircraft											
Europe/Atlantic Ocean					x						
Japan								x			
Shipboard											
Various										x	x

Legend:

ALE/GAGE	Atmospheric Lifetime Experiment/Global Atmospheric Gases Experiment
NOAA/CMDL	National Oceanic and Atmospheric Administration/Climate Monitoring and Diagnostic Laboratory
UT	University of Tokyo, Japan
FIAER	Fraünhofer Institute for Atmospheric Research (Germany)
OGIST	Oregon Graduate Institute of Science and Technology
UCI	University of California, Irvine
MRI	Meteorological Research Institute (Japan)
JPL	Jet Propulsion Laboratory, Pasadena, California
UEA	University of East Anglia, Norwich, UK
SIO	Scripps Institution for Oceanography

Table 3: *Summary of Measurement Networks*

			MOLECULE						
Network	Altitude	Stations	CFC-11	CFC-12	CFC-113	CCl_4	CH_3CCl_3	$CHCl_3$	HCFC-22
ALE/GAGE	Surface	5	x	x	x	x	x	*	
NOAA/CMDL	Surface	4	x	x					
UT	Surface	2	x	x	x	x	x		x
UEA	Shipboard	-	x	x	x	x	x		
UCI	Surface	Averaged	x	x	x				
SIO	Shipboard	-	x	x					
FIAER-CSIR	Surface	1	x			x			
FIAER	Free Trop	-	x	x	x	x	x		
MRI	Free Trop		x	x					
OGIST	Surface	5					x	x	x
Kitt Peak	Ground Based Column								x
Table Mountain	Ground Based Column								x

*For Tasmania only. $CHCl_3$ not collected at other 4 stations in network.

Germany, analyzed wind fields for the year 1987 are used in the transport model. In the other study, carried out by Michael Prather of the University of California at Irvine, winds from the general circulation model at NASA's Goddard Institute for Space Studies (GISS) were used in providing constituent transport. In the former model, there was no adjustment of dynamical parameters in fitting the data; in the latter a single parameter for horizontal diffusion was optimized to best fit the CFC-11 interhemispheric gradient in the early years of the ALE/GAGE data set. Differing statistical techniques were used with the different modeling approaches.

Table 4: *Summary of Stratospheric Data*

	Number of Balloon Profiles			ATMOS
	Tropics	Mid Latitudes	High Latitudes	30°N
CFC-11		9	6	x
CFC-12	1	9	6	x
CFC-13	1	1		
CFC-14		3		x
CCl_4		9	4	
HCFC-22	1	1		x
CH_3Cl		8	4	x
CH_3CCl_3	1	9	4	
CFC-113	1	9	5	
CFC-114	1	1		
CFC-115	1	1		
CFC-116		3		
Halon-1301	1	1		
Halon-1211	1	1		

In carrying out this analysis, attention must be given to the uncertainties in the input parameters (concentration data, emission rates and global distribution) and to determining what effect these uncertainties have on the inferred lifetimes. The most critical parameter is the uncertainty in the absolute calibration of the ALE/GAGE data. The possibility of a systematic drift in the calibration must also be considered. Additional parameters for which uncertainties need to be considered include the assumed value of emissions related to unreported production, and the geographical distribution (especially the split between the Northern and Southern Hemisphere) of the surface emission. Attention must also be paid to the possibility of a systematic change in the lifetime of methyl chloroform as a result of changes in the global distribution and integrated concentration of the hydroxyl radicals that constitute its major sink.

Table 5: *Summary of Production and Emission Data*

	Production/Emission	Comment
CFC-11	1931-1991	
CFC-12	1931-1991	
CFC-113	1970-1991	
CFC-114	1934-1991	
CFC-115	1964-1991	
HCFC-22	1970-1991	
CH_3CCl_3	1971-1991	
H-1211	1963-1991	Emission data until 1990 only
H-1301	1963-1991	Emission data until 1990 only
CH_2Cl_2	1990	
C_2Cl_4	1987, 1990	Dispersive uses only
C_2HCl_3	1987, 1990	Dispersive uses only
CH_3Br	1984-1990	

4. Photochemical Data

In the atmospheric photochemical models, those processes responsible for the destruction of CFCs must be adequately represented. As was noted above, two types of destruction dominate - photodissociation in the stratosphere, and photochemical loss in the troposphere by reaction with hydroxyl. Calculation of stratospheric photodissociation rates requires accurate knowledge of molecular absorption cross-sections for the CFCs and molecular oxygen (O_2) and the CFCs' photolytic quantum yields, which are usually assumed to be unity. In this chapter, the absorption cross-sections are given as a function of wavelength and temperature for several fully halogenated hydrocarbons. The molecules covered are indicated in the appropriate column (Chapter 4-S) of Table 1.

Photochemical reactions which can destroy these molecules include those with OH, $O(^1D)$, and Cl. Reaction with OH is the dominant one for most of the hydrogen-containing halocarbons; the others are included mainly for completeness. For reactions with $O(^1D)$ there are two possible product channels - that leading to physical quenching of $O(^1D)$ to $O(^3P)$ without chemical reaction, and that leading to chemical reaction.

There is observational evidence that methyl chloroform and carbon tetrachloride. may be destroyed in the ocean by hydrolysis. For this reason, aqueous decomposition rates and Henry's Law coefficients for the two stated molecules in water are examined as a function of temperature. Due to the salinity of the ocean, these quantities should be known as a function of ionic strength as well; to that end the salting-out coefficient of methyl chloroform was also examined.

5. Photochemical Model Calculation of Lifetimes

Lifetimes of the halogenated hydrocarbons were calculated by seven different modeling groups in Chapter 5. Six of these are two-dimensional models (in which only the dimensions of latitude and altitude are resolved; no variation is assumed in the longitudinal directions), and one is a low resolution three-dimensional model. Two types of lifetimes were calculated, steady-state lifetimes, in which fixed (time invariant) boundary conditions are assumed for all gases, and transient lifetimes, in which a time-dependent boundary condition is used to better simulate the actual evolution of CFCs in the atmosphere. The available lifetimes calculated for the different molecules by the modeling groups are given in Table 6; the symbol S is used for those constituents for which only steady-state lifetimes were calculated; T is used when both transient and steady-state lifetimes were calculated. The model-calculated lifetimes can be compared to the inferred ones for CFC-11 in Chapter 3. For CH_3CCl_3, the OH fields are not sufficiently accurate for trustworthy lifetimes to be determined, indeed the tropospheric OH levels in these models are typically adjusted in order to produce reasonable CH_3CCl_3 lifetimes.

Table 6: *Summary of Model Calculations (Model 2D unless specified)*

Molecule	AER	GSFC	LLNL	MIT (3D)	MPI	MRI	U. Wash.
CFC-11	T	T	S	T	S	T	T
CFC-12	T	T	S	T	S	T	T
CFC-113	T	T	S	T	S	T	T
CFC-114	S	S	S				
CFC-115	S	S	S				
CCl_4	T	T	S	T		T	T
N_2O	T	T	S	T	S	T	T
H-1211	T	T	S		S	T	
H-1301	T	T	S		S	T	
HCFC-22	T	T	S	S	S	T	
CH_3CCl_3	T	T	S	S	S	T	
CH_3Cl	S	S	S				
CH_3Br	S	S	S				

S: Steady State Lifetimes only calculated
T: Steady State and Transient Lifetimes calculated

Since the models obtain a range of lifetimes for CFC-11, some effort is placed on understanding the origin of the model differences. Both variations in model photochemistry and transport are considered. Photolysis rates of the CFCs and halons are compared to determine the likely magnitude of the differences between the models. Differences in transport are assessed by the use of simulated tracers in which their source distributions and/or emission rates and their destruction rates are very simply parameterized. Differences in the calculated distribution of these simulated tracers then points very clearly to the differences in particular aspects of the transport between the models.

Because of the critical role which transport plays in affecting the model-calculated distributions of CFCs and other halocarbons, model output can be analyzed in such a way that concentration profiles of constituents are considered not individually against altitude, but in pairs one against another. For molecules whose chemistry is governed by similar processes (*e.g.* slow photodissociation in the stratosphere), a good correlation is expected between their concentrations. Most typically, correlations of distributions of CFCs with those of N_2O are examined.

For HCFCs and HFCs, lifetimes are estimated using approximate tropospheric lifetimes (based on reaction rates with OH and the mean global OH distribution inferred from the CH_3CCl_3 lifetime data) and stratospheric lifetimes calculated with the AER 2-D model. The calculated tracer correlations are compared with those obtained in the stratospheric profiles presented in Chapter 1. Analytical models show that in such cases, accurate ratios of lifetimes should be obtained. The relative lifetime ratios suggested from the model calculations and the stratospheric vertical profiles can then be examined.

Summary of Results

In this section only those results most closely related to the inferred and calculated lifetimes of CFC-11 and methylchloroform will be presented. For additional results, the reader should consult the executive summary for the overall report and the summaries for each chapter.

The ALE/GAGE measurements provide a very useful data set for use in the procedure of inferring lifetimes. There is strong agreement among several measurement groups on the CFC-11 absolute calibrations, so the ALE/GAGE measurements should be usable in inference studies with some confidence. For methylchloroform, comparisons of data among several groups suggests that the absolute calibration is not yet completely fixed, and that the ALE/GAGE measurements need to be used with more attention paid to the effects of uncertainties in the calibration.

The CFC-11 lifetime inferred in Chapter 3 with the two-dimensional ALE/GAGE model and the three-dimensional MPI-Met are in reasonable agreement, with values in the 50-55 year range. These are consistent with the results calculated with the photochemical model (Chapter 5), which fall in the range 40 - 54 years (one model obtained a lifetime of approximately 60 years, but its transport differed markedly from that of the others). By consideration of the vertical profiles of N_2O and CFC-11 obtained from balloon flights and shuttle observations (see Chapter 1), the ratio of slopes suggests that the lifetime of CFC-11 is 53 years, assuming an N_2O lifetime of 110 years.

The GISS model used in Chapter 3 could only obtain an adequate fit to the data by assuming a calibration factor significantly different from that used by the ALE/GAGE Network. Fits of comparable quality can only be obtained by allowing for assumptions of a small calibration shift and a change in the magnitude of the unreported emissions; in such a case a smaller variation in the calibration adjustment would suffice.

There is clear evidence of a difference in the ALE/GAGE and GISS atmospheric models. Many of the differences in inferred lifetimes can be related to differences in the concentrations of CFCs in the two models; the connection between these quantities is very strong. The MPI-Met model may have a problem in its interhemispheric transport, as the optimally-determined interhemispheric mix of CFC-11 sources, puts an implausibly large (20%) fraction of the emission in the Southern Hemisphere.

For methyl chloroform, there is much better agreement between the ALE/GAGE and GISS models. A lifetime of the order of 6 years is computed by both assuming that the ALE/GAGE calibration factor is correct. If the actual calibration factor is appreciably lower, as was suggested by studies at the University of Tokyo (UT), then an appreciably smaller (~4 year) lifetime is needed to best explain the data.

The result that the best fit to the methylchloroform data is obtained with increasing tropospheric OH levels, is very sensitive to the actual calibration factor. Were the network calibration value to be close to the UT-derived one, the best fit to the ALE/GAGE observations would require a slow decrease in the tropospheric OH amounts. The photochemical model calculations of CH_3CCl_3 lifetime carried out in Chapter 5 do not provide a truly independent value, as the models' tropospheric OH fields are typically adjusted to provide a reasonable lifetime for CH_3CCl_3 in the first place.

In the long term it seems clear that three-dimensional models would provide the most complete way of simulating station data and thus inferring lifetimes from measurements of trace gas concentrations and estimates of emissions. In the short term, however, there is no clear consensus about the optimal approach to use in inferring lifetimes. The current two- and three-dimensional models differ substantially from each other in their use of fitted parameters, methods for data comparisons, and use of atmospheric data as input parameters. The analysis of modeling approaches and also of statistical methods should remain an active area of research in coming years.

Future Studies

This report represents a detailed look at the state of our knowledge of CFCs as of the early 1990s (data through 1990 are included in Chapter 1, for example, while production and emission data through 1991 are included). In the next few years, our ability to address several of the issues should improve. Particular areas in which improvement are likely include the following:

1. Improved Knowledge of Calibration

Recognition that the absolute calibrations for methylchloroform, carbon tetrachloride, and HCFC-22 are not fully established can be expected to lead measurement groups to refine their calibrations and determine more accurate values (both absolute and any concentration-dependence associated with detector non-linearity). Improved knowledge of HCFC-22 infrared spectroscopic parameters should also allow for more precise measurement of its atmospheric distribution as determined by ground-based column measurements.

2. Additional Surface Data

As the data record lengthens, it should become easier to do the inference process since it will correspond to a larger fraction of the lifetime. In the next few years it should be possible to detect a continuing decrease in the rate of growth of CFCs in the atmosphere as their use is phased out in response to international agreement. The behavior of the concentrations in response to this change may also shed valuable light on the relationship between production and emission. One drawback here is that unreported emissions may form a large component of the total.

3. Major Additions to the Database for Vertical Profiles of Halocarbons

Several recent measurement programs will dramatically increase the availability of vertical profiles of CFCs and other halocarbons. These will typically include simultaneous measurements of several species, which allows for their use in studies of tracer correlations. Particular measurement programs include:

(i) The Second Airborne Arctic Stratospheric Expedition (AASE-2), in which the ER-2 was fitted with a new rapid-response instrument to measure CFC-11 and CFC-113 (which accompanies an existing N_2O-measuring instrument);

(ii) The European Arctic Stratospheric Ozone Expedition (EASOE), in which there were several balloon flights where the vertical profiles of several halocarbons were simultaneously measured;

(iii) Global distributions of CFC-11 and CFC-12 will become available from the Cryogenic Limb Array Etalon Spectrometer (CLAES) instrument onboard NASA's Upper Atmosphere Research Satellite (UARS). This instrument began operating shortly after the UARS launch in September 1991 and ceased operation in May 1993, when its supply of cryogen became depleted; and

(iv) Vertical profiles of CFC-11, CFC-12, CCl_4, HCFC-22, and CH_3Cl obtained with the ATMOS instrument which flew onboard NASA's Atmospheric Laboratory for Applications and Science (ATLAS) mission in

March-April 1992 and April 1993. Some 90 profiles in the latitude range from 25°N - 55°S were obtained in the ATLAS-1 mission, while some 70 and 30, were obtained at high northern and mid-southern latitudes, respectively, during the ATLAS-2 mission.

4. Improvements in Modeling Capability

Improvements in general circulation models and availability of new sets of assimilated data should allow for better simulation of halocarbon distributions in the stratosphere. Results of ongoing model intercomparisons may provide improvements in model simulations of model transport, which are particularly important if the CFC distributions are to be accurately simulated. Advances in tropospheric chemical modeling should allow for improved calculation of OH fields; these could further enhance our capability to simulate the distribution of molecules which react with OH, such as CH_3CCl_3, this is a research activity which is to be strongly encouraged over the next 5-10 years.

Acknowledgments

We acknowledge the support of the Alternative Fluorocarbon Environmental Acceptability Study (AFEAS) which provided travel funds used to support the participation of most of the non-US scientists working on this report.

References

Intergovernmental Panel on Climate Change, *Climate Change, The IPCC Scientific Assessment,* WMO/UNEP, J. T. Houghton, G. J. Jenkins and J. J. Ephraums (Eds.), Cambridge University Press, Cambridge, UK, pp 365, 1990.

Intergovernmental Panel on Climate Change, *Climate Change 1992, The Supplementary Report to The IPCC Scientific Assessment Combined with Supporting Scientific Material,* WMO/UNEP, J. T. Houghton, B. A. Callander and S. K. Varney (Eds.), Cambridge University Press, Cambridge, UK, pp 200, 1992.

United Nations Environment Programme, Methyl bromide and the ozone layer: a summary of current understanding, Atmospheric Science Assessment in *Methyl Bromide: Its Atmospheric Science, Technology, and Economics, Montreal Protocol Assessment Supplement,* UNEP, D. L. Albritton and R. T. Watson, co-chairs of Science Assessment, 41 pp, 1992.

World Meteorological Organization, *Atmospheric Ozone 1985: Assessment of our Understanding of the Processes Controlling its Present Distribution and Change*, WMO Report No. 16, WMO Global Ozone Research and Monitoring Project, WMO/UNEP, R. T. Watson, Assessment Chair, (3 volumes) 1986.

World Meteorological Organization, *Report of the International Ozone Trends Panel 1988*, WMO Report No. 18, WMO Global Ozone Research and Monitoring Project, WMO/UNEP, R. T. Watson, Chair, (2 volumes) 1989.

World Meteorological Organization, *Scientific Assessment of Stratospheric Ozone: 1989*, WMO Report No. 20, WMO Global Ozone Research and Monitoring Project, WMO/UNEP, D. L. Albritton and R. T. Watson, co-chairs, (2 volumes) 1990.

World Meteorological Organization, *Scientific Assessment of Ozone Depletion: 1991,* WMO Report No. 25, .WMO Global Ozone Research and Monitoring Project, WMO/UNEP, D. L. Albritton and R. T. Watson, co-chairs, 1992.

Chapter 1.

Measurements

Lead Authors:

P. FRASER, M. Gunson, S. Penkett, F. S. Rowland, U. Schmidt, and R. Weiss

Additional Contributors:

F. Alyea, D. Blake, E. Brunke, J. Butler, D. Cunnold, J. Elkins, M. Hirota, F. Irion, Y. Makide, R. Prinn, R. Rasmussen, T. Sasaki, H. Scheel, W. Seiler, P. Simmonds, and H. Singh

Chapter 1
Table of Contents

Chapter 1: Measurements

1.0 Overview and Summary

Tropospheric Measurements

- Several extensive, global, long-term data sets, based on gas chromatographic techniques, are now available on surface measurements of CFC-12 (CCl_2F_2), -11 (CCl_3F), -113 (CCl_2FCClF_2), methyl chloroform (CH_3CCl_3) and carbon tetrachloride (CCl_4).

- A significant, new Northern Hemispheric data set on tropospheric HCFC-22 ($CHClF_2$), based on spectroscopic techniques, is available.

- There is a serious lack of data available on the global sources and distribution (and trends) of the important chlorine and bromine species, methyl chloride (CH_3Cl), the halons, and methyl bromide (CH_3Br), as well as several other organobromine species.

- Recent data from the mid-to-high latitudes of the Northern Hemisphere suggest that the growth rates of CFC-11 and -12 have started to decline, presumably in response to reduced emissions.

Stratospheric Measurements

- Simultaneous vertical profile measurements have been made in the stratosphere for most of the substances controlled under the Montreal Protocol and many others.

- Most data have been collected in balloon flights at mid latitudes in the Northern Hemisphere. Some data are available from polar regions and the tropics. Satellite instruments can provide global data, but they are very limited at the present time.

- Individual profiles for many molecules removed by photolysis in the stratosphere correlate well with each other confirming the good precision of the measurements.

- Profiles measured at tropical, mid- and high northern latitudes agree with model predictions as to the altitude at which photolysis begins to remove halocarbons.

- Observationally derived lifetimes can be compared with those obtained purely by calculation and serve to constrain uncertainties in the calculated values.

Calibration

- Calibration issues continue to limit our understanding of the global atmospheric distributions and trends of these species. Most activities undertaken to resolve this important issue are unsatisfactory at this stage.

- The calibration uncertainty range associated with measurements of CFC-11 and -12 by various laboratories appear to be currently less than 5%, whereas for CFC-113, CCl_4 and CH_3CCl_3 it is greater than 20%. This latter uncertainty must make a major contribution to the uncertainty of estimating atmospheric lifetimes of these species, and in the case of CH_3CCl_3, in estimating global OH levels. There have been insufficient experiments to determine whether these calibration uncertainties may have changed with time. There are insufficient data to evaluate the uncertainty in the absolute calibration of HCFC-22.

1.1 Introduction

This chapter is concerned with the measurement data base for the principal organic compounds that act as source gases for chlorine and bromine in the stratosphere. It is sub-divided with Part 2 involved with tropospheric measurements and Part 3 concerned with stratospheric measurements. Calibration issues, particularly in regard to the tropospheric measurements are also discussed in Part 4.

The tropospheric measurements are mostly collected at sites distributed between the two hemispheres in a series of long-running experiments designed to determine trends. These are supplemented by other data collected on board ship and from aircraft. The group involved in producing this chapter encompasses most of the active scientists measuring these molecules today and as such it was possible to perform an intercalibration study by direct comparison of current and past measurements of CFC-11, CFC-12, CFC-113, CCl_4 and CH_3CCl_3 in different parts of the atmosphere. This was particularly successful for the Southern Hemisphere where instantaneous variability is very low. Air in the Southern Hemisphere, particularly south of 30°S, can be considered to have a very uniform composition with respect to these stable chlorine compounds and an intercalibration exercise can be carried out independently by comparing measurements made by different laboratories at similar latitudes and times. This has the advantage of checking out the sampling technique and the analytical accuracy and precision of individuals making the measurements. The results of this exercise should constrain the tropospheric measurements to better than 4% for CFC-11 and CFC-12. Discrepancies have been shown to exist for other molecules but these probably do not exceed 20% for CFC-113 and CCl_4. The major discrepancy (30%) lies with CH_3CCl_3 and this limits its usefulness at present as a surrogate molecule for determining the atmospheric lifetimes of replacement molecules for CFCs. The molecule with the next largest data base outside those referred to above is HCFC-22. Fewer groups have measured this molecule because the normal method of halocarbon measurement (electron capture gas chromatography) is less sensitive than for molecules such as CFC-11 and CFC-12. Measurements are available, however, with spectroscopic techniques and this limits the error data to about 25%.

The stratospheric measurements are collected by balloons, and by aircraft, and satellite experiments. Most measurements are made at mid latitudes in the Northern Hemisphere but the latitudinal coverage is large with data shown in both polar regions and in the Northern Hemisphere tropics. The major omission is in the Southern Hemisphere at any altitude above 20 km.

Often these data sets are very comprehensive with both the major chlorine species, referred to in the section on the troposphere, and many minor chlorine and bromine species being determined in the same set of vertical profiles. As is shown in Chapter 5, this does allow for the determination by experiment of the stratospheric lifetimes of many species. For those molecules removed primarily by stratospheric photolysis, this constitutes an independent estimate of their atmospheric lifetimes which can then be compared with values obtained by calculation with 2-D and 3-D models.

1.2 Tropospheric Measurements

1.2.1 CFCs and Carbon Tetrachloride

CFCs -11 (CCl_3F), -12 (CCl_2F_2), and -113 (CCl_2FCClF_2) and carbon tetrachloride (CCl_4) comprise ≈65% of the total organochlorine loading of the troposphere (CFC-12, 25%; CFC-11, 20%; CCl_4, 13%; CFC-113, 6%). They are inert in the troposphere but photodissociate in the stratosphere and hence are a major source of stratospheric reactive chlorine. Their tropospheric concentrations have been measured in a number of programs and have been shown to be increasing steadily over the last fifteen years.

Table 1.1 *Updated global trends and tropospheric concentrations of CFCs, halons and related species. Adapted from WMO (1990). The global concentration data are 1990 annual means.*

Source gas	Concentration (pptv)				Long term increase pptv/year[a]				Increase 1989 - 1990				Increase 1990 - 1991		Calibration Uncertainty Range (%)
Global Data	GAGE	UT	NOAA	UCI	GAGE	UT	NOAA	UCI	GAGE	UT	NOAA	UCI	GAGE	NOAA	
CFC-12	474	478	479	478	17.6	18.4	17.7	18.6	16.6	16.0	14.8	14.2	12.1	14.0	5
CFC-11	259	254	263	256	9.4	9.1	9.7	11.0	7.0	7.5	6.4	8.8	5.5	5.2	3
CFC-113	71	71	-	75	5.8	6.2	-	6.0	7.1	7.2	-	6.0			20
CCl_4	134	-	107	-	1.6	-	-	-	0.0	-	-	-			25
CH_3CCl_3	155	125	-	-	5.5	3.5	-	-	5.0	4.0	-	-			30

Other Chlorinated Species	Concentration (pptv)	Long term increase pptv/year[a]	Uncertainty Range (%)
CFC-114	15-20	≈1	
CFC-114a	≈5	≈0.3	
CFC-13	≈5		
HCFC-22	120-130[b]	6-7	20
CH_3Cl	600[c]		
$CHCl_3$	≈15[d]		
CH_2Cl_2	≈30		
CCl_2CCl_2	≈10		
CH_2ClCH_2Cl	≈35		
$CHClCCl_2$	≈2-3		
Brominated Species			
CH_3Br	10-15[e]	0.1-0.2	
CH_2Br_2	0.5-3		
$CHBr_3$	0.2-3		
CH_2BrCl	1-2		
$CHBr_2Cl$	1		
$CHBrCl_2$	1		
$C_2H_4Br_2$	<1		
C_2H_5Br	2-3		
$CBrF_3$	1.2-2.2	0.1-0.2	80
$CBrClF_2$	1.7-2.5	0.1	30
TOTAL Cl	**3800**	**110 (2.9% per year)**	
anthropogenic ≈85 %			
TOTAL Br	**≈30**	**0.4 (≈1-2% per year)**	
anthropogenic ≈20-25 % (methyl bromide and halons)			

[a] based on linear regression; [b] projected from 1987 observations at 6-7 pptv per year; [c] 15-30% anthropogenic; [d] 50% anthropogenic; [e] 25% anthropogenic

1.2.1.1 CFC-12 and CFC-11

There are several long term measurement programs for CFC-12 (CCl_2F_2) and CFC-11 (CCl_3F). The National Oceanic and Atmospheric Administration-Climate Monitoring and Diagnostics Laboratory (NOAA-CMDL) has run a global program based on weekly flask measurements at Point Barrow, Alaska; Niwot Ridge, Colorado; Mauna Loa, Hawaii; Cape Matatula, Samoa and at the South Pole since 1977 (Thompson *et al.*, 1990; Sturges *et al.*, 1991; Montzka, *et al.*, 1992; Elkins *et al.*, 1993). CFC-12 and CFC-11 calibration problems have been identified and corrections to the NOAA-CMDL data have been made. The data are reported in the NOAA-CMDL gravimetric scale (Sturges *et al.*, 1991). Using the corrected data, the 1990 global mean concentration of CFC-12 was 479 pptv respectively (mean of hemispheric means), increasing at 17.7±0.1 pptv per year, based on linear regression of the 1977-1990 data. Similarly the 1990 global mean concentrations of CFC-11 was 263 pptv respectively, increasing at 9.7±0.1 pptv per year. The data are shown in Figures 1.2.1 and 1.2.2. The globally averaged data (mean of hemispheric means) from the NOAA-CMDL program are shown in Figure 1.2.3.

NOAA-CMDL *in situ* measurements (12 per day) of CFC-12 and CFC-11 commenced at Barrow, Mauna Loa and Samoa (1986) and at the South Pole (1987) (Thompson *et al.*, 1990; Hall *et al.*, 1990, Sturges *et al.*, 1991); preliminary CFC-12 and CFC-11 data have been reported in the recently prepared NOAA-CMDL gravimetric scale. The 1990 global mean CFC-12 and CFC-11 concentrations were approximately 480 and 260 pptv respectively, increasing at about 19 pptv and 7.5 pptv per year. These trends are higher for CFC-12 compared to the NOAA-CMDL flask data and lower for CFC-11. However the *in situ* record is of only a few years duration and experimental and calibration errors are still relatively large (Sturges *et al.*, 1991).

In situ measurements (4-12 per day) of CFC-12 and CFC-11 have been made in Ireland, Oregon, Barbados, Samoa and Tasmania since 1978 as part of the Atmospheric Lifetime Experiment/Global Atmospheric Gases Experiment (ALE/GAGE) program (Cunnold *et al.*, 1986, 1993) and are shown in Figures 1.2.1 and 1.2.2. The 1990 global mean concentrations for CFC-12 and CFC-11 were 474 and 259 pptv respectively (mean of hemispheric means), increasing at 17.6±0.1 and 9.4±0.1 pptv per year, based on linear regressions (Cunnold *et al.*, 1986, 1993). The globally averaged mean data (mean of hemispheric means) from the Global Atmospheric Gases Experiment (GAGE) program are shown in Figure 1.2.3. The data are in the SIO 1986 scale (Bullister and Weiss, 1986). The factors to convert CFC-12 and CFC-11 data from the GAGE scale (as reported in Cunnold *et al.*, 1986) and the SIO 1986 scale are discussed fully in Cunnold *et al.*, 1993.

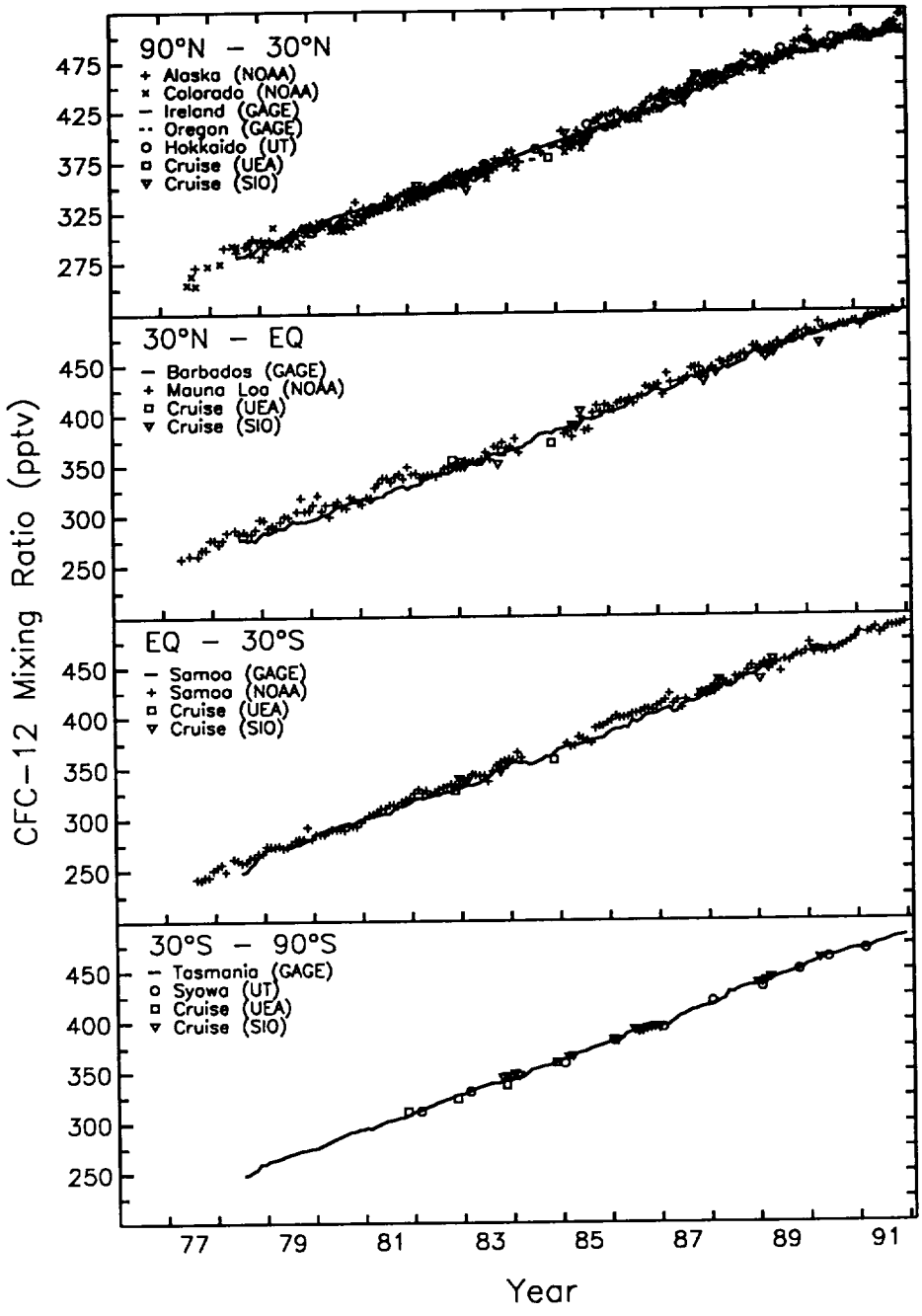

Figure 1.2.1 CFC-12 (CCl_2F_2) observations (pptv) in the four semi-hemispheres (NOAA: Montzka *et al.*, 1992; Elkins *et al.*, 1993; GAGE: Cunnold *et al.*, 1993; UT: Makide *et al.*, 1987; Makide, 1991). Some of the data are unpublished and are subject to revision. Data should not be used for further analysis without consulting the principal investigators: NOAA, J. Elkins: GAGE, R. Prinn; UT, Y. Makide; UEA, S. Penkett: SIO, R.Weiss. The NOAA data are in the NOAA-CMDL gravimentric scale and the GAGE data are in the SIO 1986 scale.

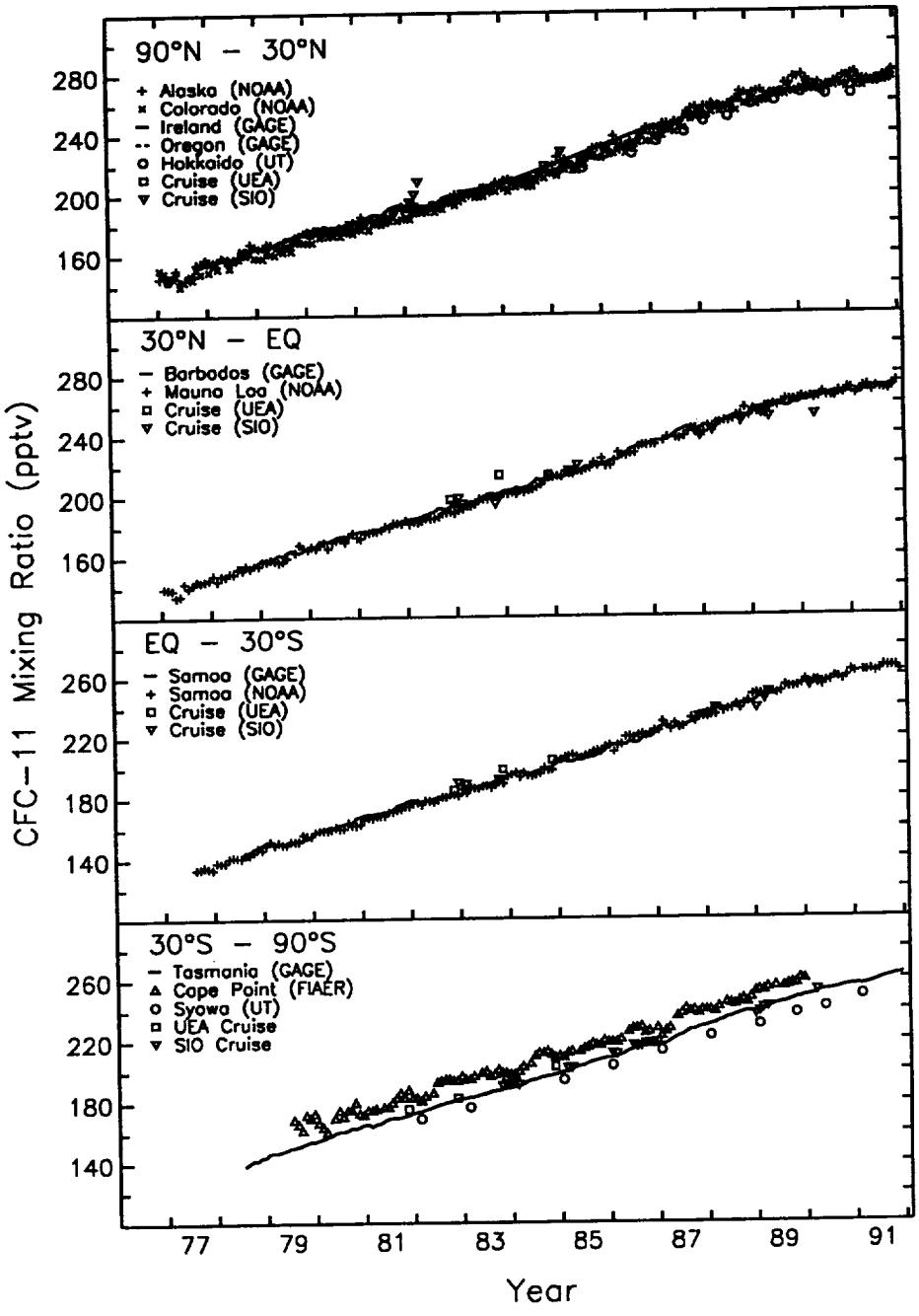

Figure 1.2.2 CFC-11 (CCl_3F) observations (pptv) in the four semi-hemispheres (NOAA: Elkins *et al.*, 1993; GAGE: Cunnold *et al.*, 1985, 1993; UT; Makide *et al.*, 1987; Makide, 1991; CSIR-FIAER: Scheel *et al.*, 1990). Some of the data are unpublished and are subject to revision. Data should not be used for further analysis without consulting the principal investigators: NOAA, J. Elkins; GAGE, R. Prinn; UT, Y. Makide; UEA, S. Penkett; SIO, R.Weiss; FIAER, H. Scheel. *Note:* the Cape Point data reported in Fraser *et al.* (1992) are not correct. The correct data are given here and in Appendix 1. The NOAA data are in the NOAA-CMDL gravimetric scale, and the GAGE data are in the SIO 1986 scale.

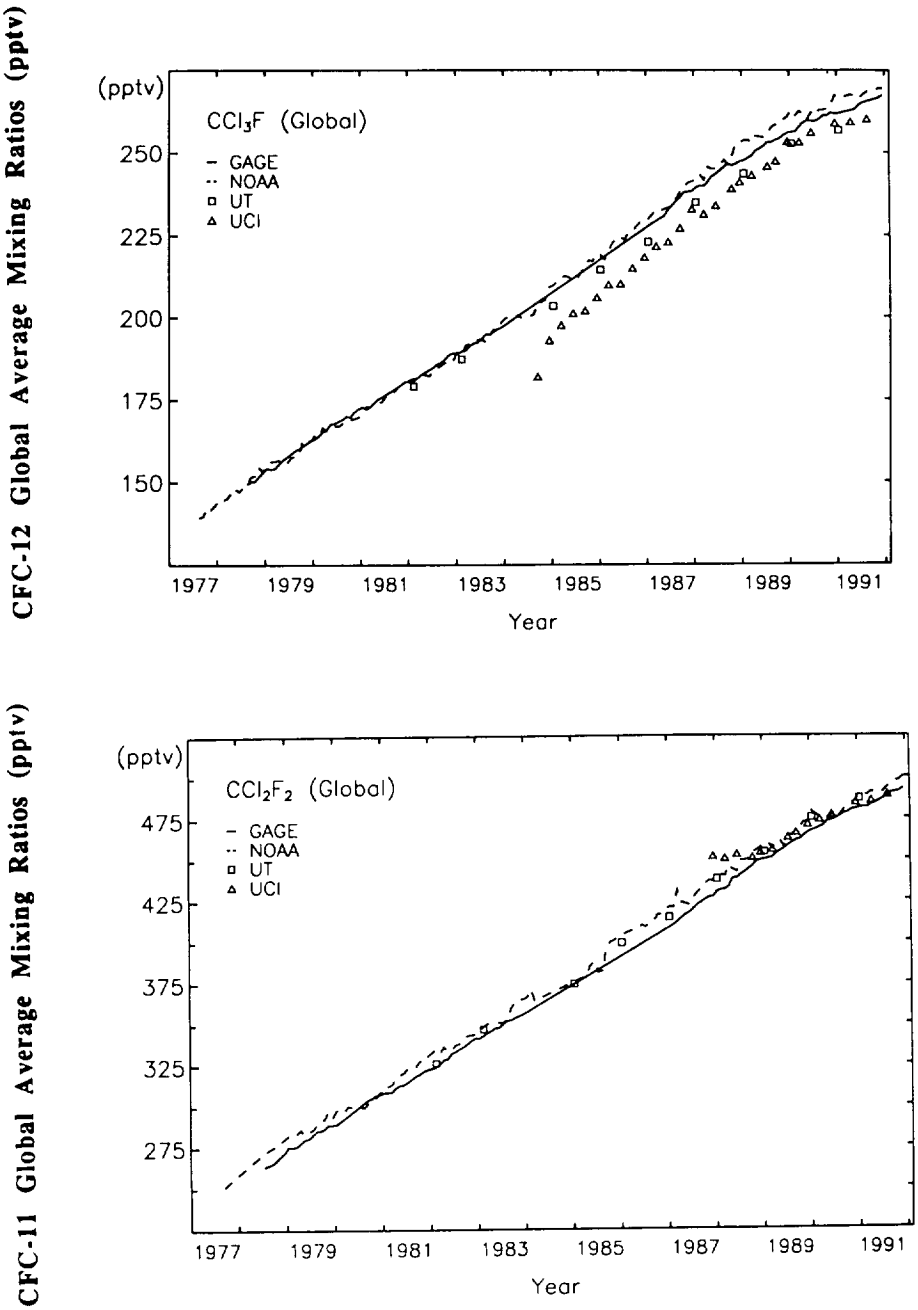

Figure 1.2.3 Globally averaged CFC-12 (CCl_2F_2) and CFC-11 (CCl_3F) observations from the GAGE *in situ* measurement program and the NOAA-CMDL, UT and UCI flask programs.

In situ CFC-11 measurements (24 per day) have been made at Cape Point, South Africa, since 1980 as part of a Fraünhofer Institute for Atmospheric Environmental Research (Germany) and the Commonwealth Scientific and Industrial Research Organization (Australia) (FIAER-CSIR) program (Scheel *et al.*, 1990; Brunke and Scheel, 1991). The 1989 annual mean CFC-11 concentration at Cape Point (34°S) was 256 pptv, increasing at 9.3±0.1 pptv per year based on a linear regression. The data are reported in the original OGIST scale and are also shown in Figure 1.2.2. The 1989 mean CFC-11 concentration and trend at Cape Point in the GAGE scale (OGIST x 0.96) are 246 pptv and 9.0 pptv per year respectively, which compare well with the 1989 mean CFC-11 concentration and trend in Tasmania (GAGE program, 41°S), 247 pptv and 9.3±0.1 pptv per year respectively.

Flask measurements of CFC-12 and CFC-11 (1 week every 6 months) have been made on Hokkaido (40°-45°N) Japan, since 1979 and at Syowa Station, Antarctica (69°S), several times per year since 1982 as part of a University of Tokyo (Japan) UT program (Makide *et al.*, 1987; Makide, 1991). The 1990 global mean concentrations for CFC-12 and CFC-11 were 478 and 254 pptv respectively (mean of hemispheric means), increasing at 18.4±0.4 and 9.1±0.2 pptv per year, based on linear regressions. The global mean data from the UT program are shown in Figure 1.2.3.

The data are reported in independently prepared UT calibration scales and are shown in Figures 1.2.1 and 1.2.2. A direct inter-laboratory comparison of the GAGE and UT CFC-12 and CFC-11 calibration scales and a comparison of CFC-12 and CFC-11 data collected at Hokkaido (UT) and Ireland (GAGE) and Syowa (UT) and Tasmania (CSIRO) has shown that GAGE data agree to within 2% for CFC-12 (GAGE lower) and within 3% for CFC-11 (GAGE higher) (Fraser and Makide, 1991). The calibration comparisons are detailed in Table 1.2.1.

Flask measurement from an extensive global network (various locations from Alaska to New Zealand) have been made for CFC-12 (since 1987) and CFC-11 (since 1984) as part of an University of California at Irvine (UCI) program (Wang *et al.*, 1991). 1990 global mean CFC-12 and CFC-11 concentrations were 478 and 256 pptv respectively and the long term increases were 18.6±0.7 and 11.0±0.3 pptv per year or 3.9% and 4.3% per year in 1990 based on linear regressions. The global data are shown in Figure 1.2.3.

Measurements of CFC-12 and CFC-11 have been made in the free troposphere via aircraft over Europe and the North Atlantic Ocean since 1976 (Scheel et al., 1988; Seiler and Scheel, 1991). CFC-12 and CFC-11 increases of 16.3±0.5 and 10.6±0.3 pptv per year have been measured over the period 1976-1987, similar to the trends observed from ground based observations in the Northern Hemisphere. These aircraft data are based on a commercially available Scott-Marrin standard.

Table 1.2.1 *A comparison of calibration scales of various trace gases employed in the ALE/GAGE* program to those of other independent laboratories, obtained by direct intercomparison of standards or by comparing respective data sets collected on or about the same time at similar latitudes in the Southern Hemisphere.*

	Laboratories†					
Species	**CMDL**	**UT**	**UEA**	**SIO**	**NIST**	**FIAER**
CCl_2F_2 (CFC-12)		1.01	1.03	1.02		
CCl_3F (CFC-11)		0.96	0.99	0.98		
CCl_2FCClF_2 (CFC-113)	0.97	1.02	0.88			
CCl_4	0.80	0.70	0.87		0.74	0.8
CH_3CCl_3	0.90	0.75	1.05			

† CMDL: Climate Monitoring and Diagnostics Laboratory (NOAA) (United States)
UT: University of Tokyo (Japan)
UEA: University of East Anglia (United Kingdom)
SIO: Scripps Institution for Oceanography (United States)
NIST: National Institute of Standards and Technology (United States)
FIAER: Fraünhofer Institute for Atmospheric Environmental Research (Germany)

*The ALE/GAGE calibration scale is based on the OGIST calibration scale derived in the late 1970s, adjusted by the following multiplicative factors, as a best estimate of absolute calibration: CCl_2F_2, 0.95; CCl_3F, 0.96; CCl_2FCClF_2, 1.40; CCl_4, 0.81; CH_3CCl_3, 0.80.

Free tropospheric measurements of CFC-12 and CFC-11 have been made via aircraft over Japan (33°-38°N) since 1978 (Hirota *et al.*, 1988; Hirota and Sasaki, 1991). CFC-12 and CFC-11 increases of 16.2±0.7 and 10.3±0.4 pptv per year have been measured over the period 1978-1990, similar to the trends observed over Europe. These aircraft data are based on a commercially available Seitetsu Kagaku and Nihon Sanso standards, whose absolute concentration is certified to ±5%.

A comparison of shipboard measurements of CFC-12 and CFC-11 from 1981 to 1984 on the North and South Atlantic (UEA; Penkett, 1991) to GAGE data from corresponding latitudes shows that the GAGE and University of East Anglia (United Kingdom) (UEA) data agree to within 3% for CFC-12 (GAGE lower) and to within 1% for CFC-11 (GAGE higher) (see Table 1.2.1). Similarly a comparison of shipboard measurements of CFC-12 and CFC-11 from 1983 to 1990 on the North and South Atlantic (SIO; Weiss, 1991) to GAGE data from corresponding latitudes shows that the GAGE and Scripps Institution for Oceanography (SIO) data agree to within 2% for CFC-12 (GAGE lower) and to within 2% for CFC-11 (GAGE higher) (see Table 1.2.1).

The atmospheric concentrations of CFC-12 and CFC-11 have been measured by several research groups for more than a decade. For most of this period the growth rates have been relatively steady at 16-20 and 8-10 pptv per year respectively. However, by the end of 1990, the rate of increase of both species has slowed down noticeably (Figure 1.2.4). The slow-down in the rate of growth of both species has appeared earlier and more strongly in the Northern Hemisphere, especially for the temperate latitudes in which the great majority of all CFC-12 and CFC-11 are emitted.

The annual increases, globally averaged, in CFC-12 and CFC-11 by the end of 1990 from the GAGE network were 14 pptv and 6 pptv respectively, the lowest annual increases observed in the 13 years of GAGE measurements (Cunnold *et al.*, 1993). In two years the global annual growth of CFC-12 has declined from 22 pptv (end of 1988) to 14 pptv (end of 1990), a 36% reduction in growth, and for CFC-11 the corresponding decline has been from 9 pptv (1988) to 6 pptv (1990), a 33% reduction in growth. The decline in growth rates appear to reflect the 20-30% reduction in emissions that has occurred for both species over the same time frame (AFEAS, 1992).

Declines in the growth rates of CFC-11 and CFC-12 have been observed in the NOAA-CMDL flask network data. Global growth rates peaked in 1988 at 11±1 and 19.5±2 pptv per year for CFC-11 and CFC-12 respectively, and subsequently declined to 4±1 and 14±2 pptv per year respectively at the end of 1992. If these observed slowdowns in growth rates continue at the same rate as in 1990-91, global atmospheric CFC-11 and CFC-12 mixing ratios will reach a maximum well before the end of the century and decline thereafter (Elkins et al., 1993).

1.2.1.2 CFC-113

Flask measurements of CFC-113 (CCl_2FCClF_2) have been made on Hokkaido (40°-45°N) Japan, since 1980 and at Syowa Station (69°S) (10 days each winter) since 1987 (Makide *et al.*, 1987; Makide, 1991). The 1990 global mean concentrations for CFC-113 was 71 pptv respectively (mean of hemispheric means), increasing at 6.2±0.2 pptv per year, based on a linear regression. On Hokkaido the mean CFC-113 increase over the period 1979-1990 was 5.5±0.2 pptv per year and 7.9±0.3 pptv per year over the period 1987-1990, based on linear regressions. The data are reported in independently prepared UT calibration scale and are shown in Figure 1.2.5. The global data (mean of Hokkaido and Syowa data) from the UT program are shown in Figure 1.2.6.

Real time measurements (12 per day) of CFC-113 have been made in Ireland, Oregon, Barbados, Samoa and Tasmania since 1982 as part of the GAGE program (Figure 1.5) (Fraser *et al.*, 1993). The 1990 global mean CFC-113 concentrations was 71 pptv (mean of hemispheric means), increasing at 5.8±0.4 pptv per year, or 8.2% per year in 1990, based on linear regressions. The global data from the GAGE program are shown in Figure 1.2.6.

The GAGE CFC-113 data (Figure 1.2.5) are obtained relative to OGIST calibration gases, but are reported in the GAGE calibration scale, which is currently based on an average of inter-laboratory comparisons to the UT (Makide *et al.*, 1987) and NOAA-CMDL (Thompson *et al.*, 1990) CFC-113 calibration scales. These comparisons showed that the UT and NOAA-CMDL CFC-113 calibration scales yielded data that are ≈40% higher than data obtained using the OGIST calibration scale (Thompson *et al.*, 1990; Fraser and Makide, 1991). It is anticipated that the entire GAGE CFC-113 data set will be calibrated with respect to new, absolute gravimetric standards prepared by R. Weiss (SIO) in 1993.

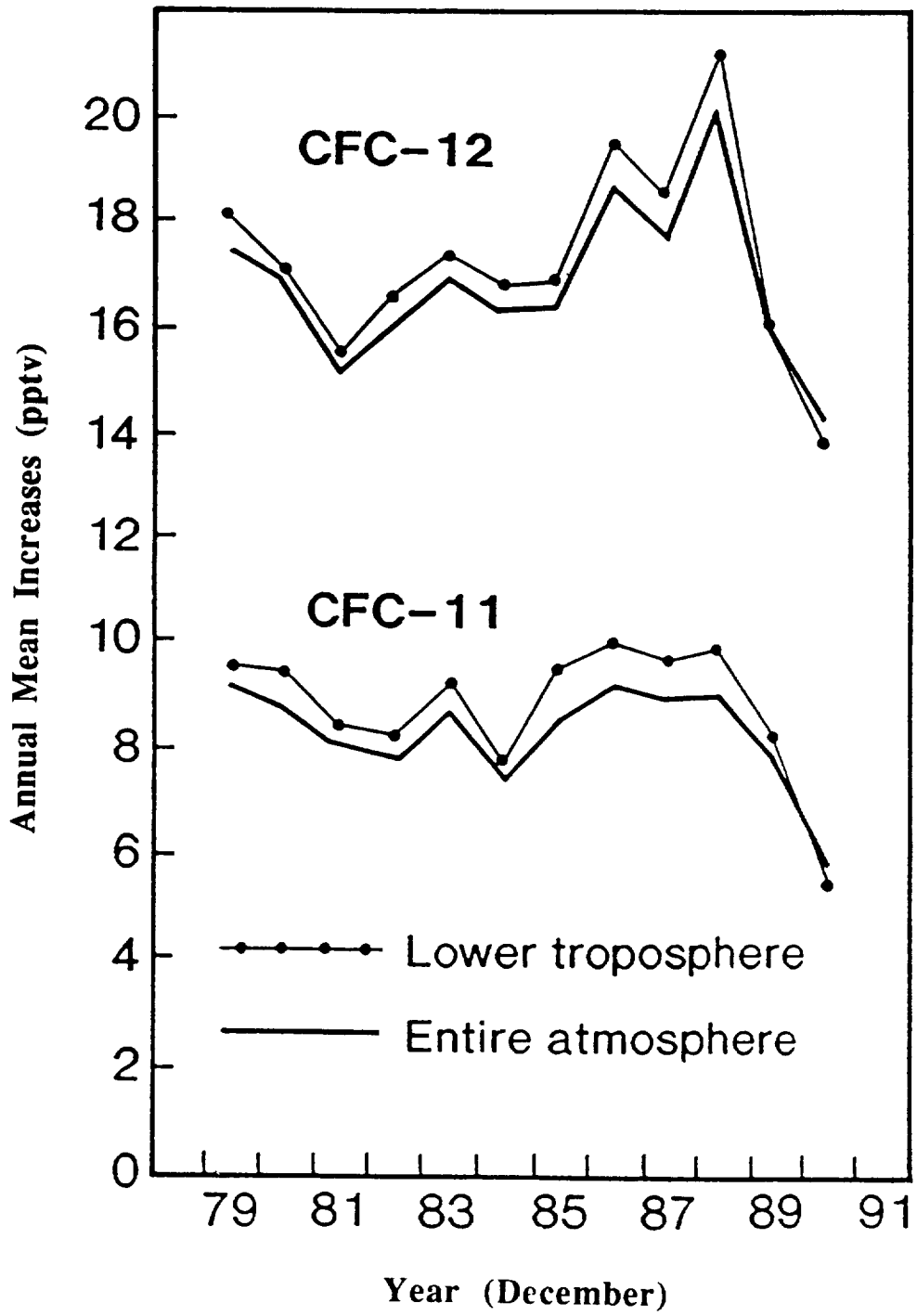

Figure 1.2.4 Annual mean increases at December of each year (pptv) of CFC-12 (CCl_2F_2) and CFC-11 (CCl_3F) estimated by combining ALE/GAGE global observations and 2-D model calculations. (Cunnold *et al.*, 1993).

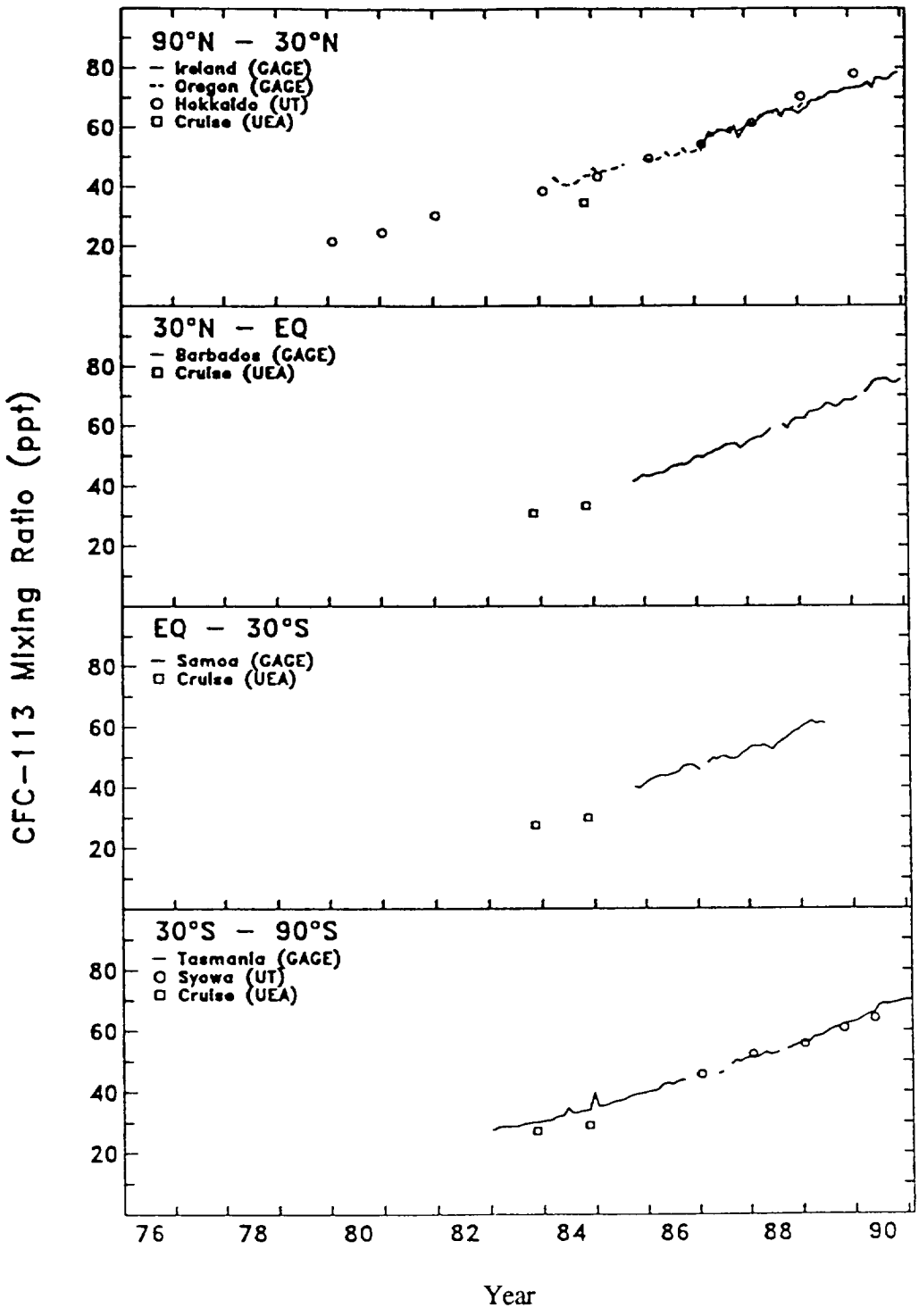

Figure 1.2.5 CFC-113 (CCl_2FCClF_2) observations (pptv) in the four semi-hemispheres (GAGE: Fraser *et al.*, 1991; Prinn *et al.*, 1991; UT: Makide *et al.*, 1987; Makide, 1991). Some of the data are unpublished and are subject to revision. Data should not be used for further analysis without consulting the principal investigators: GAGE, R. Prinn; UT, Y. Makide; UEA, S. Penkett.

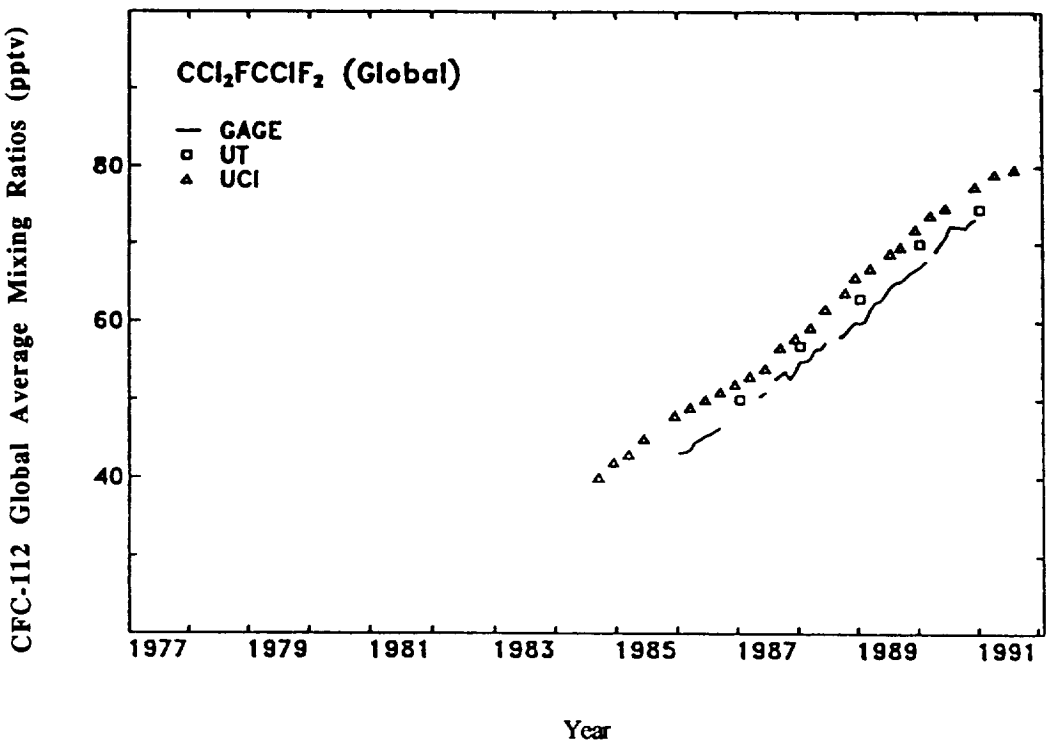

Figure 1.2.6 Globally averaged CFC-112 (CCl_2FCClF_2) observations from the GAGE *in situ* measurement program and the UT and UCI flask programs.

Flask measurements from an extensive global network have been made for CFC-113 (since 1984) (Wang *et al.*, 1991). The 1990 global mean CFC-113 concentration was 75 pptv and the long term increase was 6.0±0.1 pptv per year, based on a linear regression. The global UCI data are shown in Figure 1.2.6.

Measurements of CFC-113 in the free troposphere over Europe and the North Atlantic during the period 1982-1987 show an increase of 6.6±0.3 pptv per year (Seiler and Scheel, 1991). The data are based on a Scott-Marrin calibration standard, which gives CFC-113 concentrations that are approximately a factor of 2 higher than data obtained using OGIST calibration.

The NOAA-CMDL gravimetric CFC-113 scale is higher than the OGIST scale (NOAA-CMDL/OGIST = 1.37; Thompson *et al.*, 1990), as is the UT scale (UT/OGIST = 1.43; Fraser and Makide, 1991). The GAGE scale has been assigned a GAGE/OGIST ratio of 1.4 (average of NOAA-CMDL/OGIST and UT/OGIST). *In situ* GAGE measurements of CFC-113 at Cape Grim (41°S) have been compared to CFC-113 measurements on the South Atlantic at similar latitudes and times, which were obtained using an independent calibration scale (UEA, Penkett, 1991). The UEA data were approximately 10-20% lower than the GAGE data, which probably reflects the difference in calibration scales (i.e. GAGE/UEA = 1.1-1.2; thus UEA/OGIST = 1.2-1.3). It would appear that three independent laboratories (UT, NOAA-CMDL and UEA agree to within ±7% on CFC-113 calibration (see Table 1.2.1).

1.2.1.3 CFC-114 and CFC-114a

Rasmussen (1990) has reported growth rates for CFC-114 ($CClF_2CClF_2$) and CFC-114a (CCl_2FCF_3) from the OGIST global flask sampling network from 1979 to 1990 of approximately 6% per year. Absolute concentrations were not reported.

1.2.1.4 Carbon tetrachloride

In situ carbon tetrachloride (CCl_4) measurements have been made at the GAGE stations since 1978 (Simmonds *et al.*, 1988; Prinn *et al.*, 1991). The data (Figure 1.2.7) show the same global mean concentration in 1989 and 1990 (134 pptv), based on data from Ireland, Barbados and Tasmania, and an increase over the entire record of 1.6±0.3 pptv per year, based on a linear regression.

A similar CCl_4 increase has been observed from *in situ* measurements at Cape Point, South Africa (1.7±0.1 pptv per year) over the period 1980-1990 (Brunke and Scheel, 1991; Figure 1.2.7). This program employs the same calibration scale as the GAGE program. The 1989 mean concentration (128 pptv) at Cape Point (32°S) is very similar to that observed (130 pptv) at Cape Grim (41°S).

In situ measurements in 1989 at Samoa (14°S) and the South Pole using the new NOAA-CMDL gravimetric calibration scale gave a mean concentrations of 104 and 106 pptv respectively (Thompson *et al.*, 1990; Hall *et al.*, 1990), whereas GAGE measurements at Samoa in 1989 average about 132 pptv, suggesting that concentrations in the NOAA-CMDL scale are ≈20% lower than those in the GAGE scale. The global average CCl_4 concentration observed in the NOAA-CMDL *in situ* program (Barrow, Mauna Loa and Samoa) in 1990 was 107 pptv (Sturges *et al.*, 1991), again 20% lower than the GAGE network global average for 1990.

Flask measurements of CCl_4 on Hokkaido, Japan, over the period 1979-1990 show concentrations in 1989 and 1990 of 108 and 107 pptv respectively and an increase over the entire record of 1.2±0.2 pptv per year (Makide *et al.*, 1987; Makide 1991). A direct interlaboratory comparison between GAGE and UT indicates that the GAGE CCl_4 scale yields data that are ≈35% higher than data obtained using the UT scale (Fraser and Makide, 1991). Note that both the GAGE global data and the UT data from Hokkaido do not show any increase in CCl_4 from 1989 to 1990.

Measurements of CCl_4 in the free troposphere over Europe and the North Atlantic during the period 1976-1987 show an increase of 2.0±0.3 pptv per year (Seiler and Scheel, 1991). These data are based on a Scott-Marrin calibration standard, which gives CCl_4 concentrations that are a factor of ≈1.15 lower than those based on the GAGE calibration.

Measurements of CCl_4 at Cape Grim (41°S) have been compared to CCl_4 measurements on the South Atlantic at similar latitudes and times, which were obtained using an independent calibration scale (UEA; Penkett, 1991). The Atlantic data were approximately 15% lower, which probably reflects the difference in calibration scales (i.e. GAGE/UEA ≈1.15). A direct comparison of the National Institute of Standards and Technology (United States) (NIST) and GAGE CCl_4 standards indicates that the GAGE/NIST ratio is ≈1.35 (Fraser, 1991).

It would appear that six independent laboratories (GAGE, UT, NOAA-CMDL, UEA, FIAER (Scott-Marrin) and NIST) produce a 25% range of CCl_4 measurements. GAGE data are at the high extreme of this range. The average CCl_4 values from the five non-GAGE laboratories is approximately 20% lower than GAGE (see Table 1.2.1). These five laboratories agree to within ±10% for CCl_4.

The oceans have been identified as a significant sink for CCl_4 with 16-35% of atmospheric CCl_4 being removed by ocean mixing and hydrolysis (Butler *et al.*, 1991; Sturges *et al.*, 1991).

1.2.2 Methyl Chloroform and HCFC-22

Methyl chloroform (CH_3CCl_3) and HCFC-22 ($CHClF_2$) are important trace gases in the global atmosphere. They constitute about 14% of the tropospheric total organochlorine loading (CH_3CCl_3, 11%; $CHClF_2$, 3%) and both are partially removed from the atmosphere by reaction with hydroxyl (OH). Assuming emissions and absolute abundances of these species are known, they can be used to calculate average tropospheric OH levels (for CH_3CCl_3, see Prinn *et al.*, 1987, 1992). Methyl chloroform is used as an industrial solvent and HCFC-22 is being increasingly used as a substitute for CFCs.

1.2.2.1 Methyl chloroform, trends and global distribution

Long term, high frequency measurements (4-12 per day) of CH_3CCl_3 have been made in Ireland, Oregon, Barbados, Samoa and Tasmania (Prinn *et al.*, 1987, 1992) since 1978 as part of the GAGE program, and on Hokkaido, Japan, twice a year (10 days every 6 months) since 1979 and at Syowa Station in Antarctica (several times per year)

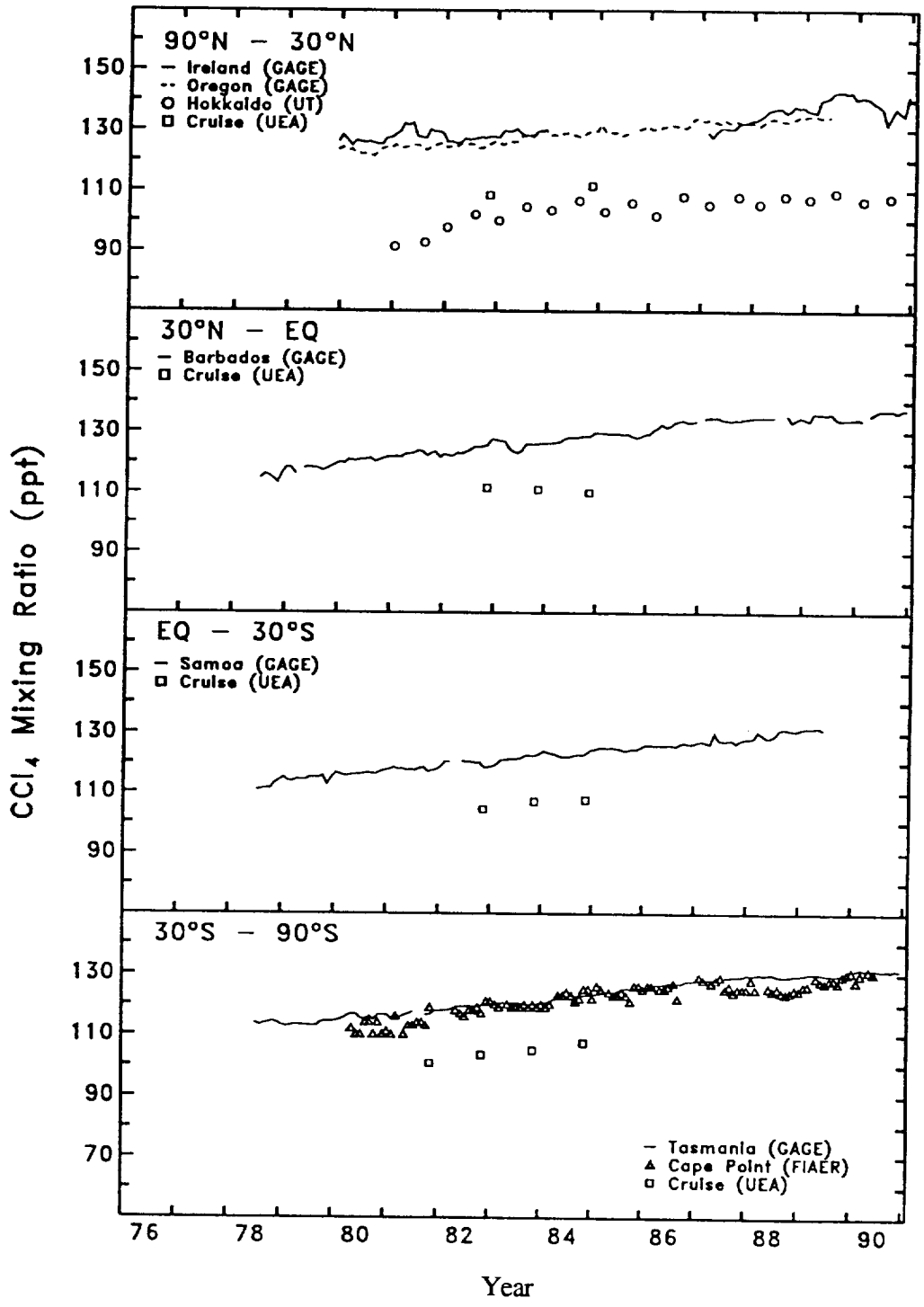

Figure 1.2.7 Carbon tetrachloride (CCl_4) observations (pptv) in the four semi-hemispheres (GAGE: Simmonds *et al.*, 1988, Prinn *et al.*, 1991; UT: Makide *et al.*, 1987; Makide, 1991; CSIR-FIAER: Scheel *et al.*, 1990). Some of the data are unpublished and are subject to revision. Data should not be used for further analysis without consulting the principal investigators: GAGE, R. Prinn; UT, Y. Makide; UEA, S. Penkett; FIAER, H. Scheel. *Note:* the Cape Point data reported in Fraser *et al.* (1992) are not correct. The correct data are given here and in Appendix I.

(Makide *et al.*, 1987; Makide, 1991). January measurements made in the NW Pacific USA and at the South Pole since 1975 have been published (Rasmussen and Khalil, 1986; Khalil and Rasmussen, 1990). Mid-tropospheric CH_3CCl_3 data have been obtained by aircraft air sampling between over Europe and the North Atlantic by FIAER since 1978 (Scheel *et al.*, 1988).

The available data are shown in Figure 1.2.8. Twelve years of ALE/GAGE CH_3CCl_3 data (July 1978-June 1990) have recently been analyzed (Prinn *et al.*, 1992) showing a global trend of 5.5±0.2 pptv per year. The 1990 global mean concentrations was 155 pptv (based on data from Ireland, Barbados and Tasmania). The global GAGE CH_3CCl_3 data are shown in Figure 1.2.9.

Flask measurements of CH_3CCl_3 (1 week every 6 months) have been made on Hokkaido (40°-45°N) Japan, since 1979 (Makide *et al.*, 1987; Makide, 1991) and at Syowa Station, Antarctica (69°S), several times per year since 1982 (Makide 1991). The 1990 global mean concentration of CH_3CCl_3 was 125 pptv (mean of hemispheric means), increasing at 3.5±0.2 pptv per year, based on a linear regression. The Hokkaido data (Makide *et al.*, 1987; Makide, 1991) show an increase of 3.7 pptv per year over the period 1980-1990 and 4.8 pptv per year over the period 1987-1990. The concentrations of CH_3CCl_3 observed on Hokkaido are about 15% lower than in Ireland or Oregon. The global UT CH_3CCl_3 data are shown in Figure 1.2.9.

The free tropospheric CH_3CCl_3 data over Europe and the North Atlantic (1978-1987) show a trend of 5.2±0.8 pptv per year (Scheel *et al.*, 1988; Seiler and Scheel, 1991).

The CH_3CCl_3 measurements at the tropical South Pacific station (Samoa) show remarkable sensitivity to El Niño/Southern Oscillation (ENSO) events, which have been attributed to modulation of cross-equatorial transport during the Northern Hemisphere winter by the interannually varying upper tropospheric zonal winds in the equatorial Pacific (Prinn *et al.*, 1992).

1.2.2.2 Methyl chloroform calibration

The absolute calibration of methyl chloroform (CH_3CCl_3) measurements in the GAGE program is based on the OGIST standard (Khalil and Rasmussen, 1984). Unfortunately there have not been any published comparisons of independently derived CH_3CCl_3 standards. A preliminary and as yet unpublished comparison between the GAGE and UT CH_3CCl_3 standards suggests that the latter are lower by about 25% (UT/GAGE = 0.75) (Fraser and Makide, 1991).

A new gravimetric CH_3CCl_3 standard has been prepared by NOAA-CMDL (Butler *et al.*, 1991). No direct comparisons have been made between this standard and the GAGE standard, but an indirect comparison can be made from observations made by both groups in the Southern Hemisphere in early 1990 (Butler *et al.*, 1991; Prinn *et al.*, 1992). This comparison suggests that the NOAA-CMDL standard is about 10% lower than the GAGE standard (NOAA-CMDL/GAGE = 0.9). Shipboard measurements of CH_3CCl_3, based on an independent calibration, have been made on the North and South Atlantic (Penkett, 1991) between 1981 and 1984. A comparison to ALE/GAGE data at similar latitudes and times indicates that the UEA standard is about 5% higher than the GAGE standard (UEA/GAGE = 1.05). Thus the current range of CH_3CCl_3 measurements based on four independent standards (GAGE, UT, NOAA-CMDL, UEA) is about 30%. The average of the four standards is approximately 10% lower than GAGE.

The long term stability of the OGIST CH_3CCl_3 standard has been possibly but not absolutely demonstrated by extensive, periodic internal comparisons of several original ALE/GAGE calibration gases and by a comparison of measurements made in 1978-1979 in the ALE/GAGE program in Tasmania with modern measurements on air archived from that period. These experiments limit the magnitude of a calibration drift component of the observed trend to about 0.2% per year, comparable to the uncertainty in the long term trend due to measurement variability (Prinn *et al.*, 1992).

1.2.2.3 HCFC-22 trends and global abundance

The available data on the global distribution and trends of HCFC-22 ($CHClF_2$) are limited, reflecting the relative difficulty in making atmospheric $CHClF_2$ measurements, which can be achieved by spectroscopy (total column), gas

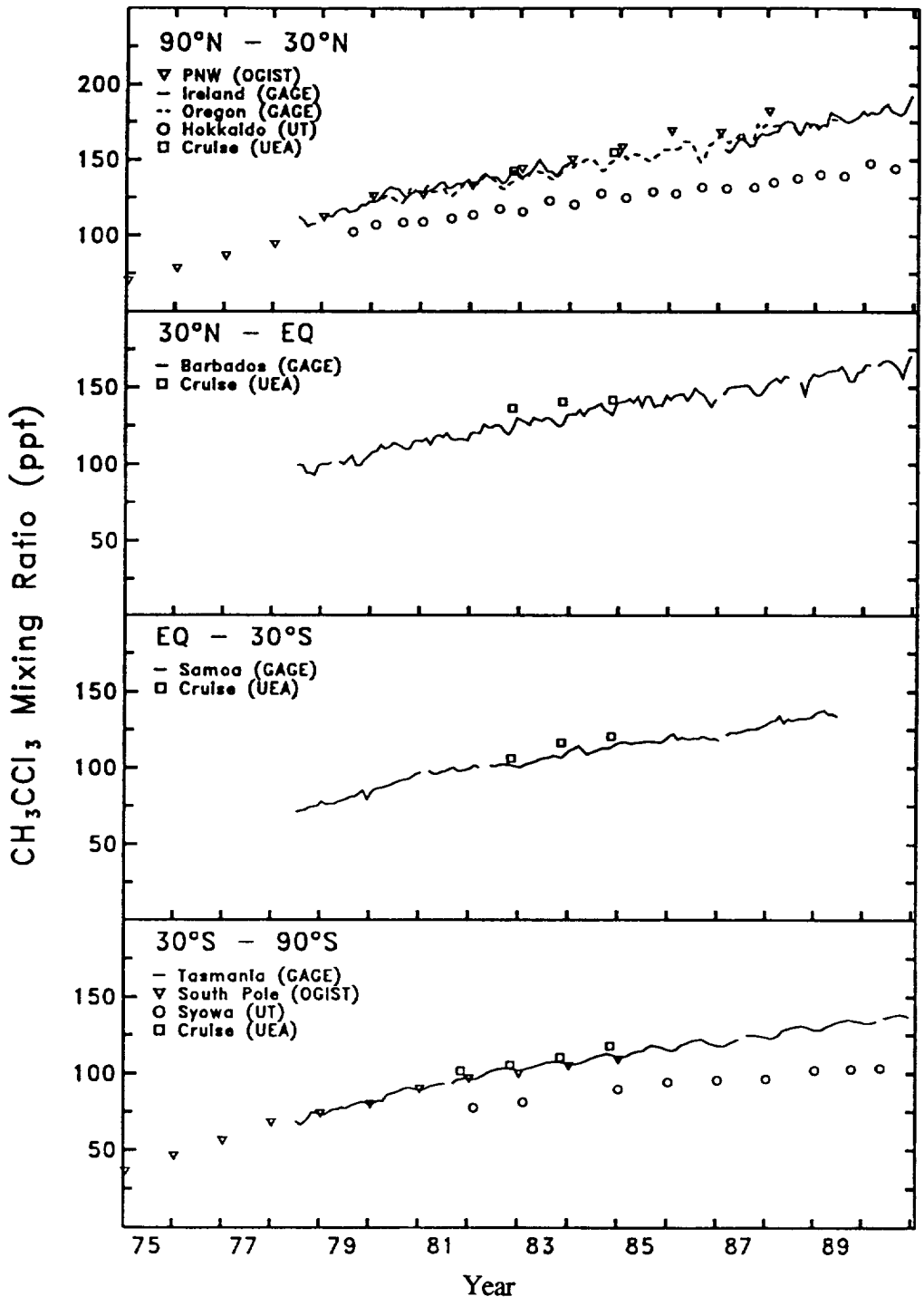

Figure 1.2.8 Methyl chloroform (CH_3CCl_3) observations (pptv) in the four semi-hemispheres (GAGE: Prinn *et al.*, 1991; UT: Makide *et al.*, 1987; Makide, 1991; OGIST: Rasmussen and Khalil, 1986; Khalil and Rasmussen, 1990). Some of the data are unpublished and are subject to revision. Data should not be used for further analysis without consulting the principal investigators: GAGE, R. Prinn; UT, Y. Makide; UEA, S. Penkett.

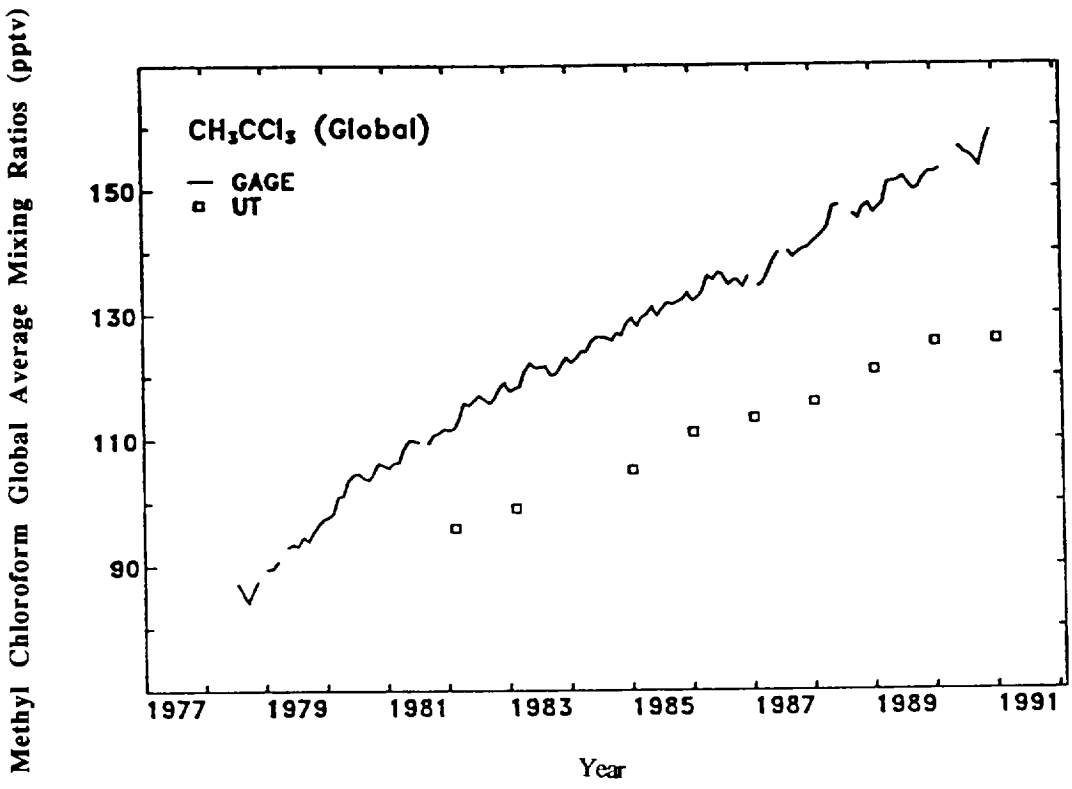

Figure 1.2.9 Globally averaged methyl chloroform (CH_3CCl_3) observations from the GAGE *in situ* measurement program and the UT flask program.

chromatographic-mass spectrometric techniques, or gas chromatography-electron capture detection involving large volume air samples.

Gas chromatographic HCFC-22 data have been regularly obtained from the Pacific North West (PNW) region of the United States and from the South Pole (Rasmussen *et al.*, 1980; Khalil and Rasmussen, 1981; Rasmussen and Khalil, 1982, 1983). The PNW data from 1976 to 1981 showed concentrations increasing by about 12±1% per year, with an absolute concentration uncertainty range of 20%. Combined PNW-South Pole data for 1979-1987 have recently been reported (Khalil and Rasmussen, 1990) which show a concentration in January 1987 of 105 pptv increasing by 6.4±0.3 pptv per year.

HCFC-22 observations (gas chromatography [GC]) for the period 1980 to 1987 have also recently reported from two locations on Hawaii (20°N), at Mauna Loa (3.4 km) and at the surface (Cape Kumukahi) (Khalil and Rasmussen, 1991). The Mauna Loa and Cape Kumukahi observations show increases of 6.5 and 6.2 pptv per year. Observations from Cape Grim, Tasmania (41°S, 1984-1987) show a mean concentration and increase in 1987 of 91 pptv and 6.5±0.3 pptv per year (Fraser *et al.*, 1989).

All of the above data, obtained from the OGIST global flask sampling program and analyzed by GC-MS, are all reported in the same calibration scale (OGIST) and are shown in Figure 1.2.10. The OGIST and UEA independent HCFC-22 calibration scales agree to within 5% (Rasmussen *et al.*, 1980).

Measurements of HCFC-22 commenced at the NOAA-CMDL stations in mid-1989. The results are now published and are reported in the recently developed NOAA-CMDL gravimetric scale (Sturges *et al.*, 1991; Montzka *et al.*, 1992, 1993) A global mean concentration of 101.8 pptv and interhemispheric difference of 13 pptv were determined for 1992. Based on data from the NOAA-CMDL flask network and from archived air samples from Ninot Ridge, Colorado, a mean growth rate from mid-1987 through 1992 of 7.3% per year has been found (Montzka *et al.*, 1993)..

Solar spectroscopic HCFC-22 measurements from Kitt Peak (32°N) over the period 1980-1988 show an increase of 7.8±1.0 % per year, with an absolute error of ±25%, arising largely from the uncertainty in the HCFC-22

spectroscopic parameter (Rinsland *et al.*, 1989). These parameters have been refined and derived concentrations increased by about 30%, resulting in improved agreement between spectroscopic and gas chromatographic measurements (in 1982 spectroscopic measurements were about 25% lower than gas chromatographic measurements); additional data from balloon borne spectrometers (31°-32°N) have been obtained (Rinsland *et al.*, 1990) and the combined data are shown in Figure 1.2.10. The combined data show a mean concentration in 1988 of 94 pptv and an increase of 5.9±0.4 pptv per year (6.3% per year in 1988), based on a linear regression. A trend of approximately 10% per year has been reported from stratospheric observations for the period 1982-1987 (Fabian *et al.*, 1989).

Between late 1985 and mid-1990, the Atmospheric Trace Molecule Spectroscopy Experiment (ATMOS) spectrometer made infrared solar measurements from Table Mountain Observatory in the San Gabriel Mountains (34°N), California. The spectroscopic data obtained have been used to derive column amounts of HCFC-22, which have been converted into local (surface) observations. The conversion assumes that HCFC-22 is well mixed in the troposphere up to 12 km, above which the profile derived by ATMOS from Spacelab 3 observations can be used. This profile was scaled to fit the ground-based observations and the tropospheric mixing ratio taken from the scaled profile. The principal error source limiting the accuracy of the spectroscopic measurements is the uncertainty in the HCFC-22 infrared absorption cross-sections. The spectroscopic parameters used in this study are those of Zander *et al.*, 1992.

The ATMOS data show a long term increase and mean concentration in 1990 of 6.3±0.4 pptv per year and 94 pptv respectively based on a linear regression. The ATMOS data from Table Mountain and the Kitt Peak spectroscopic data show good agreement, with the Table Mountain data being about 5% lower than Kitt Peak data.

1.2.3 Other Chlorinated Species

1.2.3.1 Methyl chloride

There have been little new data, further to (WMO 1990), reported on the global distribution of methyl chloride (CH_3Cl). Eight years of observations (1980-1987) at Mauna Loa and Cape Kumukahi, Hawaii, suggest background levels of 645 and 625 pptv respectively. No significant trends are reported (Khalil and Rasmussen, 1991). A global average background concentration of approximately 590 pptv (600 pptv, Northern Hemisphere; 580, pptv Southern Hemisphere) has been calculated, based on shipboard measurements made on the North and South Atlantic oceans between 1981 and 1984 (Penkett, 1991).

Measurements of CH_3Cl commenced at the NOAA-CMDL stations in mid-1989. The results as yet unpublished, are to be reported in the recently developed NOAA-CMDL gravimetric scale (Sturges *et al.*, 1991).

Source studies suggest that 15-30% of CH_3Cl may result from anthropogenic activities (Makhijani and Makhijani, 1992).

1.2.3.2 Chloroform

Chloroform ($CHCl_3$) measurements have been made regularly at Cape Grim, Tasmania, as part of the OGIST flask sampling program and as part of the GAGE *in situ* measurement program. The data have been calibrated with respect to a NIST Standard Reference Material (SRM) and are shown in Figure 1.2.11. A global background concentration in 1989 of approximately 10 pptv has been calculated from these data, based on the previously reported ratio of Northern to Southern Hemispheric measurements (Khalil and Rasmussen, 1983).

Concentrations of 13-17 pptv have recently been reported from two locations on Hawaii over the period 1980-1987. Significant trends were not observed (Khalil and Rasmussen, 1991).

A global average background concentration of approximately 15 pptv has been derived (20 pptv, Northern Hemisphere; 10 pptv, Southern Hemisphere), based on shipboard measurements made on the North and South Atlantic oceans between 1981 and 1984 (Penkett, 1991).

Approximately 40% of the $CHCl_3$ source required to maintain the observed global concentration (400 million kg per year) is anthropogenic (Khalil and Rasmussen, 1983). Termite mounds were found to contain elevated levels of $CHCl_3$, which were calculated to emit <100 million kg per year (Khalil *et al.*, 1990). Most studies have shown that there are large urban sources of $CHCl_3$ (Singh *et al.*, 1992).

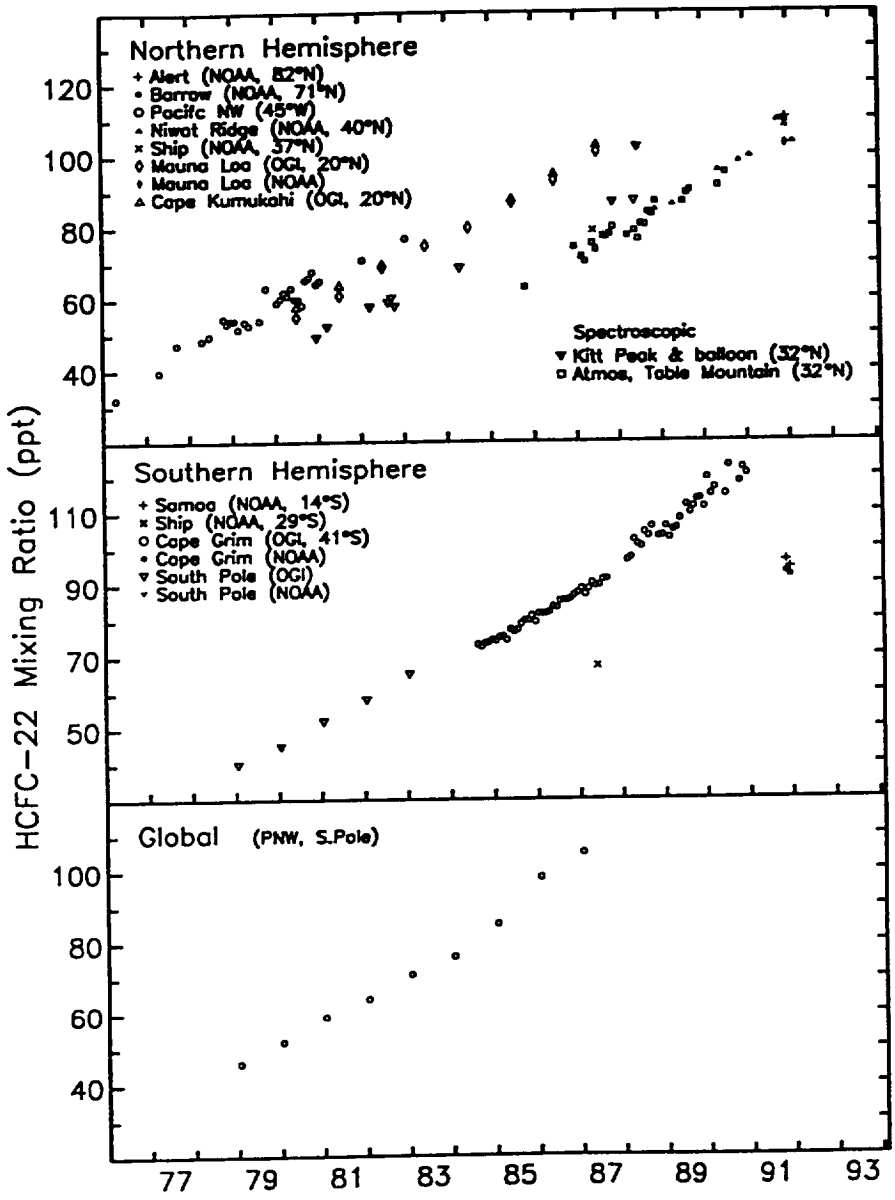

Figure 1.2.10 Northern hemispheric, southern hemispheric and global observations of HCFC-22 ($CHClF_2$) (pptv) PNW, South Pole: Khalil and Rasmussen, 1981; Rasmussen and Khalil, 1982, 1983; spectroscopic: Rinsland *et al.*, 1989, 1990: Tasmania: Fraser *et al.*, 1989; global: Khalil and Rasmussen, 1990, ATMOS: see Section 1.2.2.3, NOAA: Montzka *et al.*, 1992, 1993.

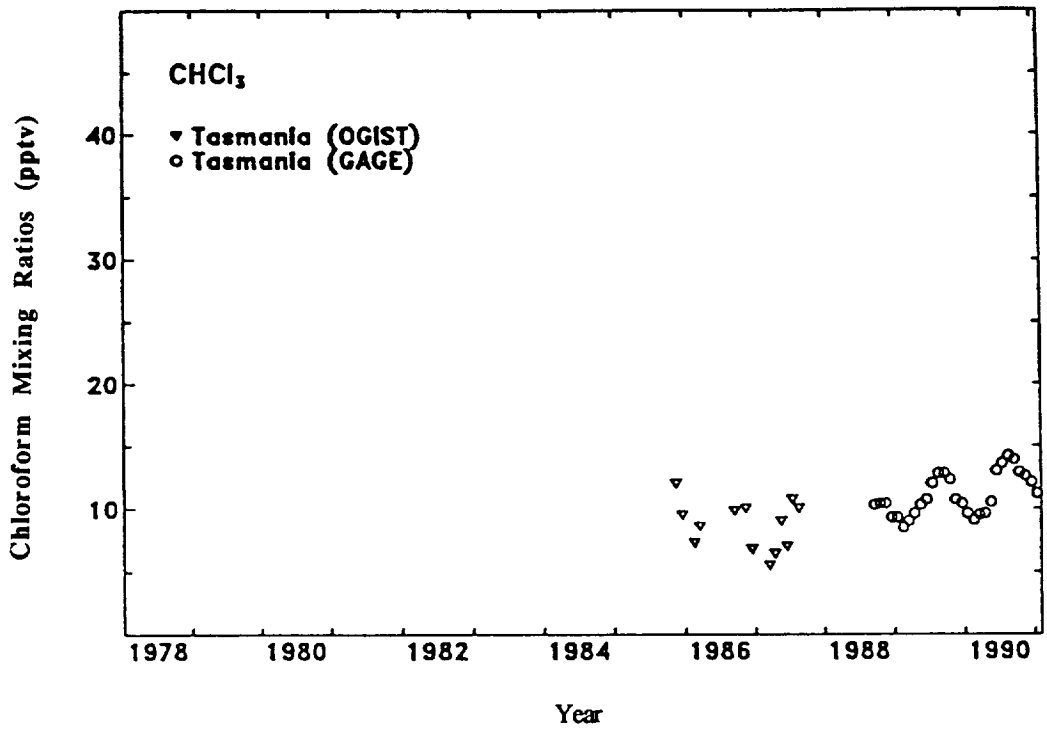

Figure 1.2.11 Chloroform ($CHCl_3$) observations (pptv) at Cape Grim, Tasmania from the OGIST flask sampling program and the GAGE *in situ* measurement program (Fraser *et al.*, 1989; Fraser, 1991). The data are unpublished and are subject to revision. Data should not be used without consulting the principal investigators: OGIST, R. Rasmussen; GAGE, P. Fraser.

1.2.3.3 Methylene chloride

A global average background concentration for methylene chloride (CH_2Cl_2) of approximately 30 pptv has been derived (50 pptv, Northern Hemisphere; 15 pptv, Southern Hemisphere), based on shipboard measurements made on the North and South Atlantic oceans between 1981 and 1984 (Penkett, 1991).

1.2.3.4 Trichloroethylene

A global average background concentration for trichloroethylene ($CHClCCl_2$) of approximately 2-3 pptv has been derived (4 pptv, Northern Hemisphere, <1 pptv, Southern Hemisphere) based on shipboard measurements made on the North and South Atlantic oceans between 1981 and 1984 (Penkett, 1991).

More recent data from Hokkaido, Japan (1979-1991) indicate Northern Hemispheric mid-latitude concentrations of 15 pptv (Makide, 1991), with significant seasonal variations (factor of two, summer minimum, winter maximum). No significant trends were observed in these data and the differences between UEA and UT data in the Northern Hemisphere are presumably due to calibration and/or regional differences.

1.2.3.5 Tetrachloroethylene

A global average background concentration for tetrachloroethylene (CCl_2CCl_2) of approximately 10 pptv has been derived (20 pptv, Northern Hemisphere, 2 pptv Southern Hemisphere), based on shipboard measurements made on the North and South Atlantic oceans between 1981 and 1984 (Penkett, 1991).

More recent data from Hokkaido, Japan (1979-1991) indicates similar Northern Hemispheric mid-latitude concentrations of 18 pptv (Makide, 1991), with significant seasonal variations (factor of two, summer minimum, winter maximum). No significant trends were observed in these data.

Flask measurements from an extensive global network have been made for CCl_2CCl_2 during 1989 and 1990 (Wang *et al.*, 1992). The global mean CCl_2CCl_2 concentrations was about 10 pptv (16 pptv, Northern Hemisphere, 4 pptv Southern Hemisphere), with significant seasonal variations (summer minimum, winter maximum).

1.2.4 Methyl Bromide, Halons and other Brominated Species

Bromine enters the atmosphere through various processes, both natural and anthropogenic. The bromine source gases that are present in the troposphere are shown in Table 1.1. There has been a recent extensive review of the sources and sinks of bromine in the lower atmosphere (Galbally *et al.*, 1991).

1.2.4.1 Methyl bromide

The most abundant organobromine species in the lower atmosphere is methyl bromide (CH_3Br), which has both natural and anthropogenic sources.

The main natural sources of CH_3Br are oceanic biological processes where it is formed with other hydrogen-containing molecules, such as CH_2Br_2, $CHBr_3$, CH_2BrCl and $CHBrCl_2$ (Singh *et al.*, 1983; Class and Ballschmitter, 1988). However measurements of CH_3Br made in both hemispheres show a significant interhemispheric gradient, with average concentrations of 12-15 pptv and 10-11 pptv being recorded in the Northern and Southern Hemispheres respectively (Penkett *et al.*, 1985; Cicerone *et al.*, 1988). This argues for a substantial land-based source, which could well be anthropogenic (fumigation). The source strength required to produce the observed abundance is approximately 100 million kg per year, assuming a lifetime of about 2-3 years (Galbally *et al.*, 1991), whereas the annual anthropogenic production is 67 million kg although a substantial fraction is probably not released to the atmosphere (Albritton and Watson, 1992). There is a clear need to investigate all identified and potential anthropogenic sources of methyl bromide, including automobile exhausts (Harsch and Rasmussen, 1977) as a matter of urgency .

A significant north-south gradient in CH_3Br argues for a larger CH_3Br source in the Northern Hemisphere compared to the Southern Hemisphere. If the oceanic source is proportional to oceanic area, then the Southern Hemispheric oceanic source is presumably larger than the Northern Hemispheric oceanic source, and therefore, there must be a significant Northern Hemispheric land-based source to produce the observed gradient. However, the oceanic sources of CH_3Br are influenced by shallow, productive coastal waters and inland seas, as well as upwelling processes, which may mean that Northern Hemispheric oceans and seas actually release more CH_3Br than the Southern Hemispheric oceans (J. Butler, NOAA-CMDL, personal communication). Clearly more research is needed to quantify these oceanic and coastal water sources before the atmospheric burden of CH_3Br can be used to calculate more accurate estimates of land-based CH_3Br sources.

Another important oceanic CH_3Br research topic is to evaluate the ability of the ocean to "buffer" any changes in the atmospheric CH_3Br burden. The flux of CH_3Br from the ocean to the atmosphere may increase with decreasing atmospheric concentrations and thus tend to offset the effect of reducing anthropogenic emissions.

Observational data records of sufficient frequency and duration to determine possible methyl bromide trends are rare. A trend in the Northern Hemisphere of approximately 0.3 pptv per year has been observed in data collected from the OGIST global flask sampling network (Albritton and Watson, 1992). NOAA-CMDL measurements of CH_3Br commenced in mid-1989 (Sturges *et al.*, 1991).

1.2.4.2 Halons

The available Halon-1211 ($CBrClF_2$) and Halon-1301 ($CBrF_3$) data from the OGIST flask sampling network up to 1986 were recently summarized (WMO, 1990), which suggested global mean concentrations and rates of increase of 1.7 and 2.0 pptv and 12 and 15% per year respectively for $CBrClF_2$ and $CBrF_3$. These data are reported in the OGIST scale. Rasmussen (1990) has recently revised the global growth rates from the OGIST flask network to be $\approx$15 and $\approx$20% per year respectively for $CBrClF_2$ and $CBrF_3$, but absolute concentrations were not reported.

NOAA-CMDL (Butler *et al.*, 1992) have recently reported shipboard data collected between 45°N and 60°S (Pacific Ocean) from 1987 to 1990 and flask data from the NOAA-CMDL network (Alaska, northern Canada, Colorado, Hawaii, Samoa, Tasmania and South Pole) from 1989 to 1992. The combined data sets show that the

global mean concentrations of $CBrClF_2$ and $CBrF_3$ in 1990 were 2.1±0.4 pptv and 1.7±0.5 pptv respectively. These data are reported in the NOAA-CMDL gravimetric scale (Sturges *et al.*, 1991). The increase in $CBrF_3$ concentration has halved from 0.3 pptv per year in 1988 to 0.15 pptv per year in 1990, whereas the increase in $CBrClF_2$ has remained relatively constant at 0.07 pptv per year. These growth rates and their recent changes are consistent with industry estimates of emissions (McCulloch, 1992), and their atmospheric concentrations may stabilize or even begin to decrease within the next few years (Butler *et al.*, 1992).

Singh *et al.*(1988) reported tropospheric concentrations for $CBrClF_2$ and $CBrF_3$ at the mid-latitudes of the Northern Hemisphere in 1987 of 2.0 and 1.3 pptv respectively. The $CBrClF_2$ data compare favorably with the OGIST Northern Hemispheric data (WMO, 1990), but the $CBrF_3$ data are ≈50% lower. These data from three independent laboratories (OGIST, NOAA-CMDL and the Max Planck Institut für Aeronomie [MPAE]) suggest that the uncertainties in calibration of $CBrClF_2$ and $CBrF_3$ are approximately ±15% and ±40% respectively.

1.2.4.3 Other brominated species

There have been little new data, further to (WMO 1990), reported on the global distribution of other brominated species. Global average background concentrations for methylene bromide (CH_2Br_2, 2-3 pptv) and bromoform ($CHBr_3$) (1 pptv) have been derived, based on shipboard measurements made on the North and South Atlantic oceans between 1981 and 1984 (Penkett, *et al.* 1985). Lower background levels of $CHBr_3$ (0.2 - 0.5 pptv) and CH_2Br_2 (0.5 - 1 pptv) have been observed at several locations in the North and South Pacific (D. Blake, UCI, unpublished data). Clearly Atlantic Ocean/Pacific Ocean differences apparent here could be real or due to calibration differences or a combination of both causes. Bromoform concentrations of 3 pptv have been observed on Hawaii (Cicerone *et al.*, 1988). Higher concentrations of both CH_2Br_2 (5-10 pptv) and $CHBr_3$ (6-8 pptv) have been observed in the Arctic regions (Berg *et al.*, 1984; Rasmussen and Khalil, 1984; Cicerone *et al.*, 1988).

1.3 Stratospheric Measurements

The purpose of this section is to review reported measurements of the stratospheric abundance and distribution of halocarbons. Clearly, the database of stratospheric measurements is much more sparse in terms of latitudinal and seasonal distribution, and lacks the same continuity as that for tropospheric measurements described in the first section. With one or two exceptions, the database of stratospheric measurements cannot be used directly to assess simple trends in the atmospheric burden of individual halocarbons. However, two of the most important questions which can be addressed using stratospheric measurements are how quickly are the halocarbons photochemically destroyed in the stratosphere to liberate active chlorine, *i.e.* what are their lifetimes, and how much active chlorine does each halocarbon contribute. Estimates of the answers to such questions are provided in later chapters where suitable models and analyses are described; below we summarize the observational database.

A number of reviews and summaries of measured stratospheric halocarbons have appeared (WMO, 1986; Prinn, 1988; Fabian, 1989), but they have considered primarily measurements made prior to 1985. Fabian (1989) derived average profiles for many of the halocarbons, based on measurements made between 1979 and 1984. They are used in subsequent figures as a guide to emphasize differences in measured profiles obtained at different latitudes. Only data obtained since 1984 have been included on an individual basis in these figures, presenting the data in the traditional format of volume mixing ratio versus altitude. However, with these figures it is difficult to distinguish variations caused by experimental uncertainty from the effects of atmospheric dynamical processes or tropospause height differences.. An alternative presentation is provided, correlation graphs, where the dynamical effects, differences in tropopause height, and wide variability seen in the measurements through the high resolution spatial sampling employed, can be removed by plotting the measured halocarbon mixing ratios against that of another tracer measured simultaneously. In these plots, following the suggestion of Plumb and Ko (1992), N_2O has been used as it is a nearly conservative tracer, which can be measured with high precision by most techniques, with a wide dynamic range of values over the altitudes of interest for maximum sensitivity. These data are used directly in Chapter 5 to determine relative atmospheric lifetimes for some of these gases. A summary of a linear fit to these data are provided in Table 1.3.1. These values were obtained from a consideration of published data from several groups

using different calibrations factors for their data. This will undoubtedly introduce bias into the linear regressions determined in Table 1.3.1 and may cause erroneous values to be determined. Some tabulations of new observational data can be found in Appendix II at the end of this chapter. These include unpublished data made available to facilitate new analyses.

Table 1.3.1 *Results of linear regressions to data included in correlation plots (halocarbon vs. N_2O). The derived fit are shown in the graphs as solid lines over the range of data used. For a discussion on the interpretation of the slopes for relative local lifetimes see Chapter 5 here and Plumb and Ko (1992).*

Molecule	CFC	Slope	Molecule	CFC	Slope
CCl_3F	CFC-11	$1.46 \pm 0.03 \times 10^{-3}$	CCl_2FCClF_2	CFC-113	$2.03 \pm 0.06 \times 10^{-4}$
CCl_2F_2	CFC-12	$1.59 \pm 0.02 \times 10^{-3}$	$CClF_2CClF_2$	CFC-114	$3.0 \pm 0.2 \times 10^{-5}$
CCl_4		$5.2 \pm 0.2 \times 10^{-4}$	$CClF_2CF_3$	CFC-115	$8.0 \pm 3.0 \times 10^{-6}$
$CClF_3$	CFC-13	$2.5 \pm 0.6 \times 10^{-6}$	$CBrF_3$	Halon 1301	$6.9 \pm 0.4 \times 10^{-6}$
CH_3Cl		$3.4 \pm 0.4 \times 10^{-3}$	$CBrClF_2$	Halon 1211	$1.5 \pm 0.1 \times 10^{-5}$
CH_3CCl_3		$1.4 \pm 0.4 \times 10^{-3}$			

Up to the mid-1980s, much of the data gathered was from analyses of whole air samples collected cryogenically, *in situ* from aircraft and balloon flights. The largest body of measurements was obtained by experiments flown on high altitude balloons launched from mid-latitude sites. Although other instrumental techniques had been used to obtain some stratospheric measurements of halocarbons, primarily infrared remote sensing experiments, these were of poorer sensitivity. Vertical profiles of the most readily measured halocarbons (CCl_3F, CCl_2F_2 and CCl_4) had been obtained at a range of latitudes along with other tracers such as N_2O and CH_4 (*e.g.*, Goldan *et al.*, 1980; Vedder *et al.*, 1981). Since 1985, additional data have been reported for different latitudes using balloon-borne cryosamplers, and vertical profiles of some of these halocarbons have been measured by optical remote sensing using a shuttle-borne infrared spectrometer. Of the gases currently regulated by the Montreal Protocol (CFC-11, CFC-12, CFC-113, CFC-114, CFC-115), few measurements of the stratospheric abundance of the latter two (Section 1.3.7) are available. Due to the instability of some of the hydro-halocarbons in whole air samples, and hence the poor measurement accuracy, there is a shortage of reliable stratospheric data on two of the more abundant hydro-halocarbons: CH_3CCl_3 (methyl chloroform) and $CHClF_2$ (HCFC-22). This comment also applies to CCl_4 (carbon tetrachloride), and whenever there is an extensive database, it may be erroneous.

Results from the balloon flight of a cryosampler, in a joint effort of the Max Planck Institut für Aeronomie (MPAE) and the Physical Research Laboratory (PRL), Abmedabad, over Hyderabad, India (17.5°N), in March, 1987 (Borchers *et al.*, 1988) have provided the basis for a set of tropical profiles for many of the key halocarbons. These confirmed qualitatively, as models have predicted, that the volume mixing ratios in the tropical stratosphere decline less quickly with altitude than at mid-latitudes, a result of the increased tropospheric upwelling counteracting the effects of their photochemical removal in the stratosphere. Conversely, measurements made during balloon ascents and aircraft flights through the Arctic winter stratosphere (68°N) with the Institut für Chemie der Kernforschungsanlage (Germany) (KFA) Jülich cryosampler (Schmidt *et al.*, 1989; Schmidt *et al.*, 1991) show a much more rapid decline with altitude in the measured halocarbons and other tracers, compared with either mid-latitude or tropical profiles of the same gases.

The ATMOS experiment was flown on board the space shuttle in April, 1985, as part of the Spacelab 3 payload (Farmer, 1987). It obtained infrared solar absorption spectra through a number of orbital sunrises and sunsets, which have subsequently been analyzed for the vertical profiles of not only the major halogenated source gases (Zander *et al.*, 1987), but also the halogen sink and reservoir species (Raper *et al.*, 1987; Zander *et al.*, 1990). The mean zonal profiles deduced from spectra obtained at sunsets around 30°N provided the most extensive data set, but some profile information was obtained during sunrises around 47°S.

Such data provide important information on the partitioning of chlorine between sources, sinks, and reservoir species, as a function of altitude, and can be used to evaluate photochemical models of the stratosphere more fully. In the upper stratosphere, where most of the organic chlorine-bearing species have been removed, measurements of hydrogen chloride (HCl) and hydrogen fluoride (HF) by experiments such as ATMOS and some of the instruments carried as part of the Upper Atmosphere Research Satellite (UARS). (see Table 1.3.2 for summary of species measurement capability of these remote sensing instruments) provide a measure of the rate of conversion of the halocarbons into inorganic chlorine and the total burden of halogens in the stratosphere. Trends in total column amounts of HCl and HF have been determined from ground-based measurements (*e.g.* WMO, 1989; Rinsland *et al.*, 1991). While the total column amounts of HCl may contain a tropospheric component, tropospheric HF is generally very low and these measurements should be representative of the trend in the stratospheric column. This can be seen, for example, by noting the very good agreement in total HF column trend results measured at Kitt Peak National Solar Observatory, USA (31.9°N, 111.6°W) and the International Scientific Station of the Jungfraüjoch, Switzerland (46.5°N, 8.0°E) (Zander and Rinsland, 1990), and the absence of significant pressure-broadening in HF lines observed in high resolution spectra. Measurement of the concentrations of HCl and HF above 50 km, where all organic halogens have been converted (with the probable exception of tetrafluoromethane [CF_4] and other fully fluorinated species) into the reservoir species, should be equivalent to the total halogen atom concentration contained in halocarbons in the troposphere, with suitable allowance for time taken for vertical transport of these gases. For May 1985, 30°N, the mean total mixing ratio for chlorine was measured to be 2.58±0.10 ppbv throughout the stratosphere, and the mean total mixing ratio of fluorine to be 1.15±0.12 ppbv (Zander *et al.*, 1992), from these ATMOS observations.

Table 1.3.2 *HCl, HF, and halocarbon measurement capabilities of current remote sensing instruments (Farmer, 1987; Reber, 1990).*

Space Shuttle:	
ATMOS	HCl, HF, CCl_3F, CCl_2F_2, CCl_4, CH_3Cl, $CHClF_2$, $ClONO_2$, CF_4
Upper Atmosphere Research Satellite:	
CLAES	HCl, CCl_3F, CCl_2F_2, $ClONO_2$
HALOE	HCl, HF

Inversion of infrared spectroscopic data to retrieve profile information is limited in accuracy by a number of factors, but the principal source of such error in the reported profiles of halocarbons using the ATMOS data continues to be the large uncertainties associated with the molecular spectroscopic parameters (Zander *et al.*, 1992). While laboratory studies have been made to determine the variation of the infrared absorption cross-sections at atmospheric temperatures and pressures (*e.g.*, McDaniel *et al.*, 1991), more laboratory data are required, particularly at a spectral resolution higher than the remote sensing data, to verify and improve the reliability of the current database with respect to halocarbons. Set against this limitation, the principal advantage of remote sensing from satellites is the wide range of latitudes that can be covered. The measurement and calibration problems associated with whole air sampling are dealt with specifically in Section 1.4 with respect to the tropospheric measurements described in Section 1.1. A further discussion of the need for prompt analyses to moderate the effects of sample decay, and other problems associated with balloon-borne sample collection is found in Knapska *et al.* (1985). With respect to these differences introduced by separate calibration standards, the reader wishing to use unpublished data tabulated in Appendix II, is encouraged to contact the source for further information.

It is clear from individual measurements of the vertical distribution of halocarbons that these long-lived gases act as tracers of atmospheric motions. Much of the structure evident in the profiles can almost certainly be attributed to such processes. The sharp decreases of volume mixing ratio with altitude of CCl_3F and CCl_2F_2 make them a sensitive indicator of atmospheric dynamics in the lower stratosphere, as has been demonstrated in the aircraft measurements during the Airborne Antarctic Ozone Experiment (AAOE) by Heidt *et al.* (1989) and Toon *et al.*

(1989). These measurements are not presented as vertical profiles, but have been included in the correlation plots and in determining the relative atmospheric lifetimes of some of these halocarbons, from the tabulations of data provided in those references.

1.3.1 CFC-11 and CFC-12

An extensive data set, spanning many years, exists of stratospheric CFC-11 (CCl_3F) and CFC-12 (CCl_2F_2) measurements. The most recent of these at high northern, mid-, and tropical latitudes are included in Figures 1.3.1, including both whole air sample measurements collected from balloon flights and profiles derived from the ATMOS SL-3 observations. The solid lines in these figures denotes the Middle Atmosphere Program (MAP) profiles taken from Fabian (1989) as a summary of measurements appearing in that source and in the WMO report (World Meteorological Organization, 1986), appropriate to northern mid-latitudes for 1982-1983. They are intended as means of visualizing and assessing differences in measurements from different latitudes, rather than to indicate any secular differences.

As with the profiles of the other CFCs and tracers measured, the high latitude profiles (Figures 1.3.1(b) and 1.3.1(e)) appear to be vertically shifted lower by 3 - 5 km over those measured at mid-latitudes, a result of subsidence caused by diabatic cooling of the Arctic vortex air (Schmidt *et al.*, 1991).

The balloon and satellite data are supplemented in the correlation plots (Figure 1.3.1 (c) and 1.3.1(g)) by whole air sample measurements made from aircraft flights during the AAOE campaigns (Heidt *et al.*, 1989). The results of linear regressions to these data are tabulated in Table 1.3.1.

1.3.2 Carbon tetrachloride

The stratospheric measurements of carbon tetrachloride (CCl_4) at northern mid-latitudes are summarized in Figure 1.3.2(a). The ATMOS/Spacelab-3 (SL-3) profile for CCl_4 at 30°N covers the 10 to 20 km altitude range (Zander *et al.*, 1987; Zander *et al.*, 1992) and is based on retrievals using the broad ν_3 band with an estimated accuracy of 15%. One of the balloon flights in 1985 from southern France was near coincident in time with the ATMOS/SL-3 measurements. The two profiles are in good agreement over the limited altitude range of the ATMOS data, although the balloon data are consistently lower than ATMOS data above 28 km, reflecting known sampling difficulties for the molecule. Figure 1.3.2(b) presents profiles obtained by balloon-borne cryosamplers flown in recent northern winters and at high latitudes (Schmidt *et al.*, 1989; Schmidt *et al.*, 1991).

1.3.3 HCFC-22

A number of problems have been encountered in measuring accurately HCFC-22 ($CHClF_2$) by analysis of whole air samples, primarily stemming from the instability of this gas in the collected samples. Consequently, only a very sparse database is available for this important and abundant man-made hydrogenated chlorofluorocarbon. Fabian *et al.* (1981) noted only preliminary values from their analyses of whole air samples collected *in situ*, as the results were unreproduceable over short periods of time. Fabian *et al.*, (1985) derived stratospheric values and the vertical distribution through improved sample handling techniques. These results showed that $CHClF_2$ decreased from its tropospheric level of around 60 pptv at 10 km to 20 pptv at 30 km, with a precision and accuracy estimated for these values of ≈10%.

Zander *et al.* (1987) analyzed the ATMOS infrared solar absorption spectra obtained from the space shuttle for the vertical distribution of $CHClF_2$. The reported profile is appropriate to mean zonal conditions around 30°N during April/May 1985. These measurements were used in conjunction with infrared measurements made during balloon flights over New Mexico by Rinsland *et al.* (1990) to deduce a rate of increase of $CHClF_2$ in the lower stratosphere of 9.4± 1.3 % $year^{-1}$, for the period March 1981 to June 1988.

1.3.4 Methyl chloride

Vertical profiles have been obtained for methyl chloride (CH_3Cl), the most abundant naturally occurring halocarbon, at northern mid-latitudes where it has been measured by balloon-borne cryosamplers and by ATMOS/SL-3 from space. The profile derived from infrared solar absorption spectra shows systematically larger values by more than

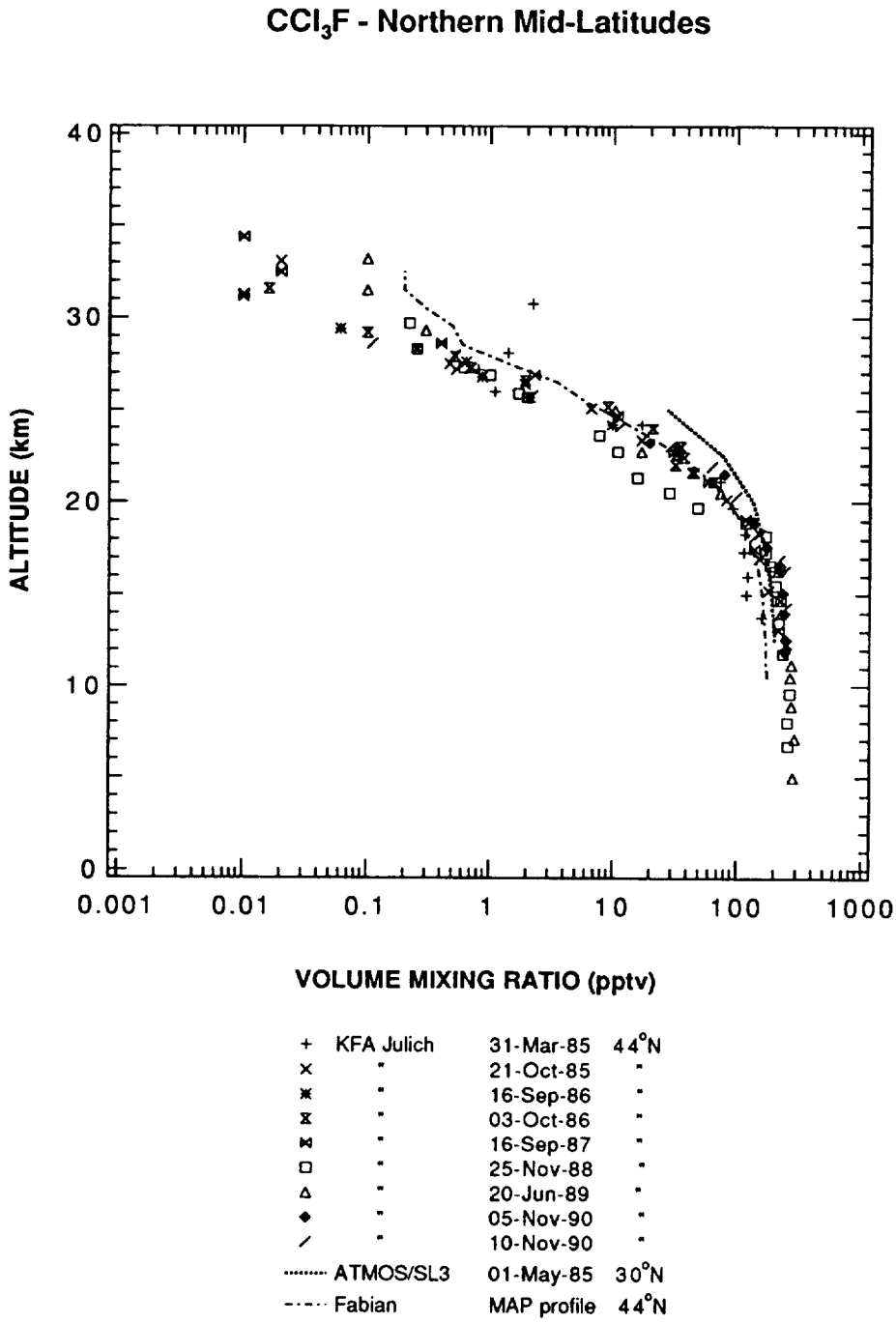

Figure 1.3.1(a) Measurements of the vertical distribution of CFC-11 (CCl_3F) at northern mid-latitudes since 1985. The KFA Jülich data (Schmidt *et al.*,1986, 1989, 1991) are from balloon-borne cryosample measurements, and are summarized in Appendix II, as are the ATMOS SL-3 data (Zander *et al.*, 1987). The MAP reference profile (Fabian,1989) is included as a guide for comparison with Figure 1.3.1(b).

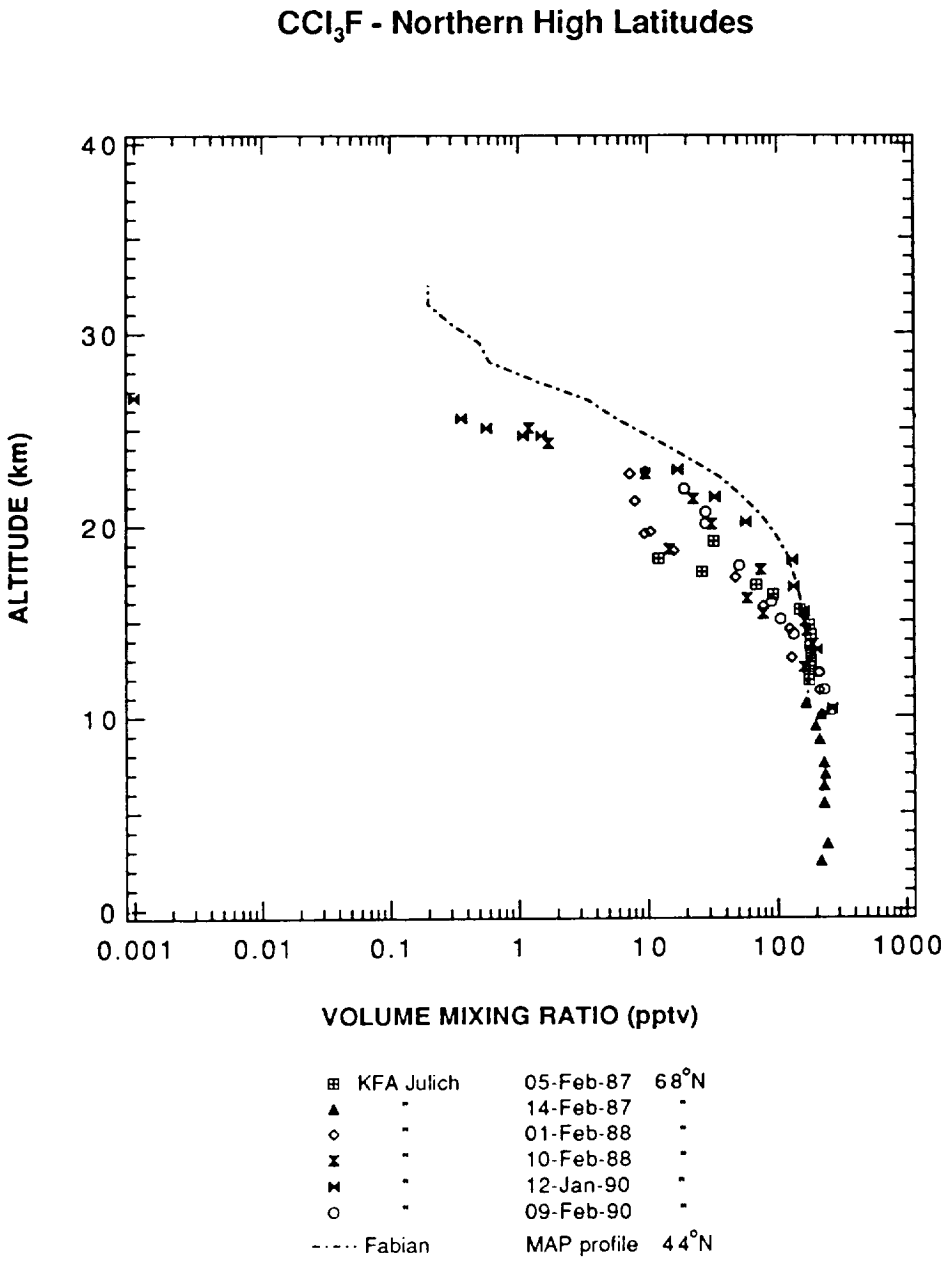

Figure 1.3.1(b) Balloon-borne cryosampler measurements of the vertical distribution of CFC-11 (CCl_3F) near Kiruna, Sweden at 68°N during winter months. The KFA Jülich data (Schmidt *et al.*,1989; 1991) are summarized in Appendix II. The MAP reference profile (Fabian, 1989) is included as a guide for comparison with Figure 1.3.1(a).

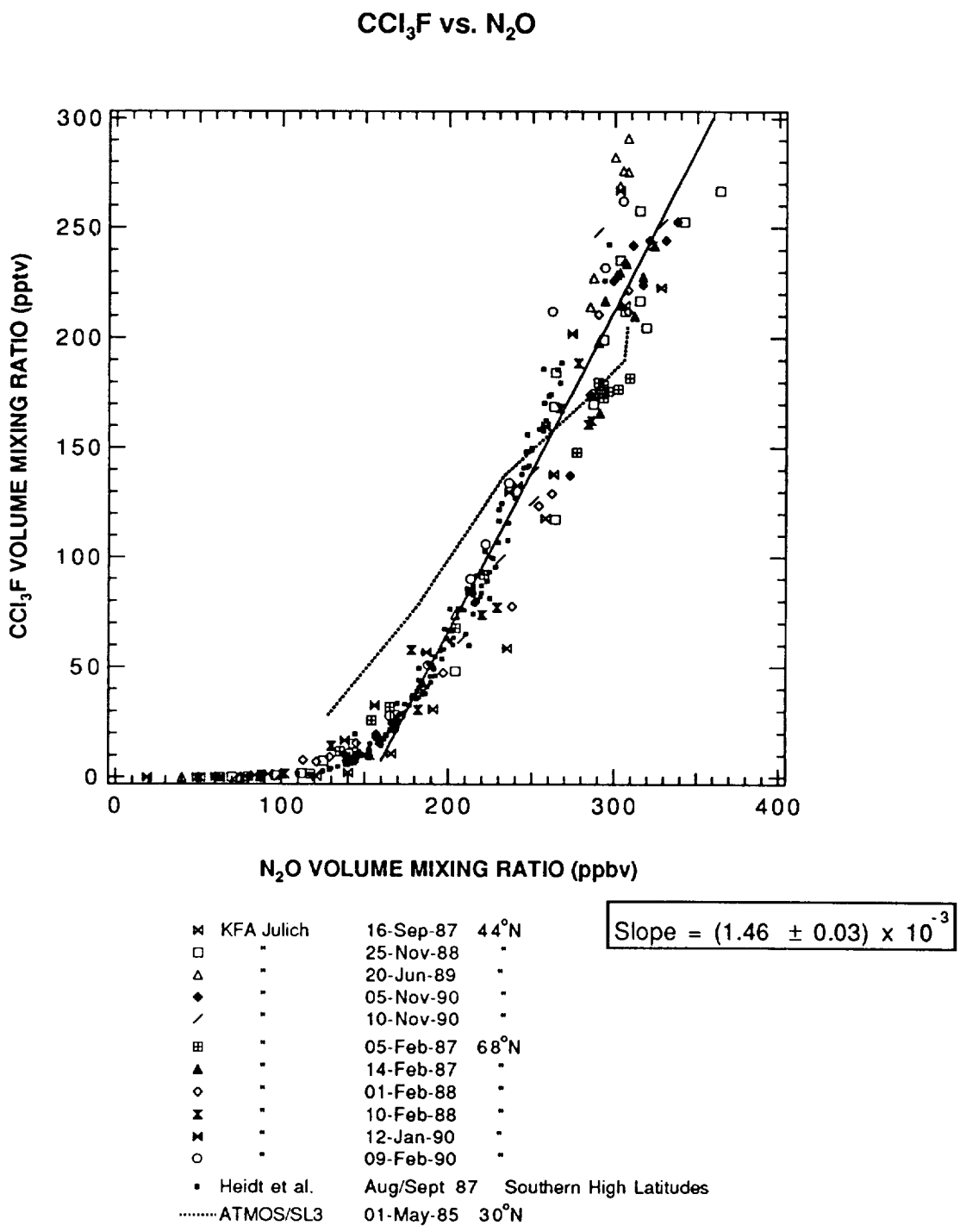

Figure 1.3.1(c) Correlation plot based on the simultaneous measurements of N_2O and CFC-11 (CCl_3F). In addition to balloon and shuttle measurements shown in Figures 1.3.1(a) and (b), aircraft *in situ* data reported by Heidt *et al.* (1989) are included. These data were collected over a range of southern mid- to high latitudes in August and September, 1987, during the AAOE campaigns. The solid line represents a linear fit to the data (excluding that of ATMOS) over the indicated region, with a slope of $(1.46 \pm 0.03) \times 10^{-3}$ part CCl_3F/part N_2O. A summary of the fits in this and other correlation plots is in Table 1.3.1.

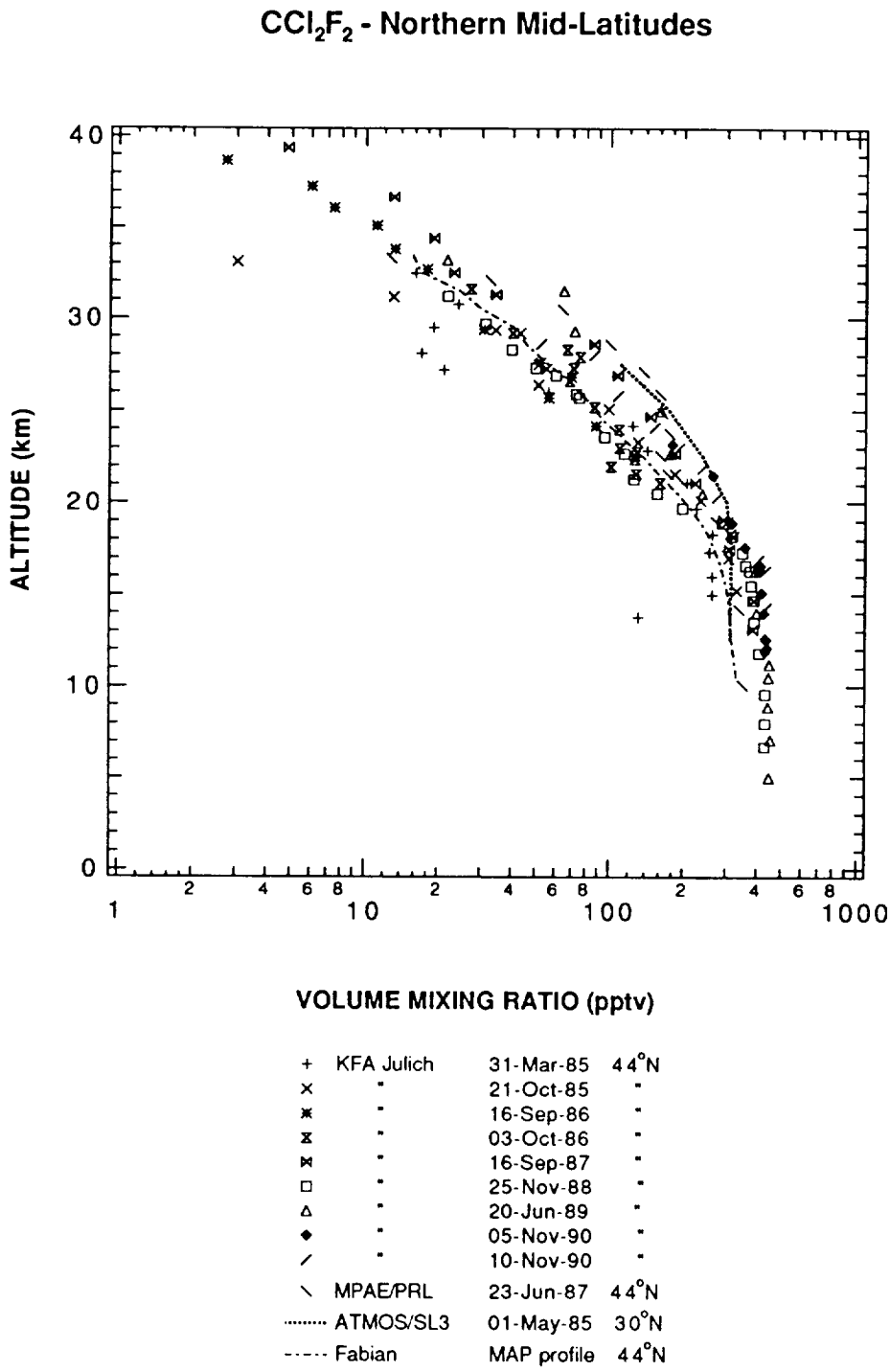

Figure 1.3.1(d) Measurements of the vertical distribution of CFC-12 (CCl_2F_2) at northern mid-latitudes since 1985. The MPAE/PRL data are from balloon-borne cryosampled measurements (Borchers *et al.*, 1988). The KFA Jülich data (Schmidt *et al.*, 1989, 1991) are from balloon-borne cryosample measurements and are summarized in Appendix II. The shuttle-based ATMOS/SL-3 measurements (Zander *et al.*, 1987) are also summarized in Appendix II The MAP reference profile (Fabian, 1989) is included as a guide for comparison with both Figures 1.3.1(e) and (f).

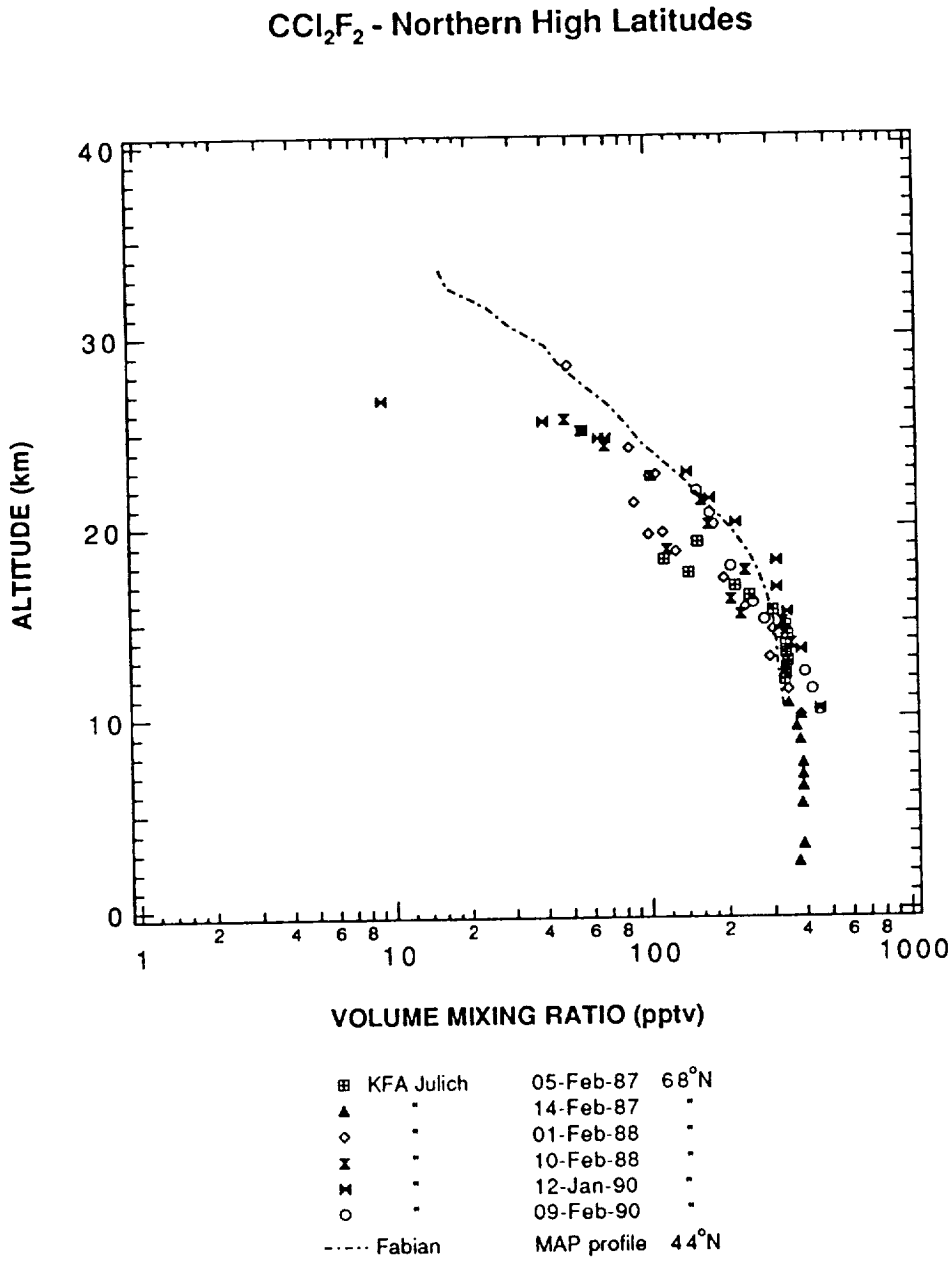

Figure 1.3.1(e) Balloon-borne cryosampler measurements of the vertical distribution of CFC-12 (CCl_2F_2) near Kiruna, Sweden at 68°N during late winter months since 1987. The data points labelled as KFA Jülich (Schmidt *et al.*, 1989, 1991) are summarized in Appendix II. The MAP reference profile (Fabian, 1989) is included as a guide for comparison with Figures 1.3.1(d) and (f)..

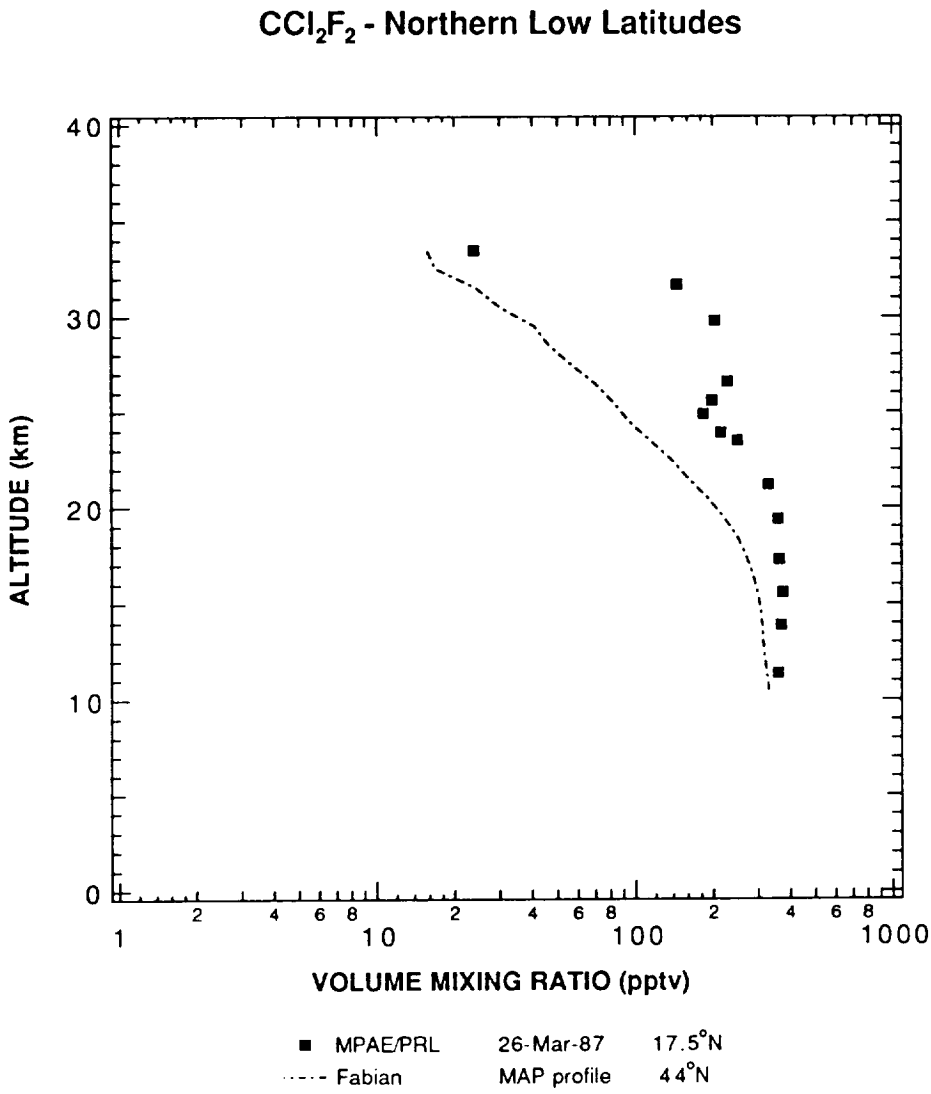

Figure 1.3.1(f) Balloon-borne cryosampler measurements of CFC-12 (CCl_2F_2) from a balloon flight over Hyderabad, India at 17.5°N (Borchers *et al.*, 1988). The MAP reference profile (Fabian, 1989) is included as a guide for comparison with Figures 1.3.1(d) and (e).

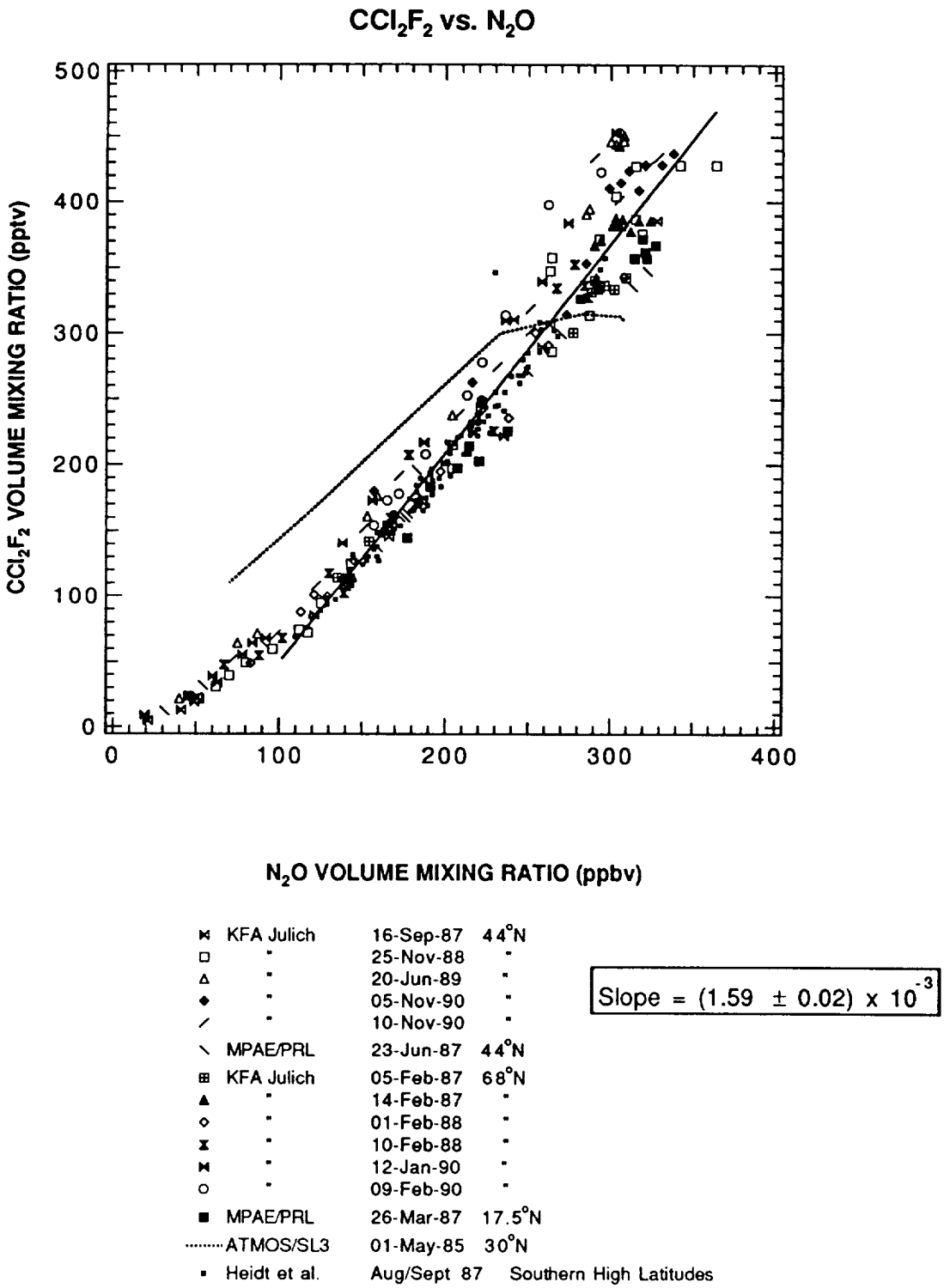

Figure 1.3.1(g) Correlation plot based on simultaneous measurements of N_2O and CFC-12 (CCl_2F_2). In addition to balloon and satellite measurements shown in Figures 1.3.1(d), (e) and (f), aircraft *in situ* data from southern mid- to high latitudes reported by Height *et al.*, (1989) are included The Height *et al.* data were collected in August and September, 1987, during the AAOE campaigns. The solid line is a linear fit to the data (excluding those of ATMOS SL-3) over the indicated region, and has a slope of (1.59 ± 0.02) $x10^{-3}$ part CCl_2F_2/part N_2O (1σ error). A summary of the fits in this and other correlation plots is in Table 1.3.1.

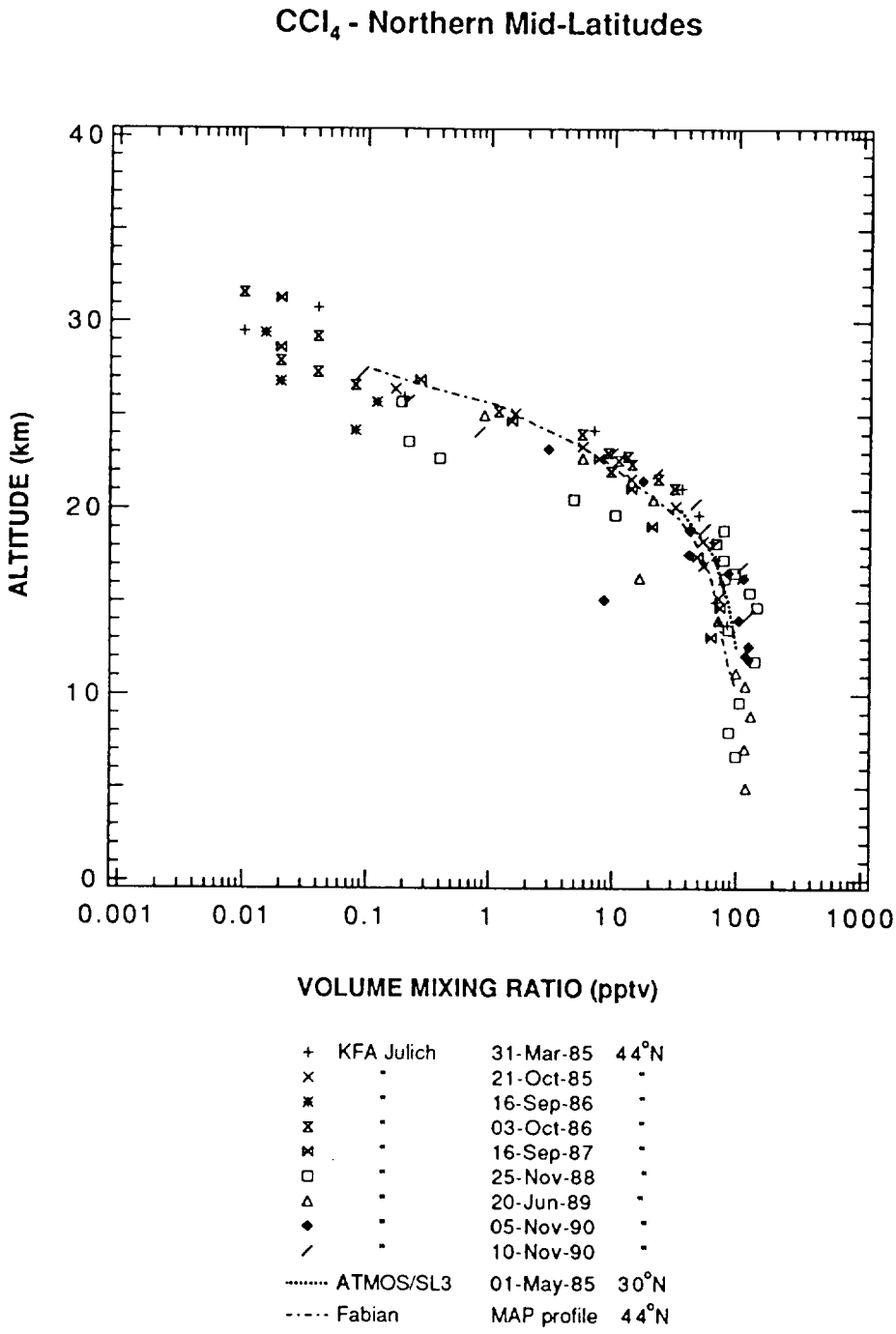

Figure 1.3.2(a) Measurements of the vertical distribution of carbon tetrachloride (CCl_4) at northern mid-latitudes since 1985. The data points labelled as KFA Jülich (Schmidt *et al.*,1986; 1991) are summarized in Appendix II. The MAP reference profile (Fabian, 1989) is included as a guide for comparison with Figure 1.3.2(b).

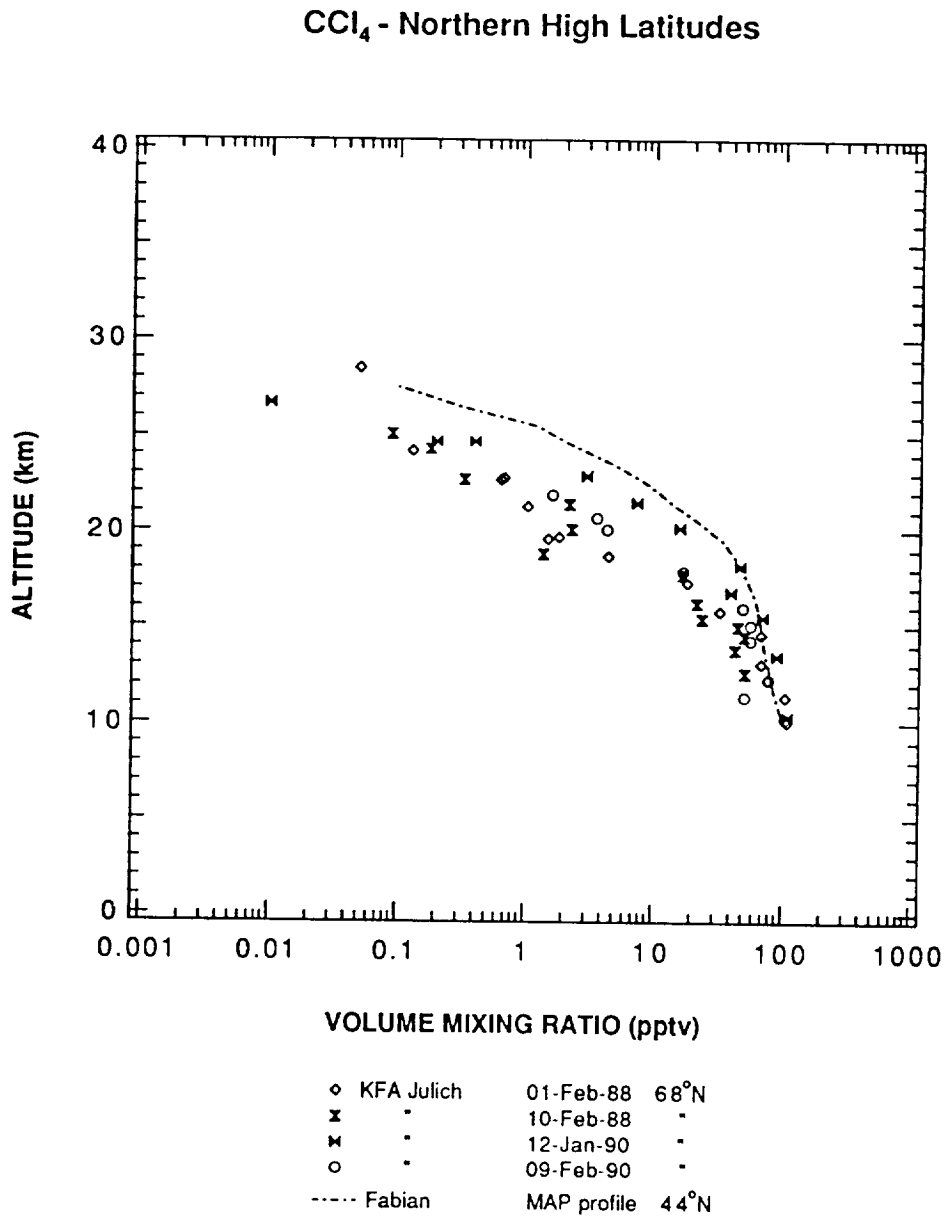

Figure 1.3.2(b) Balloon-borne cryosample measurements of the vertical distribution of carbon tetrachloride (CCl_4) near Kiruna, Sweden at 68°N during winter months since 1987. The data points labelled as KFA Jülich (Schmidt *et al.*, 1989; 1991) are summarized in Appendix II. The MAP reference profile (Fabian, 1989) is included as a guide for comparison with Figure 1.3.2(a).

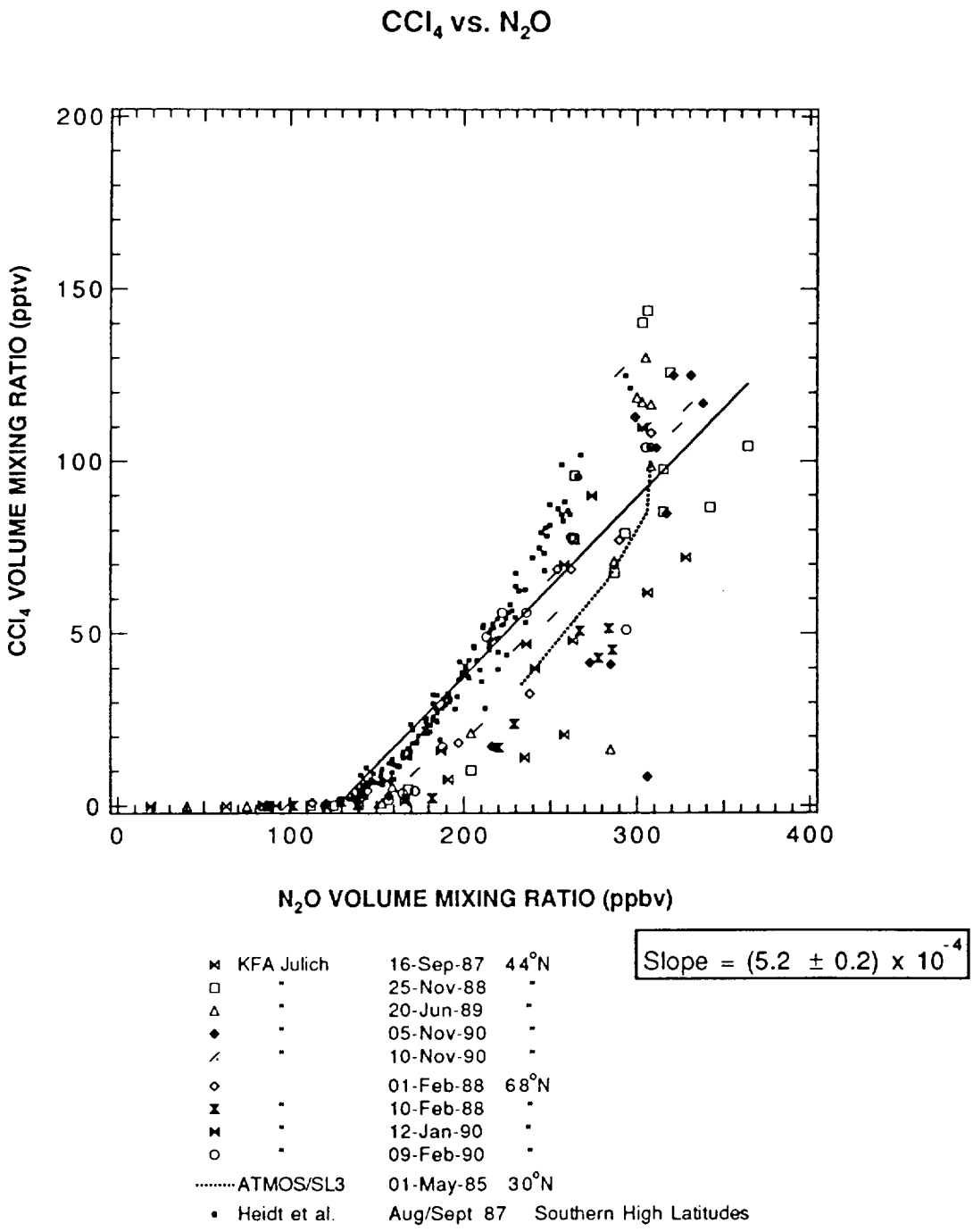

Figure 1.3.2(c) Correlation plot based on the simultaneous measurements of N_2O and carbon tetrachloride (CCl_4). In addition to data shown in Figures 1.3.2(a) and (b), aircraft *in situ* data reported by Heidt *et al.* (1989) from southern mid- to high latitudes are included. Noting that the CCl_4 data are highly dispersed when plotted against N_2O, the linear fit was made only for the Height *et al.* results, as these data are the most consistent. The slope of the line is $(5.2 \pm 0.2) \times 10^{-4}$ part CCl_4/part N_2O. A summary of the fits in this and other correlation plots is in Table 1.3.1. .

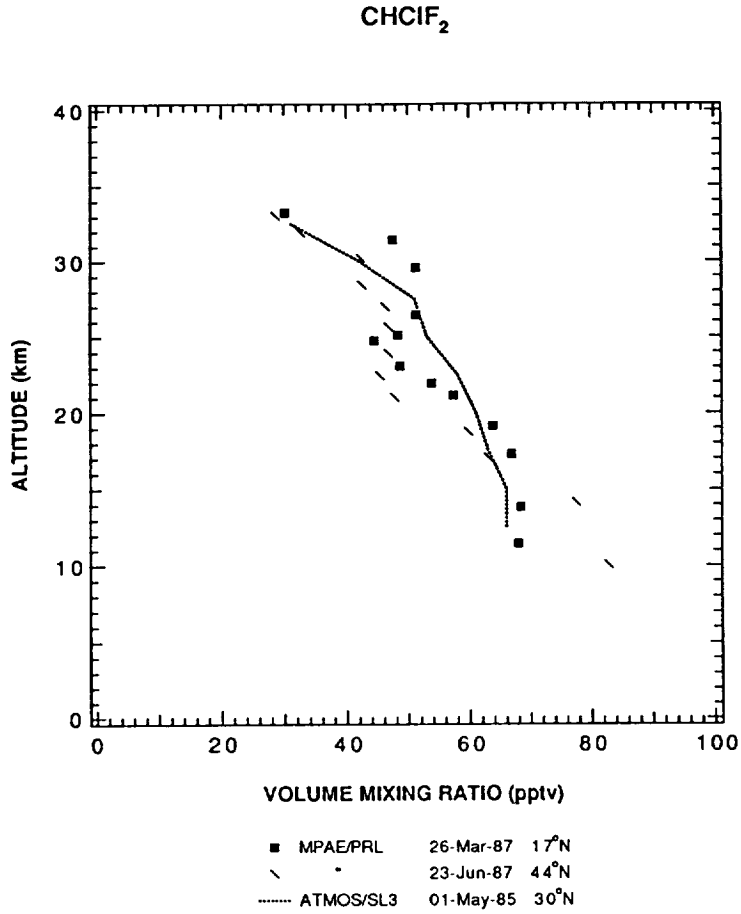

Figure 1.3.3 Measurements of the vertical distribution of HCFC-22 ($CHClF_2$). Data labelled as MPAE/PRL are from balloon-borne cryosample measurements of Fabian *et al.* (1989). The ATMOS SL-3 data (Zander *et al.*, 1987) has been scaled to reflect updated spectroscopic parameters (see Zander *et al.*, 1992). ATMOS SL-3 data is summarized in Appendix II.

25%, although this may well be a problem of calibration for either or both measurement techniques. The apparent large variability in the methyl chloride profiles derived from cryosamplers has been discussed by Schmidt *et al.* (1985) and attributed to sample instability and experimental uncertainty. This is supported by the poor correlation between methyl chloride and stable tracers such as N_2O, measured from the same samples (Figure 1.3.4(c)).

1.3.5 Methyl chloroform

Mid-latitude data (Schmidt *et al.*, 1986) are supplemented by reported values for higher northern latitudes (Schmidt *et al.*, 1991) and measurements over France and India (Borchers *et al.*, 1988). The KFA Jülich measurements were calibrated against the OGIST standard, and the conversion factors for this gas relative to other measurement standards are discussed in Section 1.2.2.2. The scatter in the correlation plot is indicative of the large measurement uncertainty, resulting mainly from methyl chloroform (CH_3CCl_3) instability in the collected samples. The outlying points evident in the correlation plot (Figure 1.3.5(d)) originate from the single set of data obtained during a balloon flight from Hyderabad, India (Borchers *et al.*, 1988), shown in Figure 1.3.5(c).

1.3.6 CFC-113

The more recent measurements of CFC-113 (CCl_2FCClF_2) at northern mid-latitudes are summarized in Figure 1.3.6(a). There is a clear difference between the bulk of the KFA Jülich data and the MAP mean profile. Although this mean profile represents earlier measurements from 1982-1984 (Fabian *et al.*, 1989; Borchers *et al.*, 1987), the difference should not be construed as a secular increase in CFC-113, but as the result of differences in calibration

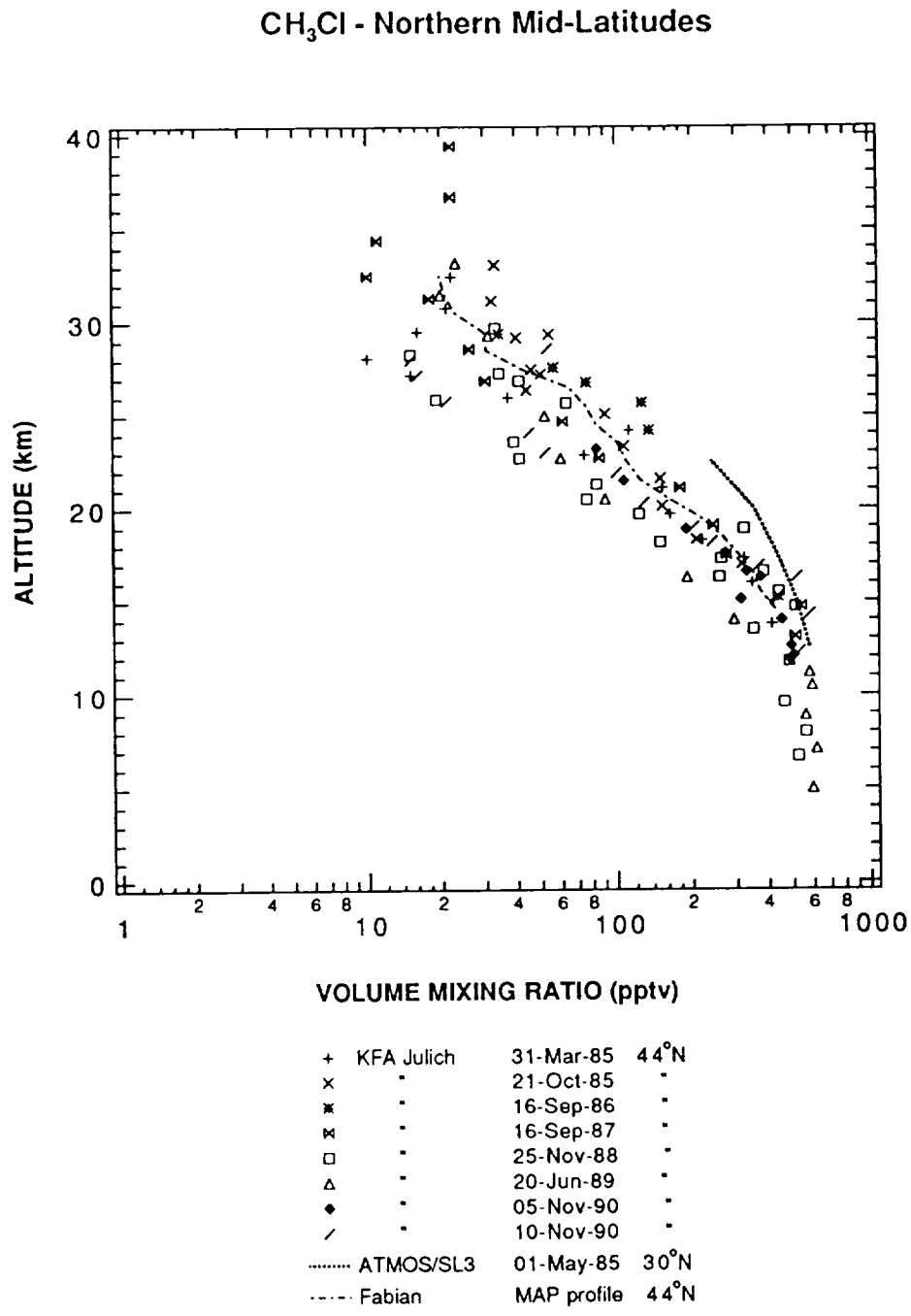

Figure 1.3.4(a) Measurements of the vertical distribution of methyl chloride (CH_3Cl) at northern mid-latitudes since 1985. The KFA Jülich data are from balloon-borne cryosample measurements (Schmidt *et al.*, 1986, 1991). The KFA Jülich data and the shuttle based measurements of ATMOS SL-3 (Zander *et al.*, 1987) are summarized in Appendix II. The MAP reference profile (Fabian *et al.*, 1989) is included as a guide for comparison with Figure 1.3.4(b).

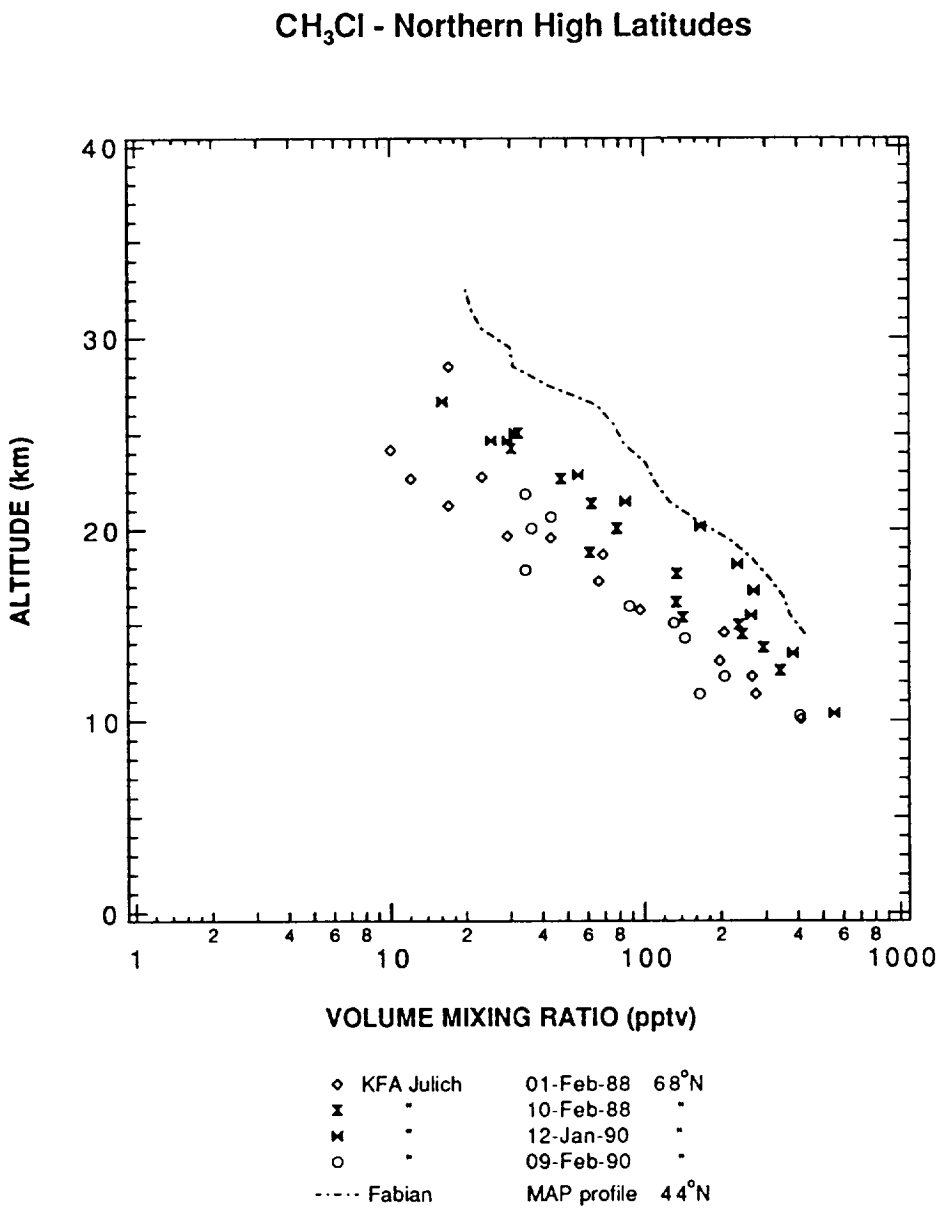

Figure 1.3.4(b) Balloon-borne cryosampled measurements of the vertical distribution of methyl chloride (CH_3Cl) near Kiruna, Sweden 68°N The KFA Jülich data are from Schmidt *et al.*,(1989; 1991) and are summarized in Appendix II. The MAP reference profile (Fabian *et al.*, 1989) is included as a guide for comparison with Figure 1.3.4(b).

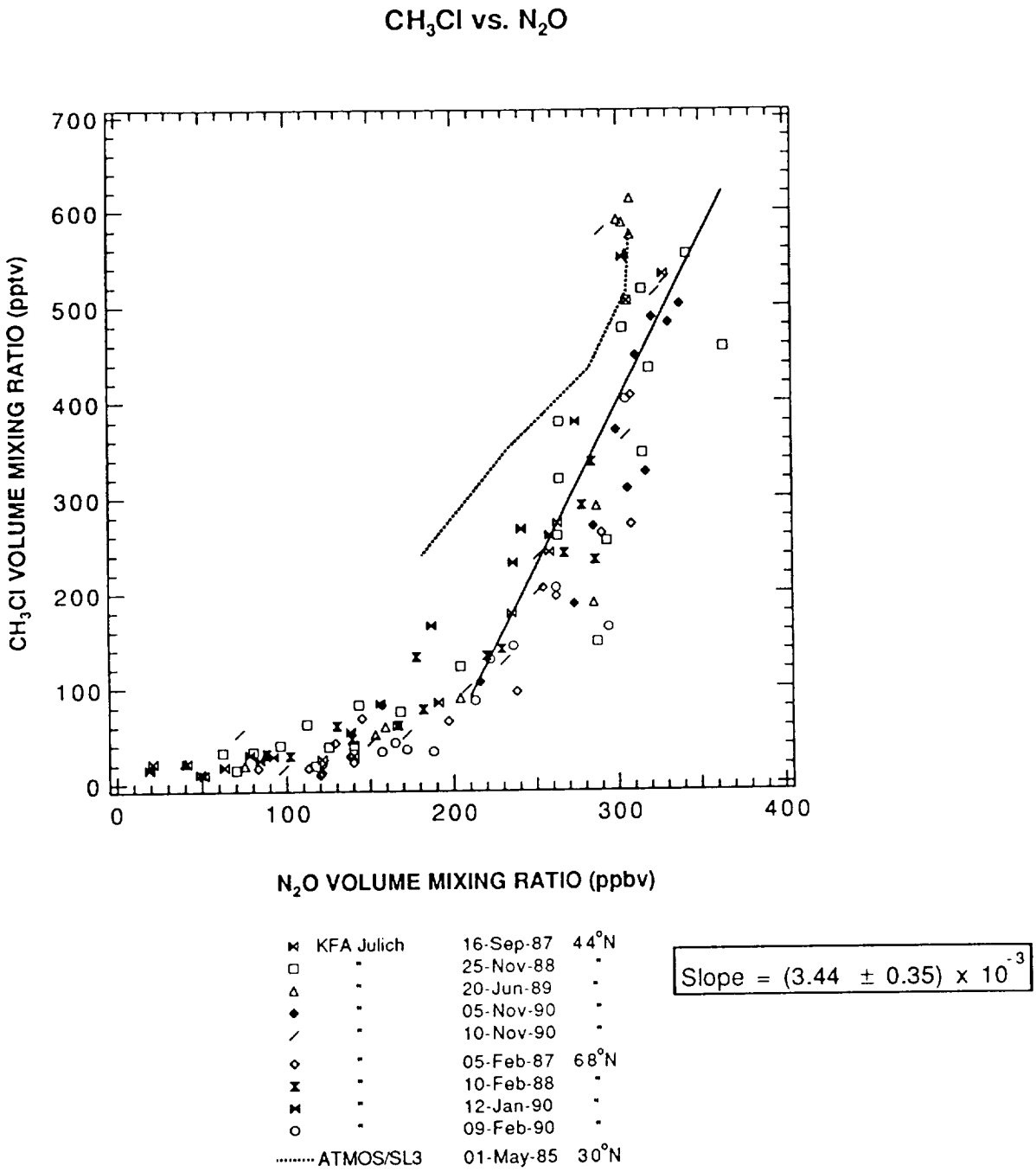

Figure 1.3.4(c) Correlation plot based on simultaneous measurement of N_2O and methyl chloride (CH_3Cl). Balloon and shuttle measurements from Figures 1.3.4(a) and (b) are included. The solid line is a linear fit to the data (excluding ATMOS) over the indicated region, and has a slope of (3.44 ± 0.35) x 10^{-3} part CH_3Cl/part N_2O (1σ error). A summary of the fits in this and other correlation plots is in Table 1.3.1.

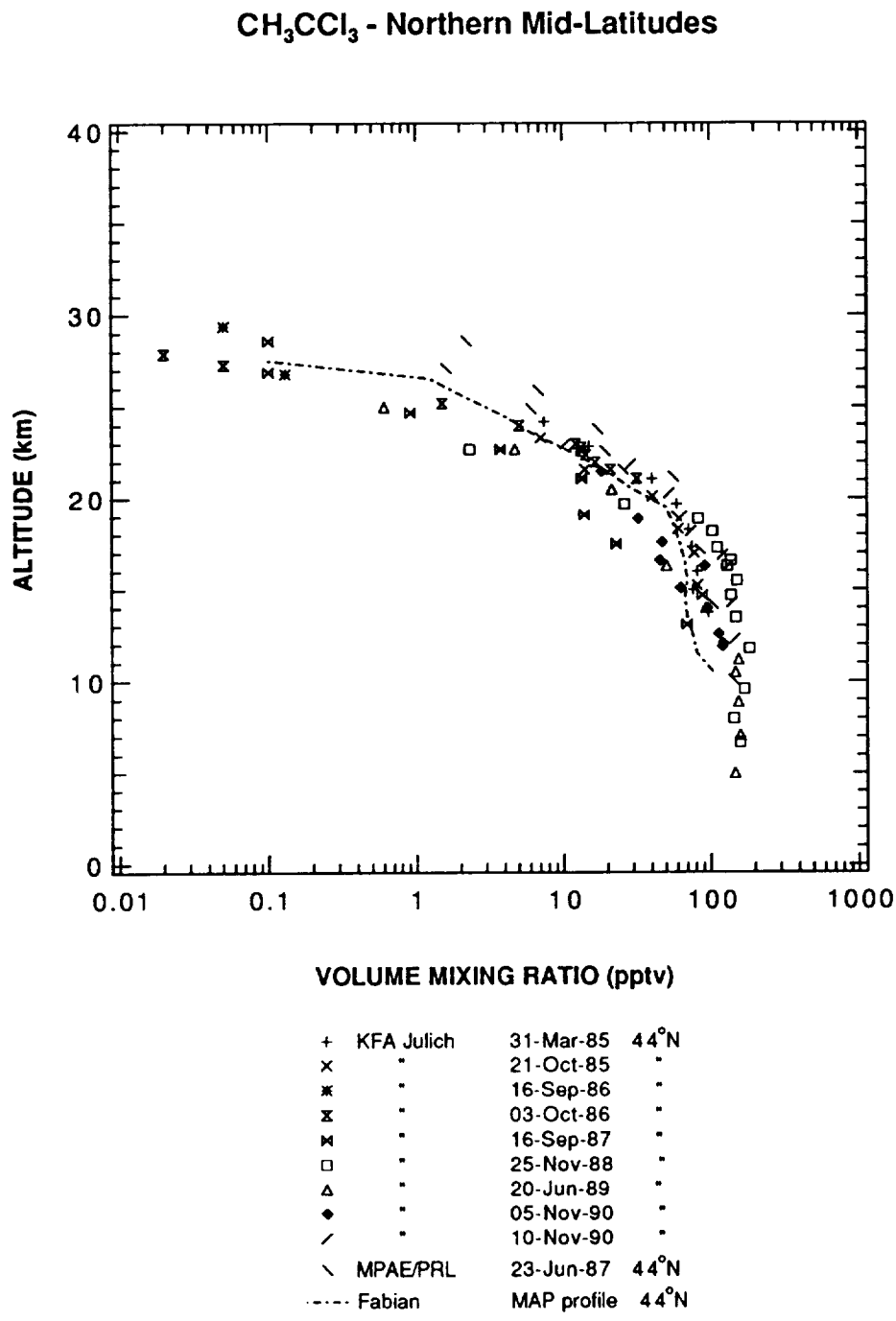

Figure 1.3.5(a) Measurements of the vertical distribution of methyl chloroform (CH_3CCl_3) at 44°N. The KFA Jülich data are cryosample measurements from Scmidt *et al.* (1986, 1991) are summarized in Appendix II. The MPAE/PRL data are from cryosample measurements of Borchers *et al.* (1989). The MAP reference profiles (Fabian, 1989) is included as a guide for comparison with Figures 1.3.5(b) and (c).

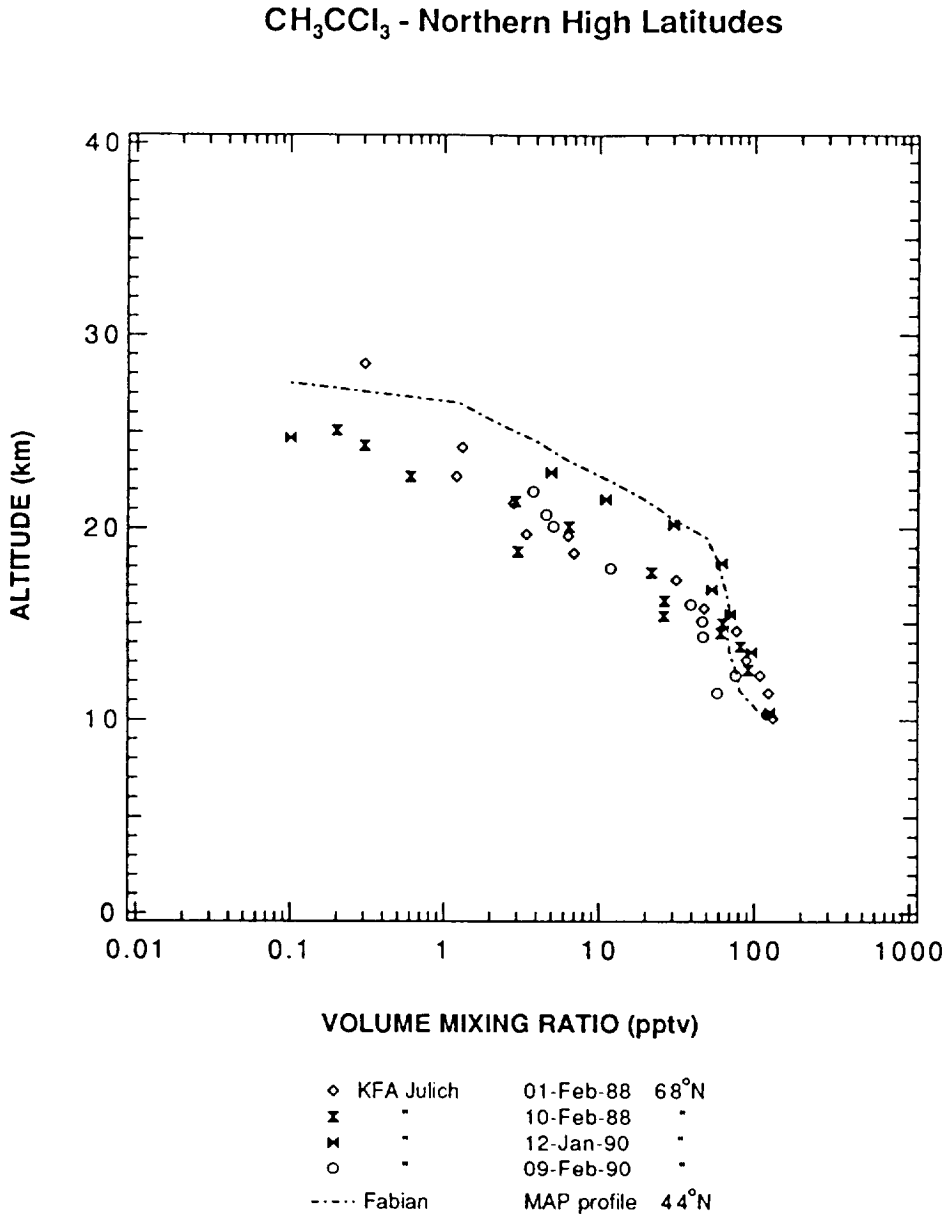

Figure 1.3.5(b) Balloon-borne cryosampled measurements of the vertical distribution of methyl chloroform (CH_3CCl_3) near Kiruna, Sweden at 68°N during winter months. The data from KFA Jülich are from Schmidt *et al.* (1989, 1991) and is summarized in Appendix II. The MAP reference profile (Fabian *et al.*, 1989) is included as a guide for comparison with Figures 1.3.5(a) and (c).

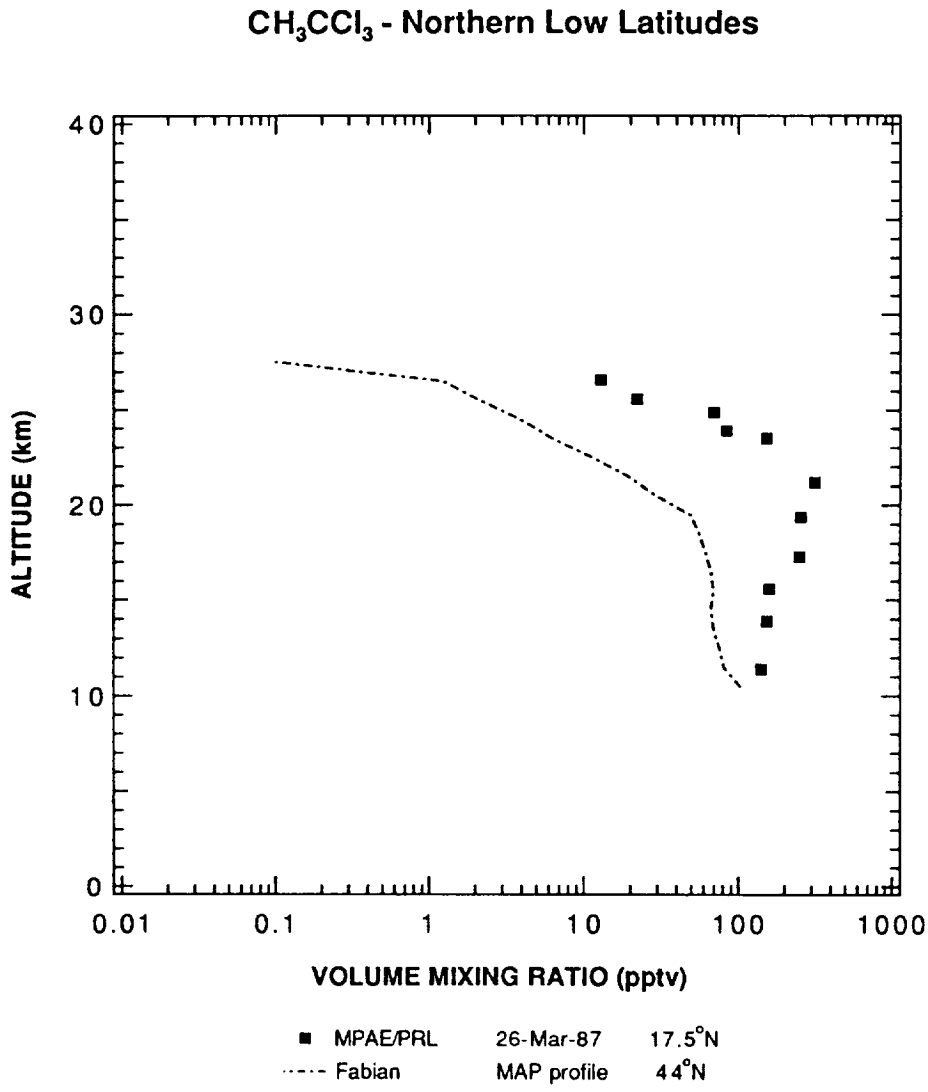

Figure 1.3.5(c) Balloon-borne cryosample measurements of the vertical distribution of methyl chloroform (CH_3CCl_3) over Hyderabad, India at 17.5°N (Borchers *et al.*, 1989). The MAP reference profile (Fabian, 1989) is included for comparison with Figures 1.3.5(a) and (b).

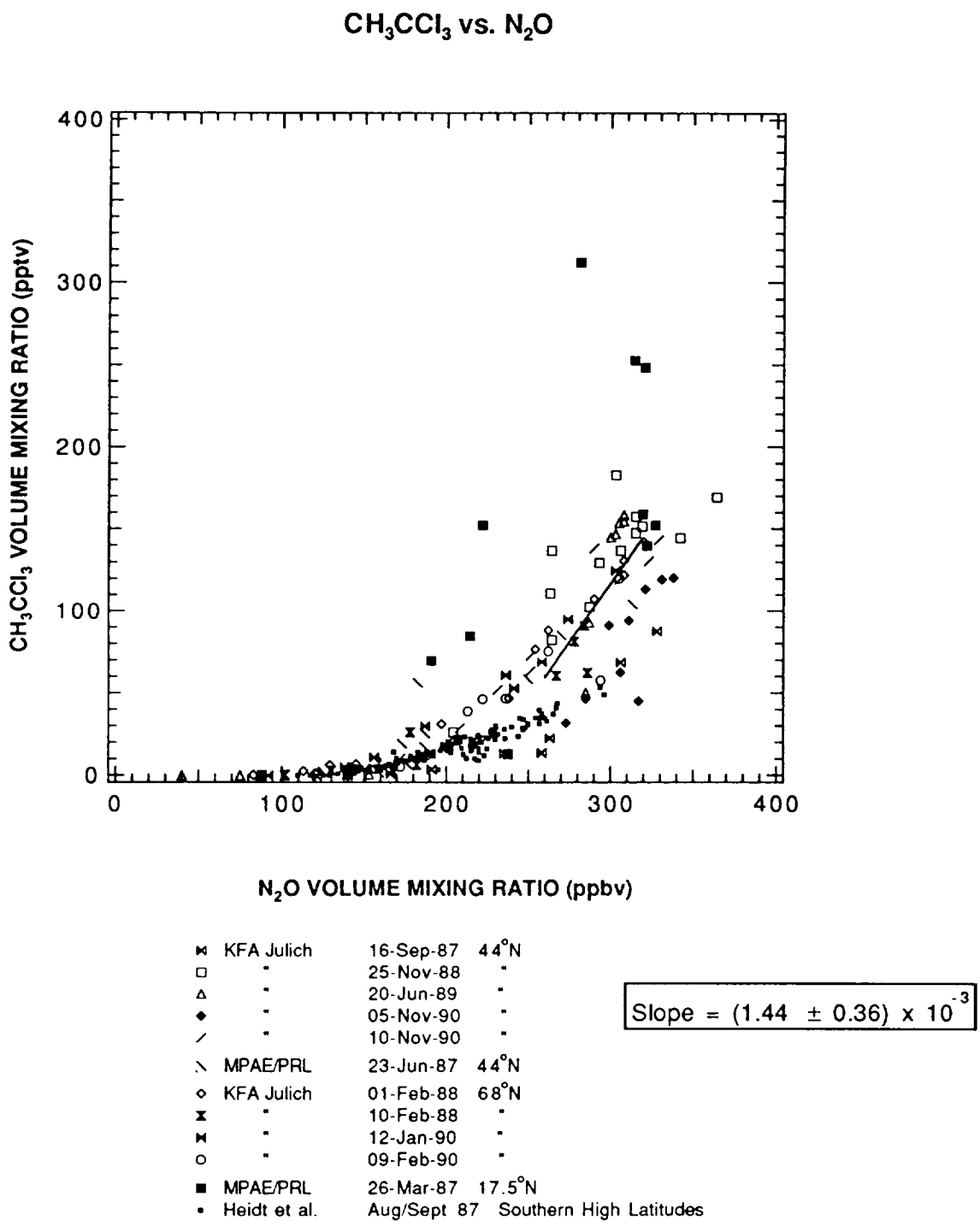

Figure 1.3.5(d) Correlation plot based on simultaneous measurements of N_2O and methyl chloroform (CH_3CCl_3). In addition to the data shown in Figures 1.3.5(a), (b) and (c), aircraft *in situ* data from southern mid- to high latitudes reported by Heidt *et al.* (1989) are included. The Heidt *et al.* data were collected in August and September, 1987 during the Airborne Arctic Ozone Experiment (AAOE) campaigns. The solid line is a linear fit to the data (excluding those of ATMOS and MPAE/PRL for 26-Mar-87) over the indicated region, and has a slope of $(1.44 \pm 0.36) \times 10^{-3}$. A summary of the fits in this and other correlation plots is in Table 1.3.1.

standards and analysis procedures. The KFA Jülich analyses were made against the OGIST standard (see Section 1.2.1.2 for a discussion on the relationship with other scales).

The high northern latitude measurements (Figure 1.3.6(b)) include data from samples collected during aircraft flights through a range of altitudes in the free troposphere. These indicate a mean value of 41 pptv which, when scaled by the 1.42 (appropriate to GAGE/OGIST scaling from Section 1.2.1.2), compares favorably with GAGE tropospheric measurements for 1987. The northern low latitude profile (Figure 1.3.6(c)) is generally consistent with the MAP mean profile; the new data and the MAP mean profile were obtained from analyses by the same group.

1.3.7 CFC-114, CFC-115 and CFC-116 (Hexafluoroethane)

These fully halogenated C_2-gases have not been measured extensively in the stratosphere. The main data source are measurements by the MPAE group of whole air samples collected during balloon flights over southern France (44°N) (Fabian *et al.*, 1981; Fabian *et al.*, 1987; Fabian 1989) and some additional data gathered during balloon flights from Hyderabad, India, (17.5°N) into the tropical stratosphere (Borchers *et al.*, 1988). These gases are increasingly more stable and long-lived in the stratosphere in proportion to the number of fluorine atoms they contain, with only relatively small differences in their measured tropospheric and stratospheric volume mixing ratios.

Fabian *et al.* (1987) re-evaluated the earliest reported profiles of CF_3CF_3 (Fabian *et al.*, 1981), suggesting they were too high by a factor of 2.4, to bring them in line with the later analyses using gas chromatography-mass spectrometry (GC-MS) techniques. These results show an upper tropospheric mixing ratio of around 2 pptv with a falloff to about 1 pptv above 30 km in the mid-latitude stratosphere (Figure 1.3.7(e)), This profile is almost certainly due to the time lag involved in tropospheric-stratospheric exchange and in air reaching altitudes of 30 km. It is not likely to be due to chemical removal since CF_3CF_3 is probably inert in the stratosphere.

1.3.8 CFC-13

Few measurements are available of CFC-13 ($CClF_3$), as was noted in WMO (1986). The MAP profile for CFC-13 was based on measurements from a single balloon ascent from southern France in September 1980 (Fabian *et al.*, 1981). The data collected later by the same group (Borchers *et al.*, 1988), while self-consistent, is as much as 50% lower than the MAP profile (Figure 1.3.8(a)). The later measurements show little difference between tropical and northern mid-latitude values, with a near constant mixing ratio of ≈2 pptv at all heights.

1.3.9 Carbon tetrafluoride

The ATMOS/Spacelab 3 measurements of CF_4 (tetrafluoromethane) (Zander *et al.*, 1987) at 30°N suggest that CF_4 has a constant volume mixing ratio up to a height of ~50 km, commensurate with its extremely long lifetime in the stratosphere. Being an inert tracer, CF_4 vertical profiles show the same features as those of CO_2 (carbon dioxide), that is, no gradient is observed above pressure levels of 50 hPa at mid-latitudes (Schmidt and Khedim, 1991). These measurements made at northern mid-latitudes are presented in Figure 1.3.9(a), together with other balloon-borne cryosampler measurements reported by Fabian *et al.*, (1987). The *in situ* values obtained between 1983 - 1985 are ≈10% larger than the profile obtained by infrared spectroscopy, but such differences are well within the uncertainties of both measurements.

1.3.10 Methyl bromide, Halon-1301 and Halon-1211

Very few measurements have been made of stratospheric brominated source gases as they are generally present at levels close to the limits of detection, declining rapidly with altitude from a few pptv in the troposphere (see earlier portions of this chapter). The main source of data are from the analyses by the MPAE group of whole air samples collected on a number of balloon flights made over southern France.

For CH_3Br, the most abundant naturally occurring brominated halocarbon, Fabian *et al.* (1981) report a value of 1.2 pptv measured at 14.4 km but that by 20 km it fell below their detection limit. No other reported measurements are available, although unpublished data from analysis of samples collected during balloon flights from France (S.

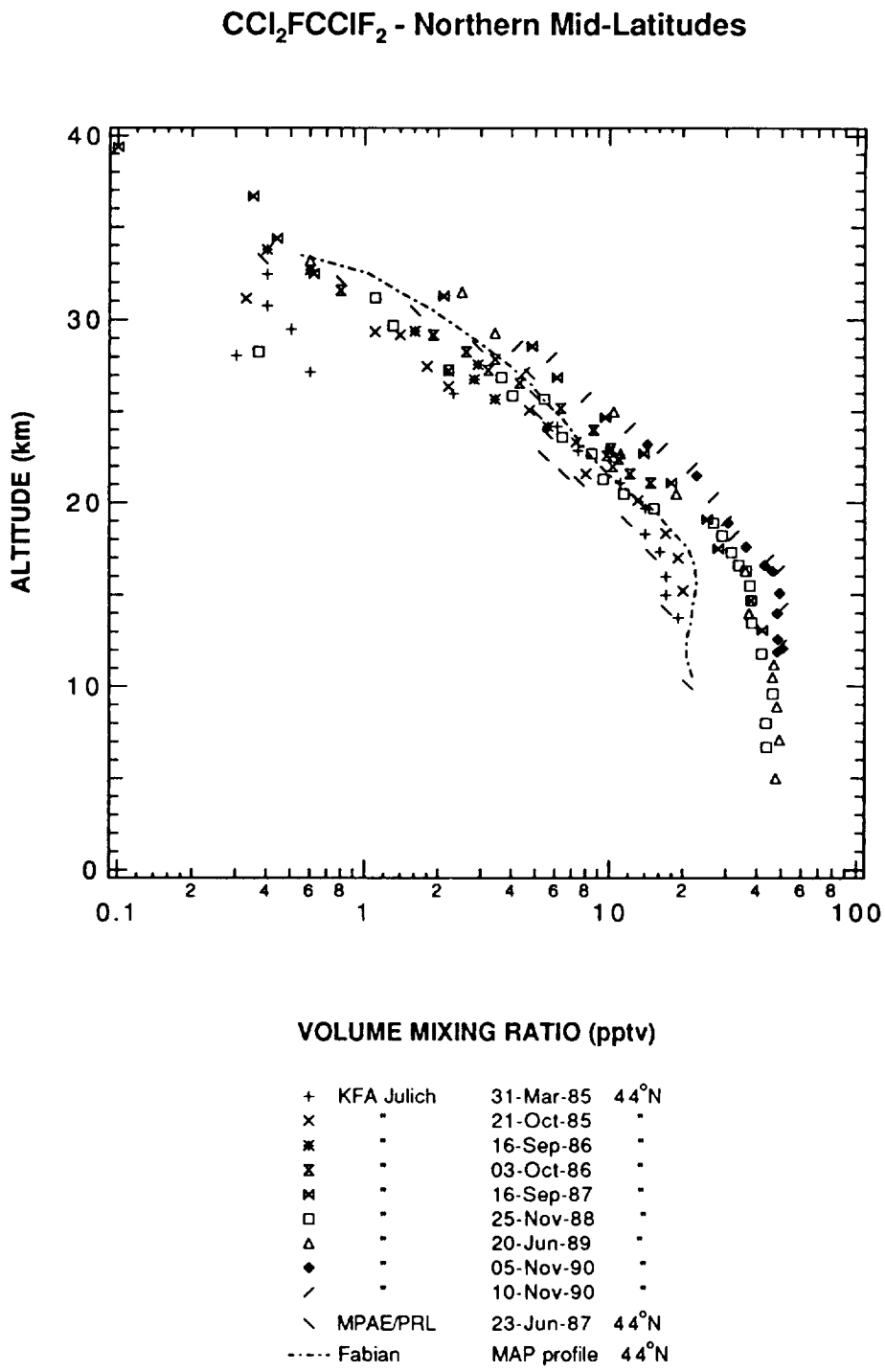

Figure 1.3.6(a) Measurements of the vertical distribution of CFC-113 (CCl_2FCClF_2) at 44°N. The data marked KFA Jülich are cryosample measurements from Schmidt *et al.*, (1986, 1991) and are summarized in Appendix II. The data marked MPAE/PRL are from cryosample measurements of Borchers *et al.* (1989). The MAP reference profile (Fabian, 1989) is included as a guide for comparison with Figures 1.3.6(b) and (c).

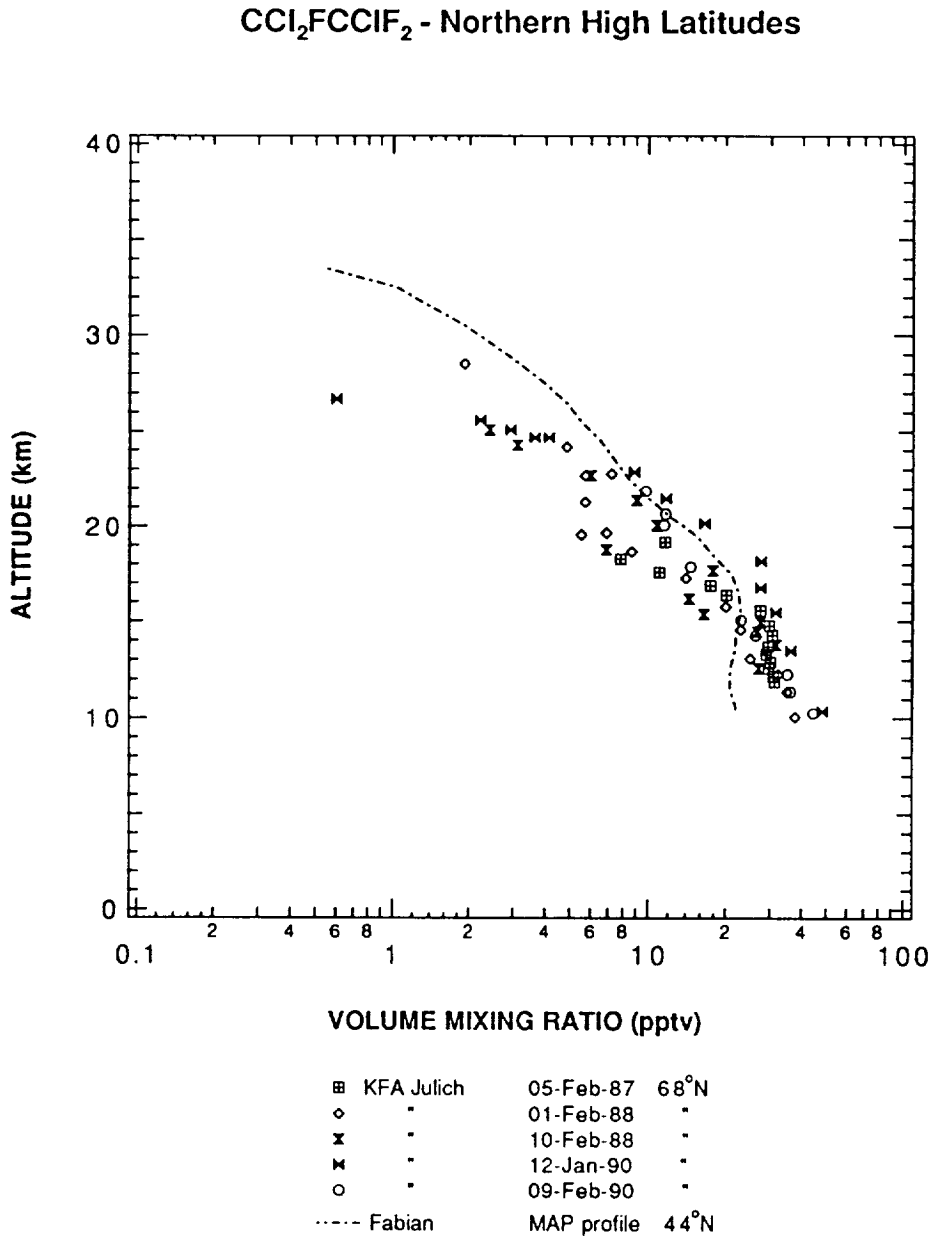

Figure 1.3.6(b) Measurements of the vertical distribution of CFC-113 (CCl_2FCClF_2) at 68°N by balloon-borne cryosampling. The data from KFA Jülich is from Schmidt *et al.* (1989) and is summarized in Appendix II. The MAP reference profile (Fabian, 1989) is included as a guide for comparison with Figures 1.3.6(a) and (c).

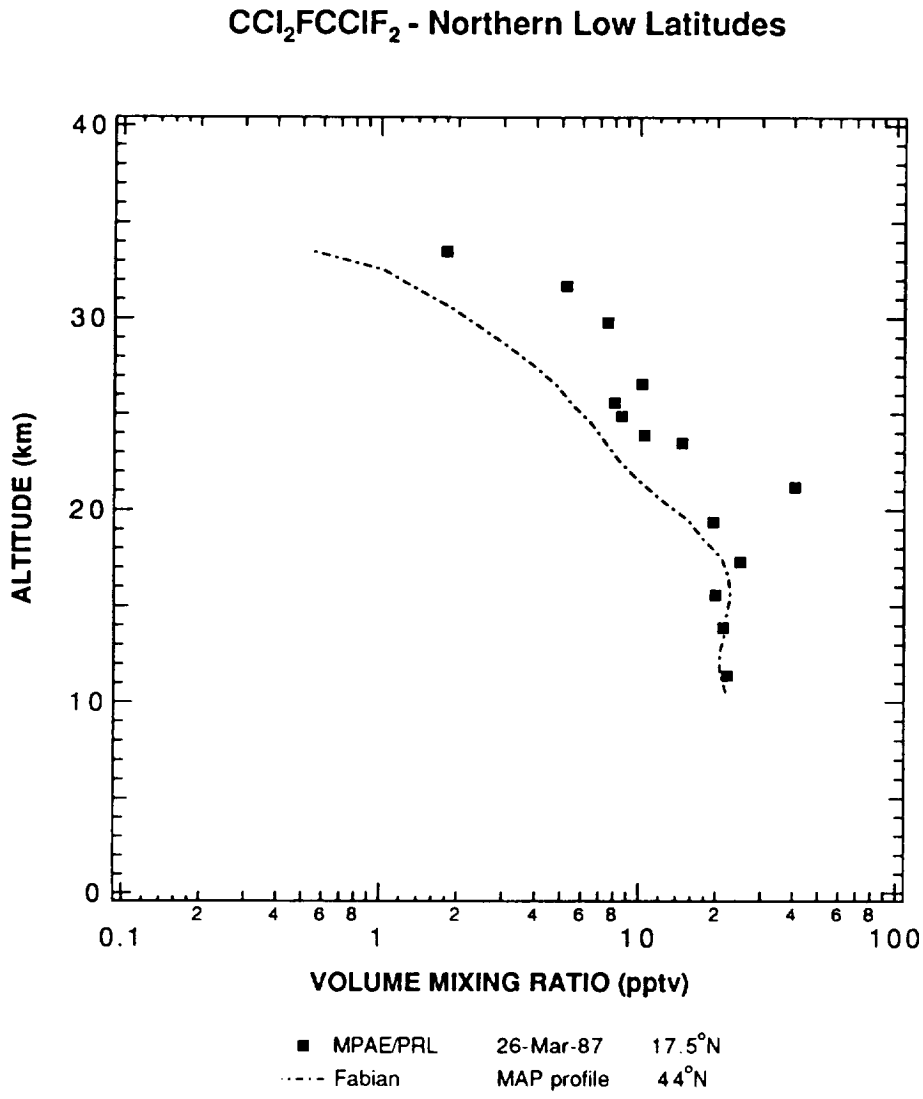

Figure 1.3.6(c) Balloon-borne cryosample measurement of the vertical distribution of CFC-113 (CCl_2FCClF_2) over Hyderabad, India at 17.5°N (Borchers *et al.*, 1989). The MAP reference profile (Fabian, 1989) is included as a guide for comparison with Figures 1.3.6(a) and (b).

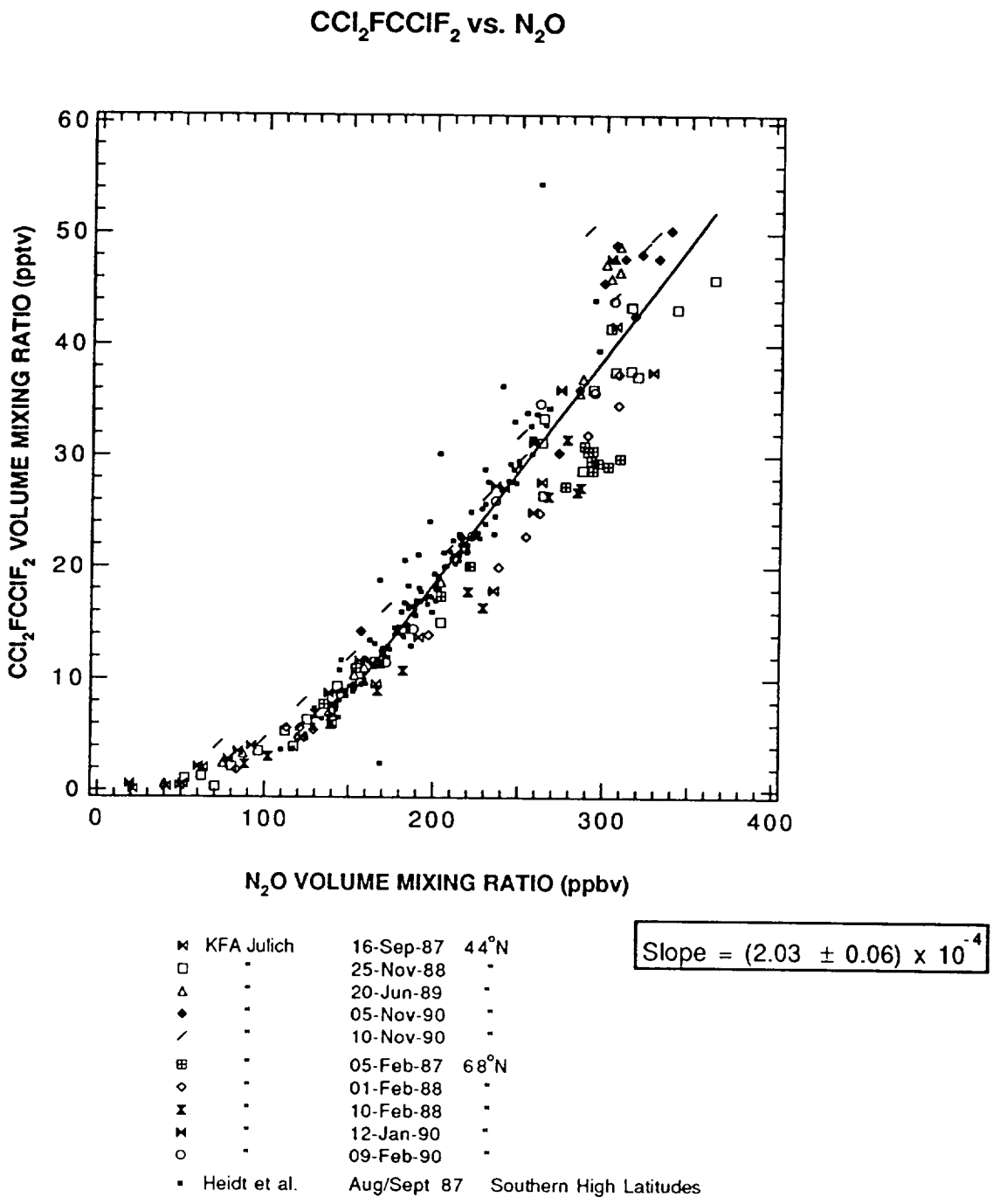

Figure 1.3.6(d) Correlation plot based on simultaneous measurements of N_2O and CFC-113 (CCl_2FCClF_2). In addition to the data shown in Figures 1.3.6(a), (b) and (c) aircraft *in situ* data from southern mid- to high latitudes reported by Heidt *et al.* (1989) are included. The Heidt *et al.* data were collected in August and September 1987 during the Airborne Arctic Ozone Experiment (AAOE) campaigns. The solid line represents a linear fit to the data over the indicated region, and has a slope of $(2.03 \pm 0.06) \times 10^{-4}$ part CCl_2FCClF_2/part N_2O (1σ error). A summary of the fits in this and other correlation plots is in Table 1.3.1.

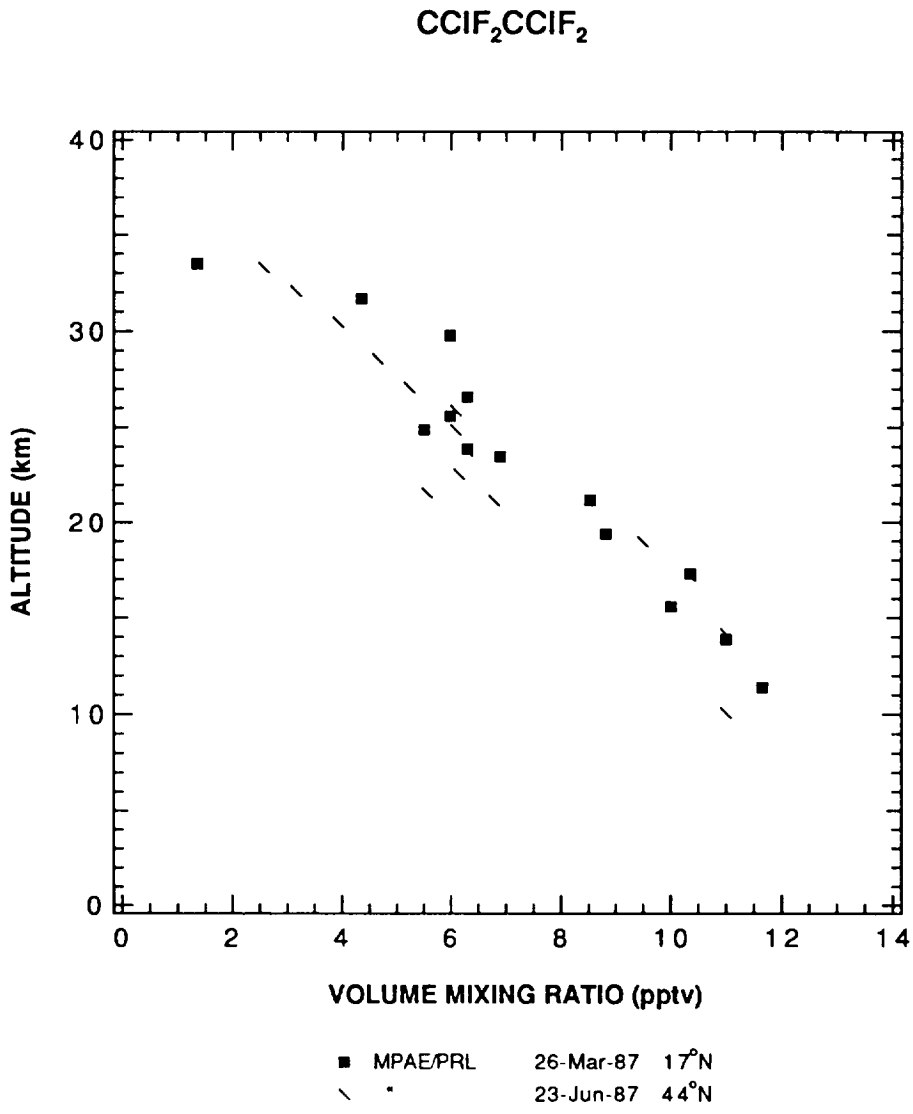

Figure 1.3.7(a) Balloon-borne cryosample measurements of CFC-114 ($CClF_2CClF_2$) at northern low and mid-latitudes reported by (Borchers *et al.*, 1989).

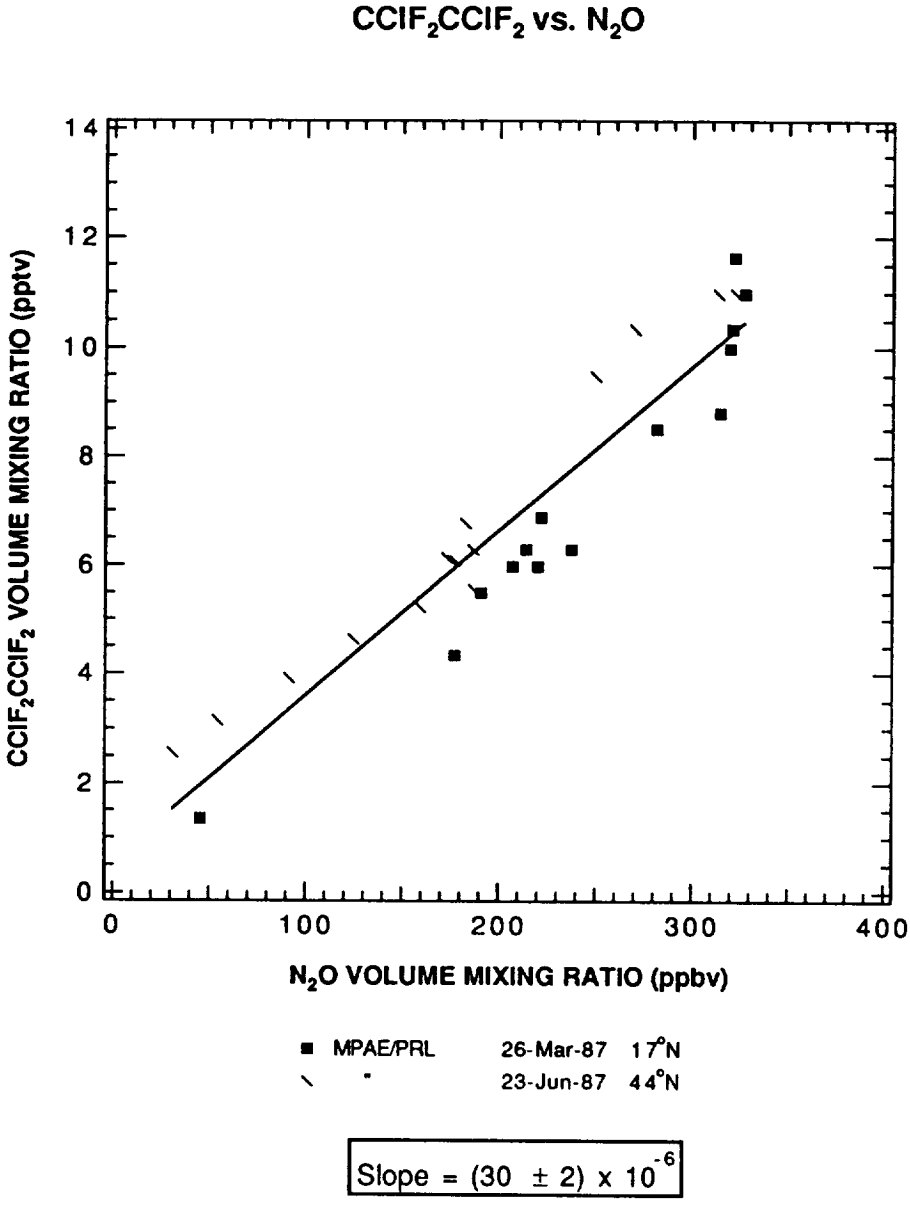

Figure 1.3.7(b) Correlation plot of CFC-114 ($CClF_2CClF_2$) vs N_2O. Data are from Borchers *et al.* (1989). The fitted line has a slope of (30 ± 2) x 10^{-6} part $CClF_2CClF_2$/part N_2O (1σ error). A summary of the fits in this and other correlation plots is in Table 1.3.1.

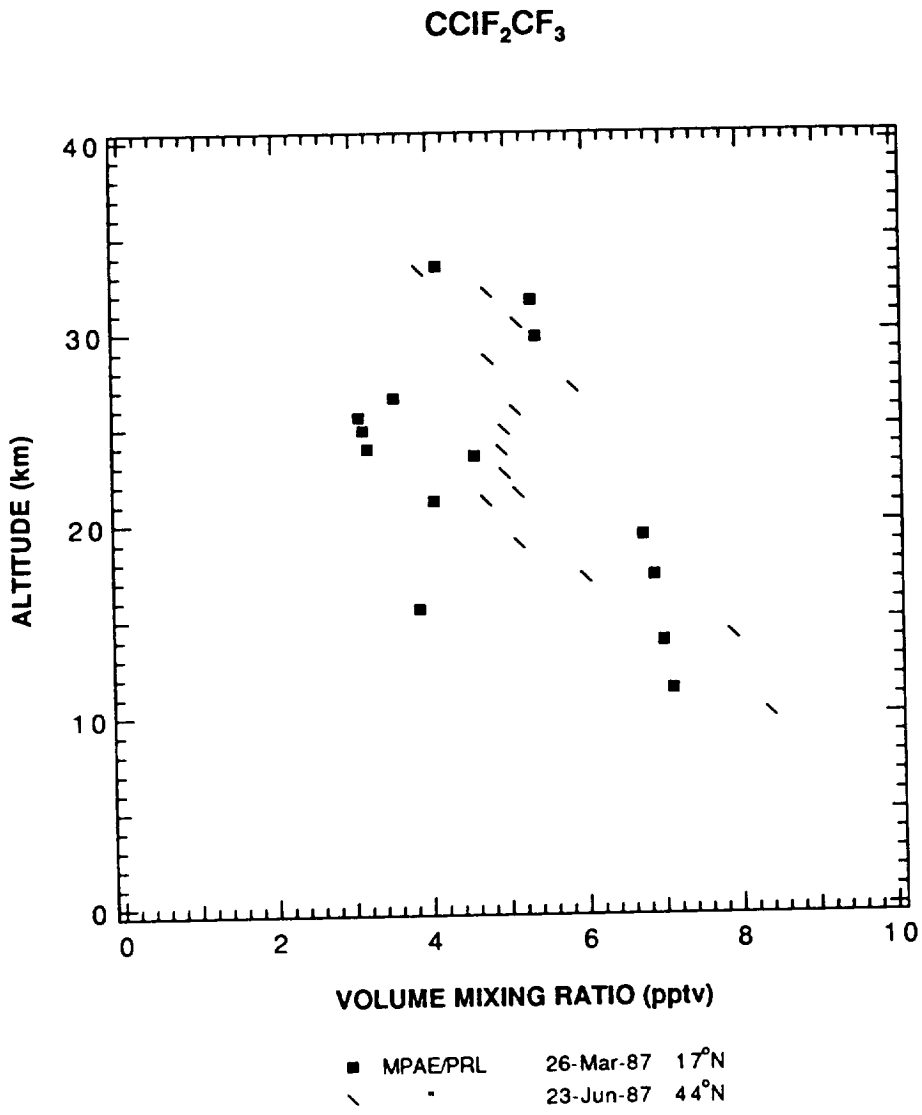

Figure 1.3.7(c) Balloon-borne cryosample measurements of CFC-115 ($CClF_2CF_3$) at northern and mid-latitudes. The MPAE/PRL data are from (Borchers *et al.*, 1989).

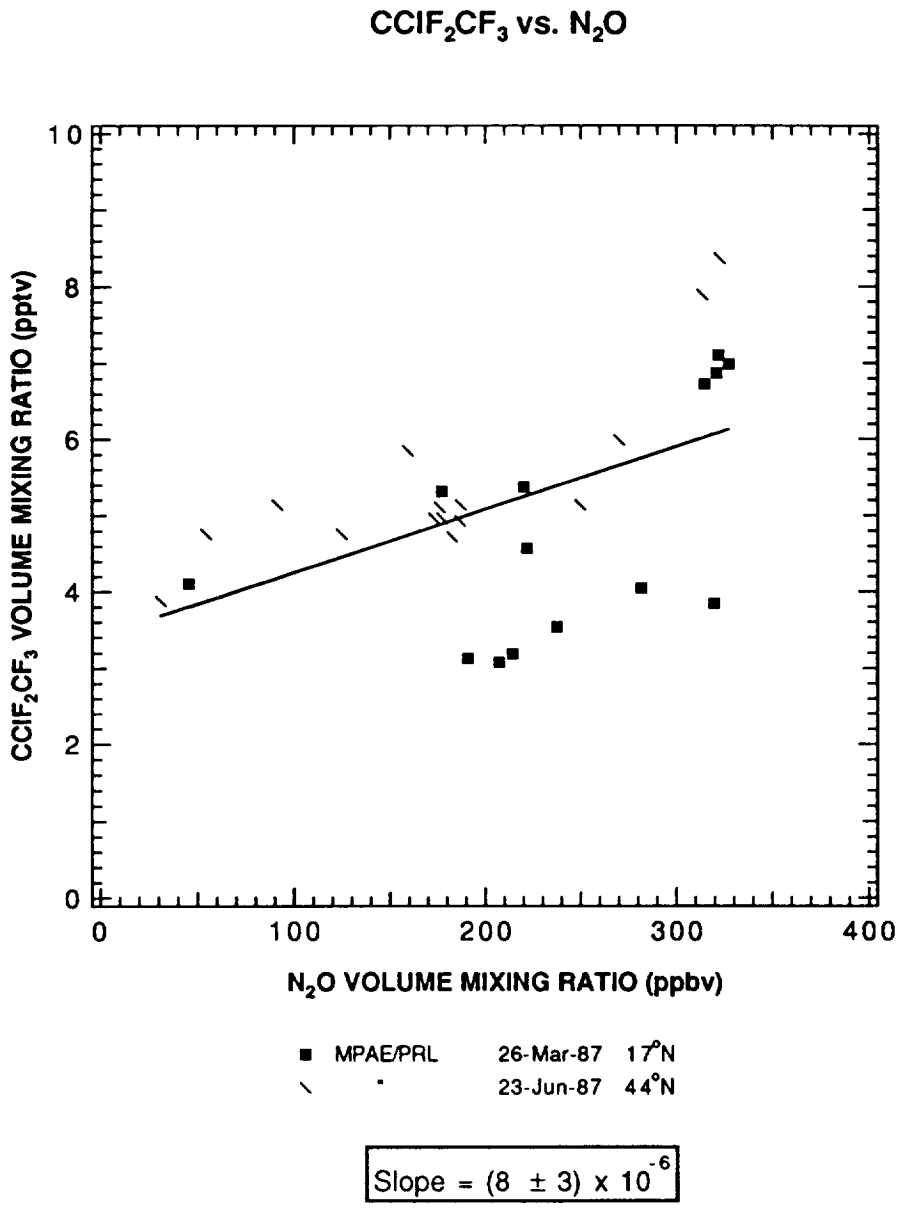

Figure 1.3.7(d) Correlation plot of CFC-115 ($CClF_2CF_3$) vs N_2O. Data are from Borchers *et al.* (1989). The fitted line has a slope of $(8 \pm 3) \times 10^{-6}$ (1σ error). A summary of the fits in this and other correlation plots is in Table 1.3.1.

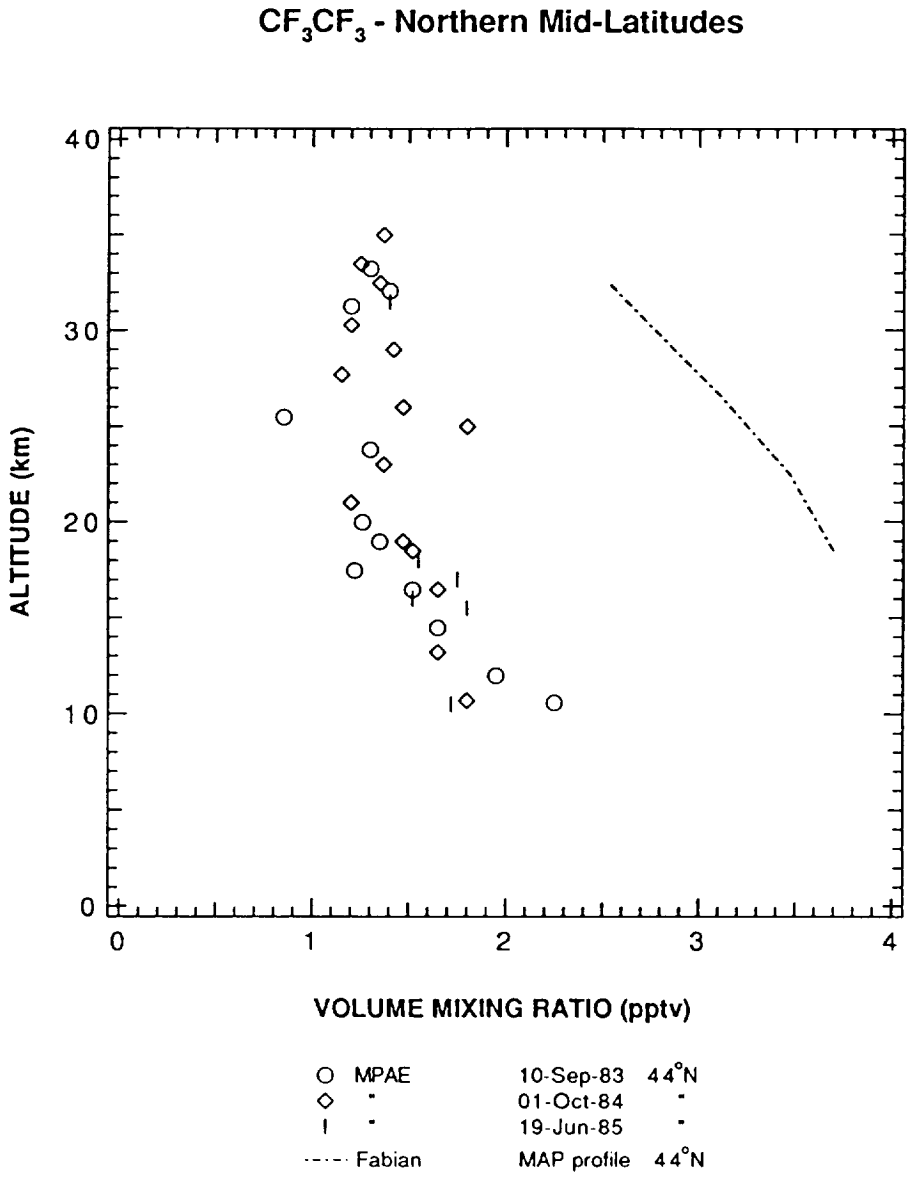

Figure 1.3.7(e) Balloon-borne cryosample measurements of CFC-116 (CF_3CF_3) at 44°N reported by Fabian *et al.*, (1987). The MAP profile (Fabian, 1989) is included for comparison.

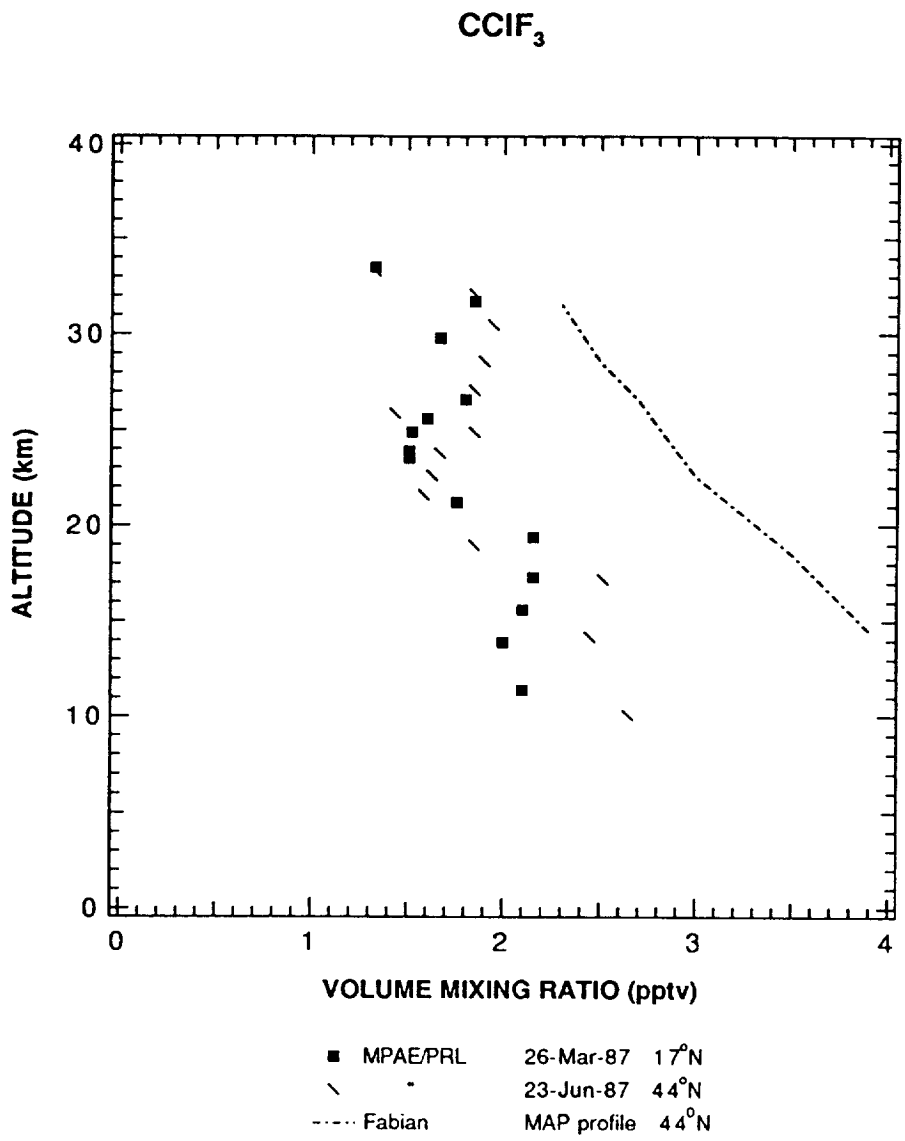

Figure 1.3.8(a) Balloon-borne cryosample measurements of CFC-13 ($CClF_3$) reported by Borchers *et al.*, (1989). The MAP profile (Fabian, 1989) is included for comparison.

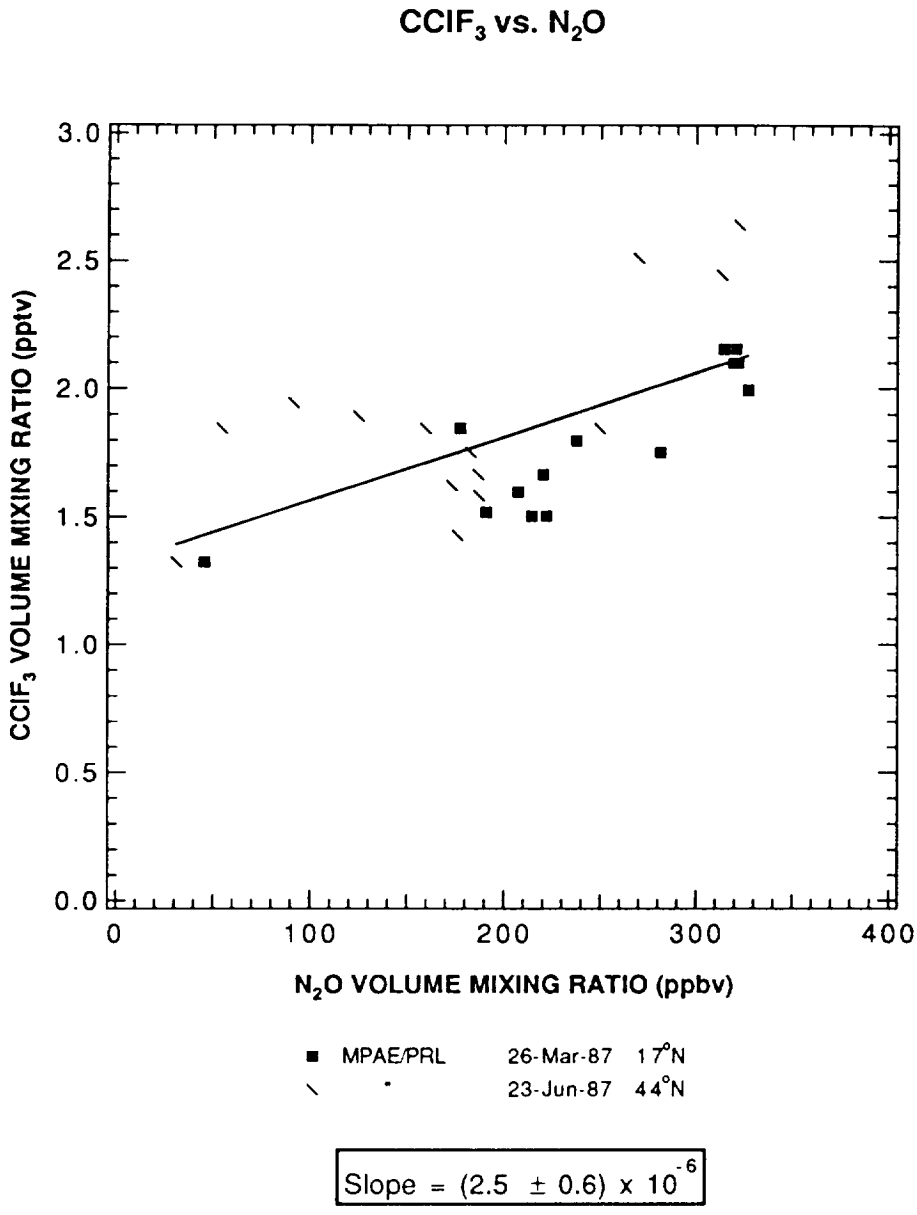

Figure 1.3.8(b) Correlation plot of CFC-13 ($CClF_3$) vs N_2O. Data are from Borchers *et al.* (1989). The fitted line has a slope of $(2.5 \pm 0.6) \times 10^{-6}$ part $CClF_3$/part N_2O (1σ error). A summary of the fits in this and other correlation plots is in Table 1.3.1.

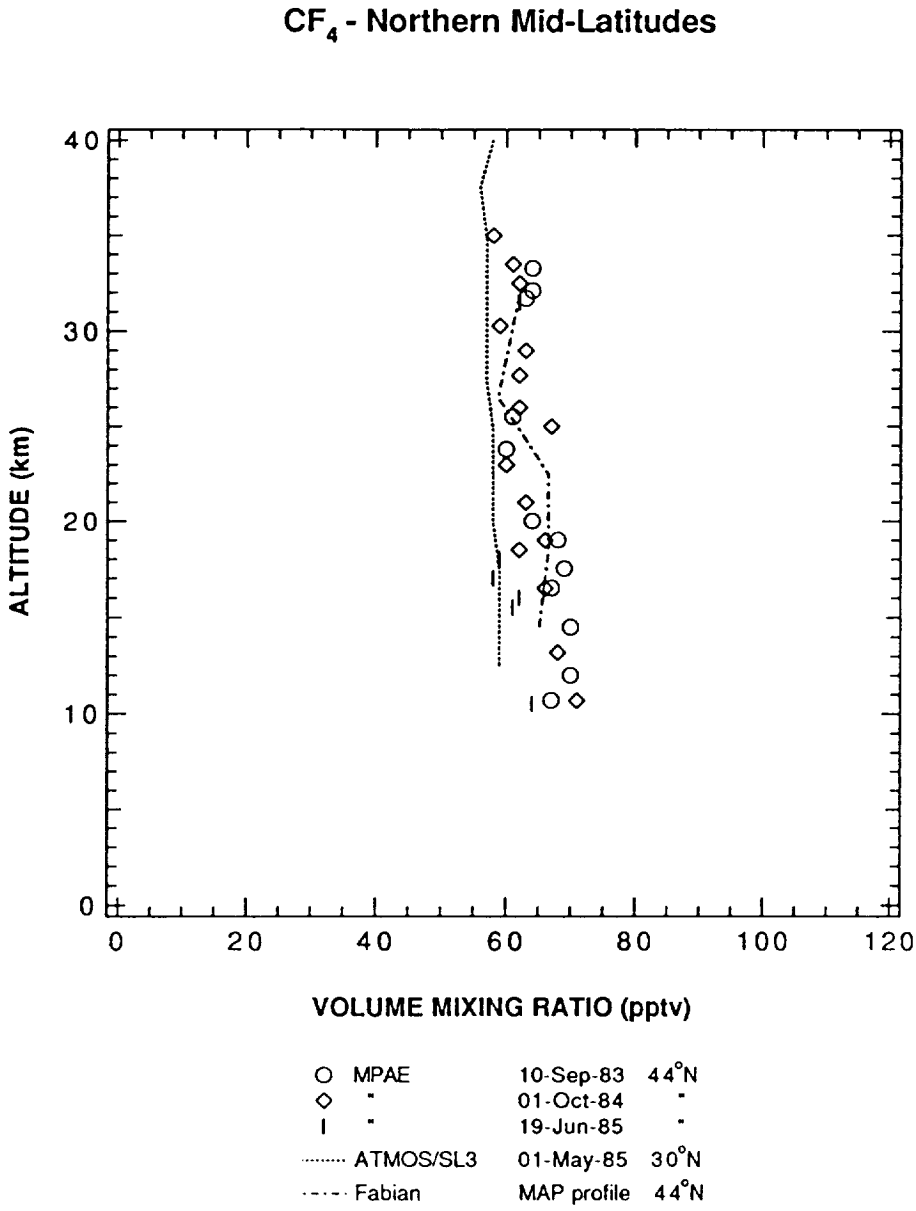

Figure 1.3.9 Measurement of carbon tetrafluoride (CF_4) at northern mid-latitudes. The MPAE data are balloon-borne cryosample measurements reported by Fabian *et al.*, (1987) and the shuttle-based ATMOS-SL-3 measurements are from Zander *et al.* (1987). The MAP profile (Fabian, 1989) is included for comparison.

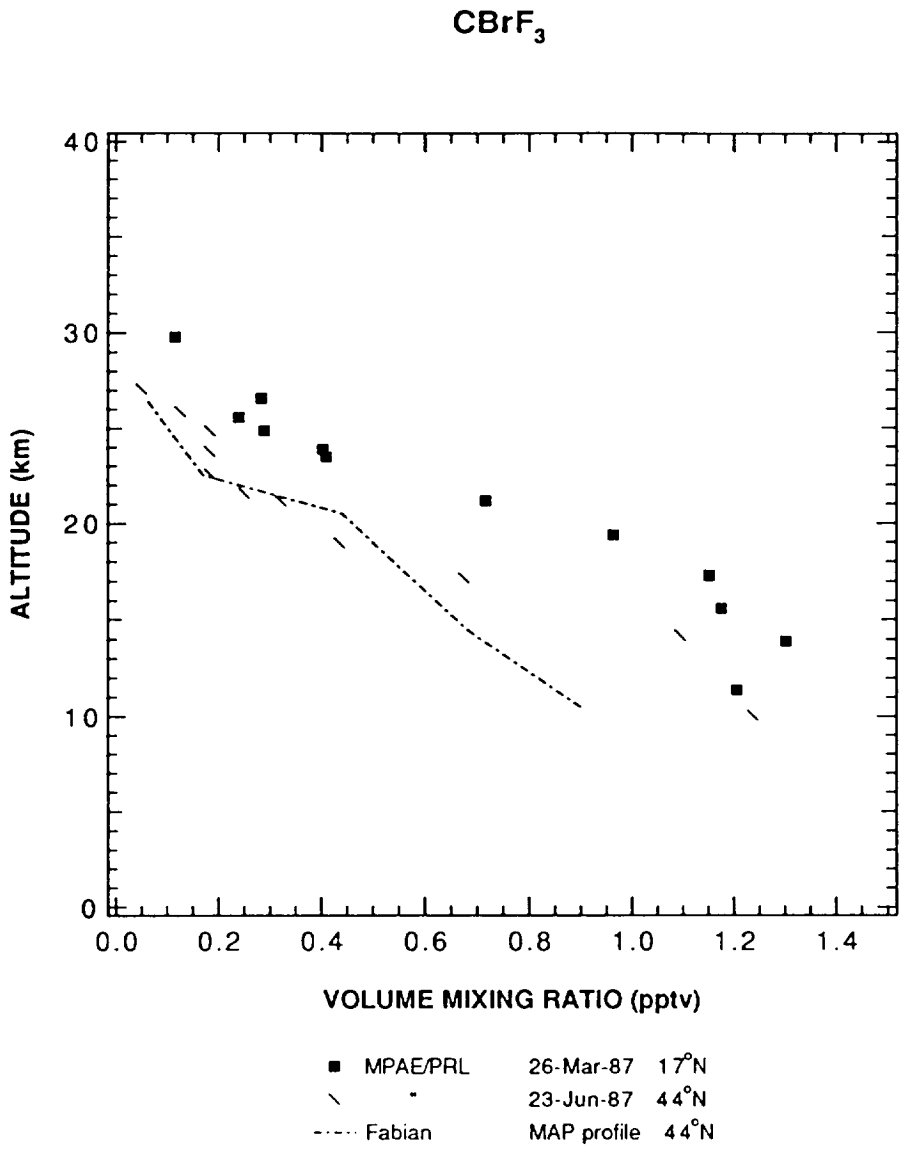

Figure 1.3.10(a) Balloon-borne cryosample measurements of Halon 1301 ($CBrF_3$) at northern low and mid-latitudes reported by Borchers *et al.*, (1989). The MAP profile (Fabian, 1989) is included for comparison.

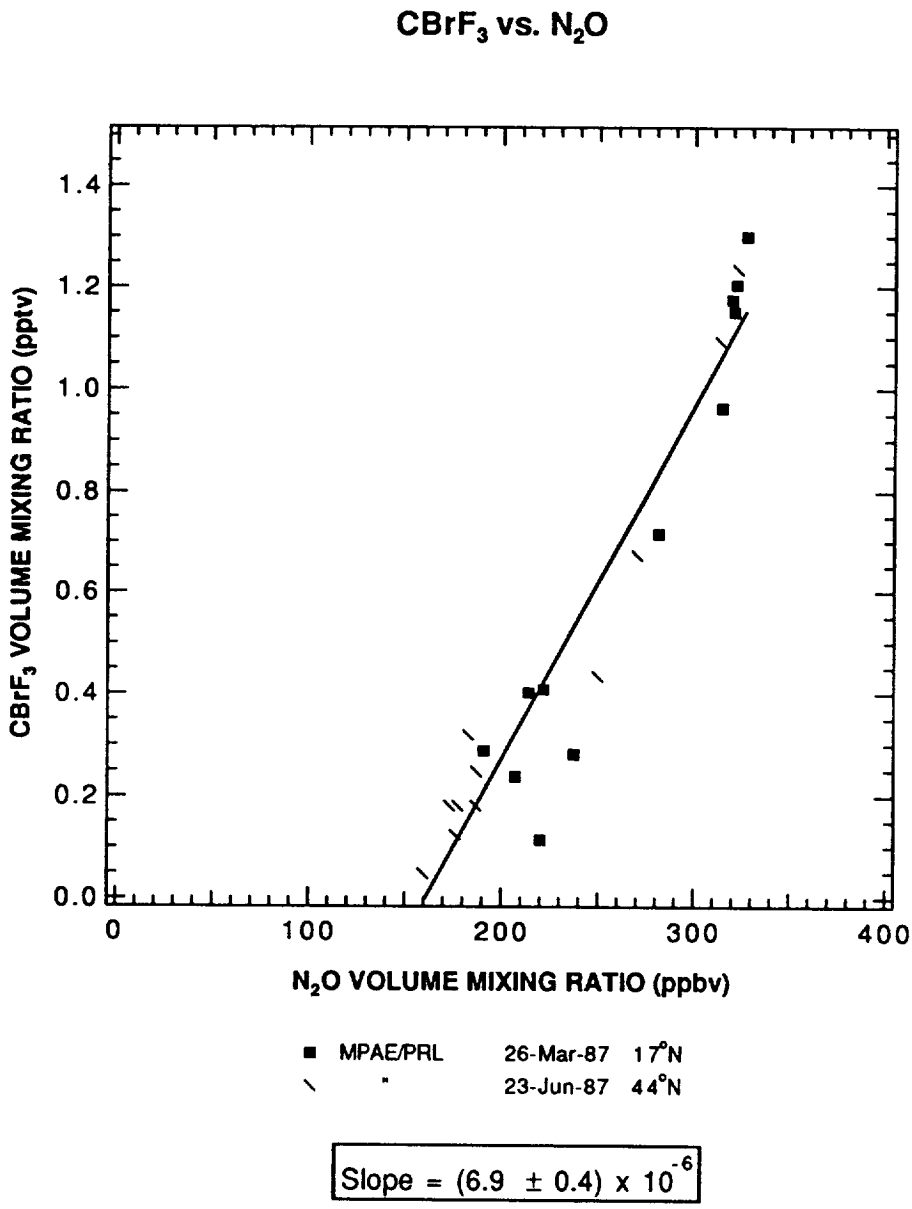

Figure 1.3.10(b) Correlation plot of Halon-1301 ($CBrF_3$) vs N_2O. Data are from Borchers *et al.* (1989). The fitted line has a slope of (6.9 ± 0.4) x 10^{-6} part $CBrF_3$/part N_2O (1σ error). A summary of the fits in this and other correlation plots is in Table 1.3.1.

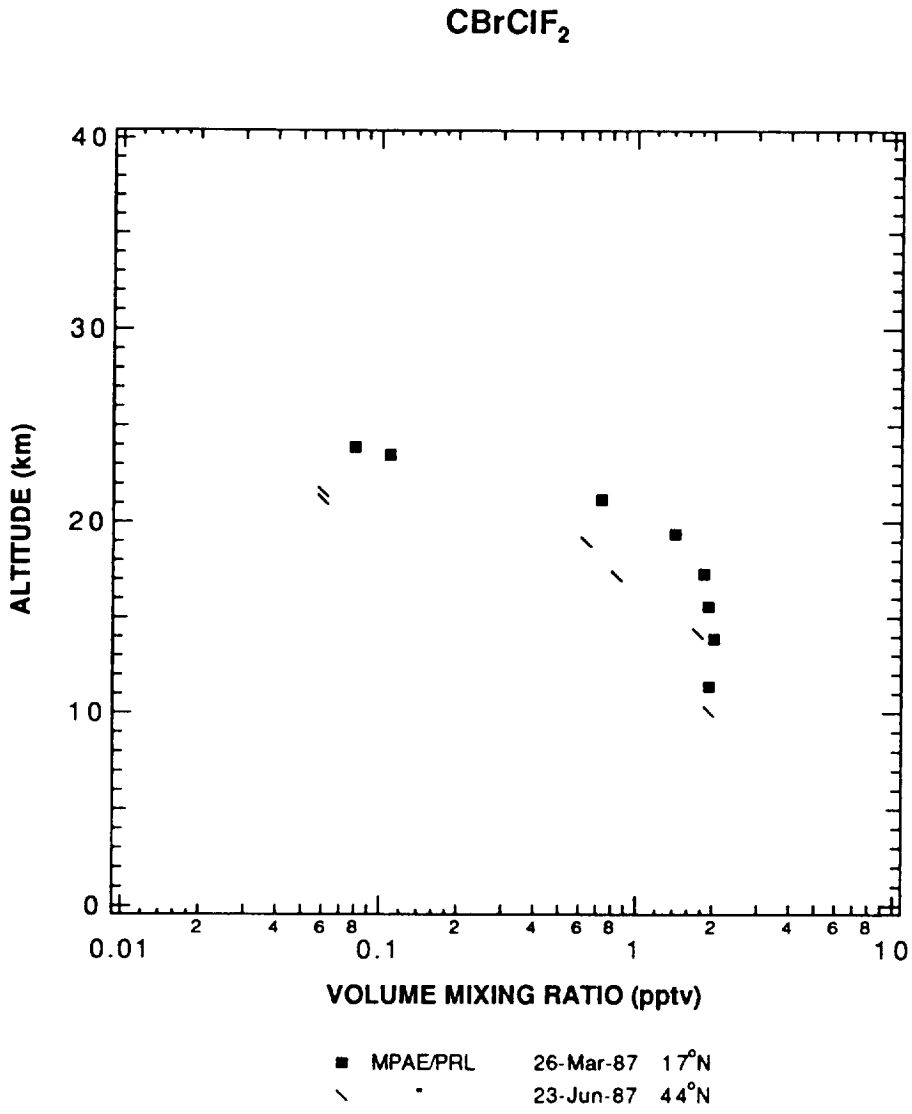

Figure 1.3.10(c) Balloon-borne cryosample measurements of Halon 1211 ($CBrClF_2$) at northern low and mid-latitudes reported by Borchers *et al.* (1989).

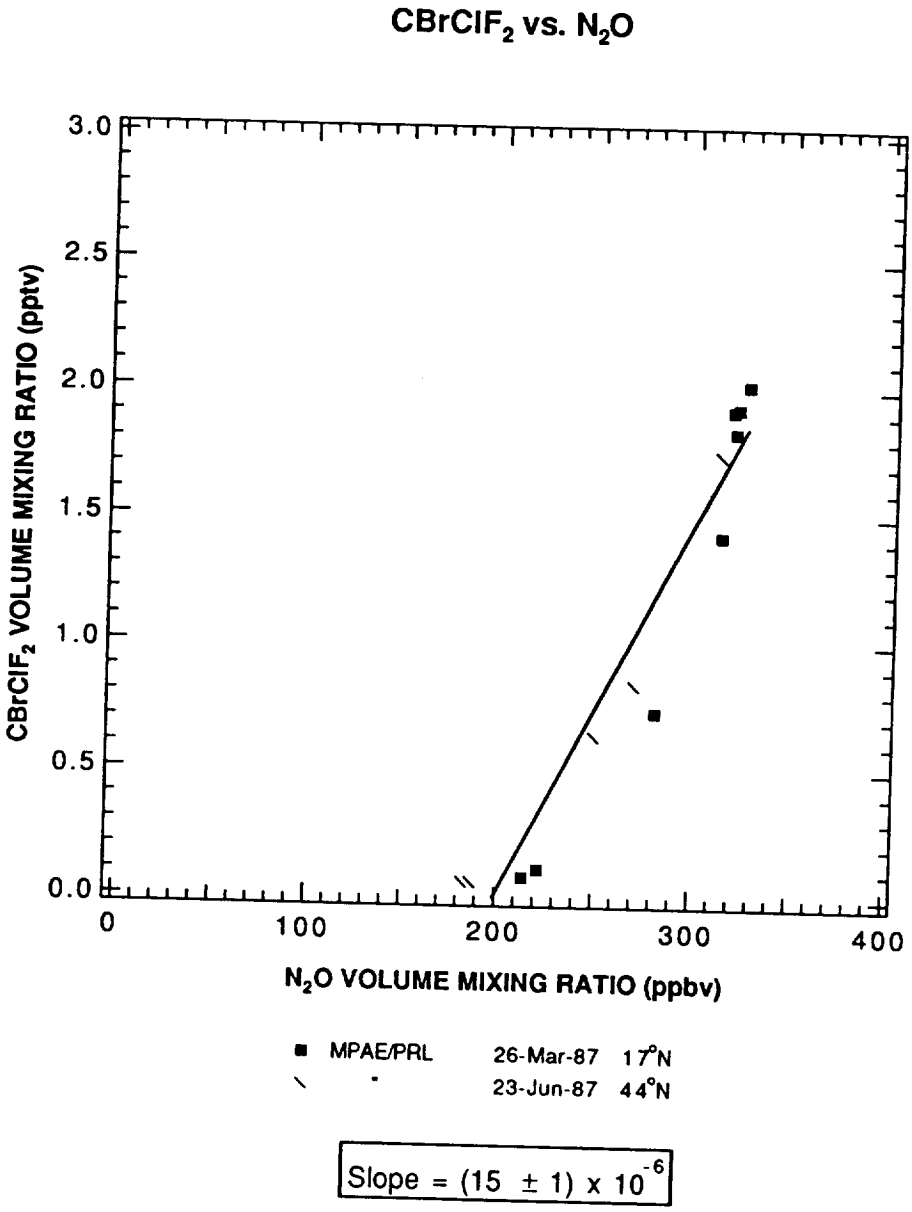

Figure 1.3.10(d) Correlation plot of Halon-1211 ($CBrClF_2$) vs N_2O. Data are from Borchers *et al.* (1989). The fitted line has a slope of (15 ± 1) x 10^{-6} part $CBrClF_2$/part N_2O (1σ error). A summary of the fits in this and other correlation plots is in Table 1.3.1.

Penkett, private communication) suggest tropospheric levels of 10-13 pptv decreasing to around 4 pptv in the lower stratosphere, at an altitude of 20 km.

More certain data are available for $CBrF_3$ (Fabian *et al.*, 1981; Fabian, 1989) and $CBrClF_2$ (Lal *et al.*, 1985; Fabian, 1989) for northern mid-latitudes, reported by the MPAE group from analyses of whole air samples obtained over southern France (44°N). This is augmented by some profile information obtained in balloon flights from Hyderabad, India (17.5°N), (Borchers *et al.*, 1988). In general, these data show a tropospheric value for both gases of just over 1 pptv, declining in the stratosphere at mid-latitude to values of less than 0.1 pptv at 25 km. The slightly larger stratospheric values measured in the tropical stratosphere may be due to the generally higher tropopause height in this region.

1.4 Calibration and Measurement Issues

The calibration and measurement issues discussed below apply particularly to the tropospheric measurements dealt with in Section 1.2. Here calibration is of extreme importance because of the use made of the data to determine atmospheric lifetimes from a comparison of atmospheric concentrations and emission data. Calibration is a less critical issue to the stratospheric measurements referred to in Section 1.3, because in this case it is generally the height profile which of interest.

The atmospheric concentrations of the organic chlorine compounds discussed in the foregoing sections are all exceedingly small, and this places severe constraints on the ways in which they can be measured and calibrated. Most measurements have been made by electron capture gas chromatography, sometimes using oxygen-doped carrier gas or pre-concentration techniques to enhance sensitivity to those compounds with low electron capture cross sections or exceptionally low concentrations. Many of the stratospheric measurements of the less common halocarbons have been made by instruments combining gas chromotography with mass spectrometry. These are of their nature less precise than measurements made by the electron capture method.

There are several important sources of potential systematic error in such low-level measurements. Calibration standards at near-ambient atmospheric concentrations are difficult to prepare accurately and, especially for some more-reactive compounds, to store reliably for calibrations of long-term time series observations. Systematic errors in preparation and storage of standards can be caused by the affinities of these compounds at such extremely low concentrations to absorb on nearly all surfaces, to dissolve in elastomers used in valves and seals, or to react chemically on clean metal surfaces.

Measurements by electron capture detection can be significantly non-linear, and this non-linearity may vary as a result of subtle changes in temperature, pressure, or carrier gas composition. The response of the electron capture detector is also vulnerable to interferences caused by co-eluting species which are not themselves detected, or to variations in trace quantities of oxygen or water vapor. Differences in overall chemical composition between samples and standards are thus a source of potential systematic errors.

The scientific implications of such potential errors in calibration or non-linearity correction are discussed elsewhere in this report. Briefly, the absolute calibration of the atmospheric measurements is of primary concern in reconciling the observed concentrations with the industrial production and release data, and thus determining the atmospheric lifetimes of these compounds. On the other hand, lifetimes determined from the rates of change of atmospheric concentrations are more dependent on uncertainties in the non-linearity correction and its variation over time, as well as on the stability of stored standards used to calibrate the measurements.

Each of the laboratories which have submitted atmospheric data for this report was asked to provide information summarizing their measurement techniques, and specifically addressing the issues of calibration, non-linearity, and long-term stability mentioned above. Unfortunately, the response has been incomplete. In some cases we have taken this information from the published literature, but very few of the published descriptions address these questions adequately enough to permit an objective assessment of their systematic uncertainties. This remains a critical area for future research emphasis.

Absolute calibration in ALE/GAGE utilizes on-site calibration gases analyzed relative to secondary standards. The calibration procedure assumes a linear relation between instrument response R and concentration x. For small values of the non-linearity parameter $e = 1 - d \ln R / d \ln x$, the error in x due to non-linearity is $-ex\Delta \ln R$ (Prinn *et al.*, 1990). The linearities of the ALE/GAGE instrument have been investigated using a suite of test tanks with x values 0.5 to 1.3 times present atmospheric values, yielding e values for each compound on each instrument. These e values are used to provide an estimate of the possible error in the trend induced by the linear assumption. For the halocarbons this error is generally very small compared to the observed trends.

The absolute calibration of the secondary standards is amendable and is based either on absolute calibrations carried out at the beginning of ALE/GAGE and/or on intercalibrations with other investigators. The long-term stability of the secondary standards is an important issue for trend determination. The relative stability of stored standards is checked using a set of specially maintained secondary tanks which are periodically analyzed relative to one another. These checks indicate that the relative stability is very high. This does not, of course, test for a systematic drift in all the tanks, although the relative stability ought to provide some measure of this drift since the internal surfaces and water content of the tanks are not identical.

Finally, as a measure of the combined effects of instrumental non-linearity, calibration stability and accuracy of the on-site tank preparations, a set of archived tanks filled each year at Cape Grim are analyzed and compared to the real-time Cape Grim measurements. For the halocarbons this restricts possible errors in the reported trends to be comparable to or less than the trend uncertainty induced by true atmospheric variability.

NOAA-CMDL flask and *in situ* measurements are reported as dry gas mole fractions relative to the NOAA 1992 gravimetric scale. Prior to 1985 these measurements were calibrated relative to two secondary standards, with frequent primary calibration against the OGIST Scale (Rasmussen and Khalil, 1986). Since 1985, the two secondary standards were calibrated directly against NOAA gravimetric primary standards. The NOAA gravimetric calibration technique is described by Novelli *et al.* (1992) for carbon monoxide standards. For primary calibrations at the lower concentrations appropriate for CFC measurements (pptv levels) the technique is similar but 2-4 dilution steps are required. Internal agreement among the NOAA primary standards is better than 1%.

Day-to-day calibrations in the NOAA program have involved only three secondary gas standards throughout the 1977 to 1992 period. An analysis of the long-term drift of these secondary standards has revealed that the first standard employed had a statistically significant drift rate during its period of use from 1977 to 1984, and that the other two standards did not drift to within experimental precision during their period of use after 1985 (Montzka *et al.*, 1992).

Measurements reported by the University of East Anglia (UEA) in this report were made on air samples collected cryogenically in 1.6 liter stainless steel canisters provided by R.A. Rasmussen. The measurements were made simultaneously in July 1984 on samples collected in each of the four years 1981, 1982, 1983 and 1984 and subsequently stored at AERE Harwell at pressures in excess of 250 psig. Calibration was made by K.A. Brice and S.A. Penkett using the following technique (Penkett *et al.* 1979):

> Samples of pure liquid CCl_3F and CCl_4 were transferred into small reservoirs on a vacuum line system. The liquids were degassed and the vapor allowed to fill a small cell of accurately determined volume to a known pressure, using a mercury manometer. Approximately 10 cm Hg pressure was typically measured out and this could be determined with a precision of about 1%. The contents of the cell were then diluted to an aluminum box with a volume of 98 l, which had been previously flushed out with compressed air. After thorough mixing 20 ml were then removed from this container and injected into a large aluminum box of volume 1 m^3 with a carefully calibrated 100 ml syringe. The larger box was previously flushed with compressed air which was passed through a molecular sieve trap to remove all traces of CCl_3F and CCl_4. By addition of successive aliquotes, mixtures from 50 to 1000 pptv could be made up with an accuracy of ±5%. These were then injected into the instrument in the same manner as outside air samples and a linear response was observed over the concentration range 0-1000 pptv for both CCl_3F and CCl_4. Since the ECD responds to the mass of electron-capturing substance in the detector, all calibrations and measurements were corrected for temperature and pressure variations of the laboratory atmosphere.

The technique described above was used in an intercalibration exercise in 1978 to produce estimates by UEA (then AERE Harwell) for concentrations of CFC-11 and CCl_4 in the standard canister of 150±10 pptv and 108±10 pptv for CCl_3F and CCl_4 respectively.

SIO shipboard measurements of atmospheric CFC-12 and CFC-11 are reported as dry air mole fractions relative to the SIO 1986 calibration scale. This calibration is based on primary standards prepared in a two-step "bootstrap" volumetric technique described in detail by Bullister (1984). In this technique, precisely measured and non-ideality corrected aliquots of CFC-12, CFC-11, and N_2O in approximately their atmospheric ratios are prepared and mixed in a volumetric static gas dilution system. Errors are minimized by using large calibrated volumes (about 12 cm^3 for the CFCs and about 35 liters for N_2O), and by using a precision mercury manometer to measure pressures. A small aliquot of this mixture is then diluted to atmospheric levels in large high-pressure Spectra-Seal aluminum cylinders using synthetic "zero air" that is free of CFC-12, CFC-11, and N_2O. The resulting N_2O concentrations are measured (Weiss, 1981) against N_2O standards with an established absolute accuracy of 0.2% (Weiss *et al.*, 1981). The product of the measured N_2O concentrations and the prepared CFC/N_2O ratios gives the CFC concentrations in these standards. The resulting calibration scale has an estimated absolute accuracy of 0.5% for CFC-12 and 1.5% for CFC-11. The larger error for CFC-11 is due to its higher boiling point and greater problems of surface adsorption during transfer of small quantities of gas mixture in the vacuum system.

SIO measurement techniques for CFC-12 and CFC-11 are described by Bullister and Weiss (1988). They involve trapping of CFCs in a cold trap and analysis by electron capture detection after separation or on a Porasil-C precolumn and column. Replicate air measurements show a standard deviation of 0.7% for CFC-12 and 0.3% for CFC-11, and are corrected for non-linearities over a wide dynamic range using a technique based on trapping multiple aliquots of standard.

Direct comparisons between three ALE/GAGE standards kept at OGC (Oregon Graduate Center, now OGIST) and SIO primary standards have shown values reported on the ALE/GAGE scale to be 1.9% lower than the SIO scale for CFC-12 and 2.5% higher than the SIO scale for CFC-11 (Weiss *et al.*, 1985).

Measurements of CFC-12, CFC-11, CCl_4 and CH_3CCl_3 reported by the FIAER group for the free troposphere over Europe and over the North Atlantic (Seiler and Scheel, 1991) are calibrated by dynamic dilution of a single 1983 Scott-Marrin gas mixture prepared in the ppmv concentration range and certified by Scott-Marrin to ±2% for each constituent. The method used by Scott-Marrin to prepare and certify these values is not discussed or evaluated.

Dynamic dilutions carried out by the FIAER group were based on Hastings mass flowmeters used in two two-stage dynamic dilution methods. In one method the Scott-Marrin gas was added through a mass flowmeter, and in the other method injections were done using an automated gas sampling valve operated by a timer, with mixing volumes in the system to smooth out pulses from these injections. The mass flowmeters were calibrated volumetrically. For CH_3CCl_3, first-stage injection through a mass flowmeter was found to be unsatisfactory, so only the results from the method using first-stage injection through the gas sampling valve were used for this compound. In all other cases, the two methods agreed.

The estimated systematic uncertainty of the dynamic dilutions is about 2%, so if one accepts the Scott-Marrin quoted uncertainty of an additional 2%, then the uncertainty of the FIAER calibration scale is around 4% for all species. The ECD measurement precision is <3% for CFC-11, and 3% for CFC-12, CH_3CCl_3, and CCl_4. Dynamic dilution experiments showed the ECD to be linear within these limits for all species except CFC-11, where non-linearities were tracked and corrected using two working standards with different concentrations.

The FIAER-CSIR measurements at Cape Point, South Africa were calibrated on the ALE/GAGE scale through collaboration with OGC.

Meteorological Research Institute (Japan) (MRI) measurements of CFC-12 and CFC-11 in free troposphere samples collected over Japan (Hirota *et al.*, 1988) were calibrated by dilution of 20 ppmv commercial mixtures prepared by Nihon Sanso and Seitetsu Kagaku, with quoted uncertainties of 5%. The method used to prepare and certify these values is not presented or discussed. MRI prepared working standards by dilution of 0.2 ml of these mixtures into 10 liters of ultra high purity (UHP) nitrogen. The systematic uncertainties associated with these additional dilutions are ~2 - 3%. (This is discussed in Hirota *et al.* (1984a) cited in Hirota *et al.* 1988). ECD

response was found to be linear in the range 0 – 500 pptv for both compounds, within the reported overall measurement precision of 4 – 5%.

The UCI calibration technique relies on the relative EC-GC response from the unknown compound of interest as compared with a fixed standard. This standard was prepared in 1985 by cryogenic trapping of nine separate halocarbons into a fixed volume which was then diluted in a static system into the atmospherically relevant range. This standard was intended to contain approximately 500 pptv of CFC-12 and 270 pptv of CFC-11, and gave 498 and 267 pptv, respectively, in direct comparison with the SIO standard. The standard concentrations of the other seven molecules (CCl_4, CH_3Cl, CH_3CCl_3, $CHCl_3$, $CHClF_2$, $CHCl{=}CCl_2$, $CCl_2{=}CCl_2$) have been calculated relative to CFC-12 as 498 pptv on the basis of their relative initial pressures. These relative calibrations have also been checked by direct comparison with a second standard prepared in a similar manner.

The standard UCI measurement technique for an unknown sample is based on the relative peak heights of the unknown and the standard. (Peak area response gives essentially identical results.) The detector response is linear and proportional to the concentration of CFC-12, $CHCl_3$ and CH_3CCl_3 over the ranges appropriate to atmospheric concentrations away from strong emission sources. The detector responses for CFC-113, CCl_4 and $CCl_2{=}CCl_2$ are not proportional to concentration, but are linear over the atmospheric range. Consequently, corrections are necessary to the directly observed response ratios for these compounds.

UCI has cross-calibrated with UT (Makide) on several occasions, with good agreement for CFC-11, CFC-12 and CFC-113. The UCI data are 13% and 23% higher than the UT data for CH_3CCl_3 and $CCl_2{=}CCl_2$, respectively.

The UT measurements are calibrated with volumetric standards prepared at near-ambient levels from the pure component gases by a three-step static dilution procedure (Makide *et al.*, 1987). Each step of the method reduces the halocarbon concentrations by roughly 10^3, using purifed nitrogen or "zero air" as the diluent gas. The dilution volumes are known to better than 1%, and the apparatus is installed in a temperature-controlled room, but no estimates are given for the accuracy of the gas volume determinations or for possible systematic errors in the dilution method including non-ideality corrections. Standard integrity during storage is checked by repeated standard preparations. Standards for CCl_4 and CH_3CCl_3 have about 10 Torr of water vapor added to protect against adsorptive loss during storage (Yokohata *et al.*, 1985).

The UT chromatographic measurements are carried out with a temperature-programmed silicone column and an ECD, using nitrogen carrier gas with methane added just before the detector. Measurement precision is about 0.5%, but measurement non-linearities are not discussed and estimates of absolute accuracy are not given.

The stratospheric data has largely been collected by two groups, KFA Jülich who use standards provided by OGIST, and MPAE who generate their own standards using a similar procedure to that reported by UEA.

References

AFEAS, Production, Sales and Atmospheric Release of CFC-11 and CFC-12 through 1990, Alternative Fluorocarbons Environmental Acceptability Study, Washington, DC, March 1992.

Albritton, D. and R. Watson, Methyl bromide and the ozone layer: a summary of current understanding, Atmospheric Science Assessment in *Methyl Bromide: Its Atmospheric Science, Technology, and Economics, Montreal Protocol Assessment Supplement,* UNEP, 41pp, 1992.

Borchers, R., P. Fabian, B. C. Kruger, S. Lal, U. Schmidt, D. Knapska, and S. A. Penkett, CFC-113 (CCl_2FCClF_2) in the stratosphere, *Planet. Space Sci., 35*, 657-663, 1987.

Borchers, R., P. Fabian, O. N. Singh, S. Lal, and B. H. Subbaraya, The vertical distribution of source gases at tropical latitudes, *Ozone in the Atmosphere*, eds. R. D. Bojkov and P. Fabian, 290-293, A. Deepak Publishing, Hampton, VA, 1988.

Brunke, E. and H. Scheel, Tropospheric CFC measurements at Cape Point, South Africa, data presented at the NASA Meeting on CFC and Halon Trends, Emissions and Lifetimes, Newport Beach, California, USA, (unpublished data) July 1991.

Bullister, J. L., Atmospheric chlorofluoromethanes as tracers of ocean circulation and mixing: measurement and calibration techniques and studies in the Greenland and Norwegian Seas, Ph.D. Thesis, University of California, San Diego, 172 pp., 1984

Bullister, J. L. and R. F. Weiss, Determination of CCl_3F and CCl_2F_2 in seawater and air. *Deep-Sea Res., 35*, 839-853, 1988.

Butler, J., J. Elkins, T. Thompson, B. Hall, T. Swanson and V. Koropalov, Oceanic consumption of CH_3CCl_3; implications for tropospheric OH, *J. Geophys. Res., 96*, 22347-22355, 1991.

Butler, J., J. Elkins, B. Hall, S. Cummings and S. Montzka, A decrease in the growth rates of atmospheric halon concentrations, *Nature, 359*, 403-405, 1992.

Cicerone, R., L. Heidt and W. Pollock, Measurements of atmospheric methyl bromide and bromoform, *J. Geophys. Res., 93*, 3745-3749, 1988.

Class, T. and K. Ballschmitter, Chemistry of organic traces in the air, VIII: sources and distribution of bromo- and bromochloromethanes in the marine and surface water of the Atlantic Ocean, *J. Atmos. Chem., 6*, 35-46, 1988.

Cunnold, D., R. Prinn, R. Rasmussen, P. Simmonds, F. Alyea, C. Cardelino, A. Crawford, P. Fraser and R. Rosen, Atmospheric lifetime and annual release estimates for CCl_3F and CCl_2F_2 from five years of ALE data, *J. Geophys. Res., 91*, 10797-10817, 1986.

Cunnold, D., P. Fraser, R. Prinn, P. Simmonds, F. Alyea, R. Weiss, A. Crawford and F. Alyea, Global trends and annual releases of CCl_3F and CCl_2F_2 estimated from ALE/GAGE measurements from July 1978 to June 1991, manuscript submitted, 1993.

Elkins, J., T. Thompson, T. Swanson, J. Butler, B. Hall, S. Cummings, D. Fisher, and A. Raffo, Decrease in the growth rates of atmospheric chlorofluorocarbons 11 and 12, *Nature, 364*, 1993.

Fabian, P., R. Borchers, S. A. Penkett, and N. J. D. Prosser, Halocarbons in the stratosphere, *Nature, 294*, 733-735, 1981.

Fabian, P., R. Borchers, B. C. Kruger, S. Lal, and S. A. Penkett, The vertical distribution of $CHClF_2$ (CFC-22) in the stratosphere, *Geophys. Res. Lett., 12*, 1-3, 1985.

Fabian, P., R. Borchers, B. C. Kruger, and S. Lal, CF_4 and C_2F_6 in the atmosphere, *J. Geophys. Res., 92*, 9831-9835, 1987.

Fabian, P., Proposed reference models for CO_2 and halogenated hydrocarbons, *MAP Handbook, Volume 31, Chapter 7*, 99-108, ed. G. M. Keating, 1989.

Fabian, P., R. Borchers, H. Duscha, B. Kruger, S. Lal and B. Subbaraya, $CHClF_2$ (HCFC-22): distribution, budget and environmental impact, in: *Ozone in the Atmosphere*, R. Bojkov and P. Fabian (eds.), 294-297, A. Deepak Publishing, Hampton, Virginia, USA, 1989.

Farmer, C. B., High resolution infrared spectroscopy of the sun and Earth's atmosphere from space, *Mikrochim. Acta [Wien], III*, 189-214, 1987.

Fraser, P., R. Rasmussen and M. Khalil, Atmospheric observations of chlorocarbons, nitrous oxide, methane, carbon monoxide and hydrogen from the Oregon Graduate Center flask sampling program, in: *Baseline 87*, B. Forgan and G. Ayers (eds.), Bureau of Meteorology/CSIRO, 40-44, 1989.

Fraser, P. and Y. Makide, Data presented at the NASA Meeting on CFC and Halon Trends, Emissions and Lifetimes, Newport Beach, California, USA, (unpublished data) July 1991.

Fraser, P., S. Penkett, R. Harriss, Y. Makide and E. Sanhueza, Source Gases: Concentrations, Emissions and Trends, Chapter 1 in *Scientific Assessment of Ozone Depletion: 1991*, WMO Report No. 25, pp 1.1-1.38, 1992.

Fraser, P., F. Alyea, D. Cunnold, R. Prinn, and P. Simmonds, Lifetime and emission estimates of 1,1,2-trichlorotrifluoroethane (CFC-113) from daily global background observations 1982-1990, manuscript in preparation, 1993.

Galbally, I., J. Sekhon and C. Marsden, Bromine in the lower atmosphere, *Clean Air, 25*, 100-105, 1991.

Goldan, P. D., W. C. Kuster, D. L. Albritton, and A. L. Schmeltekopf, Stratospheric $CFCl_3$, CF_2Cl_2, and N_2O height profile measurements at several latitudes, *J. Geophys. Res.* , *85*, 413-423, 1980.

Gunson, M. R., C. B. Farmer, R. H. Norton, R. Zander, C. P. Rinsland, J. H. Shaw, and Bo-Cai Gao, Measurements of CH_4, N_2O, CO, H_2O, and O_3 in the middle atmosphere by the ATMOS experiment on Spacelab 3, *J. Geophys. Res.*, *95*, 13867-13882, 1990.

Hall, B., J. Elkins, J. Butler, T. Thompson and C. Brunson, Improvements in nitrous oxide and halocarbon measurements at the South Pole, *Ant. J. US. 1990 Review*, *25*, 252-253, 1990.

Harsch, D. and R. Rasmussen. Identification of methyl bromide in urban air, *Anal. Lett.*, *10*, 1041, 1977.

Heidt, L. E., J. F. Vedder, W. H. Pollock, R. A. Lueb, and B. E. Henry, Trace gases in the Antarctic atmosphere, *J. Geophys. Res.*, *94*, 11599-11611, 1989.

Hirota, M., H. Muramatsu, T. Sasaki, Y. Makino and M. Asahi, Atmospheric concentrations and distributions of CCl_2F_2, CCl_3F and N_2O over Japan between 1979 and 1986, *J. Meteorol. Soc. Japan*, *66*, 703-708, 1988.

Hirota, M. and T. Sasaki, Data presented at the NASA Meeting on CFC and Halon Trends, Emissions and Lifetimes, Newport Beach, California, USA, (unpublished data) July 1991.

Khalil, M. and R. Rasmussen, Increase of $CHClF_2$ in the Earth's atmosphere, *Nature*, *292*, 823-824, 1981.

Khalil, M. and R. Rasmussen, Atmospheric chloroform ($CHCl_3$): ocean-air exchange and global mass balance. *Tellus*, *35B*, 266-274, 1983.

Khalil, M. and R. Rasmussen, Methyl chloroform: global distribution, seasonal cycles and anthropogenic chlorine, *Chemosphere*, *13*, 789-800, 1984.

Khalil, M. and R. Rasmussen, Trace gas data reported in Atmosphere and Climate, Section 24 in: *World Resources 1990-91*, a report by the World Resources Institute, UNEP-UNDP, Oxford University Press, 345-356, 1990.

Khalil, M., R. Rasmussen, J. French and J. Holt, The influence of termites on atmospheric trace gases: CH_4, CO_2, $CHCl_3$, N_2O, CO, H_2 and light hydrocarbons, *J. Geophys. Res.*, *95*, 3619-3634, 1990.

Khalil, M. and R. Rasmussen, Trace gases over Hawaii: concentrations, trends and vertical gradients, in: *Climate Monitoring and Diagnostics Laboratory, No.19 Summary Report 1989*, E. Ferguson and R. Rosson (eds.), US Department of Commerce, NOAA-ERL, Boulder, Colorado, USA, 103-104, 1991.

Knapska, D., U. Schmidt, C. Jebsen, F. J. Johnen, A. Khedim, and G. Kulessa, A laboratory test of cryogenic sampling of longlived trace gases under simulated stratospheric conditions, *Atmospheric Ozone*, eds. C. S. Zerefos and A. Ghazi, 122-128, D. Reidel, Dordrecht, 1985.

Lal, S., R. Borchers, P. Fabian, and B. Krueger, Increasing abundance of $CBrClF_2$ in the atmosphere, *Nature*, 316, 135-136, 1985.

Makhijani, A. and A. Makhijani. Biomass burning and ozone depletion, in *Saving Our Skins*, 2nd Edition, Apex Press, New York, 1992.

Makide, Y., A. Yokohata, Y. Kubo and T. Tominaga, Atmospheric concentrations of halocarbons in Japan in 1979-1986, *Bull. Chem. Soc. Jpn.*, *60*, 571-574, 1987.

Makide, Y., Data presented at the NASA Meeting on CFC and Halons Trends, Emissions and Lifetimes, Newport Beach, California, USA, (unpublished data) July 1991.

McCulloch, A., Global production and emission of bromochlorodifluoromethane and bromotrifluoromethane (halons 1211 and 1301), *Atmos. Environ.*, *26A*, 1325-1329, 1992.

McDaniel, A. H., C. A Cantrell, J. A. Davidson, R. E. Shetter, J. G. Calvert, The temperature dependent, infrared absorption cross-sections for the chlorofluorocarbons - CFC-11, CFC-12, CFC-13. CFC-14. CFC-22. CFC-113. CFC-114. amd CFC-115, *J. Atmos. Chem.*, *12*, 211-227, 1991.

Montzka, S., J. Elkins, J. Butler, T. Thompson, W. Sturges, T. Swanson, R. Myers, T. Gilpin, T. Baring, S. Cummings, G. Holcomb, J. Lobert and B. Hall, Nitrous Oxide and Halocarbons Division, Section 5 in *Climate Monitoring and Diagnostics Laboratory, No. 20 Summary Report 1991*, Department of Commerce/NOAA, Boulder, CO, pp 60-81, 1992.

Montzka, S., R. Myers, J. Butler, J. Elkins, and S. Cummings, Global tropospheric distrubution and calibration scale of HCFC-22, *Geophys.Res.Letts.*, *20*, 702-706, 1993.

Novelli, P., J. Elkins and P. Steele, The development and evaluation of a gravimetric reference scale for measurements of atmospheric carbon monoxide, *J. Geophys. Res.*, *96*, 13,109-13,121, 1991.

Penkett, S. A., K. A. Brice, R. G. Derwent and A. E. J. Eggleton, Measurement of CCl_3F and CCl_4 at Harwell over the Period January 1975 - November 1977. *Atmos. Environ. 13*, 1011-1019, 1979.

Penkett, S., B. Jones, B. Rycroft and D. Simmons, A interhemispheric comparison of the concentrations of bromine compounds in the atmosphere. *Nature*, *318*, 550-553, 1985.

Penkett, S., Data presented at the NASA Meeting on CFC and Halon Trends, Emissions and Lifetimes Meetings, Newport Beach, California, USA, (unpublished data) July 1991.

Plumb, R. A., and M. K. W. Ko, Interrelationship between mixing ratios of long lived stratospheric constituents, *J. Geophys. Res.*, *97*, 145-156, 1992.

Prinn, R., D. Cunnold, R. Rasmussen, P. Simmonds, F. Alyea, A. Crawford, P. Fraser and R. Rosen, Atmospheric trends in methyl chloroform and the global average for the hydroxyl radical, *Science*, *238*, 945-950, 1987.

Prinn, R. G., How have the atmospheric concentrations of the halocarbons changed?, *The Changing Atmosphere*, eds. F. S. Rowland and I. S. A. Isaksen, 33-48, John Wiley and Sons, 1988.

Prinn, R., D. Cunnold, R. Rasmussen, P. Simmonds, F. Alyea, A. Crawford, P. Fraser, and R. Rosen, Atmospheric emissions and trends of nitrous oxide deduced from 10 years of ALE/GAGE data, *J. Geophys. Res.*, *95*, 18,369-18,385, 1990.

Prinn, R., D. Cunnold, P. Simmonds, F. Alyea, R. Boldi, A. Crawford, P. Fraser. D. Gutzler, D. Hartley, R. Rosen and R. Rasmussen, Global average concentration and trend for hydroxyl radicals deduced from ALE/GAGE trichloroethane (methyl chloroform) data for 1978-1990, *J. Geophys. Res.*, *97*, 2445-2461, 1992.

Raper, O. F., C. B. Farmer, R. Zander, and J. H. Park, Infrared spectroscopic measurements of halogenated sink and reservoir gases in the stratosphere with the ATMOS instrument, *J. Geophys. Res.*, *92*, 9851-9858, 1987.

Rasmussen, R., M. Khalil, S. Penkett and N. Prosser, $CHClF_2$ (F-22) in the Earth's atmosphere, *Geophys. Res. Letts.*, *7*, 809-812, 1980.

Rasmussen, R. and M. Khalil, Atmospheric fluorocarbons and methyl chloroform at the South Pole, *Ant. J. US*, *17*, 203-205, 1982.

Rasmussen, R. and M. Khalil, Rare trace gases at the South Pole, *Ant. J. US*, *18*, 250-252, 1983.

Rasmussen, R. and J. Lovelock, The Atmospheric Lifetime Experiment, 2. Calibration, *J. Geophys. Res.*, *88*, 8369-8378, 1983.

Rasmussen, R. and M. Khalil, Gaseous bromine in the Arctic and Arctic haze, *Geophys. Res. Lett.*, *11*, 433-436, 1984.

Rasmussen, R. and M. Khalil, Atmospheric trace gases: trends and distributions over the last decade, *Science*, *232*, 1623-1624, 1986.

Rasmussen, R., Data reported at the Generic Cylinder Workshop, Boulder, Colorado, USA, October 22, 1990.

Reber, C. A., The Upper Atmosphere Research Satellite, *EOS Transactions*, American Geophysical Union, 71, pp. 1867-1868, 1873-1874, and 1878, December 18, 1990.

Rinsland, C., D. Johnson, A. Goldman and J. Levine, Evidence for a decline in the atmospheric accumulation rate of $CHClF_2$ (HCFC-22), *Nature*, *337*, 535-537, 1989.

Rinsland, C., A. Goldman, F. Murcray, R. Blatherwick, J. Kosters, D. Murcray, N. Sze and S. Massie, Long-term trends in the concentrations of SF_6, $CHClF_2$ and COF_2 in the lower stratosphere from analysis of high-resolution infrared solar occultation spectra, *J.Geophys.Res.*, 95, 16477-16490, 1990.

Rinsland, C. P., J. S. Levine, A. Goldman, N. D. Sze, M. K. W. Ko, and D. W. Johnson, Infrared measurements of HF and HCl total column abundances above Kitt Peak, 1977-1990: seasonal cycles, long-term increases, and comparisons with model calculations, *J. Geophys. Res.*, *96*, 15523-15540, 1991.

Scheel, H., F. Slemr, P. Matuska, J. Werhahn and W. Seiler, *Measurement of the global distribution of tropospheric trace gases and their time dependent variations, Final Report,* Fraunhofer-Institute for Atmospheric Research, Garmisch-Partenkirchen, Germany, 216pp, 1988.

Scheel, H., E. Brunke and W. Seiler, Trace gas measurements at the monitoring station Cape Point, South Africa, between 1978 and 1988, *J. Atmos. Chem.*, *11*, 197-210, 1990.

Schmidt, U., D. Knapska, and S. A. Penkett, A study of the vertical distribution of methyl chloride in the midlatitude stratosphere, *J. Atmos. Chem.*, *3*, 363-376, 1985.

Schmidt, U., C. Jebsen, F. J. Johnen, A. Khedim, E. Klein, D. Knapska, G. Kulessa, J. Rudolph, G. Schumacher, and E. Schunck, Stratospheric observations of long-lived trace gases at midlatitudes 1982-1985 (data report), *Spezielle Berichte der Kernforschungsanlage JHlich - Nr. 375*, KFA Jülich, 1986.

Schmidt, U., R. Bauer, A. Khedim, E. Klein, G. Kulessa, and B. Schubert, *In situ* observations of long-lived trace gases in the Arctic stratosphere during winter, *Ozone in the Atmosphere*, eds. R. D. Bojkov and P. Fabian, 298-301, A. Deepak Publishing, Hampton, VA, 1989.

Schmidt, U., and A. Khedim, *In situ* measurements of carbon dioxide in the winter Arctic vortex and at midlatitudes: an indicator of the 'age' of stratospheric air, *Geophys. Res. Lett.*, *18*, 763-766, 1991.

Schmidt, U., R. Bauer, A. Khedim, G. Kulessa, and C. Schiller, Profile observations of long-lived trace gases in the arctic vortex, *Geophys. Res. Lett.*, *18*, 767-770, 1991.

Seiler, W. and H. Scheel, Long term trends and latitudinal distribution of CFCs from aircraft measurements, data presented at the NASA Meeting on CFC and Halon Trends, Emissions and Lifetimes, Newport Beach, California, USA, (unpublished data) July 1991.

Simmonds, P., D. Cunnold, F. Alyea, C. Cardelino, A. Crawford, R. Prinn, P. Fraser, R. Rasmussen and R. Rosen, Carbon tetrachloride lifetimes and emissions determined from daily Singh, H., J. Salas and R. Stiles, Methyl halides in and over the eastern Pacific (40°N-32°S), *J. Geophys. Res.*, *88*, 3684-3690, 1983.

Singh, H. L.J. Salas and R. Stiles, Methyl halides in and over the eastern Pacific (40°N-32°S), *J.Geophys.Res.*, *88*, 3684-3690, 1983.

Singh, H., L.J. Salas, W. Viezee, B. Sitton and R. Ferek, Measurement of volatile organic chemicals (VOCs) at selected sites in California, *Atmos. Environ.*, *26A*, 2929-2946, 1992.

Sturges, W. (ed.), T. Baring, J. Butler, J. Elkins, B. Hall, R. Myers, S. Montzka, T. Swanson and T. Thompson, Nitrous Oxide and Halocarbons Group, Section 7 in: *Climate Monitoring and Diagnostics Laboratory, No.19 Summary Report 1990*, E. Ferguson and R. Rosson (eds.), US Department of Commerce, NOAA-ERL, Boulder, Colorado, USA, 63-71, 1991.

Thompson, T. (ed.), J. Elkins, J. Butler, B. Hall, K. Egan, C. Brunson, J. Sczechowski and T. Swanson, Nitrous Oxide and Halocarbons Group, Section 8 in: *Climate Monitoring and Diagnostics Laboratory, No.18 Summary Report 1989*, W. Komhyr and R. Rosson (eds.), US Department of Commerce, NOAA-ERL, Boulder, Colorado, USA, 64-72, 1990.

Toon, G. C., C. B. Farmer, L. L. Lowes, P. W. Schaper, J.-F. Blavier, and R. H. Norton, Infrared aircraft measurements of stratospheric composition over Antarctica during September 1987, *J. Geophys. Res.*, *94*, 16571-16596, 1989.

Vedder, J. F., E. C. Y. Inn, B. J. Tyson, C. A. Boitnott, and D. O'Hara, Measurements of CF_2Cl_2, $CFCl_3$, and N_2O in the lower stratosphere between 2°S and 73°N latitude, *J. Geophys. Res.*, *86*, 7363-7368, 1981.

Wang, C., T. Gilpin, D. Blake and F. S. Rowland, Data presented at the NASA Meeting on CFC and Halon Trends, Emissions and Lifetimes, Newport Beach, California, USA, (unpublished data) July 1991.

Wang, C., D. Blake and F. S. Rowland, Seasonal variations in the atmospheric distribution in remote surface locations of a reactive chlorine compound, tetrachloroethylene, UCI manuscript in preparation, 1992.

Weiss, R. F., Determinations of carbon dioxide and methane by dual catalyst flame ionization chromatography and nitrous oxide by electron capture chromatography, *J. Chromatog. Sci.*, *19*, 611-616, 1981.

Weiss, R. F., C. D. Keeling and H. Craig, The determination of tropospheric nitrous oxide, *J. Geophys. Res.*, *86*, 7197-7202, 1981.

Weiss, R. F., J. L. Bullister, R.H. Gammon, and M.J. Warner, Atmospheric chlorofluoromethanes in the deep equatorial Atlantic, *Nature*, *314*, 608-610, 1985.

Weiss, R., Data presented at the NASA Meeting on CFC and Halon Trends, Emissions and Lifetimes, Newport Beach, California, USA, (unpublished data) July 1991.

World Meteorological Organization, *Atmospheric Ozone 1985: Assessment of our Understanding of the Processes Controlling its Present Distribution and Change*, WMO Report No. 16, Volume II, Chapter 11, WMO Global Ozone Research and Monitoring Project, 1986.

World Meteorological Organization, *Report of the International Ozone Trends Panel 1988*, WMO Report No. 18, Volume II, WMO Global Ozone Research and Monitoring Project, 1989.

World Meteorological Organization, *Scientific Assessment of Stratospheric Ozone: 1989*, Chanin, M., D. Ehhalt, P. Fraser, J. Frederick, J. Gille, M. McCormick, G. Megie and M. Schoeberl, Chapter 2, Global Trends, in: Volume 1, WMO Global Ozone Research and Monitoring Project Report No. 20, 162-281, 1990.

Yokohata, A., Y. Makide and T. Tominaga, A new calibration method for the measurement of CCl_4 concentration at 10^{-10} v/v level and behavior of CCl_4 in the atmosphere, *Bull. Chem. Soc. Jpn.*, 58, 1308-1314, 1985.

Zander, R., C. P. Rinsland, C. B. Farmer, and R. H. Norton, Infrared spectroscopic measurements of halogenated source gases in the stratosphere with the ATMOS instrument, *J. Geophys. Res.*, *92*, 9836-9850, 1987.

Zander, R. and C. P. Rinsland, Variability and trend studies of atmospheric constituents based on infrared solar spectra recorded from the ground, *Proc. Atmos. Spac. Applic. Workshop, 6-8 June 1990*, 134-144, 1990.

Zander, R., M. R. Gunson, J. C. Foster, C. P. Rinsland, and J. Namkung, Stratospheric $ClONO_2$, HCl, and HF concentration profiles derived from ATMOS/Spacelab 3 observations- an update, *J. Geophys. Res.*, *95*, 20519-20525, 1990.

Zander, R., M. R. Gunson, C. B. Farmer, C. P. Rinsland, F. W. Irion, and E. Mahieu, The 1985 chlorine and fluorine inventories in the stratosphere based on ATMOS observations at 30° North latitude, *J. Atmos. Chem.*, *15*, 171-186, 1992.

APPENDIX I

TROPOSPHERIC MEASUREMENTS

Table 1. *Monthly mean in situ observations of CFC-12 (CCl_2F_2) (porasil column data, pptv) from the ALE/GAGE program during 1978 - 1991. Monthly means are obtained from individual measurements (ALE, 4 per day; GAGE, 12 per day). Pollution episodes are removed from the data (Prinn et al., 1983; Cunnold et al., 1986, 1993, Prinn et al., 1992). Some of the data are unpublished and subject to revision. Data should not be used for further analysis without consulting the principal investigators, GAGE, R. Prinn, P. Fraser, P. Simmonds, D. Cunnold, F. Alyea. The data are in the SIO 1986 scale (Bullister and Weiss, 1988).*

Adrigole/Mace Head, Ireland

	Jan	Feb	Mar	Apr	May	Jun	Jul	Aug	Sep	Oct	Nov	Dec
1978							280.9	282.3	282.2	285.0	284.8	289.3
1979	292.6	291.9	291.1	292.9	297.3	297.2	300.4	303.3	303.1	306.6	313.2	311.7
1980	308.6	308.7	312.8	315.1	317.9	319.2	321.6	322.7	323.4	324.7	327.1	326.7
1981	328.2	329.4	329.5	332.7	332.7	331.5	331.2	335.4	337.8	340.1	342.8	344.2
1982	339.7	341.2	342.9	345.8	344.5	350.3	351.2	353.4	356.9	360.0	361.5	360.5
1983	358.4	360.7	362.0	364.3	369.1	367.4	367.4	371.1	371.3	374.2	375.6	375.9
1984												
1985												
1986												
1987		428.2	425.4	428.2	430.9	429.9	431.9	434.2	437.5	442.0	444.1	442.8
1988	447.9	449.0	444.7	448.7	451.7	454.4	455.6	457.2	460.5	463.9	467.7	467.7
1989	467.0	468.8	468.0	471.3	471.7	473.1	474.4	475.6	479.9	478.4	480.5	482.2
1990	481.2	481.6	481.3	482.2	486.3	486.1	485.1	487.2	490.1	491.8	493.8	493.7
1991	496.1	497.4	495.6	495.0	495.0	495.6	496.7	496.3	499.8	500.8	501.4	503.1

Cape Meares, Oregon

	Jan	Feb	Mar	Apr	May	Jun	Jul	Aug	Sep	Oct	Nov	Dec
1978												
1979												
1980											322.2	321.5
1981	322.9	324.1	324.7	325.5	326.7	328.3	329.2	331.9	335.3	338.7	339.2	339.1
1982	338.7	339.4	341.0	342.1	342.3	343.4	343.8	345.4	349.0	351.2	353.6	354.1
1983	350.8	351.1	353.4	354.8	355.9	359.0	360.7	362.7	364.9	369.1	370.6	372.9
1984		372.5	371.6	374.1	374.3	375.7	376.6	376.4	380.3	386.3	387.5	388.4
1985	390.0	388.0	389.4	389.4	390.0	391.7	395.3	398.6	403.7	403.1	405.0	405.6
1986	404.4	405.9	407.7	411.0	411.3	413.0	412.3	414.6	425.1	427.6	426.7	429.4
1987	429.7	427.5	429.7	434.6	435.7	434.9	434.3	428.8	435.7	451.0	448.1	450.0
1988	450.1	449.2	450.8	453.8	455.1	455.8	456.6	459.9	465.0	467.1	465.6	467.2
1989	465.6	466.6	466.4	473.8	474.0	475.3						
1990												
1991												

Table 1. *Continued.*

Ragged Point, Barbados

	Jan	Feb	Mar	Apr	May	Jun	Jul	Aug	Sep	Oct	Nov	Dec
1978						276.1	277.3	275.5	276.5	275.2	280.6	
1979	284.0	282.4	284.1	287.4	287.7	287.6	291.1	295.2	293.4	294.2	293.8	295.0
1980	296.4	297.3	300.3	300.8	302.0	306.1	309.2	310.2	311.0	312.4	314.0	315.2
1981	316.0	316.8	313.3	317.0	318.4	318.4	322.9	323.7	326.7	328.0	329.3	325.9
1982	329.0	329.8	330.7	335.5	336.7	339.5	340.6	341.6	341.3	341.2	344.0	350.5
1983	350.5	350.1	350.6	350.6	349.9	350.3	355.6	360.1	360.7	360.2	360.7	362.6
1984	364.2	364.6	366.8	366.9	370.6	372.5	376.7	380.0	380.6	381.4	380.3	384.0
1985	384.6	384.8	386.3	386.7	391.2	389.6	395.0	394.5	394.0	395.8	396.9	402.0
1986	400.6	402.3	403.3	404.7	405.5	409.9	414.7	415.7	417.5	416.9	419.9	423.3
1987	423.3	421.8	421.9	423.2	425.0	428.1	430.4	433.6	435.8	434.5	435.7	437.3
1988	440.5	441.4	441.7	441.9	445.3	444.0	446.4	447.9	449.9	451.0	456.9	460.2
1989	460.3	458.1	459.3	460.8	463.2	467.4	469.7	468.5	469.2	472.4	472.2	
1990	475.7	475.3		477.7	479.7	481.4	483.9	485.1	485.7	482.7	485.5	486.9
1991	487.2	487.3	486.5	489.7	489.8	492.6	494.2	497.5	497.4	497.1	496.7	499.9

Cape Matatula, Samoa

	Jan	Feb	Mar	Apr	May	Jun	Jul	Aug	Sep	Oct	Nov	Dec
1978							248.0	249.5	254.5	257.9	263.5	267.0
1979	271.1	271.6	272.9	274.0	272.3	272.1	272.9	275.5	275.5	277.9	279.2	280.8
1980	285.9	286.6	288.4	290.2	291.4	292.2	293.9	295.0	296.4	292.0	297.4	299.4
1981	301.0				304.0	305.0	304.6	308.7	312.2	311.7	313.4	316.1
1982	318.8	320.0	319.4			322.7	322.7	325.1	325.4	326.0	328.1	329.5
1983	330.9	332.6	332.5	333.4	334.9	338.1	339.8	344.5	347.1	348.1	349.6	352.8
1984	356.0	354.7	354.8	355.0	352.9	353.6	355.7	357.3	360.4	359.9	363.3	367.6
1985	368.8	371.3	371.4	371.7	372.7	373.2	375.6	376.7	377.4		378.7	382.7
1986	385.3	387.3	387.1	388.9	388.3	396.1	393.6	395.8	399.8	401.3	401.1	402.4
1987	405.1		408.0	403.3	403.7	410.8	412.1	413.9	414.0	415.1	418.3	420.8
1988	422.9		426.5	430.1	428.1	428.8	431.4	437.3	439.1	440.0	439.8	441.8
1989	444.8	450.9	452.2	451.6	453.1	451.7						
1990												
1991												

Cape Grim, Tasmania

	Jan	Feb	Mar	Apr	May	Jun	Jul	Aug	Sep	Oct	Nov	Dec
1978							248.2	249.4	252.2	254.1	259.7	259.5
1979	262.8	263.4	264.4	265.7	267.5	269.1	269.9	271.6	273.0	273.1	274.4	274.9
1980	276.0								291.4	291.6	293.5	294.0
1981	295.1	294.3	296.6	298.3	300.2	301.9	302.5		305.1	305.5	307.0	310.0
1982	311.4	312.3	314.4	316.0	317.4	319.7	320.9	322.7	323.7	325.5	327.4	327.9
1983	328.7	331.1	333.2	334.5	335.9	337.2	338.7	339.1	338.7	340.5	341.6	342.5
1984	343.1	344.1	345.3	348.5	352.0	353.1	354.5	355.9	356.5	357.5	359.3	361.2
1985	362.8	364.1	365.9	368.3	369.4	370.4	372.5	374.4	375.4	376.4	378.0	379.4
1986	379.6	380.9	382.7	387.5	389.0	390.7	392.0	393.2	394.7	394.1	394.3	395.3
1987	396.0	395.4			404.5	406.1		410.6	410.9	412.8	413.7	414.4
1988	416.4	417.4	419.9	421.3	428.1	427.8	430.3	432.0	433.2	434.4	434.4	434.8
1989	435.9	437.1	439.2	441.8	443.5	444.9	445.8	447.3	448.8	450.1	451.5	454.9
1990	456.0	457.9	459.6	461.1	463.2	463.1	464.4	465.7	467.3	468.7	469.8	470.2
1991	470.1	470.4	471.6	473.3	475.3	476.2	477.6	479.2	481.3	482.0	482.6	483.8

Table 2. *Monthly mean in situ observations of CFC-11 (CCl_3F) (average of silicone and porasil column data, pptv) from the ALE/GAGE program during 1978 - 1990. Monthly means are obtained from individual measurements (ALE, 4 per day; GAGE, 12 per day). Pollution episodes are removed from the data (Prinn et al., 1983; Cunnold et al., 1986, 1993; Prinn et al., 1992). Some of the data are unpublished and subject to revision. Data should not be used for further analysis without consulting the principal investigators, GAGE, R. Prinn, P. Fraser, P. Simmonds, D. Cunnold, F. Alyea. The data are in the SIO 1986 scale (Bullister and Weiss, 1988).*

Adrigole/Mace Head, Ireland

	Jan	Feb	Mar	Apr	May	Jun	Jul	Aug	Sep	Oct	Nov	Dec
1978								162.9	162.8	163.4	164.6	
1979	164.3	164.9	164.2	165.7	167.5	169.1	169.7	170.3	171.7	173.2	173.5	175.2
1980	175.1	175.2	175.4	176.7	179.2	178.0	178.6	178.7	178.9	180.0	180.7	181.5
1981	182.4	182.8	183.7	185.6	186.5	186.5	186.1	188.6	190.9	191.8	192.8	193.4
1982	190.1	190.5	191.6	192.7	192.7	192.3	192.5	192.9	194.2	197.5	198.5	198.5
1983	197.1	198.7	199.0	201.1	202.9	203.1	202.4	204.3	203.2	205.4	206.7	206.2
1984												
1985												
1986												
1987		244.2	241.6	237.9	240.4	243.6	244.2	245.0	248.1	251.2	252.3	251.2
1988	251.5	252.6	249.9	253.5	254.4	255.0	255.1	255.7	257.8	260.3	259.0	259.3
1989	258.1	259.7	259.2	261.8	261.6	261.9	263.1	262.9	264.8	264.3	265.7	266.9
1990	265.4	265.8	266.2	267.9	268.9	268.7	266.6	267.8	269.3	270.1	271.5	269.4
1991	269.6	272.3			269.9	270.4	271.1	271.0		271.6	272.5	272.7

Cape Meares, Oregon

	Jan	Feb	Mar	Apr	May	Jun	Jul	Aug	Sep	Oct	Nov	Dec
1978												
1979												173.5
1980	173.6	171.6	174.5	176.0	176.7	176.7	176.3	178.0	180.6	182.0	182.2	181.0
1981	180.6	181.6	181.7	182.8	183.2	183.8	184.3	185.1	187.1	189.2	190.3	190.5
1982	188.9	189.2	190.1	191.5	191.3	191.4	191.6	191.9	192.9	195.6	197.3	197.7
1983	197.5	197.7	199.1	200.9	201.6	203.6	205.3	206.0	202.9	205.8	206.5	206.3
1984		207.0	206.9	208.9	209.0	208.8	208.8	207.5	210.4	212.9	213.9	214.9
1985	213.4	214.3	215.6	216.9	217.1	216.0	217.5	219.7	222.3	223.1	224.3	223.2
1986	223.4	224.4	226.0	229.3	230.6	230.9	229.8	230.4	235.1	236.1	237.1	238.5
1987	238.7	237.6	239.8	242.5	243.7	245.2	244.3	245.1	247.6	251.0	251.1	252.3
1988	251.6	251.2	252.4	253.7	254.5	254.6	254.5	256.1	258.5	259.4	259.4	259.3
1989	257.9	257.4	257.6	259.6	259.7	260.1						
1990												
1991												

Table 2 Continued.

Ragged Point, Barbados

	Jan	Feb	Mar	Apr	May	Jun	Jul	Aug	Sep	Oct	Nov	Dec
1978							154.7	155.0	154.2	154.5	154.1	157.0
1979	159.2	157.2	158.3		161.9	161.3	163.3	164.9	163.6	163.2	164.6	166.3
1980	166.8	167.6	170.8	170.0	170.5	171.3	172.7	173.6	173.9	172.7	175.5	176.3
1981	176.9	177.1	175.9	177.8	178.4	178.2	180.1	180.3	180.9	181.4	182.7	183.1
1982	184.6	185.0	185.2	186.1	187.3	188.3	189.3	191.8	191.4	191.2	192.6	194.2
1983	194.0	193.7	193.9	196.0	195.6	195.8	198.5	200.9	201.1	200.8	201.1	202.9
1984	203.2	203.7	204.9	204.3	204.8	205.7	207.4	210.4	209.8	210.4	209.6	211.5
1985	211.8	211.3	212.4	212.3	215.1	213.8	216.8	218.5	217.9	219.5	218.3	221.4
1986	220.6	222.3	222.6	223.4	224.7	227.8	230.0	231.0	232.7	231.5	232.5	234.1
1987	235.2	235.5	235.6	236.3	237.7	240.4	241.8	243.2	244.2	244.4	242.1	243.3
1988	245.2	245.1	244.2	244.1	246.4	248.3			252.1	246.0	249.9	252.4
1989	253.7		254.2	255.1	256.0	257.2	259.7	258.5	257.4	258.0	259.7	259.5
1990	261.3	260.9		265.2	265.1	264.6	265.3	266.2	267.0	264.8	266.1	266.8
1991	266.2	265.9	265.4	267.4	267.3	270.2	270.3	270.4	270.5	269.9	269.8	271.5

Cape Matatula, Samoa

	Jan	Feb	Mar	Apr	May	Jun	Jul	Aug	Sep	Oct	Nov	Dec
1978							142.3	145.1	145.4	147.5	148.1	149.7
1979	151.4	151.1	150.0	151.1	150.7	150.7	151.0	152.3	151.9	152.8	154.2	154.5
1980	157.8	158.6	159.6	160.5	161.0	161.0	162.5	162.9	163.9	163.7	166.9	167.7
1981	168.9				169.9	170.8	170.6	172.4	174.9	175.5	176.7	178.0
1982	178.3	177.9	176.8			179.4	179.4	180.2	180.5	181.1	181.0	181.5
1983	182.0	184.5	186.0	186.5	187.2	188.4	188.9	189.1	190.7	190.8	191.6	193.6
1984	195.3	196.2	196.8	196.7	195.0	195.9	197.0	197.7	199.3	198.8	200.0	203.1
1985	203.2	203.6	203.5	203.4	204.5	204.2	205.4	205.9	206.3		208.7	211.4
1986	213.2	214.5	214.0	214.9	214.3	216.6	215.4	216.0	218.4	219.3	219.2	221.6
1987	224.6	226.6	226.2	224.5	225.4	226.1	226.6	227.9	229.0	229.1	231.5	233.1
1988	235.5	234.5	237.0	239.2	237.7	238.2	238.2	239.8	241.1	241.3	241.2	242.1
1989	244.1	246.6	247.2	246.9	247.7	246.6						
1990												
1991												

Cape Grim, Tasmania

	Jan	Feb	Mar	Apr	May	Jun	Jul	Aug	Sep	Oct	Nov	Dec
1978							138.2	140.1	141.8	141.6	143.8	144.1
1979	146.6	146.8	147.1	147.8	148.7	150.0	150.5	151.4	152.4	153.5	154.4	154.5
1980	155.3	156.5	157.5	158.2	160.2	161.0	161.1	161.8	163.5	163.0	164.2	165.4
1981	165.9	164.4	165.7	166.2	167.8	169.3	169.8		170.0		171.5	172.8
1982	173.4	173.9	175.0	175.8	176.7	177.8	178.6	179.4	180.0	180.7	181.7	182.0
1983	182.4	183.1	183.3	184.0	184.8	185.4	186.4	187.1	187.2	188.2	188.8	189.4
1984	189.7	190.3	191.2	193.0	193.9	194.4	195.4	196.1	196.7	197.1	197.7	198.4
1985	199.2	199.7	200.7	202.2	202.9	203.3	204.7	205.8	206.5	207.1	207.9	208.3
1986	208.4	209.1	210.2	211.6	213.1	213.9	214.9	216.1	216.6	216.6	215.9	216.5
1987	217.2	217.6			222.3	223.2		226.7	226.7	228.0	228.7	229.2
1988	230.3	230.8	232.4	233.0	234.7	235.1	236.3	237.2	238.1	238.8	238.4	238.6
1989	239.1	239.7	241.2	242.5	243.4	244.3	244.5	245.4	246.4	247.3	247.6	248.7
1990	249.0	249.7	250.7	251.7	252.3	252.5	253.0	253.4	254.3	254.9	255.3	255.5
1991	255.8	255.5	256.0	256.7	257.5	258.6	259.6	260.4	261.1	261.8	262.1	262.8

Table 3. *Monthly mean in situ observations of CFC-113 (CCl_2FCClF_2) (silicone column data, pptv) from the ALE/GAGE program during 1978 - 1990. Monthly means are obtained from individual measurements (ALE, 4 per day; GAGE, 12 per day). Pollution episodes are removed from the data (Prinn et al., 1983, 1991). All of the data are unpublished and subject to revision. Data should not be used for further analysis without consulting the principal investigators, GAGE, R. Prinn, P. Fraser, P. Simmonds, D. Cunnold, F. Alyea.*

Adrigole/Mace Head, Ireland

	Jan	Feb	Mar	Apr	May	Jun	Jul	Aug	Sep	Oct	Nov	Dec
1987		49.8	52.4	55.9	55.3	55.9	56.7	56.4	55.4	58.1	54.2	56.1
1988	58.9	59.2	58.1	61.4	61.7	62.6	62.6	63.3	60.9	63.4	63.0	62.9
1989	62.0	63.4	64.0	66.4	66.2	66.8	67.3	68.7	69.0	68.8	69.4	70.1
1990	70.0	70.4	70.4	71.0	72.1	72.6	73.6	73.6	72.8	73.4	74.7	74.0

Cape Meares, Oregon

	Jan	Feb	Mar	Apr	May	Jun	Jul	Aug	Sep	Oct	Nov	Dec
1984				41.3	39.6	38.9	38.9	38.6	39.5	41.0	41.7	42.0
1985	44.4	42.6	43.3	43.4	43.8	44.2	44.7	45.4				
1986	47.0	47.2	46.8	47.0	48.0	49.4	47.8	48.2	48.9	50.8	48.9	49.4
1987	49.8	51.4	53.6	54.7	54.7	56.7	56.6	56.6	57.4	57.0	56.3	57.3
1988	57.8	58.0	58.9	60.5	61.6	62.2	62.3	61.1	61.9	62.7	63.1	64.4
1989	63.7	65.5	65.1	66.3	66.6	67.3						

Ragged Point, Barbados

	Jan	Feb	Mar	Apr	May	Jun	Jul	Aug	Sep	Oct	Nov	Dec
1985										39.8	40.5	41.8
1986	41.4	41.5	42.1	42.5	42.6	43.5	44.6	44.7	45.3	45.1	45.6	47.1
1987	47.8	47.3	48.2	48.7	49.6	50.0	50.9	51.5	51.5	51.8	50.3	51.4
1988	52.6	53.2	53.9	53.8	55.0	56.4			57.8	56.4	58.7	59.9
1989	59.6	59.7	61.8	62.0	62.3	63.0	64.5	64.3	63.4	64.0	65.4	65.5
1990	66.6	66.7		68.0	69.9	71.5	72.3	72.6	72.7	71.0	71.3	72.4

Cape Matatula, Samoa

	Jan	Feb	Mar	Apr	May	Jun	Jul	Aug	Sep	Oct	Nov	Dec
1985										38.6	38.1	39.3
1986	40.4	41.2	41.7	42.1	41.9	42.4	42.8	43.3	44.9	45.4	45.6	44.8
1987	43.8		46.1	47.8	47.2	48.2	48.2	47.4	47.4	47.8	49.3	50.1
1988	51.3	51.4	51.2	51.9	51.0	50.3	52.0	52.9	53.9	55.0	56.0	56.6
1989	57.8	58.5	59.6	58.4	59.0	58.6						

Cape Grim, Tasmania

	Jan	Feb	Mar	Apr	May	Jun	Jul	Aug	Sep	Oct	Nov	Dec
1982						25.8	25.8	26.0	26.0	26.3	26.6	26.5
1983	26.5	27.4	27.6	27.6	27.6	27.6	27.9	28.6	28.7	29.0	29.0	29.3
1984	29.5	29.5	30.1	30.9	31.1	31.5	31.9	31.9	32.3	32.5	32.6	33.3
1985	34.0	34.0	34.4	35.0	35.6	35.7	36.1	36.8	37.4	37.7	37.9	38.2
1986	38.5	38.6	39.2	40.7	41.0	40.6	41.3	42.0	41.9			
1987					44.1	44.7		46.9	48.4	47.7	48.6	49.0
1988	49.6	49.1	50.0	50.8	50.1	50.4	50.8		51.8	52.4	52.9	53.6
1989	53.9	53.9	55.3	55.7	56.0	57.0	57.8	58.4	58.8	59.6	59.8	60.1
1990	60.5	61.3	62.2	62.9	63.3	65.0	65.7	65.4	65.7	65.9	66.5	66.6

Table 4. *Monthly mean in situ observations of carbon tetrachloride (CCl_4) (silicone column data, pptv) from the ALE/GAGE program during 1978 - 1990. Monthly means are obtained from individual measurements (ALE, 4 per day; GAGE, 12 per day). Pollution episodes are removed from the data (Prinn et al., 1983, 1991; Simmonds et al., 1988). Some of the data are unpublished and subject to revision. Data should not be used for further analysis without consulting the principal investigators, GAGE, R. Prinn, P. Fraser, P. Simmonds, D. Cunnold, F. Alyea.*

Adrigole/Mace Head, Ireland

	Jan	Feb	Mar	Apr	May	Jun	Jul	Aug	Sep	Oct	Nov	Dec
1979												126.1
1980	128.2	126.4	124.8	126.3	126.0	125.8	125.9	125.7	125.2	125.2	127.2	127.3
1981	128.3	129.4	132.1	131.5	132.3	127.8	127.5	127.3	130.2	129.4	129.5	128.8
1982	126.0	126.2	125.6	125.8	127.1	126.8	126.9	127.3	127.5	127.3	127.8	127.7
1983	127.3	129.6	129.5	129.4	130.4	129.0	128.1	128.2	128.0	129.4	129.8	129.8
1984												
1985												
1986												
1987		129.2	127.7	129.3	130.7	130.7	130.3	130.4	131.9	132.4	132.4	133.3
1988	133.2	134.1	135.0	136.4	136.9	137.3	137.1	135.8	136.5	138.0	137.5	137.6
1989	136.6	136.2	135.8	139.9	140.3	141.0	142.6	142.6	142.2	140.0	142.6	140.5
1990	140.8	140.9	141.1	140.9	140.0	138.8	131.9	135.6	138.9	137.5	136.3	142.5

Cape Meares, Oregon

	Jan	Feb	Mar	Apr	May	Jun	Jul	Aug	Sep	Oct	Nov	Dec
1979												123.4
1980	124.1	123.0	123.5	122.1	122.1	122.0	121.7	121.3	122.6	123.7	124.2	123.9
1981	125.0	123.8	124.1	124.4	125.0	125.0	124.5	123.3	124.0	124.7	125.3	125.5
1982	124.1	124.6	124.2	125.3	125.4	125.2	125.3	124.0	123.9	124.7	125.2	126.1
1983	125.6	125.0	125.9	125.9	126.1	127.6	128.1	128.2	127.6	128.8	129.2	130.0
1984	128.1	128.3	127.9	128.7	128.8	128.7	128.1	127.7	128.4	129.2	129.6	129.6
1985	131.9	129.2	129.2	129.0	129.1	128.1	128.7	129.0		130.2	130.6	131.4
1986	130.2	130.5	130.7	131.1	131.2	131.6	131.3	130.6	130.9	131.8	133.9	133.8
1987	133.0	133.2	132.8	132.7	132.1	133.2	132.4	132.8	132.8	132.1	132.1	132.4
1988	132.0	131.6	132.6	133.4	133.8	133.4	133.2	132.8	133.2	133.6	134.5	134.1
1989	134.7	134.7	134.6	134.1	134.3	134.3						

Ragged Point, Barbados

	Jan	Feb	Mar	Apr	May	Jun	Jul	Aug	Sep	Oct	Nov	Dec
1978							114.6	116.0	115.3	114.3	113.2	116.6
1979	118.3	118.1	115.9		117.9	118.3	118.1	117.9	117.2	117.6	118.5	119.2
1980	119.9	119.6	120.8	120.4	120.5	120.9	120.9	121.2	120.2	120.6	121.2	121.7
1981	121.7	121.8	121.7	122.6	122.7	122.9	123.8	123.3	122.0	123.0	123.3	121.5
1982	122.6	122.1	122.1	123.0	122.7	123.4	123.9	125.1	124.8	125.2	125.5	127.5
1983	127.3	127.0	126.8	124.6	123.4	123.0	123.7	126.0	125.8	125.8	125.9	126.1
1984	126.2	126.2	126.3	126.7	127.7	128.2	128.2	128.1	128.4	128.5	128.4	129.6
1985	129.7	129.6	129.5	129.1	129.4	129.4	129.0	129.3	128.6	128.1	128.4	129.2
1986	129.1	130.6	131.2	132.6	131.5	132.0	133.1	133.6	133.9	133.2	133.2	133.6
1987		134.4	134.8	134.7	134.9	134.1	134.0	133.6	134.1	133.8	134.3	134.5
1988	134.7	134.7	134.9	134.7	134.9	134.9			135.5	133.3	134.2	134.9
1989	134.4	133.7	136.2	135.9	136.0	135.8	136.2	134.6	133.9	134.1	134.1	134.1
1990	134.4	134.0		135.5	136.5	137.1	137.0	137.1	137.1	136.4	137.1	137.5

***Table 4** Continued.*

Cape Matatula, Samoa

	Jan	Feb	Mar	Apr	May	Jun	Jul	Aug	Sep	Oct	Nov	Dec
1978							110.7	111.1	111.4	111.2	113.0	114.0
1979	114.9	113.8	113.6	114.3	114.2	114.2	114.9	114.9	114.8	115.6	112.6	115.0
1980	116.5	115.9	115.5	115.7	116.0	116.0	116.2	116.4	116.3	116.1	116.8	117.3
1981	117.6	118.3	117.8	118.0	117.4	117.7	117.3	118.1	118.3	116.9	117.3	117.7
1982	118.7	120.4	120.3			120.6	120.2	120.3	119.9	120.2	118.4	118.5
1983	118.7	119.7	121.0	121.0	121.3	121.3	121.2	122.0	122.6	122.3	122.4	123.0
1984	124.0	123.4	123.1	122.7	122.1	121.9	122.1	122.5	122.8	122.6	123.1	124.3
1985	124.5	125.1	125.1	124.9	125.1	124.8	124.6	124.1	124.2	124.7	124.5	125.4
1986	126.0	126.1	125.8	125.9	125.8	126.0	126.1	125.6	126.4	126.9	126.5	126.5
1987	127.0	127.3	127.0	126.4	130.0	127.8	127.4	127.5	127.8	126.7	127.6	128.2
1988	128.2	128.4	130.5	129.6	128.5	128.6	129.3	131.2	131.4	131.1	130.9	130.8
1989	131.4	131.7	131.6	131.8	131.9	131.2						

Cape Grim, Tasmania

	Jan	Feb	Mar	Apr	May	Jun	Jul	Aug	Sep	Oct	Nov	Dec
1978							113.8	113.1	113.7	113.9	114.3	113.8
1979	113.1	112.6	112.9	113.2	113.2	113.0	113.0	112.8	112.8	114.1	114.4	114.5
1980	114.5	114.8	115.3	116.2	116.8	116.6	115.3	115.1	116.1	114.9	116.4	116.4
1981	116.6	115.1	115.7	115.8	116.3	116.9	117.5			116.4	116.6	117.8
1982	117.8	118.1	118.1	118.5	119.2	119.3	119.3	119.5	119.3	119.4	119.7	119.6
1983	119.7	120.2	120.5	120.6	120.6	120.6	120.5	120.4	120.0	120.1	120.1	120.4
1984	120.5	120.7	121.0	121.8	122.6	122.7	122.8	122.9	122.8	123.1	123.0	123.1
1985	123.4	123.4	123.6	124.0	124.2	123.9	124.5	125.1	125.2	125.1	125.3	125.3
1986	125.4	125.5	125.6	126.5	126.5	126.7	126.8	126.5	126.9	126.8	127.6	127.7
1987	127.8	128.1	128.1	128.1	128.3	128.5		129.1	129.0	129.2	129.2	129.3
1988	129.8	129.6	129.8	130.0	129.6	130.0	130.0	129.4	129.2	129.2	129.4	129.6
1989	129.7	129.8	130.1	130.2	130.2	130.1	129.8	129.8	129.7	129.8	130.0	131.1
1990	131.3	131.5	131.9	131.5	131.5	131.5	131.4	131.1	131.4	131.2	131.5	131.3

C.2.

Table 5. *Monthly mean in situ observations of methyl chloroform (CH_3CCl_3) (silicone column data, pptv) from the ALE/GAGE program during 1978 - 1990. Monthly means are obtained from individual measurements (ALE, 4 per day; GAGE, 12 per day). Pollution episodes are removed from the data (Prinn et al., 1983, 1987, 1992). Some of the data are unpublished and subject to revision. Data should not be used for further analysis without consulting the principal investigators, GAGE, R. Prinn, P. Fraser, P. Simmonds, D. Cunnold, F. Alyea.*

Adrigole/Mace Head, Ireland

	Jan	Feb	Mar	Apr	May	Jun	Jul	Aug	Sep	Oct	Nov	Dec
1978							112.1	109.8	105.8	107.4	107.7	
1979	111.4	112.7	112.2	115.4	117.2	117.7	115.1	115.8	116.9	120.3	119.7	122.5
1980	121.8	123.0	126.6	130.1	132.1	130.6	130.7	127.0	124.8	127.4	129.0	129.2
1981	128.5	129.4	130.2	131.9	135.0	135.3	131.4	131.9	134.2	134.2	134.7	137.2
1982	132.4	133.8	138.9	140.9	138.5	138.8	138.3	134.5	135.5	139.8	142.8	141.4
1983	138.2	140.5	141.8	145.1	150.2	146.4	142.4	142.3	139.3	141.8	146.2	147.1
1984												
1985												
1986												
1987		156.8	154.7	157.4	162.3	164.4	162.3	159.3	159.0	164.3	167.4	166.5
1988	166.9	168.6	168.6	173.3	175.3	175.3	174.0	167.3	169.0	174.6	173.6	173.8
1989	170.2	173.4	172.7	181.6	179.8	178.6	176.7	174.6	175.4	177.0	178.5	182.3
1990	179.7	181.8	181.8	184.1	188.1	189.8	182.3	182.8	182.7	184.5	188.8	195.6

Cape Meares, Oregon

	Jan	Feb	Mar	Apr	May	Jun	Jul	Aug	Sep	Oct	Nov	Dec
1979												125.4
1980	127.7		123.9	126.4	126.3	124.1	120.8	121.5	125.4	132.1	130.1	128.2
1981	129.4	133.0	128.6	128.9	129.8	130.6	126.4	126.2	128.9	131.0	134.3	135.8
1982	134.6	135.3	136.4	139.6	139.0	136.9	134.4	131.0	130.6	134.5	135.9	138.9
1983	137.4	137.5	141.6	143.1	141.7	141.4	139.4	137.1	137.0	140.5	142.8	147.8
1984	144.2	148.0	147.9	150.0	150.3	149.9	146.8	142.5	143.8	147.8	149.5	151.6
1985	155.9	150.5	152.9	153.7	153.2	152.2	149.8	149.1	152.2	154.1	156.6	156.7
1986	156.2	156.6	157.9	162.1	162.0	161.4	153.4	148.4	151.4	159.0	161.1	164.0
1987	165.8	163.4	161.1	164.6	164.9	169.3	163.7	158.6	162.2	173.6	170.3	173.4
1988	172.0	172.3	172.9	174.7	175.1	175.3	172.0	165.7	168.4	170.1	171.8	175.5
1989	170.4	174.0	172.2	177.3	176.5	176.2						

Ragged Point, Barbados

	Jan	Feb	Mar	Apr	May	Jun	Jul	Aug	Sep	Oct	Nov	Dec
1978							99.6	99.5	94.2	94.6	92.7	99.3
1979	100.2	99.8	100.9		101.7	99.9	102.8	105.7	99.0	98.9	102.8	105.2
1980	107.8	108.5	112.5	110.1	111.0	113.8	112.9	111.3	109.6	109.9	114.9	115.4
1981	114.8	116.8	112.6	117.4	119.1	117.5	120.4	116.4	115.9	116.6	116.3	115.4
1982	120.3	120.5	120.1	126.0	123.8	124.1	125.6	125.0	121.3	119.3	123.1	130.1
1983	128.9	127.4	125.4	130.4	129.0	128.4	130.3	129.7	127.0	124.7	125.4	132.1
1984	132.6	132.3	135.5	131.6	135.8	136.5	137.7	139.6	135.4	134.2	132.0	139.6
1985	140.5	140.8	142.6	140.1	144.0	137.4	144.2	144.0	137.4	138.5	138.1	144.9
1986	141.9	144.6	145.3	145.8	141.4	144.6	149.4	146.5	145.2	141.2	137.3	142.4
1987		145.4	149.4	150.2	150.4	150.6	151.3	151.2	147.7	144.9	144.8	148.1
1988	152.0	154.5	156.2	153.2	157.4	156.6			153.4	144.6	154.2	158.8
1989	157.7	157.8	159.7	160.8	161.0	161.1	163.8	159.7	153.8	153.7	159.9	160.3
1990	165.1	164.6		164.3	166.9	167.9	167.1	165.0	162.0	156.2	165.0	171.1

Table 5 *Continued.*

Cape Matatula, Samoa

	Jan	Feb	Mar	Apr	May	Jun	Jul	Aug	Sep	Oct	Nov	Dec
1978							71.1	72.1	72.4	74.2	74.6	75.0
1979	78.0	75.8	76.6	76.2	77.9	78.5	79.7	81.2	81.3	83.0	85.1	79.1
1980	84.0	86.2	86.7	87.1	88.2	89.2	90.5	91.6	92.1	92.5	94.2	96.1
1981	96.7		97.8	96.2	95.9	97.4	97.4	99.4	100.2	97.8	97.9	98.8
1982	99.4	101.8	100.0			101.3	100.9	102.2	102.1	102.1	101.4	100.9
1983	100.2	101.8	102.9	103.4	104.6	105.9	106.6	106.8	108.2	107.6	106.6	109.1
1984	111.6	112.6	114.5	111.9	109.0	110.0	111.0	112.2	113.2	112.6	113.5	115.6
1985	116.5	117.2	116.4	115.8	116.7	116.5	117.4	117.2	117.3	116.9	116.6	118.5
1986	121.2	122.6	118.6	120.4	119.1	119.0	119.5	119.3	120.9	120.0	118.9	119.4
1987	118.1		121.7	123.5	123.1	123.5	124.2	125.3	125.4	125.5	126.3	127.4
1988	128.9	131.0	131.1	134.4	129.4	132.5	131.0	132.0	132.7	132.7	132.7	133.5
1989	136.1	137.1	137.8	135.0	135.5	133.7						

Cape Grim, Tasmania

	Jan	Feb	Mar	Apr	May	Jun	Jul	Aug	Sep	Oct	Nov	Dec
1978							68.8	66.6	68.4	70.8	74.9	74.2
1979	73.1	73.1	75.1	76.5	76.6	78.1	77.3	78.7	79.8	80.8	81.5	81.0
1980	80.6	81.0	82.4	82.0	85.9	86.8	87.6	88.7	89.9	90.8	90.6	89.4
1981	89.4	89.7	91.2	92.1	92.8	93.4	93.2		93.7	96.2	96.5	97.2
1982	96.7	96.5	97.0	98.3	99.9	101.2	102.1	103.0	103.1	103.4	103.2	102.5
1983	101.9	102.5	103.2	103.8	104.8	105.4	106.6	107.4	107.3	107.6	107.4	106.5
1984	105.9	105.7	106.3	107.0	108.1	109.4	110.3	111.4	111.8	112.7	112.3	111.4
1985	110.6	110.3	111.2	112.9	113.8	114.4	114.6	117.0	118.2	117.5	117.1	116.0
1986	115.0	114.7	115.5	118.2	119.0	120.2	121.2	121.6	122.2	120.7	119.2	118.6
1987	117.8	117.4	118.0	119.4	120.7	122.1		124.8	124.6	125.0	124.5	123.8
1988	123.4	122.6	123.3	124.6	127.9	128.6	129.4	130.2	130.5	130.6	129.9	128.8
1989	128.0	128.2	129.0	130.5	131.5	132.6	133.6	134.2	134.8	134.6	133.8	133.8
1990	132.6	132.7	132.7	133.8		135.8	136.6	137.4	138.1	138.2	137.8	136.6

Table 6. *Monthly mean flask observations of CFC-12 (CCl_2F_2) (pptv) from the NOAA-CMDL program during 1977 - 1990. Monthly means are obtained from individual flask measurements (Elkins et al., 1993). Data should not be used for further analysis without consulting the principal investigator, NOAA-CMDL, J. Elkins. The data are in the NOAA-CMDL gravimetric scale.*

Point Barrow, Alaska

	Jan	Feb	Mar	Apr	May	Jun	Jul	Aug	Sep	Oct	Nov	Dec
1977									271.2			
1978				290.5			286.2		291.6	296.1	299.4	296.8
1979	298.2	296.0	298.2	295.6	294.7	298.6	299.5	298.6	306.6	303.3	308.9	311.1
1980	312.8	307.9	310.5	316.3	315.7	313.4	309.7	313.7	319.3	318.4	327.4	335.8
1981	324.0	329.3	327.0	330.6	328.9	327.9	334.5	341.2	335.6	339.4	341.5	344.4
1982	345.3	348.5	347.0	349.0	349.9	344.6	348.9	350.1	352.5	357.9	361.3	361.1
1983	363.8	364.4	363.3	363.7	366.1	362.8	363.1	365.7	369.1	377.1	375.6	375.1
1984	383.4	385.2	377.1									
1985		404.4	392.1	392.8	397.5	404.4	391.1	394.4	406.4	414.1	417.5	419.7
1986	419.0	421.0	422.5	424.1	420.4	420.2	420.3	418.2	420.5	429.7	433.0	437.0
1987	435.2	436.2	443.6	442.3	440.7	437.8	445.3	441.4	450.0	454.7	458.0	458.4
1988	457.4	459.4	460.7	461.1	458.2	460.9	461.4	463.3	465.8	470.7	479.9	476.4
1989	479.0	473.9	475.2	475.5	476.8	472.4	480.4	476.8	480.6	484.6	491.8	493.0
1990	495.2	502.9	491.1	489.7	489.1	491.7	484.8	488.2	489.4	495.6	497.1	498.7
1991	501.1	501.9	505.0	501.0	494.7	500.4	498.8	501.3	506.3	509.9	511.7	518.7

Niwot Ridge, Colorado

	Jan	Feb	Mar	Apr	May	Jun	Jul	Aug	Sep	Oct	Nov	Dec
1977							254.2	262.8	253.1			272.5
1978			274.8			292.4	291.8			291.6	284.2	
1979	279.8	286.5		310.8	292.5	292.7	290.0	294.5	302.7	292.6	295.3	304.0
1980	308.0	311.7	315.5	310.4	314.1	307.1	307.4	308.2	306.7	311.2	310.9	314.8
1981	315.4	317.1	322.9	324.0	325.9	327.2	330.1	331.6	332.8	337.6	330.1	333.5
1982	336.9	334.8	338.1	347.7	340.6	345.4	350.9	347.4	348.2	352.0	351.9	350.6
1983	353.2	355.7	357.2	358.6	362.5	362.2	371.2	357.9	366.4	368.5	372.1	375.6
1984	373.9	372.0	368.2									
1985			383.8	387.4	389.0	392.2	386.9	393.6	399.9	405.2	413.3	407.8
1986	408.6	408.3	411.6	409.9	417.7	418.1	415.5	420.6	415.1	422.4	422.0	424.0
1987	426.6	424.7	437.8	434.6		440.9	437.7	439.6	445.8	451.8	450.3	449.2
1988	451.9	448.0	457.6	457.8	458.4	452.3	465.4	465.2	463.6	460.5	470.8	464.5
1989	465.1	469.9	461.8	467.9	471.5	472.4	476.2	478.9	479.4	476.5	484.5	482.4
1990	481.7	494.1	485.4	483.2	487.7	490.2	487.0	486.0	497.0	491.9	495.6	496.4
1991	495.4	494.5	494.1	499.9	494.1	498.3	500.4	500.7	506.3	509.0	502.3	505.2

Table 6 *Continued.*

Mauna Loa, Hawaii

	Jan	Feb	Mar	Apr	May	Jun	Jul	Aug	Sep	Oct	Nov	Dec
1977					258.0		260.8		260.4	266.6	266.8	276.5
1978	276.7	272.0	276.3	283.5		286.2	282.4	284.4	282.3	282.4	286.7	296.6
1979	296.0	288.1	290.7	288.3	294.6	299.6	298.8		304.0	317.8	304.3	305.2
1980	311.0	320.5	304.6	310.6	299.0	311.1	314.1	308.4	307.3	318.3	316.5	312.8
1981	311.2	317.9	317.5	327.7	332.5	337.3	336.9	333.1	338.4	341.3	336.4	348.1
1982	340.8	341.8	337.1	338.8	339.8	340.4	338.6	341.8	346.8	347.6	348.7	352.2
1983	346.8	353.8	352.8	353.4	352.7	355.7	362.2	355.3	367.9	366.9	372.2	366.2
1984	367.5	375.8	361.7									
1985		380.3	382.2	377.3	387.2	396.9	383.3	384.5	400.6	407.7	401.6	408.6
1986	406.5	403.4	409.7	412.2	411.3	414.3	410.0	415.7	416.9	426.3	425.0	426.4
1987	428.3	418.2	439.0	430.2		431.3	430.9	435.4	444.6	445.1	445.4	440.6
1988	440.3	445.1	442.3	450.7	449.3	450.4	454.5	453.4	457.0	458.4		465.8
1989	465.9	458.3	462.4	465.6	465.1	469.7	466.0	469.8	472.8	475.6	479.4	473.6
1990	481.4	478.8	479.3	488.7	482.9	482.5	480.9	483.2	485.9	486.4	485.9	488.9
1991	489.6	484.5	489.7	494.7	493.5	495.3	494.9	495.5	496.9	499.5	502.1	501.9

Cape Matatula, Samoa

	Jan	Feb	Mar	Apr	May	Jun	Jul	Aug	Sep	Oct	Nov	Dec
1977								242.1	241.4	243.8	244.1	250.7
1978	253.6	256.0	249.3		261.5	260.0	257.6	258.9	262.3	263.1	266.9	266.8
1979	273.8	273.4	273.1	274.0	272.3	273.2	276.0	279.5	280.4	280.6	292.1	280.8
1980	285.2	284.9	285.0	288.3	290.1	289.4	290.1	289.2	293.5	292.9	292.6	296.8
1981	300.2	303.5	304.6	306.8	309.9	310.4	313.3	313.9	312.5	316.4	318.5	319.8
1982	324.7	328.5	324.7	327.6	324.0	326.0	328.8	330.5	331.1	333.9	333.2	333.5
1983	338.6	339.5	343.2	342.5	341.9	342.1	336.5	346.1	352.2	355.0	356.6	357.9
1984	357.4	364.6	359.3									
1985		373.5	370.3	371.1	379.3	377.9	375.9	373.8	388.2	390.2	390.3	393.3
1986	395.6	399.8	397.9	398.6	399.3	402.3	402.4	404.0	406.5	406.5	405.9	409.7
1987	412.2	415.0	421.8	411.8	415.2	407.8	415.8			419.0	423.2	424.2
1988	426.5	429.8	426.3	435.2	432.2	430.3	438.1	438.0	438.1	444.6	449.2	445.3
1989	448.8	451.9	446.2	449.2	451.9	443.4	454.9	454.2	457.0	460.4	459.3	463.2
1990	471.8	461.7	464.9	464.0	462.7	466.5	463.8	467.1	468.6	471.2	473.5	476.7
1991	482.4		481.3	482.7	486.7	480.8	483.3	487.5	487.6	488.5	489.2	491.4

Table 7. *Monthly mean flask observations of CFC-11 (CCl_3F) (pptv) from the NOAA-CMDL program during 1977 - 1990. Monthly means are obtained from individual flask measurements (Elkins et al., 1993). . Data should not be used for further analysis without consulting the principal investigator, NOAA-CMDL, J. Elkins. The data are in the NOAA-CMDL gravimentric scale.*

Point Barrow, Alaska

	Jan	Feb	Mar	Apr	May	Jun	Jul	Aug	Sep	Oct	Nov	Dec
1977	145.4	148.1	143.9	145.5	150.7	143.2		146.6	147.6	154.6	155.0	157.8
1978	156.4	155.5	156.6	158.9	156.7	156.9	157.6	158.6	161.5	163.1	167.7	165.9
1979	164.6	165.3	167.8	167.3	166.1	165.7	166.1	165.6	167.8	172.2	173.1	174.9
1980	175.8	174.5	176.6	175.2	174.6	175.7	175.2	176.1	177.2	178.2	176.4	181.5
1981	180.9	185.1	182.1	183.8	182.5	183.5	183.5	184.1	183.4	187.8	190.0	192.2
1982	190.6	192.8	193.6	192.1	190.3	189.7	190.9	191.8	193.8	195.3	196.9	198.0
1983	199.5	198.9	199.1	200.8		201.6	202.1	200.1	203.9	204.4	207.5	205.8
1984	209.1	209.7	208.8	206.9	208.8	207.9	209.3	209.0	210.8	213.7	215.5	218.3
1985	218.9	224.5	220.2	222.8	221.0	218.4	218.9	223.0	223.1	227.6	229.7	230.1
1986	230.8	230.5	231.7	237.6	231.9	231.5	231.2	233.8	232.4	238.7	239.0	242.8
1987	242.1	242.3	242.4	245.2	245.5	244.6	246.7	246.4	248.6	252.7	255.3	256.2
1988	254.0	256.6	256.2	258.2	255.9	256.6	256.3	257.9	258.8	261.4	266.3	265.3
1989	263.8	265.4	266.4	267.0	265.2	263.6	264.1	263.1	265.9	271.6	271.5	275.5
1990	275.7	277.3	274.0	272.4	270.3	271.8	268.6	270.5	270.4	272.2	273.1	276.1
1991	276.0	277.8	278.6	275.0	274.1	273.7	272.7	274.1	274.1	276.5	276.8	279.6

NiwotRidge,Colorado

	Jan	Feb	Mar	Apr	May	Jun	Jul	Aug	Sep	Oct	Nov	Dec
1977	151.1	149.2	143.5	146.2	147.2	140.1	143.3	146.1	144.7	151.3	148.4	154.8
1978	149.5	153.7	151.6		158.4	152.1	156.6	157.9	163.3	160.1	161.7	158.5
1979	158.3	158.0	162.3	160.9	160.2	162.8	162.2	164.2	162.7	168.2	168.9	168.3
1980	168.0	168.4	177.1	171.8	175.6	172.3	174.1		172.5	174.7	176.7	174.1
1981	176.2	176.7	178.7	176.3	180.3	180.4	179.8	181.3	182.5	184.6	182.4	183.4
1982	184.4	183.3	187.1	188.2	187.6	188.1	190.8	188.1	190.3	190.1	193.8	193.8
1983	192.5	195.0	196.8	198.7	199.3	197.8	197.9	198.2	200.6	202.1	201.4	204.5
1984	203.1	201.3	206.4	204.3	205.7	205.5	204.3	204.7	208.0	212.1	210.1	213.4
1985	212.9	211.7	215.4	215.6	217.6	214.9	215.0	218.3	222.6	224.1	224.9	223.5
1986	223.1	227.5	225.6	226.3	227.9	229.8	226.4	230.9	228.6	233.3	237.0	233.6
1987	233.8	236.0	237.0	237.7	241.1	241.1	240.0	242.8	242.4	250.1	248.4	249.5
1988	250.1	249.2	250.7	252.5	257.6	253.1	255.7	256.1	254.5	253.6	261.7	258.0
1989	257.9	260.7	257.6	259.7	259.8	260.0	265.9	264.0	266.1	263.9	268.7	265.3
1990	266.8	268.1	270.4	266.6	266.8	267.0	265.8	267.2	270.0	269.4	271.4	270.3
1991	268.8	272.7	269.4	273.3	269.2	271.8	272.6	271.2	274.7	272.4	273.4	275.1

***Table 7** Continued.*

Mauna Loa, Hawaii

	Jan	Feb	Mar	Apr	May	Jun	Jul	Aug	Sep	Oct	Nov	Dec
1977	139.9	139.5	139.0	134.1	135.0	143.4	140.3	142.6	144.7	144.2	144.8	145.7
1978	148.6	144.8	148.4	147.9	149.9	149.5	152.7	151.9	155.1	153.2	154.9	154.7
1979	157.4	157.5	158.8	158.0	157.1	157.6	159.8		163.3	168.4	166.5	165.3
1980	167.1	165.8	168.1	169.8	165.8	169.7	171.3	171.9	169.9	173.4	175.7	172.7
1981	172.1	175.2	176.2	176.6	176.8	177.6	180.0	179.1	182.2	182.1	181.5	183.8
1982	181.4	183.0	182.5	183.4	185.1	184.7	184.9	186.2	188.2	188.7	189.1	188.2
1983	189.9	191.1	192.7	192.8	194.1	197.6	197.3	197.4	198.9	198.7	198.6	201.0
1984	200.7	201.7	200.6	202.8	201.7	203.0	203.6	205.1	206.6	209.4	212.3	211.7
1985	212.5	212.0	215.6	213.8	215.2	216.6	215.4	216.8	217.4	221.2	219.4	224.0
1986	218.8	219.1	222.5	227.7	226.0	225.7	227.0	227.4	231.6	232.7	232.8	233.1
1987	233.0		235.4	237.5		237.3	236.9	238.1	241.0	243.3	243.2	240.8
1988	240.5	244.9	241.6	246.9	247.1	248.2	248.1	249.2	251.5	252.0	256.6	251.4
1989	255.6	253.6	255.2	257.4	257.5	258.8	257.9	260.0	261.9	261.7	261.8	262.2
1990	263.7	262.9	263.6	262.3	263.3	266.8	263.9	264.0	263.5	267.2	265.5	269.3
1991	269.0	265.3	268.1	270.0	271.0	267.3	270.0	268.9	268.6	267.9	271.4	273.4

CapeMatatula,Samoa

	Jan	Feb	Mar	Apr	May	Jun	Jul	Aug	Sep	Oct	Nov	Dec
1977								133.6	133.9	135.2	134.4	133.5
1978	138.3	137.8	138.1	141.0	141.5	141.3	141.2	143.4	143.3	144.9	147.6	146.6
1979	149.4	152.1	149.7	151.3	150.2	149.8	152.1	152.2	152.0	156.4	155.5	155.4
1980	158.0	158.9	159.0	159.0	159.7	161.2	160.2	160.3	163.9	162.3	162.2	163.0
1981	165.7	166.9	166.7	168.0	168.2	168.3	170.9	170.8	171.9	172.5	174.5	174.5
1982	176.4	176.6	175.4	178.1	177.6	177.0	178.8	180.4	180.3	181.5	181.8	181.1
1983	185.6	183.0	186.8	186.2	185.8	187.4	187.5	186.4	188.0	190.8	189.3	193.7
1984	195.0	196.4	193.3	196.3	194.3	193.9	194.7	195.5	199.6	197.6	197.9	204.2
1985	204.7	206.4	207.1	208.0	206.9	205.8	207.4	208.3	210.0	210.6	209.8	213.1
1986	213.9	209.8	214.2	214.7	219.6	220.0	219.1	220.9	221.4	220.5	221.5	223.8
1987	223.5	229.5	227.0	224.4	228.5	225.6	226.3		231.9	229.7	232.5	233.5
1988	235.0	236.1	233.8	238.4	236.2	237.5	238.1	240.8	237.8	241.3	242.8	247.3
1989	248.1	247.5	246.3	248.6	248.7	248.1	249.1	253.1	252.1	252.1	252.7	254.1
1990	256.9	253.1	255.9	256.0	253.1	255.6	256.1	258.6	258.0	256.7	258.8	262.8
1991	261.7		262.4	262.5	263.0	261.8	263.2	265.6	265.2	265.3	265.2	262.9

Table 8. *Monthly mean shipboard observations of CFC-12 (CCl_2F_2), CFC-11 (CCl_3F), CFC-113 (CCl_2FCClF_2), carbon tetrachloride (CCl_4) and methyl chloroform (CH_3CCl_3) (pptv) from the UEA program in the latitude bands 30°S-90°S, EQ-30°S, 30°N-EQ and 90°N-30°N, during November 1981 - 1984 (Penkett, 1991).*

	CCl_2F_2	CCl_3F	CCl_2FCClF_2	CCl_4	CH_3CCl_3
30°S - 90°S					
1981	311.2	175.5		100.6	101.6
1982	323.9	182.6		103.4	105.6
1983	337.1	194.7	27.3	104.9	110.6
1984	359.3	202.8	29.1	107.3	117.6
EQ - 30°S					
1981					
1982	327.2	184.9		104.3	106.3
1983	352.0	198.7	27.5	107.0	116.5
1984	357.4	204.6	30.0	107.5	120.7
30°N - EQ					
1981		197.6			
1982	354.9	213.6		111.5	136.4
1983	362.7	213.1	30.8	111.0	140.7
1984	371.2		33.3	109.9	141.8
90°N - 30°N					
1981					
1982	353.1	195.6		108.4	142.6
1983					
1984	378.5	218.2	34.6	111.6	155.0

Table 9. *Monthly mean shipboard observations of CFC-12 (CCl_2F_2) (pptv) from the SIO program within the latitude band 30°S-90°S, EQ-30°S, 30°N-EQ and 90°N-30°N, during 1982 - 1990. Monthly means are obtained from individual measurements (Weiss, 1991).*

30°S - 90°S

	Jan	Feb	Mar	Apr	May	Jun	Jul	Aug	Sep	Oct	Nov	Dec
1983										343.7	344.7	345.1
1984	347.9	345.9										
1985		364.5	365.2									
1986	381.6	381.0				391.1	389.6	390.3	392.4	393.5	394.3	393.6
1987												
1988												435.9
1989	436.6	438.8	441.9									
1990			460.5									

EQ - 30°S

1982												338.5
1983		336.6								345.7		
1984												
1985												
1986												
1987											421.4	420.9
1988	423.0	423.5	434.8									
1989	435.3		446.3	454.8								
1990		464.4		463.6								

30°N - EQ

1982												347.3
1983	352.7	348.1								350.1		
1984												
1985				388.0	385.9	401.9						
1986												
1987											436.0	430.7
1988			439.1									
1989		459.7	454.7	458.8	458.9							
1990				468.0								

90°N - 30°N

1982		345.2	351.2	343.2								
1983			346.9									
1984												
1985			401.9	393.9		395.6		397.8	399.8			
1986												
1987											459.5	

Table 10. *Monthly mean shipboard observations of CFC-11 (CCl_3F) (pptv) from the SIO program within the latitude band 30°S-90°S, EQ-30°S, 30°N-EQ and 90°N-30°N, during 1982 - 1990. Monthly means are obtained from individual measurements (Weiss, 1991).*

30°S - 90°S

	Jan	Feb	Mar	Apr	May	Jun	Jul	Aug	Sep	Oct	Nov	Dec
1983										190.2	191.5	191.4
1984	191.9	190.9										
1985		201.5	201.8									
1986	211.5	210.8				216.7	215.6	216.0	217.6	217.9	218.1	218.5
1987												
1988												236.7
1989	238.5	240.8	241.7									
1990			252.0									

EQ - 30°S

1982												189.6
1983		188.7								191.6		
1984												
1985												
1986												
1987											232.6	233.4
1988	233.1	234.1	238.3									
1989	238.2		244.1	248.6								
1990		252.6		254.4								

30°N - EQ

1982												193.6
1983	198.1	194.2								194.3		
1984												
1985				215.9	214.3	219.5						
1986												
1987											240.6	238.3
1988			241.7									
1989		254.5	252.7	252.5	250.6							
1990				251.9								

90°N - 30°N

1982		194.4	199.6	208.1								
1983			199.9									
1984				251.9								
1985			227.7	217.1		216.8		221.4	222.2			
1986				251.9								
1987											249.5	

Table 11. *Monthly mean in situ observations of CFC-11 (CCl_3F) and carbon tetrachloride (CCl_4) (pptv) from the FIAER-CSIR program at Cape Point, South Africa, during 1976 - 1987. Monthly means are obtained from individual measurements (Scheel et al., 1990; Brunke and Scheel, 1991). Some of the data are unpublished and subject to revision. Data should not be used for further analysis without consulting the principal investigators, FIAER, H. Scheel; CSIR, E. Brunke.*

CCl_3F

	Jan	Feb	Mar	Apr	May	Jun	Jul	Aug	Sep	Oct	Nov	Dec
1979							169.0	166.0	162.0	172.0	170.0	173.0
1980	167.0	164.0	161.0	169.0	170.0	175.0	171.0	175.0	175.0	180.0	173.0	172.0
1981	175.0	175.0	176.0	176.0	177.0	177.0	180.0	183.0	186.0	183.0	188.0	183.0
1982	183.0	181.0	184.0	186.0	186.0	193.0	194.0	195.0	195.0	194.0	194.0	197.0
1983	195.0	195.0	197.0	198.0	199.0	200.0	197.0	198.0	201.0	199.0	199.0	198.0
1984	198.0	200.0	203.0	205.0	205.0	210.0	212.0	212.0	213.0	211.0	209.0	210.0
1985	209.0	212.0	213.0	214.0	213.0	215.0	216.0	218.0	217.0	217.0	220.0	219.0
1986	219.0	219.0	221.0	222.0	226.0	228.0	228.0	229.0	225.0	226.0		228.0
1987	223.0	226.0	228.0	233.0	236.0	238.0	241.0	239.0	240.0	238.0	240.0	240.0
1988	240.0	239.0	242.0	242.0	245.0	244.4	243.7	245.6	246.9	245.1	248.1	251.7
1989	252.8	252.6	254.5		255.5		255.1	256.2	256.9	257.1	260.2	259.8

CCl_4

	Jan	Feb	Mar	Apr	May	Jun	Jul	Aug	Sep	Oct	Nov	Dec
1980				109.0	112.0	110.0	110.0	114.0	114.0	110.0	114.0	110.0
1981	111.0	110.0	116.0	115.0	110.0	113.0	113.0	114.0	114.0	113.0	119.0	
1982				118.0	118.0	117.0	116.0	118.0	118.0	119.0	117.0	121.0
1983	121.0	120.0	119.0	120.0	120.0	119.0	119.0	119.0	120.0	119.0	120.0	119.0
1984	120.0	119.0	120.0	121.0	123.0	123.0	124.0	123.0	121.0	122.0	125.0	125.0
1985	122.0	126.0	125.0	124.0	124.0	123.0	123.0	124.0	123.0	121.0	126.0	126.0
1986	125.0	126.0	126.0	125.0	125.0	125.0	126.0	127.0	122.0			
1987		129.0	128.0	126.0	127.0	128.0	129.0	125.0	126.0	124.0	125.0	125.0
1988	125.0	128.0	125.0	125.0		125.4	124.5	125.2	124.1	123.6	124.0	124.9
1989	124.6	125.9	126.2		128.9	127.7	127.2	128.0	128.1	127.1	129.5	130.2
1990	130.8	127.5	129.9	131.4	131.2	130.5						

Table 12. *Monthly mean aircraft observations of CFC-11 (CCl_3F), CFC-12 (CCl_2F_2), CFC-113 (CCl_2FCClF_2), carbon tetrachloride (CCl_4) and methyl chloroform (CH_3CCl_3) (pptv) from the FIAER program in the free troposphere (3-13 km) over Europe and the North Atlantic Ocean, during 1976 - 1987. Monthly means are obtained from individual measurements (Scheel et al., 1988; Seiler and Scheel, 1991). Some of the data are unpublished and subject to revision. Data should not be used for further analysis without consulting the principal investigator, FIAER, H. Scheel.*

CCl_2F_2

	Jan	Feb	Mar	Apr	May	Jun	Jul	Aug	Sep	Oct	Nov	Dec
1976											248.2	252.7
1977						249.2			258.5			
1978						271.1						
1979					302.0	312.8		307.6	313.0		307.6	
1980		309.0	318.4									
1981			322.9									
1982			340.0			340.5			346.8			354.2
1983			361.5									366.0
1984						380.2				382.8		
1985		393.2	400.4									
1986												
1987						424.1						

CCl_3F

	Jan	Feb	Mar	Apr	May	Jun	Jul	Aug	Sep	Oct	Nov	Dec
1976											127.0	125.7
1977						127.0			132.0			
1978						144.5						
1979					145.0	156.1		156.4	155.4		162.7	
1980		161.1	162.1									
1981												
1982			182.6			183.3			185.8			185.6
1983			203.5									199.4
1984						208.0				209.2		
1985		214.5	222.7									
1986												
1987						235.1						

***Table 12** Continued.*

CCl_2FCClF_2

	Jan	Feb	Mar	Apr	May	Jun	Jul	Aug	Sep	Oct	Nov	Dec
1978						24.0						
1979					21.0	22.4		23.5	21.0		23.5	
1980		23.0	25.0									
1981												
1982			28.5			28.4			27.7			31.5
1983			34.2									37.0
1984										45.7		
1985		44.1										
1986												
1987						60.6						

CCl_4

	Jan	Feb	Mar	Apr	May	Jun	Jul	Aug	Sep	Oct	Nov	Dec
1976											67.1	76.9
1977						79.2			78.3			
1978						79.5						
1979					86.9	93.0		86.0	86.0		81.4	
1980		83.7	83.1									
1981												
1982			79.4			85.2			88.0			85.6
1983			94.6									91.9
1984						94.4				95.0		
1985		97.7	97.2									
1986												
1987						98.6						

CH_3CCl_3

	Jan	Feb	Mar	Apr	May	Jun	Jul	Aug	Sep	Oct	Nov	Dec
1978						80.9						
1979					87.5	94.0		91.4	97.6		105.1	
1980		105.8	107.2									
1981												
1982			80.1			93.4			88.3			104.3
1983			121.9									116.3
1984						118.6				120.9		
1985		133.5	140.0									
1986												
1987						135.9						

Table 13. *Monthly mean aircraft observations of CFC-12 (CCl_2F_2) and CFC-11 (CCl_3F) (pptv) from the MRI program in the free troposphere (3-9 km) over Japan, during 1978 - 1990. Monthly means are obtained from individual measurements (Hirota et al., 1988; Hirota and Sasaki, 1991). Some of the data are unpublished and subject to revision. Data should not be used for further analysis without consulting the principal investigator, MRI, M. Hirota.*

CCl_2F_2

	Jan	Feb	Mar	Apr	May	Jun	Jul	Aug	Sep	Oct	Nov	Dec
1978												282.0
1979												
1980	299.0											
1981												
1982												335.0
1983												
1984		349.0										361.0
1985												
1986		389.0									390.0	
1987												425.0
1988												
1989	452.0									453.0		
1990								463.0				

CCl_3F

	Jan	Feb	Mar	Apr	May	Jun	Jul	Aug	Sep	Oct	Nov	Dec
1978												162.0
1979												
1980	179.0											
1981	184.0											
1982		188.0										194.0
1983												
1984		209.0										218.0
1985												
1986		227.0									238.0	
1987												
1988												
1989	265.0									277.0		
1990								282.0				

Table 14. *Monthly mean chloroform ($CHCl_3$) observations (pptv) at Cape Grim, Tasmania from the OGIST flask sampling program (1985-1987) and the GAGE in situ measurements program (1988-1990; Fraser et al., 1989; Fraser, 1991). The data are unpublished and subject to revision. Data should not be used for further analysis without consulting the principal investigators, OGIST, R. Rasmussen; GAGE, P. Fraser.*

$CHCl_3$

	Jan	Feb	Mar	Apr	May	Jun	Jul	Aug	Sep	Oct	Nov	Dec
1985											12.0	9.5
1986		7.3	8.6						9.8		10.0	6.8
1987			5.5	6.4	9.0	7.0	10.7	10.0				
1988									10.3	10.4	10.4	9.3
1989	9.3	8.5	9.0	9.6	10.3	10.7	12.0	12.8	12.8	12.3	10.7	10.4
1990	9.6	9.1	9.5	9.6	10.5	13.0	13.6	14.2	13.9	12.9	12.6	12.1

Table 15. *Monthly mean HCFC-22 ($CHClF_2$) observations (pptv) at Cape Grim, Tasmania from the OGIST flask sampling program (1984-1987) (Fraser et al., 1989). The data are unpublished and subject to revision. Data should not be used for further analysis without consulting the principal investigator, OGIST, R. Rasmussen.*

$CHClF_2$

	Jan	Feb	Mar	Apr	May	Jun	Jul	Aug	Sep	Oct	Nov	Dec
1984								73.2	72.6	73.5	73.7	74.4
1985	74.2	75.2	75.4	74.4	77.3	76.7	77.2	78.9	79.9	79.8	81.1	79.4
1986	81.7	81.6	81.8	82.2	83.7	83.4	85.2	85.4	85.4	85.9	86.8	87.5
1987	88.6	87.0	88.6	90.3	89.4	89.6	91.2	91.4				

APPENDIX II

STRATOSPHERIC MEASUREMENTS

The tabulations in this appendix include previously unreported data, and data used in the section on stratospheric measurements of halocarbons, and the figures therein. This data is provided to facilitate new analyses. If using this data for new studies, the reader is encouraged to contact the original source of the measurements for further clarification.

Table 1. *Independent analysis (S. Penkett, unpublished data) of air samples collected over Aire sur l'Adour.*

Date: Latitude: 44°N
Origin: Aire sur l'Adour Method:

Hght. km	N_2O ppbv	CCl_3F pptv	CCl_2F_2 pptv	CCl_2FCClF_2 pptv	CH_3Cl pptv	$CHClF_2$ pptv	$CClF_2CClF_2$ pptv	$CClF_2CF_3$ pptv	CF_3CF_3 pptv	$CClF_3$ pptv	CF_4 pptv	CF_3Br pptv
11	310	144.00	241.00	—	477.0	79.20	7.0	4.20	3.99	5.10	72.2	0.87
15	314	178.00	289.00	10.40	424.0	44.70	8.5	3.10	—	3.90	65.2	0.68
20	224	90.30	189.00	5.10	183.0	7.20	6.0	2.30	3.7	3.52	79.3	0.44
23	180	14.70	129.00	2.73	119.0	1.04	5.4	1.70	3.47	2.99	66.5	0.17
26	69	0.28	39.60	1.00	44.0	—	3.8	1.36	3.12	2.65	66.5	—
29	48	0.09	20.80	0.60	34.0	—	4.4	1.26	2.92	2.45	58.8	—
33	18	—	8.96	—	54.5	—	2.7	1.0	2.53	2.26	61.8	—

Table 2. *Vertical profiles of nitrous oxide (Gunson et al., 1990) and halocarbons (Zander et al., 1992) from analysis of infrared solar absorption spectra obtained by the ATMOS experiment during the Spacelab 3 mission.*

Date: 30 Apr - 1 May 1985 Latitude: 26 to 32°N
Method: IR Solar Absorption Spectra Ident.: ATMOS/Spacelab 3

Hght. km	Pres. · mbar	Temp. K	N_2O ppbv	CCl_3F pptv	CCl_2F_2 pptv	CH_3Cl pptv	CCl_4 pptv	$CHClF_2$ pptv	CF_4 pptv
12.5	189.00	207.2	308.0	205	310	580	100	66	59
15.0	122.60	204.4	306.0	190	313	515	85	66	59
17.5	82.40	207.2	283.0	72	315	435	65	63	59
20.0	54.50	211.2	233.0	137	300	350	35	61	58
22.5	36.90	214.9	182.0	78	240	240	—	58	58
25.0	24.50	220.8	128.0	28	175	—	—	53	58
27.5	17.10	226.7	70.2	—	110	—	—	51	57
30.0	11.70	232.1	50.4	—	—	—	—	42	57
32.5	8.27	236.2	45.6	—	—	—	—	31	57
35.0	5.75	242.6	46.6	—	—	—	—	—	57
37.5	4.12	250.2	46.3	—	—	—	—	—	56
40.0	2.95	256.4	40.5	—	—	—	—	—	58
42.5	2.14	263.2	32.2	—	—	—	—	—	59
45.0	1.53	269.9	22.8	—	—	—	—	—	59
47.5	1.14	273.3	16.5	—	—	—	—	—	60

Table 3. *Results from recent balloon flights from southern France and Sweden of the KFA Jülich air sampler (Schmidt et al., 1991, U. Schmidt, unpublished data).*

Date: 16 Sep 1986 Latitude: 44°N
Origin: Aire sur l'Adour Ident.: BII9.KFA Method: CRYO/GC Tropopause: 160 hPa

Hght. km	Pres. mbar	Temp. K	CH_4 ppmv	CCl_3F pptv	CCl_2F_2 pptv	CO_2 ppmv	CH_3Cl pptv	CH_3CCl_3 pptv	CCl_4 pptv	CCl_2FCClF_2 pptv
38.7	3.5	250.6	0.46	—	2.7	335.2	—	—	—	—
37.3	4.2	250.4	0.55	—	6.0	336.1	—	—	—	—
36.1	5.0	244.8	0.62	—	7.4	336.2	—	—	—	—
35.1	5.7	245.7	0.71	—	11.1	336.7	—	—	—	—
33.8	6.7	240.8	0.72	—	13.2	338.2	—	—	—	0.4
32.7	8.0	238.0	0.74	—	17.9	336.5	—	—	—	0.6
29.4	13.0	231.5	0.85	0.06	30.6	336.4	34.0	0.05	0.015	1.6
27.6	17.1	228.7	0.92	0.64	52.0	336.6	56.3	—	—	2.9
26.8	19.2	229.1	0.90	0.86	69.6	337.1	75.8	0.13	0.020	2.8
25.7	22.8	225.7	0.89	2.09	56.1	338.0	126.4	—	0.120	3.4
24.2	28.8	222.6	0.99	9.74	87.7	336.9	134.9	—	0.080	5.6

Table 3. *Continued.*

Date: 3 Sep 1986 Latitude: 44°N
Origin: Aire sur l'Adour Ident.: BI10.KFA Method: CRYO/GC Tropopause: 145 hPa

Hght km	Pres. mbar	Temp. K	CH_4 ppmv	CCl_3F pptv	CCl_2F_2 pptv	CO_2 ppmv	CH_3Cl pptv	CH_3CCl_3 pptv	CCl_4 pptv	CCl_2FCClF_2 pptv
31.6	9.4	227.3	0.78	0.02	27.1	339.0	—	—	0.01	0.8
29.2	13.5	221.0	0.86	0.10	40.0	339.0	—	—	0.04	1.9
28.3	15.3	220.3	0.91	0.25	66.8	338.0	—	—	—	2.6
27.9	16.5	220.2	—	0.52	75.5	—	—	0.02	0.02	3.4
27.3	17.9	220.1	0.91	0.69	70.9	339.0	—	0.05	0.04	3.2
26.6	20.0	219.0	0.92	1.93	68.4	338.0	—	—	0.08	4.3
25.2	24.7	218.0	1.00	9.00	86.5	336.6	—	1.50	1.17	6.3
24.0	29.7	216.8	1.06	20.80	109.3	338.0	—	5.00	5.56	8.6
23.0	34.8	217.5	1.11	35.20	109.5	339.0	—	12.10	9.00	10.1
22.8	35.9	216.6	1.11	33.30	128.5	338.5	—	13.20	13.10	10.0
22.6	36.9	216.5	1.10	32.60	126.5	337.5	—	13.30	11.00	9.7
22.4	38.1	216.2	1.12	37.50	126.5	338.0	—	14.30	14.10	10.9
22.0	40.0	216.5	1.14	31.90	100.9	339.0	—	16.40	9.50	10.3
21.6	43.0	215.4	1.19	43.80	127.9	338.5	—	21.00	23.20	12.1
21.1	46.3	216.3	1.28	64.30	160.1	340.0	—	31.50	31.10	14.7

Table 3. *Continued.*

Date: 5 Feb 1987 Latitude: 68°N
Origin: Kiruna Ident.: BII11.KFA Method: CRYO/GC Tropopause: 299 hPa

Hght. km	Pres. mbar	Temp. K	CH_4 ppmv	N_2O ppbv	CCl_3F pptv	CCl_2F_2 pptv	CO_2 ppmv	CH_3Cl pptv	CH_3CCl_3 pptv	CCl_4 pptv	CCl_2FCClF_2 pptv
19.2	63.0	203.6	1.00	165	32	154	336.9	—	—	—	11.6
18.3	71.5	205.2	0.98	135	12	114	340.3	—	—	—	7.8
17.6	80.0	205.6	1.06	154	26	142	341.0	—	—	—	11.0
16.9	89.0	206.3	1.24	204	68	215	337.7	—	—	—	17.4
16.4	96.5	206.9	1.34	221	92	244	337.7	—	—	—	20.1
15.6	110.0	207.5	1.53	277	148	301	343.3	—	—	—	27.3
14.8	124.0	207.9	1.59	292	175	334	343.3	—	—	—	29.6
14.3	134.5	208.6	1.60	290	180	341	346.1	—	—	—	30.4
13.7	148.5	211.1	1.60	302	177	334	342.8	—	—	—	29.1
13.3	158.5	212.1	1.60	293	179	336	341.5	—	—	—	28.7
12.9	167.5	212.7	1.62	309	182	343	344.0	—	—	—	29.8
12.6	177.0	214.2	1.61	296	176	337	343.0	—	—	—	29.4
12.2	186.5	215.7	1.60	293	173	336	345.4	—	—	—	30.5
11.9	197.5	215.9	1.59	288	175	332	347.3	—	—	—	30.9

Table 3. *Continued.*

Date: 16 Sep 1987 Latitude: 44°N
Origin: Aire sur l'Adour Ident.: BII12.KFA Method: CRYO/GC Tropopause: 105.0 hPa

Hght. km	Pres. mbar	Temp. K	CH_4 ppmv	N_2O ppbv	CCl_3F pptv	CCl_2F_2 pptv	CO_2 ppmv	CH_3Cl pptv	CH_3CCl_3 pptv	CCl_4 pptv	CCl_2FCClF_2 pptv
39.4	3.15	250.8	0.55	21	—	4.8	336.9	22	—	—	0.10
36.7	4.45	242.0	0.67	41	—	13.0	338.1	22	—	—	0.35
34.4	6.15	238.4	0.69	49	.01	19.0	336.9	11	—	—	0.44
32.5	8.20	233.8	0.68	51	.02	23.0	337.2	10	—	—	0.62
31.3	9.75	230.5	0.74	63	.01	34.0	337.0	18	—	0.02	2.10
28.6	14.70	225.7	0.95	121	0.40	86.0	338.1	26	0.10	0.02	4.80
26.9	19.00	223.8	1.01	140	2.30	107.0	338.9	30	0.10	0.27	6.10
24.7	26.80	222.3	1.08	166	10.90	146.0	335.6	61	0.91	1.50	9.60
22.7	36.50	219.4	1.16	191	30.90	184.0	335.7	85	3.71	7.60	13.80
21.1	46.20	216.8	1.27	235	58.80	222.0	338.5	179	13.30	14.00	17.90
19.1	63.50	213.3	0.00	258	118.00	290.0	—	243	13.80	20.70	25.00
17.5	82.20	212.5	1.50	263	138.00	307.0	342.1	273	22.80	48.00	27.70
14.7	126.50	211.7	1.70	328	223.00	386.0	344.9	534	87.50	72.10	37.60
13.1	163.50	217.3	1.70	306	215.00	382.0	342.5	506	68.80	61.80	41.70

Table 3. *Continued.*

Date: 1 Feb 1988 Latitude: 68°N
Origin: Kiruna Ident.: BI13.KFA Method: CRYO/GC Tropopause: 207.0 hPa

Hght. km	Pres. mbar	Temp. K	CH_4 ppmv	N_2O ppbv	CCl_3F pptv	CCl_2F_2 pptv	CO_2 ppmv	CH_3Cl pptv	CH_3CCl_3 pptv	CCl_4 pptv	CCl_2FCClF_2 pptv
28.5	18.2	194.7	0.80	83	—	49.2	—	17	0.3	0.05	1.9
24.2	29.1	196.8	0.95	120	—	84.8	—	10	1.3	0.13	4.8
22.8	35.4	197.8	1.03	140	9.5	107.2	—	23	—	0.68	7.2
22.7	37.0	197.7	0.97	121	7.2	100.9	—	12	1.2	0.64	5.7
21.3	45.0	197.2	0.93	113	7.9	87.9	—	17	2.8	1.03	5.7
19.7	65.2	199.8	1.00	138	10.5	113.3	—	29	3.4	1.82	6.9
19.6	58.4	199.5	0.97	129	9.4	99.7	—	43	6.3	1.49	5.5
18.7	67.1	200.4	1.06	145	15.8	127.7	—	69	6.9	4.48	8.6
17.3	84.5	202.3	1.22	197	47.6	194.8	—	66	31.4	18.30	14.0
15.8	107.0	203.3	1.34	238	77.8	236.0	—	96	47.1	32.70	20.0
14.6	128.5	205.1	1.49	254	123.7	300.9	—	206	76.6	68.70	22.8
13.1	161.5	207.6	1.51	262	129.3	291.3	—	197	88.5	68.70	24.9
12.3	185.5	207.9	1.61	290	210.8	339.4	—	263	107.8	77.10	31.9
11.4	213.0	208.1	1.65	308	212.0	343.5	—	272	122.4	104.20	34.6
10.1	261.0	209.1	1.72	308	221.7	383.0	—	407	131.0	108.40	37.4

Table 3. *Continued.*

Date: 10 Feb 1988 Latitude: 68°N
Origin: Kiruna Ident.: BII14.KFA Method: CRYO/GC Tropopause: 223 hPa

Hght. km	Pres. mbar	Temp. K	CH_4 ppmv	N_2O ppbv	CCl_3F pptv	CCl_2F_2 pptv	CO_2 ppmv	CH_3Cl pptv	CH_3CCl_3 pptv	CCl_4 pptv	CCl_2FCClF_2 pptv
25.7	23.0	196.7	—	67	—	47.9	—	—	—	—	—
25.1	25.1	196.8	0.86	88	1.2	54.9	337.8	32	0.2	0.09	2.4
24.3	28.7	196.8	0.89	102	1.7	68.2	336.8	30	0.3	0.18	3.1
22.7	36.1	198.8	0.98	139	9.6	102.2	336.0	47	0.6	0.33	6.0
21.4	44.2	199.3	1.12	167	22.4	160.1	337.2	62	2.9	2.19	9.0
20.1	54.4	201.8	1.15	182	30.8	170.9	336.2	78	6.4	2.30	10.8
18.8	66.3	202.5	1.01	130	14.6	117.3	336.3	61	3.0	1.38	6.9
17.7	79.5	202.7	1.33	220	74.1	236.1	337.3	134	21.8	17.00	17.8
16.2	100.0	206.3	1.26	178	58.1	207.4	337.3	133	26.3	21.80	14.4
15.4	113.0	206.8	1.31	229	77.3	226.0	338.8	141	26.2	23.90	16.4
15.0	121.0	206.2	1.55	286	162.6	327.8	340.2	235	62.4	45.30	27.2
14.5	132.0	207.1	1.57	267	168.3	335.2	341.1	242	60.7	50.80	26.4
13.8	145.5	209.8	1.59	278	188.8	352.8	342.2	292	81.2	43.00	31.5
12.6	178.0	211.9	1.61	284	160.8	337.0	341.5	338	90.9	51.50	26.8

Table 3. *Continued.*

Date: 25 Nov 1988 Latitude: 44°N
Origin: Aire sur l'Adour Ident.: B15.KFA Method: CRYO/GC Tropopause: 203 hPa

Hght. km	Pres. mbar	Temp. K	CH_4 ppmv	N_2O ppbv	CCl_3F pptv	CCl_2F_2 pptv	CO_2 ppmv	CH_3Cl pptv	CH_3CCl_3 pptv	CCl_4 pptv	CCl_2FCClF_2 pptv
33.7	6.7	223.3	—	27	—	—	—	—	—	—	—
31.2	9.8	219.4	0.74	52	—	21.7	334.6	—	—	—	1.1
29.7	12.2	217.0	0.77	62	0.22	31.0	336.2	33	—	—	1.3
28.3	15.5	215.2	0.80	70	0.25	39.6	337.4	15	—	—	0.4
27.3	17.9	215.1	0.83	80	0.61	49.6	337.4	34	—	—	2.2
26.9	19.0	214.3	—	96	1.00	59.9	—	41	—	—	3.6
25.9	22.0	213.6	0.90	117	1.70	72.3	340.1	19	—	—	4.0
25.7	23.0	213.3	—	112	2.00	74.4	—	63	—	0.19	5.4
23.6	31.5	210.7	0.94	125	7.70	94.7	338.8	39	—	0.22	6.4
22.7	36.3	210.9	0.98	140	10.90	113.9	336.4	41	2.3	0.39	8.4
21.3	45.8	208.4	0.99	143	15.60	125.0	331.3	83	—	—	9.4
20.5	51.5	207.8	1.07	168	28.60	156.0	333.8	76	—	4.78	11.4
19.7	58.5	207.0	1.29	204	48.30	197.7	—	123	26.2	10.32	15.1
18.9	66.0	205.6	—	264	117.40	286.4	—	320	82.3	77.37	26.5
18.2	73.5	206.0	1.47	287	169.90	314.1	344.5	149	102.7	67.73	28.7
17.3	83.5	205.7	1.55	263	169.00	347.7	343.6	260	111.1	77.85	31.2
16.6	95.0	209.2	—	264	184.40	357.7	—	380	137.0	95.84	33.4
16.3	99.0	209.5	1.63	293	199.30	371.9	349.0	255	129.6	79.21	36.0
15.5	112.0	209.8	—	319	204.80	375.9	—	436	151.6	125.90	37.2
14.7	128.0	210.4	—	306	212.00	382.0	—	506	137.0	143.80	37.6
13.5	152.0	211.2	1.65	315	216.90	387.1	343.0	347	147.8	85.40	37.7
11.8	200.0	212.3	1.70	303	235.50	404.6	342.2	478	182.9	140.30	41.5
9.6	280.0	224.6	1.73	364	266.70	428.3	349.6	458	169.4	104.50	45.9
8.0	360.0	236.7	1.73	342	252.80	428.3	343.5	555	144.6	86.60	43.2
6.7	430.0	247.5	1.74	315	257.70	427.4	335.4	518	157.7	97.60	43.4

Table 3. *Continued.*

Date: 20 Jun 1989 Latitude: 44°N
Origin: Gap Ident.: BII16.KFA Method: Cryo/GC Tropopause: 191 hPa

Hght. km	Pres. mbar	Temp. K	CH_4 ppmv	N_2O ppbv	CCl_3F pptv	CCl_2F_2 pptv	CO_2 ppmv	CH_3Cl pptv	CH_3CCl_3 pptv	CCl_4 pptv	CCl_2FCClF_2 pptv
33.2	7.4	245.0	0.65	40	0.1	21.6	341.7	23	0.0	0.0	0.6
31.5	9.6	242.0	0.87	75	0.1	64.7	344.8	20	0.0	0.0	2.5
29.3	13.3	237.0	0.86	87	0.3	71.7	344.8	31	0.0	0.0	3.4
25.0	25.4	227.7	1.08	153	10.3	161.1	344.6	52	0.6	0.9	10.4
22.7	36.4	223.7	1.11	159	17.0	176.7	349.2	60	4.7	5.6	11.1
20.5	51.2	220.9	1.25	204	73.9	238.0	344.6	90	21.4	21.2	18.7
16.3	98.6	217.2	1.62	285	214.3	390.9	349.2	190	50.3	16.4	35.7
14.0	142.0	219.6	1.61	287	227.5	395.1	350.8	291	93.0	71.0	37.0
11.2	221.0	216.9	1.75	308	275.6	446.5	352.2	575	154.6	98.6	46.6
10.5	245.0	221.9	1.73	303	269.1	444.4	352.3	588	146.9	117.3	46.0
8.9	313.0	234.2	1.76	305	275.9	442.8	353.4	555	153.5	130.1	47.8
7.1	406.0	225.8	1.77	308	291.1	450.9	354.2	613	158.6	116.6	48.9
5.0	540.0	258.1	1.75	300	282.2	446.1	353.5	591	145.0	118.7	47.3

Table 3. Continued.

Date: 12 Jan 1990 Latitude: 68°N
Origin: Kiruna Ident.: BI17.KFA Method: CRYO/GC Tropopause: 210 hPa

Hght. km	Pres. mbar	Temp. K	CH_4 ppmv	N_2O ppbv	CCl_3F pptv	CCl_2F_2 pptv	CO_2 ppmv	CH_3Cl pptv	CH_3CCl_3 pptv	CCl_4 pptv	CCl_2FCClF_2 pptv
26.7	19.5	188.7	0.52	19	0.00	19.1	347.5	16	—	0.01	0.6
25.6	23.2	188.5	0.72	60	0.36	39.3	344.4	—	—	—	2.2
25.1	25.1	188.4	0.81	78	0.56	55.9	345.7	31	—	—	2.9
24.7	26.7	188.6	0.84	84	1.09	64.4	344.0	25	—	0.40	3.6
24.7	26.5	188.1	0.87	92	1.50	68.3	346.4	29	0.1	0.20	4.1
22.9	35.5	191.1	1.09	138	16.90	141.0	347.3	55	4.9	3.00	8.8
21.5	44.0	193.5	1.13	156	32.80	173.0	348.2	84	11.0	7.40	11.7
20.2	53.8	189.3	1.25	187	56.90	217.0	348.1	166	30.0	16.00	16.5
18.2	73.8	193.8	1.42	236	130.00	310.0	348.1	232	61.0	47.00	27.4
16.8	91.5	195.5	1.44	241	133.00	311.0	349.0	267	53.0	40.00	27.2
15.5	113.0	198.2	1.51	258	160.00	340.0	349.8	261	69.0	70.00	31.2
13.5	154.0	200.2	1.59	274	202.00	384.0	351.6	380	95.0	90.00	36.0
10.4	250.0	206.9	1.75	303	267.00	453.0	349.3	551	125.0	110.00	47.8

Table 3. *Continued.*

Date: 9 Feb 1990 Latitude: 68°N
Origin: Kiruna Ident.: BII18.KFA Method: Cryo-GC Tropopause: 294 hPa

Hght. km	Pres. mbar	Temp. K	CH_4 ppmv	N_2O ppbv	CCl_3F pptv	CCl_2F_2 pptv	CO_2 ppmv	CH_3Cl pptv	CH_3CCl_3 pptv	CCl_4 pptv	CCl_2FCClF_2 pptv
21.9	40.9	200.8	1.09	157	19	154	346.7	34	3.8	1.6	9.7
20.7	49.6	204.3	1.13	165	28	173	343.6	43	4.6	3.6	11.6
20.1	54.2	205.2	1.14	172	28	178	344.3	36	5.1	4.3	11.5
17.9	76.5	208.2	1.21	188	51	208	345.0	34	11.9	17.0	14.5
16.0	103.4	213.1	1.31	213	90	253	346.8	87	38.9	49.0	—
15.1	119.7	214.7	1.34	222	106	278	348.4	130	46.5	56.0	22.8
14.3	136.3	213.8	1.42	236	134	314	351.0	144	46.6	56.0	26.0
12.3	185.9	217.5	1.59	262	212	398	350.4	206	75.5	78.0	34.7
11.4	214.5	217.1	1.66	294	232	423	350.0	164	57.6	51.0	35.7
10.3	252.3	214.4	1.70	305	262	453	352.3	403	120.0	104.0	43.9

Table 3. *Continued.*

6Date: 05 Nov 1990 Latitude: 44°N
Origin: Aire sur l'Adour Ident.: BII19.KFA Method: Cryo/GC Tropopause: 211 hPa

Hght. km	Pres. mbar	Temp. K	CH_4 ppmv	N_2O ppbv	CCl_3F pptv	CCl_2F_2 pptv	CO_2 ppmv	CH_3Cl pptv	CH_3CCl_3 pptv	CCl_4 pptv	CCl_2FCClF_2 pptv
23.2	33.3	216.6	1.13	157	19.7	180.2	348	83	—	3.0	14.3
21.5	43.7	214.1	1.32	216	79.7	262.8	350	107	18.1	17.3	22.7
18.9	65.8	213.6	1.43	273	137.5	315.0	350	189	32.1	41.7	30.3
17.6	94.9	216.0	1.68	317	224.2	409.2	354	327	45.3	84.8	42.6
16.3	99.0	215.2	1.70	299	226.3	410.7	353	371	91.2	113.0	45.6
15.1	118.5	214.3	0.00	306	234.2	415.1	—	310	62.7	8.5	49.0
14.0	141.3	215.5	1.74	311	242.2	424.2	353	449	94.4	104.0	47.8
12.6	177.8	216.3	1.76	321	244.5	428.6	357	489	113.7	125.0	48.2
12.1	190.3	216.0	1.75	338	252.7	437.6	352	502	120.8	117.0	50.3
11.9	196.8	216.4	1.75	331	244.6	428.8	350	483	119.7	125.0	47.8

Table 3. *Continued.*

Date: 10 Nov 1990
Origin: Aire sur l'Adour

Latitude: 44°N
Ident.: BI20.KFA

Hght. km	Pres. mbar	Temp. K	CH_4 ppmv	N_2O ppbv	CCl_3F pptv	CCl_2F_2 pptv	CO_2 ppmv	CH_3Cl pptv	CH_3CCl_3 pptv	CCl_4 pptv	CCl_2FCClF_2 pptv
28.6	14.7	213.3	0.80	72	0.11	52.2	348	53	—	—	4.2
28.0	16.2	213.1	0.93	121	0.52	86.0	349	15	—	—	5.8
27.2	18.2	213.4	0.86	98	0.53	71.0	347	16	—	0.09	4.5
25.8	22.5	213.7	0.96	122	2.20	108.0	348	21	—	0.22	8.0
24.1	29.3	209.4	1.05	151	11.30	152.0	349	45	—	0.82	12.1
23.0	34.6	211.0	1.13	172	29.10	191.5	349	52	10.3	9.80	16.4
21.9	41.4	209.5	1.24	208	63.10	238.7	347	100	28.7	22.70	21.6
20.3	52.9	209.5	1.33	231	99.30	274.6	347	129	51.9	46.40	26.5
19.0	64.3	209.8	1.41	251	126.10	302.2	349	203	63.4	54.90	29.8
18.2	73.2	210.5	1.46	251	139.40	319.3	351	240	72.5	66.70	32.0
16.9	90.3	208.8	1.67	305	219.40	401.8	353	365	119.4	110.00	44.3
16.3	99.1	207.8	1.73	323	242.20	428.0	353	515	130.5	110.00	48.8
14.3	135.9	212.2	1.76	290	248.10	434.2	350	579	138.2	126.00	50.3
12.3	186.3	220.6	1.76	329	251.90	434.7	353	528	143.4	116.00	49.8

Chapter 2.

Production and Emission of CFCs, Halons, and Related Molecules

Lead Authors:

D. A. FISHER, T. Duafala, P. M. Midgley, and C. Niemi

Additional Contributors:
A. Makhijani and S. Seidel

Chapter 2
Table of Contents

Chapter 2: Production and Emission of CFCs, Halons, and Related Molecules

2.0 Summary of Production and Emissions

- Production of CFC-11 and CFC-12 peaked in 1987 and their estimated emissions have decreased substantially since 1988.

- The major uncertainties in the calculations of current, global emissions for CFC-11 and CFC-12 are the lack of data from companies not reporting to industry panels along with the estimation of banking times for long-term uses.

- For CFC-11, CFC-12 and CFC-113, reporting companies are estimated to account for 85-90% of total production; higher percentages are believed for most other CFCs and methyl chloroform. At least 95% of the CFC production and emission is believed to take place in the Northern Hemisphere.

- The proportion of emissions of CFC-11 and CFC-12 from non-reporting companies is projected to increase as production is phased out under the Montreal Protocol. In addition, the fraction of total emissions arising from the service bank of CFCs will also increase as new production decreases. Emission levels are therefore likely to fall off less rapidly than production, and the uncertainty in emission relative to production will grow.

- Methyl chloroform emissions increased during the 1980s, partly due to its substitution for restricted substances, including CFC-113 and other volatile organic compounds. There are no industrial estimates for current production of carbon tetrachloride produced for dispersive uses. Somewhat inprecise production and emission data are available for methylene chloride (CH_2Cl_2), trichloroethylene ($CHClCCl_2$) and perchloroethylene (CCl_2CCl_2), which are short-lived compounds whose study may help shed light on global average distributions of tropospheric OH.

- HCFC-22 emissions have increased at approximately 8.5% per year since 1980. This increase is due in part to substitution for restricted CFCs. There are no industrial estimates for other HCFCs since they are significantly lower and presently have not met the agreed-upon criteria for industry reporting.

- Some proportion of methyl chloride emissions, may be due to anthropogenic sources (15-30%), probably almost all from biomass burning. The rest of the emissions are from natural sources, primarily the oceans.

- Methyl bromide emissions to the atmosphere have a number of sources. These include a significant natural component, most likely from the oceans, and various anthropogenic sources, such as fumigant use. There is considerable uncertainty about both the anthropogenic and natural emissions of methyl bromide.

2.1 Introduction

In order to infer the lifetimes of CFCs, halons, and related molecules from atmospheric composition data, it is necessary that the spatial and temporal dependence of their emissions into the atmosphere be accurately quantified. To do this, several steps are necessary. First, accurate estimates of the total molecular production must be obtained. Then, information about the end use of each compound must be obtained, preferably with information about the time and location of its actual use. Finally, the time lag between production and emission of the molecule must be determined for each end use.

In this chapter, the processes necessary to evaluate all three of these steps and the results obtained are considered. In particular, the survey process used by industrial, governmental, and international organizations to gather the necessary information is described. Results from a variety of these data collections exercises form the bulk of the data in this chapter. Molecules examined include five fully halogenated CFCs (CFC-11, -12, -113, -114, -115), HCFC-22, and other HCFCs, methylchloroform, the Halons (H-1211, H-1301, H-2402), methyl chloride, other chlorocarbons such as trichloroethylene and tetrachloroethylene, and methyl bromide. There is also an explicit treatment of the estimated uncertainties in the emissions of CFC-11, CFC-12, and methyl chloroform.

The emissions data obtained in this chapter will be used in the model calculations in Chapter 3 together with the ALE/GAGE surface concentration data given in Chapter 1 in the inference of molecular lifetimes.

The text is presented mainly as explanatory notes to the various tables and figures contained within the chapter. The style is therefore of necessity different from other chapters which are more concerned with the discussion of scientific data collected by atmospheric and laboratory measurements, and in the calculated interpretation of such data.

2.2 Reported Production Surveys

Production surveys for a number of industrial gases have been carried out by trade associations of companies responsible for their commercial manufacture. Because the gases and the trade associations vary, the extent of coverage both in terms of geographical locations and time span also vary.

During the 1970s, the trade association representing most of the world's producers of CFCs 11 and 12, the Chemical Manufacturers Association: Fluorocarbon Program Panel (CMA FPP), organized the first authoritative survey of world production of these chemicals. Participating companies included all producers in Europe, Japan, and North America, which, with their subsidiaries, were responsible for the production in those regions plus Australia, Argentina, Brazil, Mexico, South Africa, Spain, and Venezuela. In the early years, the panel attempted to quantify production in other parts of the world, most notably in the Commonwealth of Independent States (C.I.S.) and Eastern Europe. These attempts were later abandoned when it became clear that there were no reliable sources of data accessible at that time and extrapolations were introducing unreasonably high errors.

For the past decade, industrial producers have published only their own data which, for CFCs 11 and 12, have been estimated to represent over 85% of the world production throughout much of the 1970s and '80s; however, over the past few years, these surveys are estimated to represent a much smaller portion of the world's production — approximately 75% (AFEAS, 1992).

Total global production and consumption data have been reported to the United Nations Environment Programme (UNEP, 1991) under the provisions of the Montreal Protocol which makes possible estimates of truly global production; however, unlike the industrial survey, the UNEP data collection process does not survey use data which are required to make reasonable estimates of emissions.

Over the past few years, producers of CFCs 113, 114, 115, methyl chloroform, HCFC-22, and methyl bromide initiated data collection exercises that were similar to the survey of CFCs 11 and 12. The reporting producers accounted for production in essentially the same regions as the survey of CFCs 11 and 12. Each survey represented

varying fractions of the global production total during the 1980s: over 85% for the CFCs, over 90% for HCFC-22, over 98% for methyl chloroform, and over 95% for methyl bromide

The procedure for each survey was basically the same: 1) collect production and sales data, 2) categorize the sales into various end uses, and 3) estimate the time delay for release to the atmosphere from each end use in order to calculate an estimate for the overall annual emissions. In each of these surveys, companies have submitted their individual survey inputs to an independent auditor thereby preserving commercial confidentiality. Thus, each year, producers report net production — that is, the total produced less the amount used or sold as a chemical intermediate (which is consumed and thus never released to the atmosphere) — to the auditor. The auditor then aggregates production and sales categories from all survey participants.

The survey of Halons 1211 and 1301 was structured in much the same manner. The companies were asked to estimate the percentage of the production that is lost to the atmosphere rather than report specific end uses. As we will see later, the result of this exercise shows significant changes in emission patterns over the commercial life of these compounds and also significant changes compared to previous estimates of emissions.

2.3 Emission Calculations

To calculate the overall release rate of a chemical, the time delay following sale before release (service life) is first estimated for each of its various uses. For some applications, statistical studies have been completed which characterize the time delay from the point of sale to the emission into the atmosphere. For uses where no firm data were available, informed experts from user industries were consulted to make appropriate estimates for delay times.

Once the time delay for emissions was estimated, fluxes into the atmosphere are calculated from:

$$\text{Emission (year i)} = \sum_{j=0}^{i} \sum_{k=1}^{N_u} [\, f(i-j,k) * p(j,k) \,]$$

where: p(j,k) is the amount sold in year j for end-use k;
f(t,k) is the fractional emission to the atmosphere during the t^{th} year following sale for use category k.

where $\sum$ f(t,k) = 1 for each k;
t = i-j, the time delay from sale to release; and
N_u = Number of use categories.

Additional details of the appropriate categories will be given in Section 2.5 relative to the individual gases.

2.4 Unreported Production and Emissions

Since the production of some industrial gases in some countries is not covered by the surveys of the various chemical associations discussed above, estimation of "unreported production" is needed to evaluate global trends. Recently, several new sources of information have been developed that provide limited, albeit useful, material on both production and consumption of CFCs, HCFCs, and halons in countries not covered by the voluntary industry data reporting. Three data sources available are: studies from United Nations Development Programme; survey by the Alternative Fluorocarbons Environmental Acceptability Study (AFEAS) of non-reporting countries; and data collected by UNEP for the production of eight controlled substances.

2.4.1 United Nations Development Programme

A number of large developing countries not covered by the industry data have prepared detailed studies of their current production and use of these gases in an effort to understand the costs of complying with the international treaty on ozone layer protection (the Montreal Protocol). These studies covered production in two major countries: China and India.

China: A recent analysis was conducted in China by a team of experts under the auspices of the United Nations Development Programme. The *Report of a United Nations Development Programme Mission to Investigate Ozone*

Layer Protection in China (Isaksen *et al.*, 1990) included data on production during 1989 given in Table 2.4-1. This report also listed a breakdown of uses for these chemicals for 1990 as shown in Table 2.4-2.

***Table 2.4-1** 1989 Chinese Production of Fluorochemicals*

CFC-11	5,500	tonnes
CFC-12	14,000	tonnes
CFC-113	1,500	tonnes
HCFC-22	15,000	tonnes
Halon-1301	10	tonnes
Halon -1211	3,500	tonnes

In reviewing these two tables, it is important to note that the difference between production and use would be accounted for by imports and exports. It is also important to recognize that a large percentage of the production of HCFC-22 was consumed as a chemical intermediate.

***Table 2.4-2** 1990 Chinese Use of Fluorochemicals (tonnes)*

	Ref/AC	Com. Ref	Fire	Aerosol	Plastics	Solvents
CFC-11	7300	6073			4000	
CFC-12	3111	1543		4700		
CFC-113	24					1096
HCFC-22	2315	774				
Halon-1301			500			
Halon-1211			4500			

India: A similar analysis of use of these compounds in India (Billimoria, 1990) was undertaken in 1989. Table 2.4-3 shows the breakdown by compound and by end use for the period from 1985 to 1991 (estimated). Detailed production data for India was not available, but little or no production of either CFC-113 or halons has occurred to date.

2.4.2 AFEAS Estimates

The AFEAS Steering Committee collated a list of other "non-reporting" producers and estimated their 1989, 1990, and 1991 production levels so that more complete estimates of total global production for CFCs 11, 12, and 113 plus HCFC-22 could be made. There are two possible flaws with this exercise: 1) several plants are "swing" plants, capable of producing CFCs 11 and 12 and/or HCFC-22 and it is not easy to define their production separately, and 2) for HCFC-22, it was assumed that the production data given represented dispersive uses (*i.e.*, that the amount used or sold as chemical intermediate was already deducted as was done in the AFEAS report for HCFC-22) but this distinction was not specifically requested. So this exercise, if in error, tends to overstate non-reported production. Results of this exercise are shown in Table 2.4-4. As seen, no reports were received for production in Hungary or Poland which were listed in Gamlen *et al.* (1986) as possible producers.

Table 2.4-3 *Indian Fluorochemical Consumption (tonnes)*

Summary of CFC Usage By CFC	1985	1986	1987	1988	1989	1990	1991
CFC-11	277	426	613	763	945	1139	1382
CFC-12	1054	1162	1353	1520	1723	1928	2173
CFC-113	336	397	453	502	569	654	742
HCFC-22	544	566	620	709	785	863	960
Halon-1301	40	80	120	150	168	198	234
Halon-1211	50	90	140	178	205	252	310
CCl_4	1910	1984	2099	2238	2826	3096	3391
Methyl Chloroform	300	360	430	520	600	1200	2400
TOTAL	4510	5065	5828	6580	7821	9331	11592
Summary of CFC Usage By End Use							
- Refrig	657	735	805	910	998	1113	1262
- Air Cond.	260	291	310	333	366	405	454
- Aerosol	226	322	550	673	868	1037	1238
- Foam	192	247	310	375	445	525	616
- Cleaning	1790	1984	2181	2462	2853	3704	5176
- Misc.	750	750	793	790	1133	1234	1343
- Fire	90	170	260	328	373	450	544
Sub Total	3966	4499	5208	5872	7036	8468	10632
-HCFC-22 uses	544	566	620	709	785	863	960
TOTAL	4510	5065	5828	6580	7821	9331	11592

Table 2.4-4 *AFEAS survey of non-reported production (tonnes)*

	1989 Non-Rep'ted (range)	1990 Non-Rep'ted (range)	1991 Non-Rep'ted (range)	Producing Countries
CFC-11 &-12	157,050 (±42,050)	163,325 (±39,475)	145,124 (±48,876)	P. R. China, Czechoslovakia, former GDR* India, Korea, Rumania, Taiwan, & C.I.S.
CFC-113	19,000 (±5,000)	18,650 (±3,150)	17,592 (±8,875)	P. R. China, Korea, Taiwan, & C.I.S.
HCFC-22	22,450 (±4,000)	23,625 (±2,850)	23,590 (±7,448)	P. R. China, former GDR*, Greece*, India, Korea, Rumania, & C.I.S.

* denotes countries where producers started reporting production in 1990

2.4.3 UNEP Data

UNEP has published 1986 production and consumption data (UNEP 1991) for eight controlled substances: CFCs 11, 12, 113, 114, 115 and Halons 1211, 1301, and 2402; no historical data have been given. These data are a combination of external reports and UNEP's own estimates.

Consumption (defined as Consumption = Production + Imports - Exports) is broken down in the following regional groupings:

- Africa
- Asia and Pacific
- Western Europe and others — including the European Economic Community (EEC), Australia, North America
- Eastern Europe
- Latin America and the Caribbean

(Reports distinguish between exports to Parties and to non-Parties to the Montreal Protocol.)

Production was reported by 13 Parties: Argentina, Australia, Brazil, Canada, Czechoslovakia, EEC, the former German Democratic Republic (GDR), Japan, Mexico, South Africa, USA, Commonwealth of Independent States (C.I.S), former USSR, and Venezuela. These production data are specified by compound as shown in Table 2.4-5.

UNEP estimated production of regulated compounds by non-Parties to be 5,256 metric tons (tonnes).

***Table 2.4-5** UNEP Report of 1986 Production by Parties (tonnes)*

Substance	Production by Parties
CFC-11	392,114
CFC-12	472,644
CFC-113	221,518
CFC-114	17,241
CFC-115	11,110
Total (CFCs)	1,114,627
Halon-1211	13,378
Halon-1301	11,599
Halon-2402	3,724
Total (halons)	28,701
TOTAL	1,143,329

2.5 Production and Emissions of Individual Gases

2.5.1 Trichlorofluoromethane (CFC-11)

A. Surveyed Production Data

Annual production surveys for this compound and for CFC-12 started in the mid-1970s and continued to 1989 under the auspices of the Chemical Manufacturers Association, Fluorocarbon Program Panel (CMA FPP). AFEAS assumed responsibility for data collection in 1990.

Participating producers, listed in Table 2.5.1-1, account for all production in the European Economic Community, Japan, and North America and their subsidiaries, as well as some producers in India, Australia, and South America. This survey was estimated to represent over 85% of global production during much of the 1980s. Data reported to UNEP indicate that production by Parties to the Montreal Protocol was 392.1 kt (kilotonnes) in 1986 (total consumption including non-signatory countries was 394.2 kt) which means that the industrial survey accounted for 89% of reported global production (350.1 kt). However, the more recent AFEAS estimates indicate that the amount of CFCs 11 and 12 covered by the survey represents a smaller portion of the total global production, *i.e.*:

Year	Fraction Survey Coverage	
1975	86%	(McCarthy *et al.*, 1977)
1982	88%	(Gamlen *et al.*, 1986)
1986	89%	(UNEP, 1991)
1989	81%	(AFEAS, 1992)
1991	75%	(AFEAS, 1992)

The diminished coverage is due, in part, to the fact that use in surveyed countries has decreased more rapidly than in the non-surveyed countries — consistent with the provisions of the Montreal Protocol for lesser-developed countries.

Global sales reports also distinguish by hemisphere and show that over 95% of the material has been sold, and therefore presumably released, in the Northern Hemisphere.

Uncertainties in the production data themselves are probably not more than ±0.5%, given that plant losses are accounted for separately.

Table 2.5.1-1 *Participants in Survey of CFC 11 and 12 Production and Sales*

Listing of Survey Reporting Companies inclusive of any Related Subsidiaries and/or Joint Ventures Reporting Data

- Akzo Chemicals BV (Holland)
- Allied-Signal, Inc. (U.S.)
  - -- Allied Canada, Inc. (Canada)
  - -- Quimobasicos, S.A. (Mexico)
- Ausimont S.p.A. (formerly Montefluos S.p.A.) (Italy)
- Chemiewerk Nünchritz GmbH (Germany) [joined in 1990]
  - -- Dohna-Chemie GmbH (Germany)
- E. I. du Pont de Nemours & Company (U.S.)
  - -- Du Pont Argentina (Argentina)
  - -- Du Pont do Brasil S.A. (Brazil)
  - -- Du Pont Canada, Inc. (Canada)
  - -- Du Pont International (Europe)
  - -- Du Pont S.A., de C.V. (Mexico)
- Elf Atochem, S.A. (France)
  - -- Elf Atochem Espana (Spain)
  - -- Elf Atochem North America (U.S.)
  - -- Pacific Chemical Industries Pty. Ltd. (Australia)
  - -- Produven (Venezuela)
- Hoechst AG (West Germany)
  - -- Hoechst Iberica (Spain)
  - -- Hoechst do Brasil Quimica e Farmaceutica S.A. (Brazil)
- ICI Chemicals and Polymers, Ltd. (England)
  - -- African Explosives & Chemical Industries, Ltd.
- Japan Flon Gas Association (Japan)
  - -- Asahi Glass Co., Ltd.
  - -- Central Glass Co., Ltd
  - -- Daikin Industries, Ltd.
  - -- Du Pont-Mitsui Fluorochemicals Co., Ltd.
  - -- Showa-Denko, K.K.
- LaRoche Chemicals, Inc. (formerly Kaiser Aluminum & Chemical Corp. (U.S.)
- Rhône-Poulenc Chemicals, Ltd. (U.K.)
- Société des Industries Chimiques du Nort de la Grèce, S.A.(Greece)
- Solvay S.A. (Belgium)
  - -- Kali-Chemie Iberia SA (Spain)
  - -- Solvay Fluor und Derivate GmbH (formerly Kali-Chemie Aktiengesellschaft) (Germany)

B. End Use Categories

The survey partitions sales into five classifications:

- Hermetically Sealed Refrigeration — service life 12 years
- Non-Hermetic Refrigeration — mean service life 4 years
- Closed-Cell Foam Blowing — 10% initial losses followed by 4.5% per year loss for 20 years
- Open-Cell Foam Blowing — 6-month delay
- Aerosol Propellants — average of 6 months from sale to emission

These five categories cover the major uses for CFC-11. For the minor fraction remaining, the emissions are assumed to occur 6 months following sale. The categorization of end uses is discussed in detail in Gamlen *et al.* (1986).

C. Emission Results

Results for the survey production plus calculated emissions of CFC-11 through 1990 are shown in Table 2.5.1-2. As shown, both production and emissions peaked in 1974 and later in 1987-88 before production diminished in accordance with the Montreal Protocol.

***Table 2.5.1-2** Production and Calculated Emissions of CFCs 11 and 12 (kt)*

	Reporting Companies Only				Global Estimates			
	CFC-11 Prod.	CFC-11 Emiss.	CFC-12 Prod.	CFC-12 Emiss.	CFC-11 Prod.	CFC-11 Emiss.	CFC-12 Prod.	CFC-12 Emiss.
1931	0.0	0.0	0.5	0.1	0.0	0.0	0.5	0.1
1932	0.0	0.0	0.1	0.1	0.0	0.0	0.1	0.1
1933	0.0	0.0	0.3	0.1	0.0	0.0	0.3	0.1
1934	0.0	0.0	0.7	0.2	0.0	0.0	0.7	0.2
1935	0.0	0.0	1.0	0.3	0.0	0.0	1.0	0.3
1936	0.1	0.0	1.7	0.5	0.1	0.0	1.7	0.5
1937	0.1	0.0	3.1	0.8	0.1	0.0	3.1	0.8
1938	0.1	0.1	2.8	1.2	0.1	0.1	2.8	1.2
1939	0.1	0.1	3.9	1.7	0.1	0.1	3.9	1.7
1940	0.2	0.1	4.5	2.3	0.2	0.1	4.5	2.3
1941	0.3	0.1	6.3	3.0	0.3	0.1	6.3	3.0
1942	0.3	0.1	5.9	3.7	0.3	0.1	5.9	3.7
1943	0.4	0.2	8.2	4.5	0.4	0.2	8.2	4.5
1944	0.4	0.2	16.7	6.1	0.4	0.2	16.7	6.1
1945	0.4	0.3	20.1	8.0	0.4	0.3	20.1	8.0
1946	0.7	0.6	16.6	13.9	0.7	0.6	16.6	13.9
1947	1.3	1.3	20.1	21.3	1.3	1.3	20.1	21.3
1948	3.0	2.3	24.8	24.8	3.0	2.3	24.8	24.8
1949	4.5	3.8	26.1	26.6	4.5	3.8	26.1	26.6
1950	6.6	5.5	34.6	29.5	6.7	5.5	35.1	29.7
1951	9.1	7.6	36.2	32.4	9.2	7.7	36.9	32.8
1952	13.6	11.0	37.2	33.7	13.7	11.1	38.0	34.2
1953	17.3	15.0	46.5	37.9	17.4	15.1	47.4	38.5
1954	20.9	18.6	49.1	42.9	21.0	18.7	50.2	43.7
1955	26.3	23.0	57.6	48.2	26.4	23.1	58.9	49.2
1956	32.5	28.7	68.7	56.1	32.7	28.9	70.2	57.3
1957	33.9	32.2	74.2	63.8	34.2	32.4	75.9	65.2
1958	29.5	30.2	73.4	66.9	29.8	30.4	75.6	68.6
1959	35.6	30.9	87.6	74.8	35.9	31.2	90.1	76.8
1960	49.7	40.5	99.4	89.1	50.1	40.9	102.4	91.6
1961	60.5	52.1	108.5	99.7	61.0	52.6	111.9	102.7
1962	78.1	65.4	128.1	114.5	78.7	65.9	132.2	118.0

1963	93.3	80.0	146.4	133.9	94.0	80.6	151.2	138.2
1964	111.1	95.0	170.1	155.5	111.9	95.7	175.8	160.6
1965	122.8	108.3	190.1	175.4	123.8	109.1	196.8	181.3
1966	141.0	121.3	216.2	195.0	142.2	122.3	224.1	201.8
1967	159.8	137.6	242.8	219.9	161.1	138.8	252.1	228.0
1968	183.1	156.8	267.5	246.5	184.7	158.1	278.8	256.2
1969	217.3	181.9	297.3	274.3	219.9	183.8	311.4	286.2
1970	238.1	206.6	321.1	299.9	241.0	209.0	336.8	313.8
1971	263.2	226.9	341.6	321.8	266.6	229.7	360.5	338.0
1972	306.9	255.8	379.9	349.9	311.1	259.1	401.7	368.9
1973	349.1	292.4	423.3	387.3	354.3	296.6	447.4	408.8
1974	369.7	321.4	442.8	418.6	377.5	327.1	473.5	444.3
1975	314.1	310.9	381.0	404.1	323.4	318.4	418.5	435.5
1976	339.8	316.7	410.7	390.4	350.5	325.4	450.3	424.9
1977	320.5	303.9	382.8	371.2	332.8	313.8	424.5	406.0
1978	308.9	283.6	372.1	341.3	323.0	294.7	416.0	376.8
1979	289.5	263.7	357.2	337.5	305.8	275.9	403.4	375.4
1980	289.6	250.8	350.2	332.5	308.4	264.5	399.0	373.4
1981	286.9	248.2	351.3	340.7	308.6	263.7	402.7	385.1
1982	271.4	239.5	328.0	337.4	296.3	257.1	382.2	385.3
1983	291.7	252.8	355.3	343.3	320.4	273.4	412.4	394.3
1984	312.4	271.1	382.1	359.4	345.4	295.1	442.3	413.5
1985	326.8	280.8	376.3	368.4	364.8	308.3	439.7	426.0
1986	350.1	295.1	398.4	376.5	393.8	326.8	465.2	437.4
1987	382.1	310.6	424.7	386.5	431.2	345.8	499.8	451.0
1988	376.0	314.5	421.0	392.8	431.2	353.6	505.5	462.7
1989	302.5	265.2	379.8	364.7	364.6	304.7	474.8	436.9
1990	232.9	216.1	231.0	310.5	297.5	255.2	329.7	385.6
1991	213.5	188.3	224.8	271.6	270.8	223.0	312.6	344.6

Figure 2.5.1-1 shows calculated global emissions including non-reported production — estimates for "non-reported" production from the CMA FPP through 1975 were used in combination with more recent UNEP and AFEAS estimates as previously described. Non-reported production for intervening years were interpolated and, in the absence of any better information, use categorization for this production was assumed to be the same as for reported production. It has been suggested that this assumption is likely to yield overestimated emissions and underestimated size of the bank for this portion. Lastly, the generally increasing divergence between production and emission curves in later years reflects the growing fraction used in markets characteristically having longer service times.

2.5.2 Dichlorodifluoromethane (CFC-12)

A. Surveyed Production Data

The survey for CFC-12 is the same as the one used for CFC-11 so that the coverage, both in terms of geographic and temporal, is the same.

Interhemispherical split of sales indicates that 94.5% of the material is sold in the Northern Hemisphere. Furthermore, comparison with the UNEP reported total production for 1986 indicates that the survey amount (398.4 kt) amounts to 86% (86.5 % if non-Parties are included) of the 462.6 kt (465.7 including non-Parties) global value.

B. End Use Categories

Sales categories for the CFC-12 survey are the same as for CFC-11 (Gamlen *et al.*, 1986). The release delays are the same as with CFC-11 with the exception of material used for closed-cell foams. CFC-12 is used as a blowing agent for extruded polyolefin foams which have a very thin cross section. As such, CFC-12 is lost to the atmosphere more

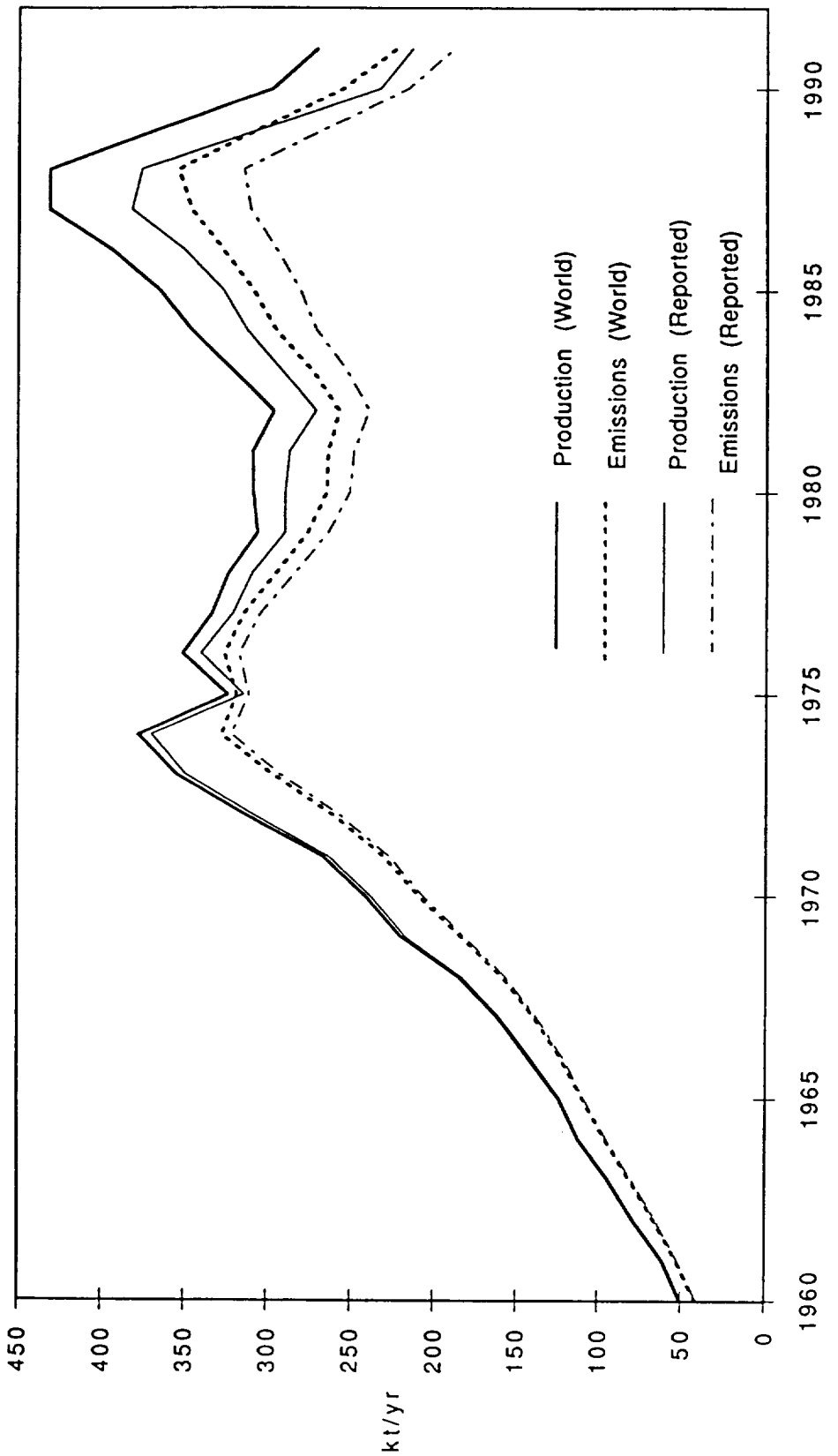

Figure 2.5.1-1 Production and emission of CFC 11 (Reporting Companies and World Estimates)

rapidly — within two years — than the comparable application for CFC-11 (12-year timescale for CFC-11 used as a blowing agent principally in rigid polyurethane foams).

C. Emission Results

Production and emission results for CFC-12 through 1990 are also shown in Table 2.5.1-2 and Figure 2.5.2-1. As shown, patterns for both production and emissions are similar to the results for CFC-11. Again, diminished production and emission levels are evident after the Montreal Protocol enactment.

Figure 2.5.2-1 also shows results which include non-reported production. As with CFC-11, early information from the CMA FPP was used to estimate "non-reported" production in conjunction with the more recent estimates outlined in Section 2.4. Intervening years were interpolated and use categorization for "non-reported" production was assumed to be the same as for the reported production.

2.5.3 1,1,2-Trichlorotrifluoroethane (CFC-113)

A. Surveyed Production Data

Annual production amounts of CFC-113 were reported by participating companies of the CMA FPP for each year from 1980 to 1989 to an independent accounting firm. Cumulative sales figures prior to 1980 were also collected. The auditing firm compiled confidential reports from individual producers and then reported only the total production figure. Participating companies are listed in Table 2.5.3-1. Additional surveys covering 1990 and 1991 have been completed by AFEAS (AFEAS, 1992). More complete details of this survey are available from Fisher and Midgley (1993).

The participating companies include all the producers in Canada, the EEC, Japan, and the USA (as well as their subsidiaries). Current estimates indicate that these reporting companies still account for over 85% of total world production of CFC-113, although the fraction of non-reported production appears to be growing (AFEAS, 1992). The survey also indicates that the vast majority has been released in the Northern Hemisphere (98.9%). Data collection from 1990 onwards has been carried out by AFEAS.

B. End Use Categories

To calculate release rates of CFC-113, the time delay between production and emission was estimated for each end use. Product applications were then reviewed and grouped into categories according to the timescale of their emission to the atmosphere from date of sale. In cases where firm data on the time delay did not exist, informed experts from various user industries were consulted to make appropriate time estimates and group use categorizations. The auditor's questionnaire solicited sales data from the producers classified by release category.

CFC-113 sales were divided into the following categories:

Aerosols
Cleaning, drying, dry-cleaning
Blowing agent, phenolic foams
Long-lived refrigerant use
Heat transfer fluid
Other uses

This categorization allows major markets that have similar delays between production and release to be grouped for the purpose of estimating emission rates.

- Short time scale (average service life = 6 months): includes material used in aerosols, cleaning, and other uses plus fugitive emissions (plant losses).
- Long time scale (characteristic time = 12 years): includes product used in refrigeration, as a blowing agent for rigid phenolic foams, and as a heat transfer fluid.

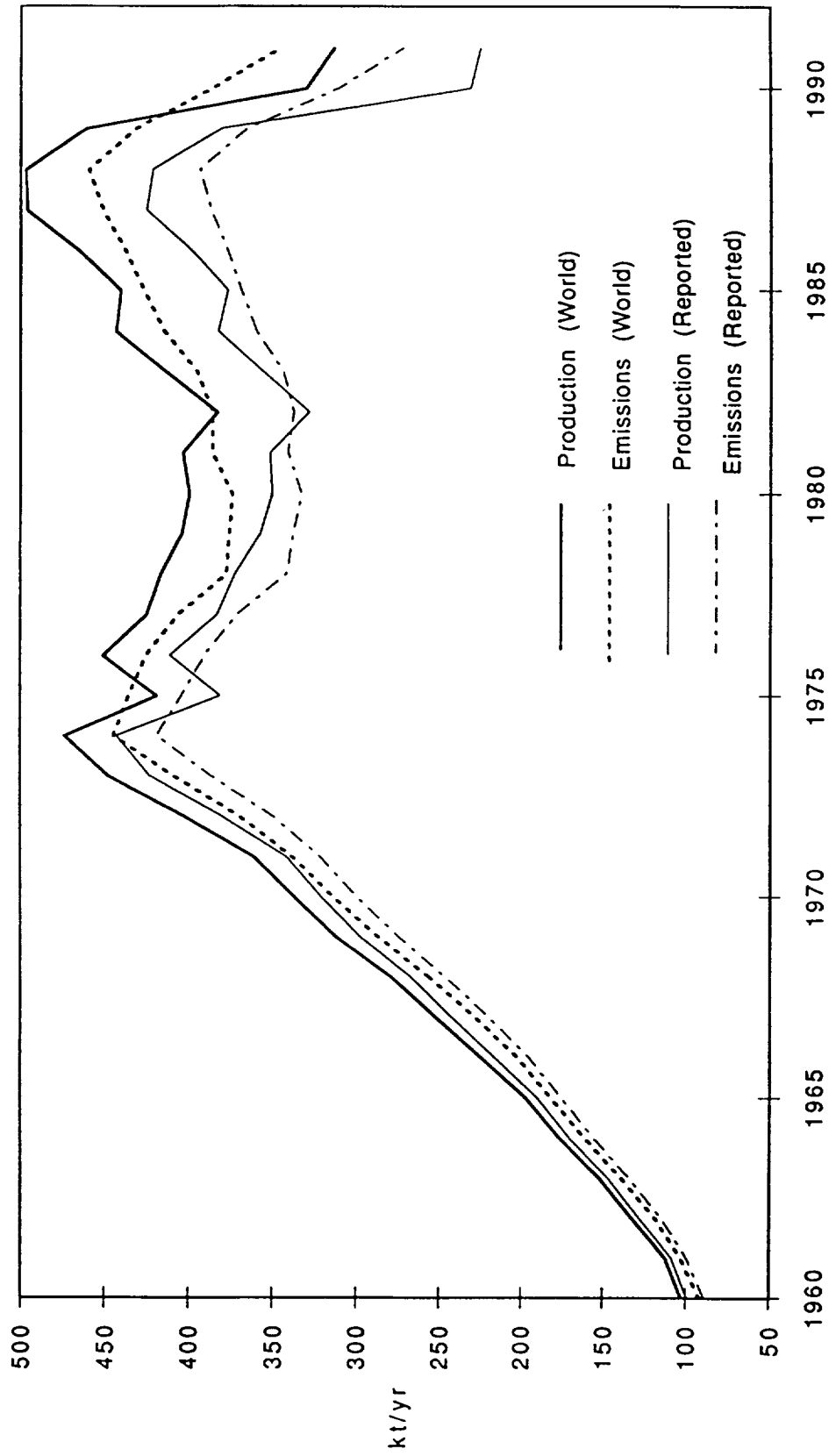

Figure 2.5.2-1 Production and emission of CFC 12 (Reporting Companies and World Estimates)

***Table 2.5.3-1** Participants in Survey for Production and Sales of CFCs 113, 114, and 115*

Listing of Survey Reporting Companies inclusive of any Related Subsidiaries and/or Joint Ventures Reporting Data
• Akzo Chemicals BV (Holland)
• Allied-Signal, Inc. (U.S.)
-- Allied Canada, Inc. (Canada)
-- Quimobasicos, S.A. (Mexico)
• Ausimont S.p.A. (formerly Montefluos S.p.A.)(Italy)
• Chemiewerk Nünchritz GmbH (Germany)[joined in 1990]
-- Dohna-Chemie GmbH (Germany)
• E. I. du Pont de Nemours & Company, Inc. (U.S.)
-- Du Pont Argentina (Argentina)
-- Du Pont do Brasil S.A. (Brazil)
-- Du Pont Canada, Inc. (Canada)
-- Du Pont International (Europe)
-- Du Pont S.A., de C.V. (Mexico)
• Elf Atochem, S.A. (France)
-- Elf Atochem Espana (Spain)
-- Elf Atochem North America (U.S.)
-- Pacific Chemical Industries Pty. Ltd. (Australia)
-- Produven (Venezuela)
• Hoechst AG (West Germany)
-- Hoechst Iberica (Spain)
-- Hoechst do Brasil Quimica e Farmaceutica S.A. (Brazil)
• ICI Chemicals and Polymers, Ltd. (England)
-- African Explosives & Chemical Industries, Ltd.
• Japan Flon Gas Association (Japan)
-- Asahi Glass Co., Ltd.
-- Central Glass Co., Ltd.
-- Daikin Industries, Ltd.
-- Du Pont-Mitsui Fluorochemicals Co., Ltd.
-- Showa-Denko, K.K.
• LaRoche Chemicals, Inc. (formerly Kaiser Aluminum & Chemical Corp. (U.S.)
• Rhône-Poulenc Chemicals, Ltd. (U.K.)
• Société des Industries du Nord de la Grèce, S.A. (joined in 1990)
• Solvay S.A. (Belgium)
-- Kali-Chemie Iberia SA (Spain)
-- Solvay Fluor und Derivate GmbH (formerly Kali-Chemie Aktiengesellschaft) (Germany)

C. Emission Results

Both Table 2.5.3-2 and Figure 2.5.3-1 show the production and emission results from this survey. The use of CFC-113 grew steadily in the 1980s. Because most of the sales are in the short service life category, the emission results closely mirror production levels.

Figure 2.5.3-1 also shows the global production and emission results including "non-reported" production. Both the UNEP and the AFEAS estimates have been used to develop data for world emission levels for years between 1986 and 1991. In the absence of any other information for years before 1986, world production levels were assumed to be 12.2% above the surveyed production levels — the same as derived for 1986 from the UNEP data — but this may overstate total production. Use categories were assumed to be the same as for reported production.

Table 2.5.3-2 Production and Calculated Emissions of CFC 113 (kt)

	Reporting Companies Only		Global Estimates	
	Prod.	Emiss.	Prod.	Emiss.
1970	26.6	25.0	29.8	28.0
1971	30.5	28.6	34.2	32.1
1972	35.0	32.9	39.3	36.9
1973	40.0	37.6	44.9	42.2
1974	45.9	43.1	51.5	48.4
1975	52.6	49.4	59.0	55.5
1976	60.2	56.6	67.5	63.5
1977	69.0	64.9	77.4	72.8
1978	79.0	74.3	88.6	83.4
1979	90.5	85.1	101.5	95.5
1980	103.7	97.5	116.3	109.4
1981	108.5	106.4	121.8	119.4
1982	113.0	111.1	126.8	124.6
1983	132.7	123.3	148.9	138.3
1984	171.1	152.5	192.0	171.1
1985	187.0	179.8	209.8	201.7
1986	196.6	193.1	220.6	216.6
1987	225.8	213.1	248.1	236.4
1988	247.4	238.7	268.1	260.3
1989	251.3	251.5	270.3	271.6
1990	174.8	214.7	193.5	233.8
1991	147.6	163.1	165.2	181.5

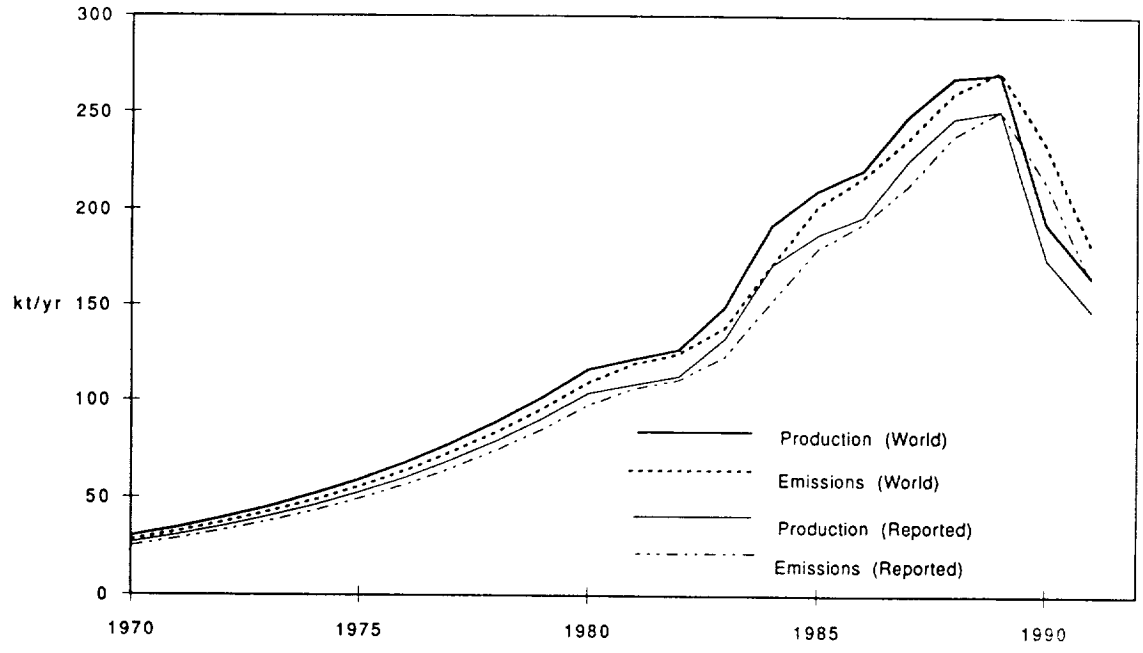

Figure 2.5.3-1 Production and emission of CFC 113 (Reporting Companies and World Estimates)

2.5.4 1,2-Dichlorotetrafluoroethane (CFC-114)

A. Surveyed Production Data

Production and sales of CFC-114 were covered under the same survey described above for CFC-113; thus survey coverage is the same. The data once again indicate that almost all of the material is released in the Northern Hemisphere (97.4%); however, no detailed estimates are available for the production in non-reporting countries. The UNEP report of production by Parties of the Montreal Protocol indicates less production than reported in the industry survey for 1986 [17,241 (UNEP, 1991) vs 19,101 tonnes (survey)].

B. End Use Categories

As with the CFC-113 survey, market applications were grouped according to time scale of use; however, both the major applications and the groupings are somewhat different.

CFC-114 sales were divided into the following categories:

Aerosols
Blowing agent, polyolefin foams
Long-lived refrigerant use
Other uses

This categorization allows major markets that have similar delays between production and release to be grouped for the purpose of estimating emission rates.

- Short time scale (average service life = 6 months): includes product used in aerosols, polyolefin foams, and the other uses plus fugitive emissions.
- Long time scale (characteristic time = 12 years): includes product used in refrigeration.

C. Emission Results

Both Table 2.5.4-1 and Figure 2.5.4-1 show the production and emission results from this survey. The use of CFC-114 has grown steadily over the past decade although at a rate less than for CFC-113. Again, because most of the sales fall in the short service life category, the emissions pattern closely reflects the production growth. Levels of "non-reported" production are not quantified, and so no estimates of total global production have been made.

Table 2.5.4-1 *Production and Calculated Emissions of CFCs 114 and 115 (kt) (Reporting Companies only)*

	CFC-114		CFC-115	
	Production	Emissions.	Production	Emissions
1934	2.6	0.1	0.0	0.0
1935	2.7	0.1	0.0	0.0
1936	2.8	0.1	0.0	0.0
1937	2.9	0.1	0.0	0.0
1938	3.0	0.2	0.0	0.0
1939	3.1	0.2	0.0	0.0
1940	3.3	0.3	0.0	0.0
1941	3.4	0.5	0.0	0.0
1942	3.5	0.7	0.0	0.0
1943	3.7	0.9	0.0	0.0
1944	3.8	1.2	0.0	0.0
1945	4.0	3.2	0.0	0.0
1946	4.1	5.4	0.0	0.0
1947	4.3	5.8	0.0	0.0
1948	4.4	6.2	0.0	0.0
1949	4.6	6.5	0.0	0.0
1950	4.8	6.8	0.0	0.0
1951	5.0	7.0	0.0	0.0
1952	5.2	7.2	0.0	0.0

Table 2.5.4-1 *Continued*

	CFC-114		CFC-115	
	Production	Emissions.	Production	Emissions
1953	5.4	7.4	0.0	0.0
1954	5.6	7.4	0.0	0.0
1955	5.8	7.3	0.0	0.0
1956	6.0	7.2	0.0	0.0
1957	6.3	7.2	0.0	0.0
1958	6.5	7.1	0.0	0.0
1959	6.7	7.1	0.0	0.0
1960	7.0	7.1	0.0	0.0
1961	7.3	7.2	0.0	0.0
1962	7.6	7.4	0.0	0.0
1963	7.8	7.6	0.0	0.0
1964	8.1	7.7	0.9	0.1
1965	8.4	8.0	1.1	0.2
1966	8.8	8.3	1.2	0.3
1967	9.1	8.7	1.4	0.5
1968	9.5	9.0	1.7	0.8
1969	9.9	9.4	2.0	1.1
1970	10.2	9.7	2.3	1.3
1971	10.6	10.1	2.6	1.6
1972	11.1	10.5	3.1	1.9
1973	11.5	10.9	3.6	2.2
1974	11.9	11.3	4.2	2.5
1975	12.4	11.7	4.8	3.0
1976	12.9	12.2	5.6	3.5
1977	13.4	12.7	6.5	4.0
1978	13.9	13.2	7.6	4.7
1979	14.4	13.7	8.9	5.4
1980	15.0	14.2	9.3	6.3
1981	14.0	14.1	10.0	7.2
1982	13.6	13.5	10.4	8.1
1983	14.8	13.9	11.6	8.9
1984	15.6	14.9	11.2	9.6
1985	17.1	15.9	10.0	10.1
1986	19.1	17.7	11.8	10.6
1987	17.1	18.0	12.8	11.0
1988	16.5	16.0	13.6	11.4
1989	15.0	14.3	14.2	11.9
1990	8.3	10.3	11.3	12.2
1991	6.7	6.3	12.3	12.6

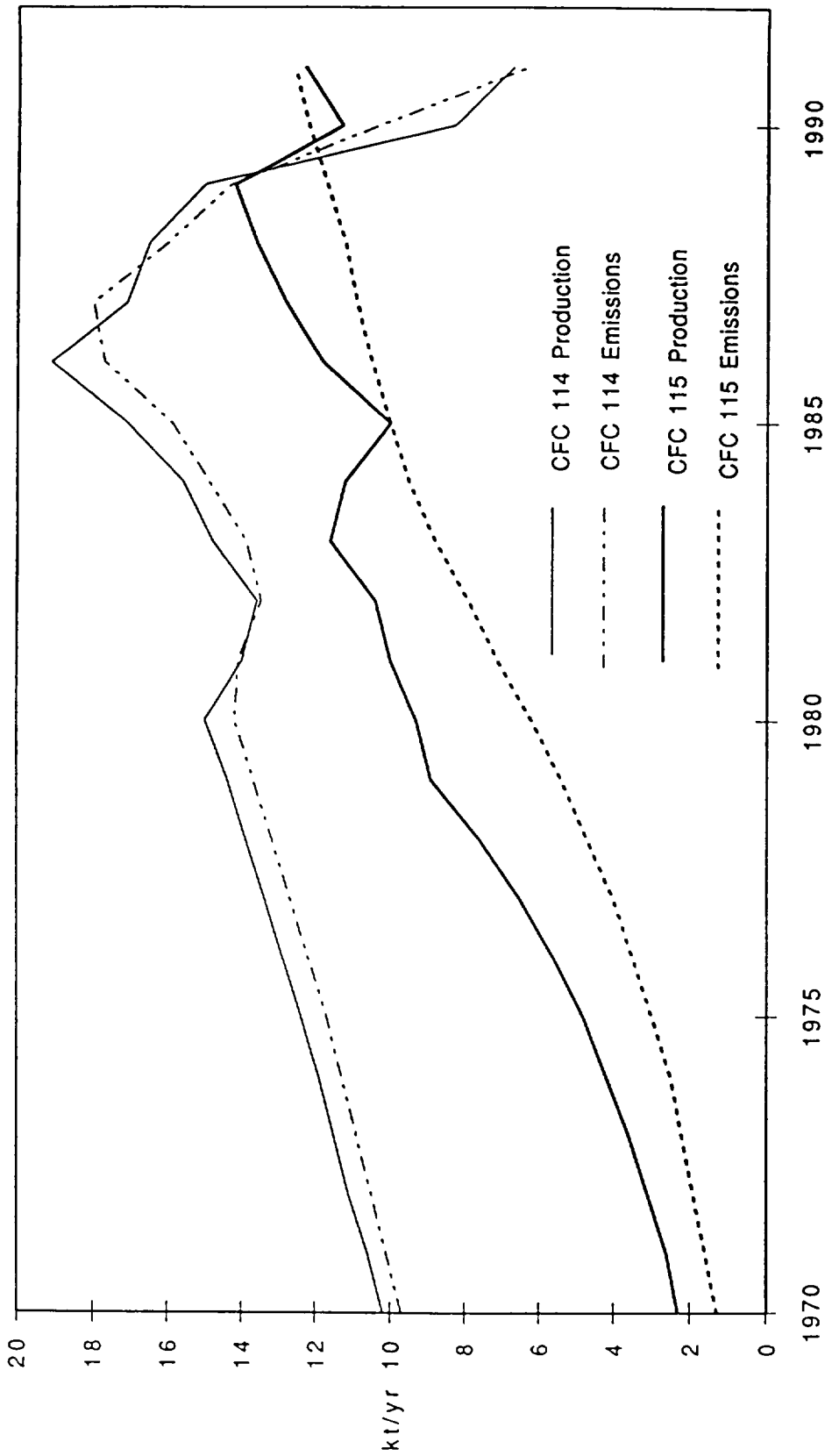

Figure 2.5.4-1 Production and emission of CFCs 114 and 115 (Reporting Companies only)

2.5.5 Chloropentafluoroethane (CFC-115)

A. Surveyed Production Data

Production and sales of CFC-115 were covered under the same survey described above for CFC-113 so that the survey coverage is identical. The data once again indicate that almost all of the material is released in the Northern Hemisphere (96.3%); however, no detailed estimates are available for the production in non-reporting countries. The UNEP report of production by Parties of the Montreal Protocol indicates less production than reported in the industry survey for 1986 [11,110 (UNEP 1991) vs. 11,818 tonnes (survey)].

B. End Use Categories

As with the CFC-113 survey, market applications were grouped according to time scale of use but with a slight realignment.

CFC-115 sales were divided into the following categories:

Aerosols
Short-lived refrigerant use
Dielectric fluid
Other uses

This categorization allows major markets to be grouped for the purpose of estimating emission rates.

- Short time scale (average service life = 6 months): includes CFC-115 used in aerosols and the other uses plus fugitive emissions.
- Long time scale (characteristic time = 4 years): includes material used in refrigeration. This delay time is shorter than for refrigerant uses of either CFC-113 or -114 since it is used in a different type unit. Use as a dielectric fluid is included here although this application is minor.

C. Emission Results

Both Table 2.5.4-1 and Figure 2.5.4-1 show the production and emission results from this survey. The use of CFC-115 has grown steadily over the past decade at a rate somewhat like CFC-113. Levels of "non-reported" production are not quantified, and so no estimates of total global production have been made.

2.5.6 Chlorodifluoromethane (HCFC-22)

A. Surveyed Production Data

Annual production and sales of HCFC-22 since 1980 have been surveyed and reported by AFEAS. In this survey, annual production totals only were reported for the years 1970-1979. The results of this retrospective survey were published in June 1991. The participating companies, listed in Table 2.5.6-1, include all the producers in Japan, North America, Western Europe as well as their subsidiaries, which cover production in South America and Africa. Some production is believed to occur in India, Korea, the People's Republic of China, and the former USSR, but much of this is used as a chemical intermediate and thus not released to the atmosphere. More complete details of this survey are available in Midgley and Fisher, 1993.

Current estimates indicate that the reporting companies account for over 90% of the total world production of HCFC-22. Sales were allocated to the following regions: 0°-30°N, 30°-90°N, and 0°-90°S. Production data uncertainties are probably not greater than ±0.5%, given that plant losses are accounted for by the auditor.

B. End Use Categories

A sizeable portion of the HCFC-22 production is consumed as a chemical intermediate to make fluoropolymers and halons and is not released to the atmosphere. Therefore, this quantity is deducted from the production total. The remainder of the sales were reported in the following categories:

- Short-term emissions (less than 1 year): aerosols, blowing agents for open cell foams and extruded foams; also fugitive emissions (plant losses) are included with this total in the emissions calculation. These fugitive

losses account for losses both at the production step as well as in the use of HCFC-22 as a chemical intermediate.

- Medium-term emissions (1-10 years): essentially refrigeration and air conditioning, account for largest fraction of total production.
- Long-term emissions (more than 10 years): primarily used as a blowing agent for closed cell thermoset foams.

***Table 2.5.6-1** AFEAS member companies*

Akzo Chemicals BV
Allied-Signal Inc.
Ausimont S.p.A.
Dohna-Chemie GmbH (formerly Chemiewerke Nünchritz GmbH) (joined in 1990)
E. I. du Pont de Nemours & Company
Elf Atochem
Hoechst AG
ICI Chemicals & Polymers, Ltd.
Japan Flon Gas Association
LaRoche Chemicals Inc.
Rhône-Poulenc Chemicals/ISC Division
Société des Industries du Nord de la Grèce, S.A. (joined in 1990)
Solvay Fluor und Derivate GmbH

C. Results

The results of the HCFC-22 survey are given in Tables 2.5.6-2 and 2.5.6-3 and Figure 2.5.6-1. Use of this compound has shown steady growth with the majority (>90%) of the product included in the refrigeration and air conditioning category. The long-term emission category accounts for a very small portion of overall sales.

***Table 2.5.6-2** Sales of HCFC-22 by Emission Category and Region (kt) (Reporting Companies only)*

	Emission Category			Region		
	Short	Medium	Long	30°-90°N	0°-30°N	0°-90°S
1980	5.7	120.5	0.1	112.3	8.2	5.9
1981	6.0	124.8	0.1	116.1	8.9	5.8
1982	5.8	117.7	0.2	108.6	9.1	5.9
1983	6.8	137.0	0.1	126.7	10.7	6.5
1984	7.8	144.4	0.1	134.0	11.6	6.7
1985	8.5	144.7	0.2	132.3	13.4	7.7
1986	8.9	156.0	0.1	138.2	18.2	8.6
1987	10.0	163.1	0.2	148.6	15.0	9.8
1988	16.0	187.3	0.3	176.6	16.4	10.6
1989	25.1	194.1	0.3	191.4	18.7	9.4
1990	31.0	180.8	1.8	181.9	20.2	11.6
1991	27.1	201.9	7.7	207.2	19.8	9.8

Table 2.5.6-3 Production and Calculated Emissions of HCFC-22 (kt)

(Reporting Companies only)

	Production	Emission
1970	56.1	41.4
1971	60.6	45.8
1972	63.3	50.1
1973	74.3	57.5
1974	83.4	65.0
1975	75.0	65.7
1976	90.7	74.0
1977	101.4	82.4
1978	111.7	90.1
1979	117.9	96.7
1980	126.3	104.3
1981	130.8	110.3
1982	123.6	111.9
1983	143.9	122.8
1984	152.4	131.8
1985	153.4	137.2
1986	165.0	145.6
1987	173.3	153.7
1988	203.5	171.4
1989	219.5	188.7
1990	213.7	195.2
1991	236.8	204.3

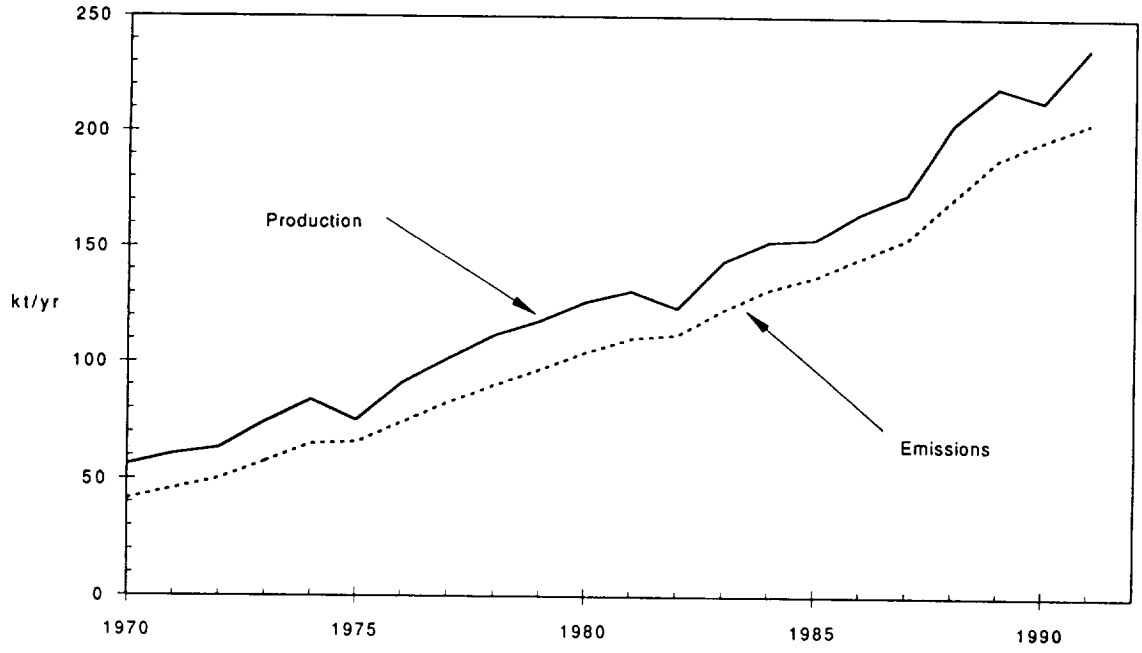

Figure 2.5.6-1 Production and emission of HCFC 22 (Reporting Companies only)

2.5.7 Methyl Chloroform (1,1,1-trichloroethane)

A. Surveyed Production Data

Worldwide producers of methyl chloroform (1,1,1-trichloroethane) have surveyed production and use covering 1980-1991; production totals only are reported for 1970-1980. The survey participants are listed in Table 2.5.7-1 and results are given in Table 2.5.7-2. Survey participants believe that this survey accounts for at least 97% and possibly greater than 99% of methyl chloroform production in the world.

Table 2.5.7-1 *Participants in Methyl Chloroform Survey*

Asahi Glass Company
Asahi Chemical Industry Company Ltd.
Atochem Group Elf Aquitaine
Central Class Company Ltd.
The Dow Chemical Company
ICI PLC
Kanto Denka Industry Company Ltd.
PPG Industries
Solvay et Cie
Toagosei Chemical Industry Ltd.
Tosoh Company Ltd.
Vulcan Chemicals

Table 2.5.7-2 *Production and Emissions of Methyl Chloroform (Reporting Companies only) [kt]*

		PRODUCTION		EMISSIONS
Year	Total	Release:	Release:	
		0-6 mo.	6-12 mo.	Total
1971	175	*166*	9	170
1972	227	*216*	11	214
1973	279	265	14	266
1974	314	298	16	305
1975	307	292	15	309
1976	407	*387*	20	382
1977	480	456	24	462
1978	524	498	26	513
1979	506	*481*	25	511
1980	551	525	26	539
1981	548	521	27	548
1982	512	487	25	521
1983	540	518	22	534
1984	600	577	23	584
1985	587	567	20	591
1986	608	585	23	602
1987	627	605	22	622
1988	679	658	21	666
1989	694	673	21	690
1990	726	705	21	718
1991	605	*585*	20	610

Note: Data in *italics* are based on assumed release categorization data (see text).

Only two known production facilities are not covered by the production survey. A single production facility in India with a capacity of 3,000 tonnes per year was established in 1985. Due to technical problems, production did not exceed 20% of the capacity although it was expected to produce at full capacity by 1991. Additionally, a plant with a 15,000 tonnes per year capacity in the former USSR has been reported to sporadically produce methyl chloroform at less than capacity. A delegate from the former Soviet Union to a meeting of the Montreal Protocol Parties acknowledged the existence of a small development plant in Russia, but indicated that it would undoubtedly be shut down.

B. End Use Categories

The surveyed methyl chloroform producers reported their data not by specific end use but rather according to the timescale of expected emissions to the atmosphere in less than 6 months, between 6 months and 1 year, and more than 1 year. About 95 - 98% of the 1980 through 1990 production was into end uses which emit methyl chloroform in less than 6 months. The balance was a single, minor use with a medium release delay of 6 to 12 months. No production was reported for any end uses with long timescale (greater than one year) release. The largest use of methyl chloroform, worldwide, is for metal cleaning in a wide variety of industrial processes.

C. Emission Results

Calculated emissions, based on surveyed methyl chloroform production/sales, are shown in Table 2.5.7-2 and Figure 2.5.7-1. This emission calculation has been based on the following assumptions : the immediate and the medium release categories are assigned service lives of 0.25 and 0.75 years respectively (Midgley, 1989). The medium category was assumed to be 5% of total sales prior to 1980, consistent with the fraction in 1980. Also, 20 kt were assumed for this category in 1991 consistent with use at the end of the 1980s. Fugitive emissions, calculated at 0.25% of total sales, were included during each production year. All material sold was assumed to be emitted.

Figure 2.5.7-2 and Table 2.5.7-3 display the geographical pattern of its use. Note that the Northern Hemisphere covers the vast majority of manufacture and use for this compound — in fact the three regions of Europe, United States/Canada, and the Far East are the dominant regions and are of comparable size throughout the entire period. Substantial decreases in sales were realized in 1991.

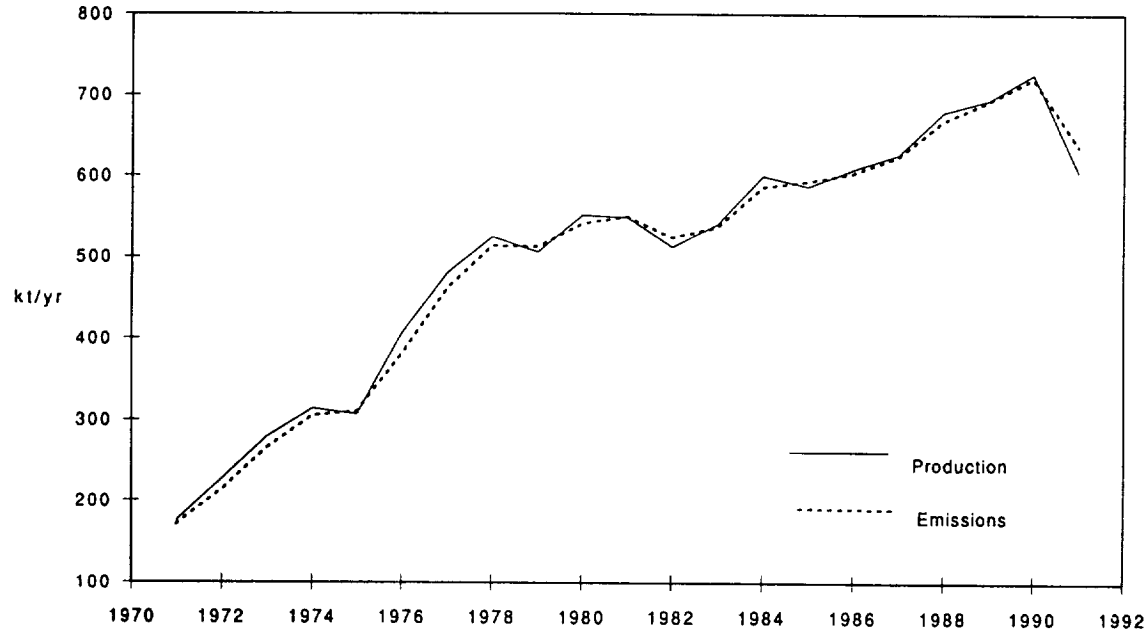

Figure 2.5.7-1 Production and emission of Methyl Chloroform (Reporting Companies only)

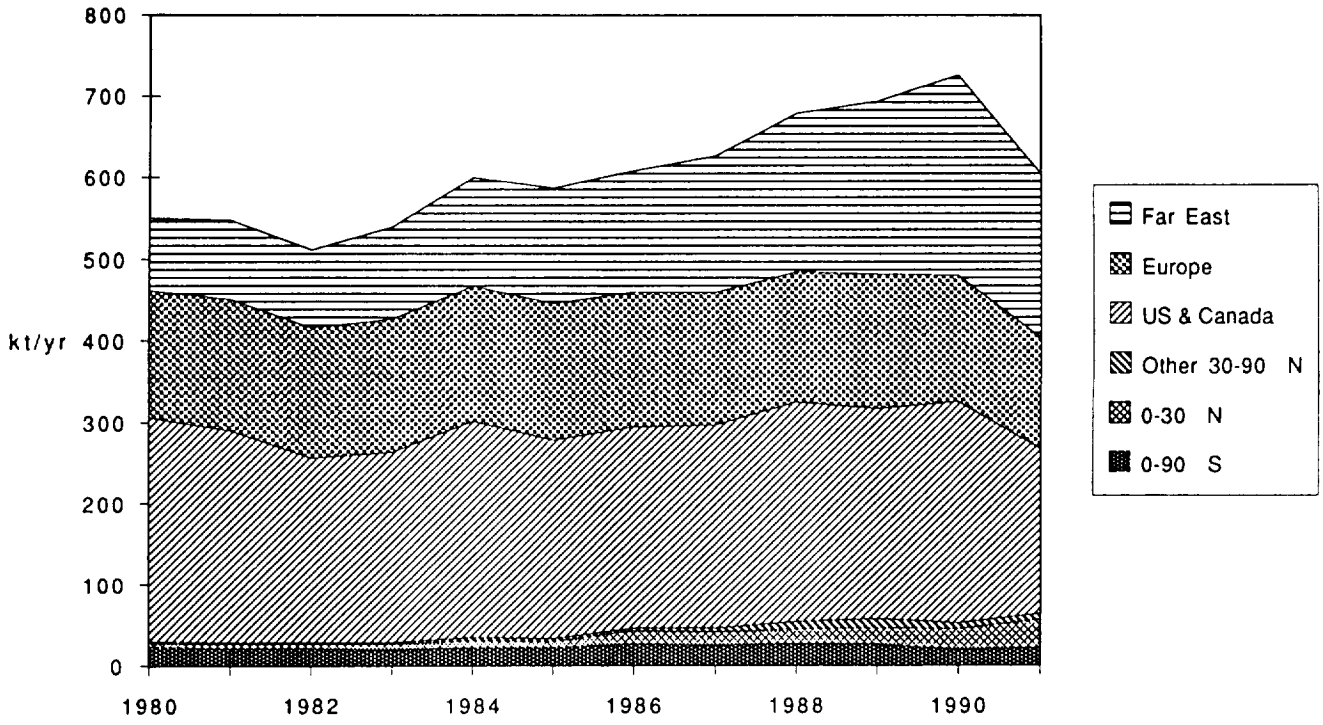

Figure 2.5.7-2 Regional Sales of Methyl Chloroform (Reporting Companies only)

Table 2.5.7-3 *Methyl Chloroform Sales by Region (reporting companies only) in kt*

	0-90°S	0-30°N	30°N-90°N			
			US & Canada	Europe	Far East	Other 30°N-90°N
1980	24.0	4.2	276.3	156.2	87.8	2.0
1981	20.6	5.6	262.3	160.7	96.4	2.0
1982	20.8	5.7	228.1	159.8	95.9	1.5
1983	19.5	7.5	234.6	163.5	112.7	2.1
1984	22.0	8.7	266.9	165.8	132.0	4.3
1985	22.0	7.7	245.5	167.2	141.4	3.3
1986	26.6	16.3	248.7	165.9	147.6	3.0
1987	24.6	16.2	251.1	162.6	167.0	5.3
1988	27.2	17.5	271.5	160.0	193.7	9.0
1989	25.9	20.1	259.7	165.4	211.3	11.4
1990	19.6	25.0	273.7	155.2	244.7	7.7
1991	21.1	34.8	204.2	136.0	201.0	7.7

2.5.8 Halons

2.5.8.1 Bromochlorodifluoromethane (Halon-1211) and Bromotrifluoromethane (Halon-1301)

The halon producers within the OECD (Organization for Economic Cooperation and Development), listed in Table 2.5.8-1, conducted a data collection exercise for Halons 1211 and 1301 ($CBrClF_2$ and $CBrF_3$). Annual production totals up to 1991 have been reported to independent auditors. To preserve commercial confidentiality for the early years during which there were few producers, only cumulative totals were reported up to 1980 for Halon-1211, and up to 1972 for Halon-1301 (McCulloch, 1992). The uncertainties in the production data were ±0.5%.

***Table 2.5.8-1** OECD (Organization for Economic Cooperation and Development) Halon Producers*

Producers in:
Australia
Canada
Japan
New Zealand
United States
European countries

Production of Halons -1211 and -1301 outside the OECD (*e.g.*, People's Republic of China and the C.I.S.) is relatively insignificant with virtually none in the C.I.S.

Realistic estimates were developed for the percentage of production released to the atmosphere by surveying the OECD producers. These estimates took into account the amount due to "incidents" (fires, accidental discharge, training, and testing), and during initial filling, servicing, and disposal of equipment. To accommodate changes in use and containment patterns, separate estimates were made for different time periods. The responses reflected a wide disparity of opinion. These more realistic release estimates are greater than the percentages previously assumed (20 to 30%), especially for Halon-1211. The results, quoted in Table 2.5.8-2, were used to calculate annual emissions from the reported annual production totals which are given in Table 2.5.8-3. Figure 2.5.8-1, which displays the production and emission data for these compounds, graphically shows that both production and emissions peaked between 1985 and 1987, and have since steadily declined.

***Table 2.5.8-2** Annual percentages of Halon production emitted to the atmosphere from all sources*

	Halon-1211	Halon-1301
1969-1980	66	36
1981-1985	69	52
1986-1990	58	33

2.5.8.2 1,2-Dibromotetrafluoroethane (Halon-2402)

Limited quantities of Halon-2402 ($CBrF_2CBrF_2$) were reported to the Montreal Protocol Secretariat as part of the data requirements under the Protocol. Total reported data for 1986 was 3724 tonnes. Since not all countries reported, this amount may not represent total global production. The C.I.S. and other Eastern European countries account for about 90% of the consumption of Halon-2402.

Table 2.5.8-3 *Annual global production and calculated emissions of Halons (tonnes)*

Year	Halon-1211		Halon-1301	
	production	emissions	production	emissions
1963	50	33	10	4
1964	100	66	20	7
1965	200	132	30	11
1966	300	198	40	14
1967	500	330	50	18
1968	700	462	60	22
1969	900	594	100	36
1970	1260	832	200	72
1971	1700	1122	550	198
1972	2200	1452	839	302
1973	2750	1815	1292	465
1974	3300	2178	1461	526
1975	3800	2508	2019	727
1976	4356	2875	3172	1142
1977	5000	3300	3550	1278
1978	5650	3729	4015	1445
1979	6280	4145	4718	1698
1980	6910	4561	4877	1756
1981	6689	4615	5694	2961
1982	7485	5165	7565	3934
1983	8259	5699	7386	3841
1984	10408	7353	8692	4520
1985	12491	8876	9781	5086
1986	13731	8307	11076	3655
1987	17058	10322	11604	3829
1988	20181	12563	12551	4142
1989	16182	10243	11152	3680
1990	14852	9472	9115	3008
1991(#)	9037	xxx	9617	xxx

Note: To preserve commercial confidentiality, data prior to 1980 for Halon 1211 and 1972 for Halon 1301 are based on the cumulative total production to that date with a reasonable extrapolation back to the start of production.

(#) For 1991, production data was reported by Conseil Europeen des Federations de l'Industrie Chimique. No emission data is available since use patterns have shifted significantly and emission factors based on previous poll results are not valid.

2.5.9 Methyl Chloride (CH_3Cl)

Annual emissions of methyl chloride have been variously estimated to be in the range of 2 to 5 million tonnes, depending largely on assumptions about lifetime. A lifetime of 1.5 years yields an estimate of about 3.5 million tonnes per year. Most of these emissions are thought to come from natural sources, probably from biological processes in the oceans (Singh, 1988; WMO, 1990). There are, however, some anthropogenic sources that may be significant. Global industrial production/sales of methyl chloride in 1990 was about 662 kt; however, essentially all of this was used for chemical feedstock, primarily in the manufacture of silicones, but also to make agricultural chemicals and butyl rubber (SRI, 1992). As such, the product was consumed and only process fugitive emissions escape to the atmosphere which are likely to be small and a very minor contributor to the global atmospheric methyl chloride.

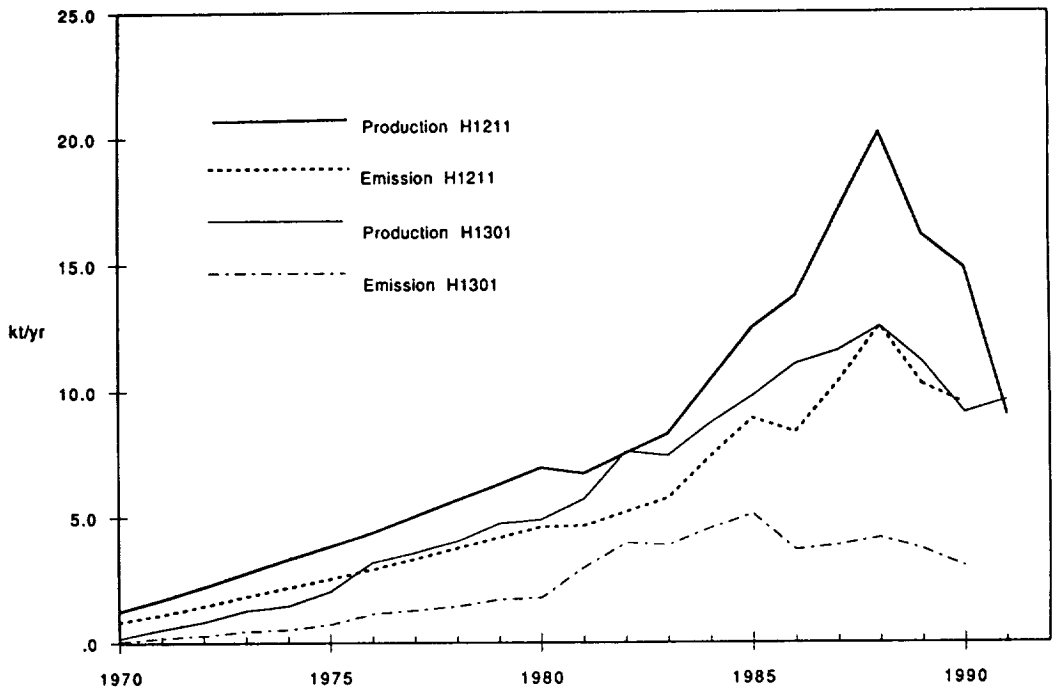

Figure 2.5.8-1 Production and emission of Halons 1211 and 1301 (Reporting Companies only)

The principal source of anthropogenic methyl chloride emissions is probably from diverse kinds of biomass burning in open fires, including burning of forests and savannahs, and the use of biomass as a fuel. High temperature, complete combustion of biomass does not result in significant methyl chloride emissions. There are large uncertainties in the amounts of methyl chloride emitted from biomass burning due to variations in specific emissions from different types of biomass, a variety of combustion conditions, and uncertainties about the total amount of biomass burned (Rasmussen *et al.*, 1980, Crutzen *et al.*, 1979). A reasonable range for total emissions of methyl chloride due to biomass burning based on current data is 0.5 to 1 million tonnes per year, though the actual uncertainties are even larger (Levine, 1990; Makhijani, 1990; Andreae, 1991). This range is equivalent to approximately 15 to 30 percent of total methyl chloride emissions, based on a total source term of 3.5 million tonnes.

2.5.10 Other Chlorocarbons

It would be useful to have accurate production and emission data on a number of other chlorine-containing chemicals, specifically methylene chloride (CH_2Cl_2), perchloroethylene (CCl_2CCl_2), trichloroethylene ($CHClCCl_2$), and carbon tetrachloride (CCl_4) as input to modeling destructive process of the more reactive compounds. There are currently no industry-wide data collections on any of these; however, global totals for methylene chloride, perchloroethylene and trichloroethylene can be estimated from the data given in Table 2.5.10-1.

It is more difficult to estimate emissions of carbon tetrachloride. The principal use of carbon tetrachloride is as a feedstock for the production of CFCs, rather than for dispersive uses; however, feedstock applications can account for only a small proportion of the releases that can be inferred from atmospheric measurements (Simmonds *et al.*, 1983).

There are a number of other sources of carbon tetrachloride emissions. These include uses as a solvent and fire extinguishant, and emissions from inadvertent production in a range of industrial chlorination processes. Together, these sources are responsible for the vast majority of emissions of carbon tetrachloride. It is not possible, at the

present time, to partition accurately the emissions among these various sources. Part of the difficulty arises from the fact that there are a number of significant producers who have not reported data so far. An order of magnitude estimate of annual emissions inferred from atmospheric concentrations is 100,000 tonnes per year (WMO, 1986; Simmonds *et al.*, 1983; Penkett *et al.*, 1979).

Table 2.5.10-1 *Estimates and Reported Data on Methylene Chloride, Perchloroethylene, and Trichloroethylene*

Methylene Chloride - kt

	Geographic Region					Notes
Year	Global	USA	W. Europe	Japan	Rest of World	
1990	657	213	275	75	94	Production data (SRI 1992)
1990	594	164	183	78	170	Consumption data (SRI 1992)
1988		177				Dispersive Uses (paint stripper, aerosol, polyurethane foam, metal cleaning, electronics) (Chem. Market Rep 1989)
1990	530	200	261	69	(*)	Sales Data (MITI 1991)

Notes: (*) Rest of world is included with W. Europe.
No data for production in E. Europe and C.I.S. but thought to be very small, if not zero.

Perchloroethylene* - kt

	Geographic Region					Notes
Year	Global	USA	W. Europe	Japan	Rest of World	
1990	358	129	220	15	small	Production for dispersive uses (SRI 1992)
1987	386	154	193	39	small	Production for dispersive uses (SRI 1988)

* Additional perchloroethylene emissions of up to 100 kt/yr could come from residue processes in developing nations.

Trichloroethylene* - kt

	Geographic Region					Notes
Year	Global	USA	W. Europe	Japan	Rest of World	
1990	267	79	131	57	small	Production data (SRI 1992)
1987	248	57	142	49	small	Production data (SRI 1988)

* Additional trichloroethylene emissions of up to 50 kt/yr could come from residue processes in developing nations.

2.5.11 Other HCFCs

AFEAS members have agreed to collect data on other HCFCs in the future, subject to the following conditions: for each compound, the combined data will be disclosed once there are at least three producers and total sales or dispersive uses exceed 20,000 tonnes per year. The compounds that could likely to be covered in future surveys are HCFCs -123 ($CHCl_2CF_3$), -124 ($CHClFCF_3$), -141b (CH_3CCl_2F), -142b (CH_3CClF_2) -225ca ($CHCl_2CF_2CF_3$), and -225cb ($CHClFCF_2CClF_2$) (see Table 2.5.11-1).

***Table 2.5.11-1** Hydrochlorofluorocarbons of Commercial Interest*

HCFC	Chemical Formula
22	$CHClF_2$
123	$CHCl_2CF_3$
124	$CHClFCF_3$
141b	CH_3CCl_2F
142b	CH_3CClF_2
225ca	$CHCl_2CF_2CF_3$
225cb	$CHClFCF_2CClF_2$

2.5.12 Methyl Bromide (CH_3Br)

A substantial portion of methyl bromide (CH_3Br) emitted into the atmosphere is thought to come from natural, oceanic sources. Measurements of methyl bromide in sea water (Singh *et al.*, 1983) show significant supersaturation suggesting that oceans are a significant natural source of methyl bromide. Measurements of larger tropospheric mixing ratios for methyl bromide in the Northern Helmisphere (Penkett *et al.*, 1985) suggest a larger source in the north.

The primary fraction of industrially produced methyl bromide is used as a fumigant. As a fumigant, methyl bromide's largest use is to treat soils for production of crops in intensive agricultural systems — it is also used for essential import/export quarantine treatments and for treatment of enclosed spaces for insect and rodent control. Additionally, a portion of industrial sales goes into chemical raw material feedstocks, but this portion is consumed and therefore not dispersed to the atmosphere.

In 1992, an industry-wide survey of production and sales by uses was released by the Methyl Bromide Global Coalition of the CMA (MBGC CMA, 1992). This survey covers the seven-year period 1984-1990. (Data prior to 1984 could not be reconstructed since records from a major producer, which has since sold its business, could not be retrieved.) This seven-year coverage, however, should be sufficient for assessment of anthropogenic source strengths since the "held-in-use" times for these applications are comparatively short, also atmospheric measurements of methyl bromide are relatively recent and limited, and the estimated atmospheric lifetime for methyl bromide is only ~2 years (WMO, 1992 and UNEP, 1992).

Companies from the United States, western Europe, and Japan (see Table 2.5.12-1) participated in this survey such that reporting companies accounted for at least 95% of world production. The MBGC-CMA survey indicates that in 1990, total methyl bromide production amounted to 61,724 (metric) tonnes and 62,951 tonnes sold for dispersive use. Detailed results of the MBGC-CMA survey are given in Tables 2.5.12-2 and 2.5.12-3.

***Table 2.5.12-1** Participants in Survey for Production and Use of Methyl Bromide*

Listing of Reporting Companies Inclusive of any Related Subsidiaries and/or Joint Ventures that Reported Production and Release Data

- Association of Methyl Bromide Industry Japan (Japan)
  - -- Sanko Kagaka Koguyo Co., Ltd.
  - -- Teijin Chemicals, Ltd.
  - -- Nippoh Chemicals Co., Ltd.
  - -- Dohkal Chemical Industry Co., Ltd.
  - -- Nippon Kayaku Co., Ltd.
  - -- Ichikawa Gohsei Chemical Co., Ltd.
- Atochem S.A. (France)
  - -- Derivados Del Etilo, S.A. (Spain)
- Dead Sea Bromine Group
  - -- AmeriBrom (U.S.)
  - -- Dead Sea Bromine (U.S.)
  - -- Eurobrom B.V. (The Netherlands)
- Ethyl ,Corporation (U.S.)
  - -- Ethyl S.A. (Belgium)
- Great Lakes Chemical Company (U.S.)
- Societa Azionaria Industria Bromo Italiano (Italy)

Table 2.5.12-2 *Annual Production of Methyl Bromide 1984 through 1990. Reporting Companies Only (Tonnes)*

Year	Production
1984	44,856
1985	48,013
1986	48,754
1987	56,224
1988	61,546
1989	64,628
1990	61,724

Total	385,745

Table 2.5.12-3 *Methyl Bromide Sales Tabulated by Use Category 1984 through 1990. Reporting Companies only (Tonnes)*

Year	Pre-Plant	Post Harvest	Structural	Residential/ Commercial	Chemical Intermediates	Total Sales
1984	30,408	9,001	1,285	881	3,997	45,572
1985	33,976	7,533	1,274	983	4,507	48,273
1986	36,090	8,332	1,030	999	4,004	50,455
1987	41,349	8,708	1,763	1,160	2,710	55,690
1988	45,131	8,028	1,910	1,737	3,804	60,610
1989	47,542	8,919	2,083	1,530	2,496	62,570
1990	51,306	8,411	1,740	1,494	3,693	66,644
Total	285,802	58,932	11,085	8,784	25,211	389,814

Not all of the methyl bromide used as a fumigant actually reaches the atmosphere. For typical agricultural treatments, methyl bromide is applied to the soil under a sheet of polyethylene film — such containment increases the efficacy of the treatment and diminishes loss to the atmosphere. Preliminary estimates indicate that roughly 40 to 70% of the material is chemically transformed while contained by the plastic, and the remainder eventually escapes to the atmosphere. The methyl bromide industry has initiated additional emission studies to better quantify the primary factors (moisture levels, application techniques, etc.) affecting the fraction emitted to better estimate global methyl bromide emissions from fumigation.

Apart from the methyl bromide produced for sale, some material is produced as by-products of other industrial production and eventually vented to the atmosphere. In the United States, emissions from inadvertent industrial sources amounted to ~1 kt in 1990 (EPA, 1992) or <1% of the annualized global emissions.

In summary, recognizing that the total emission level of methyl bromide is 100-150 kt/year (calculated to balance the atmospheric budget of methyl bromide in terms of atmospheric burden and chemical destruction rate) (UNEP, 1992) and assuming a 50% fumigant emission factor for dispersive uses, it appears that these industrial uses could account for as much as one-third of the total global emissions. These numbers are highly uncertain, however.

2.6 Uncertainty Analyses

2.6.1 General

Uncertainties in input data to the emission simulation contributes to the uncertainty in the resultant calculation. It is therefore important to examine the sensitivity of each derived parameter, *i.e.*, 1) production levels, 2) emission levels, and 3) amount of material remaining unreleased in the "bank," to the imprecisions that are present in the input parameters. This section examines uncertainties related to calculated emissions of CFCs 11 and 12 as well as for methyl chloroform.

Production levels:
Three factors can contribute to errors in production data generated from the various industrial surveys used in this study: errors in the reported production; errors in estimates in unreported production; and the possibility of inadvertent production.

High levels of accuracy for reported production are noted for all surveys utilized by this chapter. Error limits on the order of ±0.5% are typical for the surveys detailed above, given that fugitive emissions have been accounted for both at the manufacturing site and at the point of use as a chemical feedstock. Furthermore, transfers among co-producers, as well as adjustments for inventory levels at year-end, are recognized to be important factors and are dealt with appropriately.

Errors in the estimates for non-reported production can contribute significantly to the inaccuracies in the derived global figures. Levels of certainty vary significantly among the surveyed compounds and obviously depend on the fraction of global production that falls outside the survey region. At one extreme is methyl chloroform which has extremely limited production apart from what is covered by the surveys. At the other extreme are such compounds as carbon tetrachloride and perchloroethylene which are believed to have significant production and dispersive uses, but mainly in areas that have previously proved impossible to survey thereby rendering the attempt at such an exercise as impractical.

Certain compounds are produced inadvertently and emitted as by-products from chemical processes and could contribute to uncertainties in reported production levels. There is no known inadvertent production of the chemicals that have been surveyed. Conversely, inadvertent production of such products as carbon tetrachloride could contribute significantly to potential errors for any attempted survey for this compound.

Emission levels:
Uncertainties in calculated emission levels can best be understood by examining the impact of individual sources of potential errors to the resultant calculated emissions. Uncertainties in the basic production levels have a one-to-one correspondence to the derived emission data — therefore, each of the possible errors discussed above directly affects calculated emissions.

Calculated emission levels are sensitive to uncertainties in the emission functions. With the exception of material that is recovered and recycled, or that is consumed in chemical processing, virtually all material produced is eventually emitted to the atmosphere. Thus, there is little uncertainty about this aspect of the exercise; however, there are uncertainties surrounding the time pattern of release (*i.e.*, the emission function). It also follows that material used in applications where it is released soon after production (*e.g.*, CFC-113 and methyl chloroform, used primarily in cleaning applications) can be estimated much more directly than for applications where the materials are held for very long periods (*e.g.*, CFC-11 as a blowing agent in closed cell foams) since the time scale of general interest for emission data is one year.

Banked Amount:
Uncertainties in the quantity of material unreleased to the atmosphere mirror the uncertainties in the emissions since the banked amount is the difference between cumulative production and cumulative emissions. Here again, the uncertainties for the amount of material held in service are, in general, greater for applications experiencing long service life and smallest for applications involving complete release soon after production. These generalizations are shown explicitly in the sensitivity calculation below.

2.6.2 Sensitivity Analysis for CFCs 11 and 12
The significance of underlying uncertainties can be established by evaluating the sensitivity of calculated parameters to the individual sources of uncertainty. The significance of the individual uncertainties depends on how the release estimate is to be used. For lifetime calculations based on global atmospheric inventory, it is primarily the absolute errors in the release total that matter, *i.e.*,

$\sum_i R_i$ (where R_i is the release in year i). For lifetime calculations based on global trends, it is the uncertainties in the release trend that matters, i.e., $\frac{R_{1990}}{\sum_i R_i}$.

Furthermore, it is useful to estimate uncertainties in the amount held in the service "bank," i.e., $\sum_i P_i - \sum_i R_i$ (where P_i is the net production in year i), to estimate the amount of unreleased material that potentially could be emitted.

Table 2.6.2-1 lists the uncertainties associated with the calculated emissions of CFC-11 and 12. The sensitivity tests are analogous to the tests outlined in Gamlen *et al.* (1986), but applied in 1990 conditions. Although the uncertainties cannot be statistically defined as 2σ limits, they appear to approximate the 95% confidence limits, *i.e.*, less than 5% chance that the true value falls outside these limits.

Table 2.6.2-1 *Sources of uncertainty and their impact on calculated emissions of CFCs 11 and 12*

	Resulting % change in $\Sigma_{1990}R_i$		Resulting % change in $R_{1990}/\Sigma_{1990}R_i$		Resulting % change in Bank $_{1990}$	
	CFC-11	CFC-12	CFC-11	CFC-12	CFC-11	CFC-12
A) Reported Production is off by 0.5%	±0.5	±0.5	--	--	--	--
B) Non-Reported production ±25% of derived estimates	±1.3	±2.7	±2.5	±2.6	±1.6	±2.4
C) Non-Reported	+1.8	+1.3	+3.0	+4.9	-10.2	-14.3
Production all aerosol or 4	-0.5	-1.2	+3.8	+1.3	+ 2.8	+12.4
year release delay						
D) Long-lived refrig.	--	-0.6	--	-0.2	--	+6.9
comprises 3.5 ±2% of						
refrig. total	--	+0.5	--	+0.2	--	-5.3
E) Fugitive Emissions	±0.4	±0.4	--	--	--	--
± .4%						
F) Aerosol release delay 6	--	--	±0.9	±0.6	±0.2	±0.5
months ±1 month						
G) Short Refrigeration	±0.2	±1.1	±0.2	±0.1	±1.2	±12.
4 ± 0.5 yr						
H) Open Cell Foam	--	--	±0.4	--	±0.3	--
Release delay 2 ± 1 month						
I) Closed Cell Foam, fast	+4.5	--	+6.4	--	-25.7	--
and slow limits	-7.8		-16.0		+45.0	
J) "Other" category treated	-0.4	-0.2	-0.3	-0.9	+2.5	+1.7
as short lifetime refrig not						
aerosol.						

This table shows significant uncertainties in the release and banking estimates are:

For CFC-11,

(1) the closed-cell foam release scenario,

(2) the end-use pattern for non-reported production,

(3) the production level in non-reporting countries.

For CFC-12,

(1) the production levels in non-reporting countries,
(2) the end-use pattern for non-reported production,
(3) the short lifetime refrigeration emission scenario.

This analysis reemphasizes the need for production and use data from regions not covered by the survey, as well as a better understanding for short lifetime refrigeration category and, in particular, the closed-cell foam application. It should be noted that the cumulative emission uncertainty resulting from the closed cell foam has grown significantly from the level reported by Gamlen *et al.*, simply because the total time for release for the slow limit (100 years) involves material manufactured over the entire commercial life for CFC-11, whereas the base case involves sales only over the most recent 20 years.

2.6.3 Sensitivity Analysis for Methyl Chloroform (CH_3CCl_3)

Emission uncertainties for methyl chloroform can be analyzed in a manner similar to the CFC-11 analysis. The following analysis is based on the uncertainties outlined in Midgley (1989). Sources of uncertainty are estimated for each of the major input components for the emission calculation, namely the uncertainties in the reported production, in the non-reported production, and in characterization of the emission delays.

A) Reported Production

Production/sale levels of CH_3CCl_3 have been collected from participating companies using well-established procedures. The uncertainty for these data is 2.1%.

B) Non-Reported Production

Not all producers participated in this survey. However, as outlined previously, very little production occurs outside the reported region such that survey results should represent between 97% and 100% of the global production.

C-E) Release Categorization

The next step is to examine the uncertainties that arise from the form of the emission functions used in the calculation. For the "immediate" category, sensitivity of the lag uncertainties of ±1 month have been examined. Similarly, for the "medium" category, sensitivities of ±2 months were examined. Since no material is reported to the long time category, no sensitivity tests were run for this class of material. Additionally, categorization of material to each of the sales category is cited to be 4.1%. The uncertainty associated with this categorization was tested assuming that the "medium" category was either zero or double the survey fraction since the survey fraction is <4.1% for all years.

F) Fugitive Emissions

Release of material during the production and packaging operations are estimated by the producers to be 0.2-0.3% of total production. Thus sensitivity tests of ±0.05% have been examined.

The results of these sensitivity calculations are summarized in Table 2.6.3-1. Results are reported as changes in cumulative production amounts for 1980 through 1990, the period over which detailed use data were collected, as well as changes in trends, through examination of the change of 1990 emissions relative to the cumulative emissions — in this case for years 1980 through 1990.

***Table 2.6.3-1** Sources of Uncertainty and Impact on Calculated Emissions for CH_3CCl_3*

	% change in $\sum_{i=1980}^{1990} R_i$	% change in $\frac{R_{1990}}{\sum_{i=1980}^{1990} R_i}$
A) Uncertainty for net Production {±2.1%}	±2.1%	--
B) Uncertainty in non-surveyed production {97% to 99.5%}	+0.0 +3.0%	--
C) Short lived [<6 mo.] category certain to within {± 1 mo.}	-0.3 +0.5%	+0.1 -0.1
D) Medium lived [>6 mo.,<12 mo.] uncertainty of {± 2 mo}	±0.01%	--
E) Uncertainty for split into release categories {± 1X size of med. category}	±0.03%	--
F) Uncertainty in Fugitive emissions {±0.05%}	±0.05%	--

As shown in Table 2.6.3-1, the main uncertainties for CH_3CCl_3 emission estimates are associated with:

1) the production level in non-reporting countries, and
2) the imprecisions in the survey of reported production.

Uncertainties of input parameters have very little impact on emission trend. However, trend data may still be sensitive to some of these uncertainties for the following reason: in applying each sensitivity test, the uncertainty was applied uniformly over the historical results. Therefore such a test would not examine the impact of time variant application of these uncertainties, *e.g.*, if the actual production levels varied from year to year within the 2.1% uncertainty range, such a variation would not be represented by this analysis. No formal methodology has been developed for such a time variant analysis.

Since the amount of material held in use for methyl chloroform is comparatively small, the sensitivity of the "bank" size to each of the uncertainties was not analyzed.

2.6.4 Sensitivity Analysis for Other Compounds

A similar analysis has been carried out for HCFC-22 and is reported in Midgley and Fisher (1993). Details of that analysis are not reported here since that compound is not of central interest to the analysis of Chapter 3. However, in qualitative terms, that analysis showed that calculated emissions of HCFC-22 presently have higher levels of associated uncertainty than do the emission data for methyl chloroform. This result primarily reflects the higher levels of non-reported production and the uncertainties associated with emissions from longer service refrigeration uses of the material for HCFC-22.

References

AFEAS, Alternative Fluorocarbons Environmental Acceptability Study, Chlorofluorocarbons (CFCs) 11 and 12, Annual report of Production, Sales and Atmospheric Release of CFC-11 and CFC-12 through 1991, Washington, D.C., September 1992.

AFEAS, Alternative Fluorocarbons Environmental Acceptability Study, Chlorofluorocarbons (CFCs) 113, 114, and 115, Annual report of Production, Sales and Atmospheric Release of CFC-113, CFC-114, and CFC-115 through 1991, Washington, D.C., September 1992.

AFEAS, Alternative Fluorocarbons Environmental Acceptability Study, Hydrochlorofluorocarbon-22 (HCFC-22), Annual report of Production, Sales and Atmospheric Release of HCFC-22, Washington, D.C., September, 1992.

Andreae, M. O., Biomass Burning: Its History, Use, and Distribution and Its Impact on Environmental Quality and Global Climate in *Global Biomass Burning: Atmospheric, Climatic and Biospheric Implications*, J. S. Levine, Editor, MIT Press, Cambridge, 1991.

Billimoria, S. B. & Co., for Ministry of Environment and Forests, Government of India, Interim Report on the Supply and Use of Ozone Depleting Substances in India, Part-B, Sectoral Analysis, New Delhi, February 1990.

CMR, *Chemical Marketing Reporter,* Feb. 20, 1989.

Crutzen, P. J., L. E. Heidt, J. P. Krasnec, W. H. Pollock, and W. Seiler, Biomass burning as a source of atmospheric gases CO, H_2, N_2O, NO, CH_3Cl, and COS, *Nature, 282,* 253-256, 1979.

EPA, Environmental Protection Agency, Publication 700-S-92-002, *1990 Toxic Release Inventory - Public Data Release*, CAS 74-83-9, 1992.

Fisher, D. A. and P. M. Midgley, The production and release to the atmosphere of CFCs 113, 114, and 115, *Atmos. Environ.,* 27A, 271-276, 1993.

Gamlen, P. H., B. C. Lane, P. M. Midgley, J. P. Steed, The production and release to the atmosphere of $CFCl_3$ and CF_2Cl_2 (Chlorofluorocarbons CFC-11 and CFC-12), *Atmos. Environ., 20,* 1077, 1986.

Isaksen, I., L. Roke, and M. Fergus, for People's Republic of China National Environmental Protection Agency (NEPA), *Report of a United Nations Development Programme Mission to Investigate Ozone Layer Protection in China*, Beijing, May 28, 1990.

Levine, J. S., Global biomass burning: atmospheric, climatic and biospheric implications, *Eos, Transactions*, American Geophysical Union, September 11, 1990.

Makhijani, A. and A. Makhijani, Biomass Burning and Ozone Depletion: An Assessment of the Problem and Its Implications for the Ozone Layer, Institute for Energy and Environmental Research, Takoma Park, MD. 1990.

MBCG CMA, Report of the Methyl Bromide Global Coalition of the CMA, Chemical Manufacturers Association, Washington, D.C., 1992.

MITI, Yearbook of Chemical Statistics, Tokyo, 1991.

McCarthy, R. L., F. A. Bower, J. P. Jesson, The Fluorocarbon-Ozone Theory-I Production and Release: World Production and Release of $CFCl_3$ and CF_2Cl_2 (fluorocarbons 11 and 12) through 1975, *Atmos. Environ., 11,* 491, 1977.

McCulloch, A., Global production and emissions of bromochlorodifluoromethane and bromotrifluoromethane (Halons 1211 and 1301), *Atmos. Environ., 26A*, 1325-1329, 1992.

Midgley, P., The production and release to the atmosphere of 1,1,1-trichloroethane (methyl chloroform), *Atmos. Environ., 23,* 2663-2665, 1989.

Midgley, P. M., The production and release to the atmosphere of halocarbons, *Ber. Bunsenges. Phys. Chem. 96,* 293-296, 1992.

Midgley, P. M. and D. A. Fisher, The production and release to the atmosphere of chlorodifluoromethane (HCFC-22), *Atmos. Environ., 27A, No. 14,* 2215-2223; 1993.

Penkett, S. A., B. M. R. Jones, M. J. Rycroft and D. A. Simmons, An interhemispheric comparison of bromine compounds in the atmosphere, *Nature, 318,* (6046), 550-553, 1985.

Rasmussen, R. A., L. E. Rasmussen, M. A. K. Khalil, and R. W. Dalluge, Concentration distribution of methyl chloride in the atmosphere, *J. Geophys. Res., 85,* pg. 7350-7356, 1980.

Simmonds, P. G., F. N. Alyea, C. A. Cardelino, A. J. Crawford, D. M. Cunnold, B. C. Lane, J. E. Lovelock, R. G. Prinn, and R. A. Rasmussen, The Atmospheric Lifetime Experiment, 6, Results for carbon tetrachloride based on 3 years data, *J. Geophys. Res., 88,* 8427-8441, 1983.

Singh, H. B., L. J. Salas and R. E. Stiles, Methyl halides in and over the Eastern Pacific (40°N-32°S), *J. Geophys. Res., 88,* pg. 3684-3690, 1983.

Singh, H. B. and J. F. Hasting, Chlorine-hydrocarbon photochemistry in the marine troposphere and lower stratosphere, *J. Atmos. Chem., 7,* 261-285, 1988.

SRI, Chemical Economics Handbook, SRI International, 1988.

SRI, Chemical Economics Handbook, SRI International, 1992.

UNEP, United Nations Environment Programme, Report of the Secretariat on the Reporting of Data by the Parties in Accordance with Article 7 of the Montreal Protocol, report presented at the third meeting of the Parties to the Montreal Protocol on substances that deplete the ozone layer, Nairobi, June 1991.

UNEP, United Nations Enviornment Programme, *Methyl Bromide: Its Atmospheric Science, Technology, and Economics*, Synthesis Report of the Methyl Bromide Interim Scientific Assessment and Methyl Bromide Interim Technology and Economic Assessment, UNEP, 41pp, June 1992.

WMO, World Meteorological Organization, *Atmospheric Ozone 1985*, WMO Global Ozone Research and Monitoring Project, Report No. 16, Sponsored by WMO, NASA, NOAA, FAA, UNEP, CEC, and BMFT, 1986.

WMO, World Meteorological Organization, *Scientific Assessment of Stratospheric Ozone: 1989*, WMO Global Ozone Research and Monitoring Project — Report No. 20, 1990.

WMO, World Meteorological Organization, *Scientific Assessment of Ozone Depletion:1991*, WMO Global Ozone Research and Monitoring Project — Report No. 25, 1992.

Chapter 3.

Inferred Lifetimes

Lead Author:

P. BLOOMFIELD

Additional Contributors:

M. Heimann, M. Prather, and R. Prinn

Chapter 3
Table of Contents

Chapter 3: Inferred Lifetimes

3.0 Summary

This chapter examines the empirical models used to derive the atmospheric residence lifetimes of the industrial halocarbons using four components: observed concentrations, history of emissions, a predictive atmospheric model, and an estimation procedure for describing an optimal model. The model describes both the mixing of the trace gas throughout the atmosphere and its chemical loss. The predictions of model plus emissions are compared with the observations. The estimation procedure is used to select a "best fit" for a range of chemical losses (and hence lifetimes), including uncertainties in emissions and observed concentrations.

We present here three efforts to infer the lifetime of $CFCl_3$ (CFC-11), two of which are also applied to CH_3CCl_3 (methyl chloroform). All studies used the same emissions (see Chapter 2) and observations (that is, monthly means of unpolluted air from the five ALE/GAGE surface sites). "Optimal inversion" results are those obtained by the ALE/GAGE researchers using their published statistical method for empirical determination of the atmospheric residence time for industrial halocarbons, whereas "least squares" refers to results obtained in the course of preparation of this report using a GISS atmospheric model with least squares and related methods to determine the atmospheric residence time. In addition, the Hamburg 3-D model was used to infer a "best" lifetime or emission source for CFC-11.

These studies considered one or more of the following key quantities to be "uncertain" in terms of optimizing the model simulation of the reported observations:

- "lifetime", the atmospheric lifetime of a gas. (Although the chemical loss of either $CFCl_3$ or CH_3CCl_3 is a complex pattern in space and time, only a uniform scaling of the loss frequencies was considered here.)
- "pseudo-calibration", an adjustment factor applied to the observed concentrations to give the best fit to the modeled concentrations. (This quantity effectively includes absolute errors in the calibrations and systematic offsets in the model predictions of surface concentrations.) If allowed to change with time, it can include drifts in the calibration as well.
- "estimated emissions", the emissions of $CFCl_3$ estimated from the non-reporting segment of global production. (See Chapter 2.)

The following quantities were not considered as formal uncertainties in these studies:

- the atmospheric circulation or parameterized mixing
- the location of chemical losses
- the emissions from reporting companies.

The different approaches used here have reported formal confidence intervals in various units. Scientific credibility is normally tied to 95% confidence intervals as reported in this chapter for the "least squares" approach; but the "optimal inversion" results here are available only as 1-σ uncertainties. In this summary alone, we compare the 1-σ range with 68% confidence intervals. Those associated with "optimal inversion" estimates reflect measurement error, natural variability, and emissions uncertainty; "least squares" intervals do not allow for emissions uncertainty.

CFC-11 Lifetime

For the case of fixed emissions (as tabulated in Chapter 2) and no pseudo-calibration we infer a lifetime of

50 (+24, -13) yr for "optimal inversion",

100 yr for "least squares" (fit is too poor, no statistical uncertainty).

When the methods allow the pseudo-calibration to be determined by the optimization procedures, the lifetimes become

40 (+10, -7) yr for "optimal inversion"

39 (+4, -3) yr for "least squares" (the pseudo-calibration factor (PCF) is 0.88, equivalent to reducing the absolute calibration by 12% from 0.948 to 0.839).

When the pseudo-calibration is allowed to drift by +2% per decade (to 0.88 in 1990, interpreted as either calibration drift or calibration nonlinearity) and the non-reporting emissions are halved, the lifetime is

56 (+5 -3) yr for "least squares"

The range in pseudo-calibration factors chosen by some of the optimization procedures is outside the expected uncertainty in the laboratory calibration. The PCF may also account for inaccuracies in the atmospheric model which is discussed below. If we accept the emissions history, then the preferred fit from the "least squares" is 39 years with a 95% confidence range of 34 - 47 yr.

Methyl Chloroform Lifetime

For the case of fixed emissions ("optimal inversion" assumes slightly different emissions from those derived from industry survey in Chapter 2) and adopting current ALE/GAGE calibration, the inferred lifetime is

6.1 (+1.4, -1.0) yr by "optimal inversion",

6.4 (+0.2, -0.2) yr by "least squares".

When the pseudo-calibration is determined separately at each station (which, for example, may also be considered as a systematic error in the atmospheric model's ability to predict concentrations at a given site) the lifetime is inferred to be

4.8 (+0.6, -0.7) yr by "optimal inversion" with average,

4.2 yr by "least squares" with average.

If the pseudo-calibration is fixed and the atmospheric loss frequency (L) is allowed to change linearly over the period, then the inferred lifetime is

5.7 - 5.9 yr with L = +1 (+0.6, -0.6) %/yr for pseudo-calibration = 1.00 from both methods,

4.9 yr with L = +0.5 %/yr for pseudo-calibration = 0.875,

4.3 yr with L = -0.3 %/yr for pseudo-calibration = 0.75.

Thus, the possible identification of a trend in tropospheric chemistry (for example, OH) will depend on the determination of the CH_3CCl_3 absolute calibration.

Atmospheric Models

Much of the difference between the optimal inversion-ALE/GAGE results and the least squares-GISS results can be attributed to the atmospheric models. The distribution of trace gases in the atmosphere relative to the surface sites (where comparisons are made with observations) can be equated to a shift in the pseudo-calibration factor. The differences between estimates obtained from different atmospheric models (1-box global mean, ALE/GAGE 12-box, GISS 3-D/8000-box) are not trivial, when no adjustment of calibration is allowed. In the case of CFC-11, the differences between the ALE/GAGE and GISS atmospheric models account for most of the differences in lifetimes (50 versus 100 yr) with the standard calibration. Likewise, both models give similar lifetimes in fitting the trend (40 versus 39 yr) but with substantially different pseudo-calibration factors. The lifetime inferred for more short-lived gases such as CH_3CCl_3 is much less sensitive to the atmospheric model.

3.1 Introduction

The long atmospheric residence times (henceforth, "lifetimes") of molecular species such as CFC-11 ($CFCl_3$) mean that they continue to have an impact on the atmosphere for decades after they are first released. Information about their lifetimes is therefore critical to the assessment of their overall impact, both on future ozone levels and on global temperature. One method for estimating lifetimes is to compare measurements of the atmospheric concentration of a particular species with its rate of release. An atmospheric model incorporating transport of the species and mechanisms for its local removal (sinks) is used to construct a prediction of the concentration for the given release history. The magnitude of the sink is then scaled to give the best fit between the predictions and the observed concentrations. Finally, the scaled loss rates and the predicted atmospheric distribution of the species are used to compute the global lifetime.

In this chapter, complementary approaches involving both two and three dimensional models are used in the inference of molecular lifetimes. By using substantially differing model methodologies, the effects of the assumptions underlying the atmospheric transport models on the inferred lifetimes can be examined.

The basic scheme described above was used for example by Cunnold *et al.* (1983) to infer the atmospheric lifetime of CFC-11 from 3 years of concentrations observed by the ALE/GAGE network. The atmospheric model used in this and several similar studies by the same team of researchers is relatively simple, consisting of 9 or 12 boxes: 2 tropospheric layers divided at the Equator and at ±30°, and a single stratospheric box (4 stratospheric boxes in the 12-box version). The model transport is adjusted for each set of concentration data to give satisfactory matching to aspects of the observed distribution of the species, such as the interhemispheric gradient.

The concentration of a halocarbon predicted at a given observing site by the 3-D models depends critically on the location of the observing site relative to the sources. The atmospheric circulation cannot be parameterized to fit the observations. One exception for the GISS model is the addition of a single scalar for horizontal diffusion that was chosen to match the interhemispheric gradient in CFC-11 from 1978 to 1983.

This chapter discusses the ALE/GAGE lifetimes deduced using the 12-box model and lifetimes inferred using more detailed atmospheric models. Martin Heimann of the Max-Planck-Institut für Meteorologie (MPIMet) and Michael Prather of NASA's Goddard Institute for Space Studies (GISS) have used their respective three-dimensional models to compute predicted atmospheric concentrations for several chemical loss scenarios. The MPIMet model output has been used to produce a preliminary lifetime estimate for CFC-11, and to explore the use of such a model to infer aspects of the release of CFC-11 such as its geographical distribution and temporal structure. Statistical methods have been used with the GISS model output to assess the uncertainty in the lifetime estimate and to explore the sensitivity of the estimate to assumptions about the temporal structure and geographical distribution of releases, and drift and nonlinearity of calibration. GISS model output with tropospheric loss has been used similarly to assess the lifetime of methyl chloroform (CH_3CCl_3).

For clarity we shall refer in this chapter to the inversions performed with the ALE/GAGE 12-box model as "optimal inversion" and to those done with the 3-D models as "least squares fitting".

3.2 Methods

3.2.1 Basic Approach

The approach is based on four components: (1) a release history of the appropriate species, giving the amounts released by location and time; (2) an atmospheric model, to predict concentrations at specific locations and times, from the release history; (3) observed atmospheric concentrations for comparison with the predictions; and (4) a statistical model to describe the differences between the observed and predicted concentrations.

The release history typically consists of annual emission totals by large regions (North America, Europe, Southern Hemisphere, etc.), estimated from production or sales data and an emission model. These data are discussed in Chapter 2. The various atmospheric models used in this exercise are described later in this chapter. The

observations of atmospheric concentrations are described and tabulated in Chapter 1. The statistical model used in conjunction with the 3-D atmospheric models is described in greater detail in the Appendix.

3.2.2 3-D Model Formalism

Both chemical transport models (CTMs) (GISS and MPIMet) have been used in forward studies for which the global sources, S(t), are specified as a function of time and the geographic emission patterns are defined (see references above). In this traditional mode, the tracer is emitted into the surface layer every time step (on the order of an hour) is removed by local chemistry over the same period, and is then redistributed by the circulation (winds, convection, diffusion).

In this report we take the novel approach of linearly decomposing the tracer history: each year of tracer emissions is followed throughout the period of interest, from 1931 through 1990. Since the CFC and HCFC species in these simulations are linear (*i.e.*, the sources and loss frequencies do not depend on the tracer distribution), we may derive the tracer distribution at a given time by summing the separate histories from each individual year of emissions prior to and including the current year.

These models make the further simplifying assumption that the atmospheric circulation is the same from year to year (*i.e.*, cyclo-stationary). The GISS model is based on a general circulation/climate model, and hence a single year of climatologically "typical" winds is recycled (with a discontinuity at April 1). The MPIMet model is based on analyzed wind fields and thus corresponds to a single year which is also recycled. The highest quality European Centre for Medium Range Weather Forecasts (ECMWF) data available at the start of this project were for 1987, which is the year that is used.

With the cyclo-stationary approximation, the computation of the history of one-year's emission from a given calendar year is identical to any other calendar year. This change in formulating the problem allows, for the first time, statistical optimization procedures to be combined with 3-D transport models.

Therefore, for a given loss frequency a single basis function, g, can be derived which describes the tracer distribution at all subsequent times due to a continuous emission of 1 kg of tracer over a single calendar year (1 Jan through 31 Dec). We archived the tracer distribution at the ALE/GAGE surface sites as monthly medians in order to minimize the influence of local pollution (*i.e.*, equivalent to the ALE/GAGE reporting of "unpolluted" monthly means). The median concentration for month m, station k, and in the year y following the continuous emission of 1 kg of tracer (mean mol.wt. of 137.5) is described by the basis function g(m,y,k). The year, y=1, corresponds to the year in which the emissions occur; for all subsequent years, emissions are zero. The CTM calculations are continued for 5 (GISS) or 7 (MPIMet) years, by which time the tracer is globally uniform at the 0.1% level in the case of no chemical loss. The basis functions are extended to subsequent years by scaling the last CTM year of monthly medians with a single annual decay factor, $e^{-1/L}$, corresponding to the tracer mass loss predicted for the final year of the CTM run:

$$g(m,y,k) = g(m,5,k) \exp[-(y-5)/L], \qquad (3.1)$$

for all years subsequent to year 5 in the GISS simulations (subsequent to year 7 in the MPIMet simulations).

The transient-decay lifetime L used in this formula is the reciprocal of the loss rate attained after several years of zero emissions. It is neither the instantaneous lifetime (*i.e.*, described as "transient" in Chapter 5, and corresponding to a 2-3 year lag between tropospheric buildup and stratospheric destruction) nor the steady-state lifetime in which emissions are maintained at a constant rate. For CFC-11 the transient-decay lifetime will be slightly shorter than the steady-state lifetime, which will in turn be slightly shorter than the instantaneous lifetime when CFC concentrations are increasing (see Chapter 5). These differences become insignificant for gases with tropospheric losses (*e.g.*, methyl chloroform).

The monthly median concentration, χ, for month m, year Y at station k is calculated as the sum of the products of the basis functions and the emissions over previous years,

$$\chi(m, Y, k) = \Sigma_{y=1931}^{Y} \; S(y)\, g(m, Y-y+1, k) \qquad (3.2)$$

Table 3.2.1 *Summarizes the different CTM simulations performed for this report.*

CTM model simulatons				
Simulation	Emission pattern	Stratospheric loss	Tropospheric loss	Lifetime (years)
#1	standard*	none	none	infinite
#2	standard	CFC-11	none	49.1
#3	standard	2×CFC-11	none	30.0
#4	N. Hem. only	none	none	infinite
#5	Far East only	none	none	infinite
#6	N. Amer. only	none	none	infinite
#7	standard	0.75×MeCF	0.75×MeCF	8.73
#8	standard	1.5×MeCF	1.5×MeCF	4.47
#9	standard	0.75×MeCF	0.75×MeCF + ocean	7.06

*the standard geographic emission pattern supplied by Hartley and Prinn has 92.9% located in the N. Hemisphere and 7.1% in the S. Hemisphere. The N. Hemisphere is broken down into 36.3% in N. America, 14.1% in the Far East, and 42.5% in Europe and the remainder of Asia.

The technique employed in the separate MPIMet statistical analyses (described briefly here) consists of a nested two-stage process. Within the inner stage the model solution to a prescribed loss rate is decomposed into a series of base components, which are determined from running the model with individual spatio-temporal source patterns. A linear combination of these base components is subsequently fit to the observations using a weighted least squares procedure (*i.e.* basically a linear regression problem). Within the outer stage the inner stage is repeatedly performed with different values of the atmospheric loss rate, which is determined by minimizing the weighted prediction error.

In the analysis of the GISS output (documented here), the inner optimization stage is omitted; instead, the optimization of the loss rate is repeated for various specific combinations of components, corresponding to a base case and certain perturbations used for sensitivity analyses.

The GISS 3-D CTM used here has been developed at GISS in collaboration with Harvard University. This version of CTM uses the circulation statistics from the 4°×5° GCM (Hansen *et al.*, 1983) and is documented in various chemical tracer studies (Prather *et al.*, 1987; Jacob *et al.*, 1987; Jacob and Prather, 1990; Spivakovsky *et al.*, 1990). The CTM has 8° latitude by 10° longitude resolution with 9 vertical levels (the upper 2 are generally stratospheric). The tracer is redistributed by advection (winds), convection (both shallow and deep cumulus), and horizontal diffusion (parameterized to achieve correct interhemispheric transport of $CFCl_3$). The photochemical loss of CFCs occurs only in the upper two levels (above 150 mbar) and is based on a highly resolved 1-D photochemical model (Prather *et al.*, 1987). The tropospheric loss (in some of the studies) uses the 3-D tropospheric OH fields applied in the CH_3CCl_3 study (Spivakovksy *et al.*, 1990).

For the CFC-11 simulations the MPIMet model used the TM2 transport model (Heimann and Keeling, 1989; Heimann *et al.*, 1989; Brost and Heimann, 1991) with the low resolution (~8° × 10°, 9 layers in the vertical). Advective transport (*i.e.* transport resolved on the model grid and time step) is obtained from the meteorology of the year 1987 from the ECMWF analyses. The model cycles through these windfields for each simulated year. There is no explicit horizontal diffusion but a vertical diffusion term that depends on the local stability of the troposphere has been applied (Louis, 1979). Cloud transport is performed with a version of the Tiedke (1989) mass flux scheme.

Model mixing ratios in the MPIMet CTM at the locations of the stations are obtained by interpolation within the model grid using Hermite bicubic polynomials. The stations are assumed to lie in the lowest model layer. The model-predicted 12 hourly instantaneous mixing ratios are recorded. From these a monthly value is obtained by taking the median value of the instantaneous values during one month.

3.2.3 ALE/GAGE 2D model inversion

To interpret their measurements in terms of surface emissions, atmospheric circulation, and atmospheric destruction the ALE/GAGE investigators utilize an optimal estimation inversion technique based on a linear Kalman Filter

(Cunnold *et al.*, 1983, 1986). The technique includes the use of a two-dimensional model of the atmosphere (8 tropospheric boxes, 4 stratospheric boxes). Unsimulated oscillations are accounted for by including two empirical statistical models designed to describe the spectrum of the differences between the observations and the model. The vector Y containing the unknowns (reciprocal lifetimes) is updated using each new month of data (contained in vector X with elements for each ALE/GAGE station) using

$$\Delta Y = CP'[PCP'+N]^{-1}(X-X_C) \tag{3.3}$$

where P is a matrix of the partial derivatives of the elements of X_C (the model predictions) with respect to the elements of Y. The matrix N is a variance-covariance matrix comprising products of the standard deviations in the monthly observations and C is a variance-covariance matrix comprising products of the standard errors in the unknowns. The matrices P and C are updated as the inversion proceeds.

It is important to note that the update equation for C,

$$C_t = C_{t-1}(1 - CP'[PCP' + N]^{-1}P), \tag{3.4}$$

means that its diagonal elements (which are interpreted as the squares of the uncertainty in the unknowns in Y) are determined by a combination of the initializing uncertainties (contained in the first guess for C) and the measurement standard deviations (contained in N).

The gases studied in this way are $CFCl_3$ and CF_2Cl_2 (Cunnold *et al.*, 1986; 1992, private communication) CH_3CCl_3 (Prinn *et al.*, 1987, 1992), N_2O (Prinn *et al.*, 1990), CCl_4 (Simmonds *et al.*, 1988), and $CF_2ClCFCl_2$ (Fraser *et al.*, 1992, private communication). For some of these compounds updates of these published calculated lifetimes have been made to take into account the longer time series of observations now available and new estimates of industrial emissions.

3.2.4 Observed concentrations and estimated release histories

The ALE/GAGE CFC-11 observations are discussed in Section 1.2.1.1 (see Table 2 in the Appendix to Chapter 1). The CFC-11 emissions are discussed in Section 2.5.1, and global totals are given in Table 2.5.1-2. These emission rates are derived from industry statistics on CFC-11 production and are independent of the atmospheric mixing ratio record. The geographical distribution of CFC-11 release has been estimated by Hartley and Prinn (1990), and introduces some unknown level of uncertainty in these calculations.

3.2.5 Estimation procedures

Cunnold *et al.* (1983; 1992, private communication) used an optimal inversion method to estimate loss rates. The method yields associated standard errors, but these share the weakness of least squares standard errors, namely that they must be corrected for data containing correlated residuals. Most atmospheric science data contain *serial correlation*, meaning that anomalies tend to persist for some time, high values tending to be followed for some time by further high values, and conversely. Recognizing the need for standard errors that are valid when the observed concentrations show serial correlation, Cunnold *et al.* (1983) applied an *ad hoc* correction based on the power spectrum of the residuals. The lifetimes discussed in this chapter obtained from the GISS model output were constructed using a regression model with an explicit time series model for the serial correlation. This produces standard errors that take account of the correlation structure without the need for such corrections.

The separate MPIMet statistical analyses used a weighted least squares estimation procedure (WLS), which accounts for the dependence of the reliability of a monthly mean on the within-month variability and the number of observations available for summary. The procedure minimizes the weighted prediction error defined as:

$$L = \mathbf{e}^T\mathbf{W_e}\mathbf{e} \tag{3.5}$$

where $\mathbf{e}$ denotes the vector of errors $(X_{Model,i}-X_{obs,i})$ for each month and station where data are available. Restricting the time interval under study to the years 1978 through 1989 there exist 617 data points (*i.e.* i=1,...,617). The matrix $\mathbf{W_e}$ is diagonal with elements $W_{e,ii} = \sigma_i^{-2}$ and σ_i is the estimated standard deviation of observation point i as recorded in the ALE/GAGE data set. The MPIMet method was used to infer the lifetime of CFC-11 from 1978-1990 emissions, with the initial (1978) atmospheric concentration optimized (not based on model output for

1930-1977 emissions). It was also used to explore the hemispheric distribution of sources, and to infer emissions for a given lifetime.

The analysis of the GISS model output allowed for serial correlation in the residuals for each station by incorporating an autoregressive (AR) model for the errors (see Appendix), but did not allow for the varying reliability of monthly means. The criterion that was minimized may be written

$$\Sigma_{\text{station}} L_{AR}(e_{\text{station}}) \tag{3.6}$$

where L_{AR} denotes a more general likelihood criterion (see Appendix), and e_{station} is the vector of errors for a particular station. The special case of a zero'th order model reduces to (ordinary, or unweighted) least squares (OLS).

The GISS CTM predicts seasonal cycles in the tracer distribution due to seasonal variation in the atmospheric circulation. The Barbados site, adjacent to the South American continent, is observed (and predicted in both the MPIMet and GISS CTMs) to have large seasonal oscillations as the nearby tropical convergence zone moves seasonally. The one year of winds used in the GISS model does not reproduce the observed cycles (Spivakovsky *et al.*, 1990; Hartley and Prinn, 1991; Spivakovksy *et al.*, 1991) and hence the residuals have large seasonal variations; see Figure 3.3. Here, we focus on the long-term trends and do not wish to penalize the optimization of the fit or bias the statistical error model by the large residual variance due to inadequately modeled seasonal cycles. Thus, we subtract estimated signals at 6- and 12-month cycles.

3.2.6 Sensitivity studies

In attempting to estimate molecular lifetimes from concentration data, it is important to verify how sensitive the inferred lifetimes are to the various assumptions which go into the model calculations. Particular assumptions which will be examined here include those related to the absolute value and long-term stability of the calibration factors in the ALE/GAGE Network, to the magnitude of unreported emissions, and to the uncertainty in the the geographical distribution of emission.

Uncertainty in the absolute value and stability of the ALE/GAGE Network calibration must be considered on the basis of data on calibration scales from different laboratories. Data on the uncertainty in the absolute calibrations are summarized in Table 1.2.1. Calibration values relative to the ALE/GAGE calibration can range from small to large. For example for CFC-11 (the molecule with the smallest range), three other calibrations differ by only 1-4% from the ALE/GAGE calibration, while for CH_3CCl_3, which has the largest range, the other calibrations range from 5% higher to 25% lower than ALE/GAGE.

There is also the possibility that the calibration factors in the ALE/GAGE Network are time and/or concentration dependent. Such a dependence could partially offset or enhance the observed concentration increase. While the networks go to substantial effort to minimize this possibility (see Section 1.4), including studies of detector linearity and stability of secondary standards, some residual uncertainty can still remain. The most likely source of such an error is the non-linearity of the electron capture detectors used in the GAGE Network; the maximum possible errors are -0.15%/yr and -0.55%/yr for CFC-12 and CFC-11, respectively (see Section 1.2.1.1). For CH_3CCl_3, the calibration drift appears to be limited to 0.2%/yr (see Section 1.2.2.2).

Uncertainty in the magnitude of the non-reported production can be one of the largest contributors to the overall uncertainty in the molecular emissions. For example, for CFC-11, a 25% uncertainty in the amount of non-reported production can have a ±2.5% effect on its annual release trend (see Section 2.6.2 and Table 2.6.2.1). For CH_3CCl_3, uncertainty in the unreported production has the potential to be the largest source of uncertainty in the overall emissions (see Section 2.6.3, Table 2.6.3.1) but will still be of minor significance.

The geographical distribution of molecular emissions has been assembled from various data sets by Hartley and Prinn (1990). The interhemispheric split they derived for CFC-11 emissions (92.9% NH, 7.1% SH; see footnote to Table 3.2.1) is reasonably consistent with the result in Section 2.5.1 that over 95% of CFC-11 has been sold in, and is therefore assumed to be released in, the Northern Hemisphere. Similar dominance of the Northern Hemisphere in CH_3CCl_3 emissions is also assumed (see Section 2.5.6, Figure 2.5.7.2 and Table 2.5.7.3).

3.3 Least Squares Fitting Results: CFC-11

3.3.1 Base analysis

Various lifetimes inferred for CFC-11 are shown in Tables 3.3.1 and 3.3.2. Base case calculations use all available data, specified calibration factors, and tabulated emissions. The other cases are used in various sensitivity studies, discussed below.

Table 3.3.1 Inferences for CFC-11, MPIMet atmospheric model.

Inferences for CFC-11, MPIMet atmospheric model		
Case	Result	L
Base	Lifetime = 55.61 yr	2591.96
Hemispheric distribution	80.7% NH, 19.3% SH, lifetime = same	957.60
Europe/N. America distribution	Europe + 40%, N.A. -40%	919.87
Emissions history, lifetime = 55.61 yr	See Figure 3.5	1976.80
Emissions history, infinite lifetime	See Figure 3.5; 15-20% smaller	

In Table 3.3.2, "Cal" refers to the pseudo-calibration factor, which is applied to the ALE/GAGE absolute calibration of 0.948. "Unreported emissions" refer to emissions from producers who do not participate in the CMA reporting scheme. The table in Chapter 2 contains estimates of such emissions, used in constructing global emissions. This part of the global emissions is considerably less certain than the reported part, and some analyses in Table 3.3.2 explore this uncertainty by arbitrarily halving the estimates of the unreported emissions.

Confidence intervals were not computed in several cases, where the residuals showed substantial trend. Trending residuals cannot reasonably be viewed as having been sampled from a statistical model, which is a prerequisite for obtaining credible standard errors and confidence intervals. Where calculated, the 95% confidence intervals are almost symmetric on the reciprocal lifetime scale.

Among the GISS results with the pseudo-calibration factor left free, the error model giving the widest, and hence most conservative, interval is the fourth order autoregressive model (AR(4)), for which the interval is 6.1 times wider than that given by ordinary least squares. The last column gives values of Akaike's Information Criterion (AIC; see Appendix), a criterion for the quality of the fit for a given model. Small values are desirable, suggesting that the AR(3) model gives the most satisfactory fit.

Figure 3.1 shows some aspects of the log likelihood as a function of the lifetime and pseudo-calibration, for the case of a third order autoregressive error model, AR(3). The maximum likelihood estimates, the coordinates of the minimum of the function, are 39.08 years and 0.8847, respectively. The solid contour indicates a level such that the projection of the contour onto either axis is a 95% confidence interval for the corresponding parameter. The confidence interval for lifetime extends from 33.56 to 46.97 years.

The shape of the contour shows the connection between the estimates of lifetime and of the pseudo-calibration. Note that if the pseudo-calibration had been known *a priori* to be 0.8847, the confidence interval for lifetime would have been the intersection of the contour with a horizontal line at this level, which is much shorter than the interval obtained by projection. The extra length of the projected interval shows the loss of precision incurred by the need to estimate the adjustment factor from the observed atmospheric concentrations.

Table 3.3.2 *Inferred lifetimes for CFC-11, GISS atmospheric model.*

	Cal F/V	Cal Val	UNR Fact	Drift	Model	Lifetime	Limits	AIC
GISS	F	1.0	1.0	0	OLS	99.60	-	
	F	1.0	1.0	+1.0	OLS	94.79	-	
	F	1.0	0.5	0	OLS	127.0		
	F	0.95	1.0	0	OLS	61.46	-	
	F	0.95	1.0	1.0	OLS	59.42		
	F	0.95	0.5	1.0	OLS	68.88	68.35-69.44	
	F	0.95	0.5	1.0	AR(3)	66.83	64.23-69.30	
	V	0.87	1.0	0.0	OLS	37.24	36.27-38.25	2701.836
	V	0.86	1.0	0.0	AR(1)	34.34	31.99-37.89	2022.653
	V	0.88	1.0	0.0	AR(2)	37.82	32.86-44.17	1978.211
	V	0.88	1.0	0.0	AR(3)	39.08	33.56-46.97	1947.732
	V	0.89	1.0	0.0	AR(4)	39.64	33.66-47.62	1951.445
	V	0.90	1.0	+1.0	OLS	41.60	40.50-42.75	2627.206
	V	0.88	0.5	0	OLS	43.82	42.70-44.96	2519.218
	V	0.91	0.5	+1.0	OLS	49.66	48.36-51.05	2467.476
	V	0.91	0.5	+1.0	AR(3)	49.36	44.23-57.67	1916.311
	V	0.93	0.5	+2.0	OLS	56.90	55.31-58.62	2460.992
	V	0.93	0.5	+2.0	AR(3)	56.08	50.61-65.75	1908.771

Legend: Cal — Pseudo-Calibraton
F: Fixed
V: Varies

Cal Val — Pseudo-Calibration Factor Relative to ALE/GAGE Value

UNR Fact: — Unreported Emission Multiplicative Factor

Drift: — Assummed Pseudo-Calibration Drift in %/decade

Model: — WLS: Weighted Least Squares
OLS — Optimal Least Squares
AR(n): — Autoregressive Model of order (n)

Lifetime: Inferred Lifetime in years

Limits: — 95% Confidence Limits

AIC: — Akaike's Information Criterion

The GISS results for standard calibration may be closely approximated by

1/lifetime = 0.01004 yrs^{-1}

-0.00216 yrs^{-1} if the unreported part of global emissions is halved

+0.00051 yrs^{-1} if the calibration is assumed to drift +1% per decade

+0.00626 yrs^{-1} if the calibration factor is set to 0.95 (in 1990, when there is drift)

The adjustments are very nearly additive. The GISS results when the calibration factor is left free may be similarly summarized as

1/lifetime = 0.02685 yrs^{-1}

-0.00403 yrs^{-1} if the unreported part of global emissions is halved

-0.00281 yrs^{-1} if the calibration is assumed to drift +1% per decade

with 95% confidence limits of around ±0.003, and

pseudo-calibration factor = 0.8729

+0.0112 if the unreported part of global emissions is halved

+0.0241 if the calibration is assumed to drift +1% per decade

with 95% confidence limits of around ±0.02.

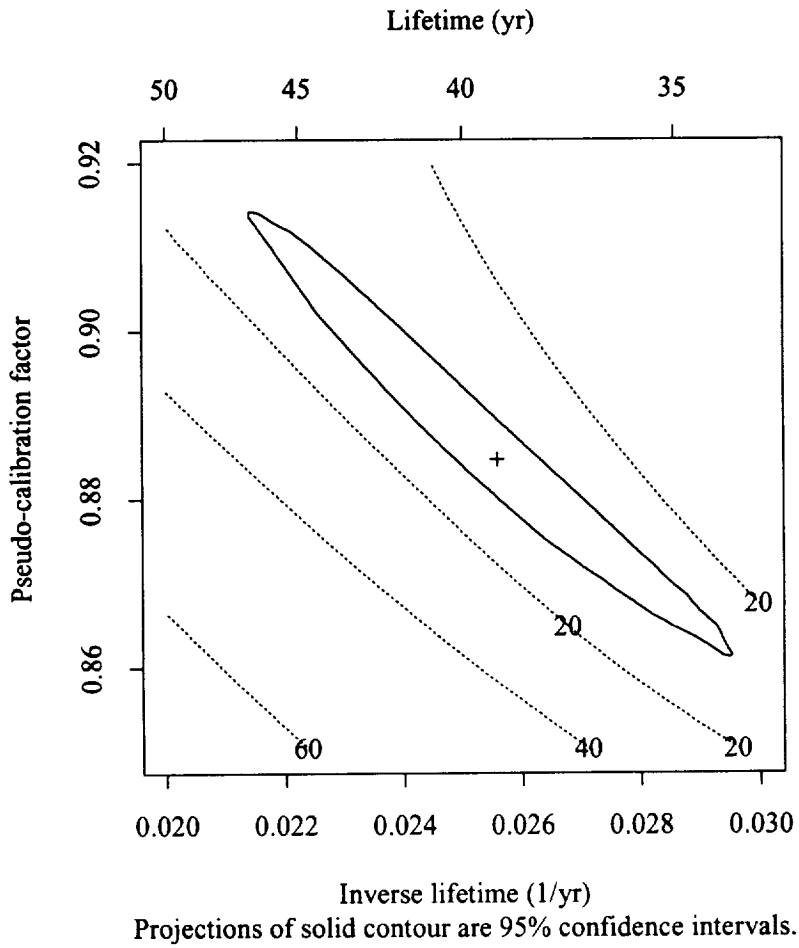

Figure 3.1 Log likelihood function for lifetime and pseudo-calibration factor, CFC-11. Solid contour represents a level of 3.84, and its projections onto the axes form 95% confidence intervals for lifetime and pseudo-calibration factor, respectively.

Figure 3.2 shows the observed concentration data and the model predictions for the (AR(3)) estimated lifetime of 39.08 years, and the estimated pseudo-calibration of 0.8847. The overall fit is good, in that both the temporal trend within each station's observations and the latitudinal gradient are matched. Figure 3.3 shows the residuals (differences between observations and predictions) from Figure 3.2. Recall that the seasonal behavior in the residuals, especially strong at Barbados, is removed before calculating the sums of squares. The nonseasonal part of the residuals is shown by the broken line in Figure 3.3. The figures show that there is a small but systematic difference between the observed data and the predictions, even after removal of the seasonal structure.

It is worth noting that the optimal inferred pseudo-calibration factor of 0.8847 (95% confidence interval from 0.86 to 0.91) is well outside the range of calibration factors measured in the laboratory. Values of 0.96, 0.99 and 0.98 relative to the ALE/GAGE factor were obtained at the University of Tokyo, University of East Anglia, and Scripps Institute of Oceanography, respectively. These results suggest two alternatives, then: either the laboratory-derived calibration values for CFC-11 are substantially in error, or there are problems with the model simulation which can be removed only by allowing for an altered calibration factor (in essence, a uniform adjustment of the observed amounts of CFC-11). Consideration of the origins of the differences between this analysis and that of the ALE/GAGE investigators, summarized in Section 3.6.1, shows that there is a strong connection between the amounts of molecule assumed and the inferred lifetime (a 1% error in data for a long-lived gas can lead to a 5% error in the lifetime). Thus if the model somehow led to an unphysically large, but globally distributed, build-up of the trace molecule, an altered pseudo-calibration factor would be needed for the model to adequately fit the data.

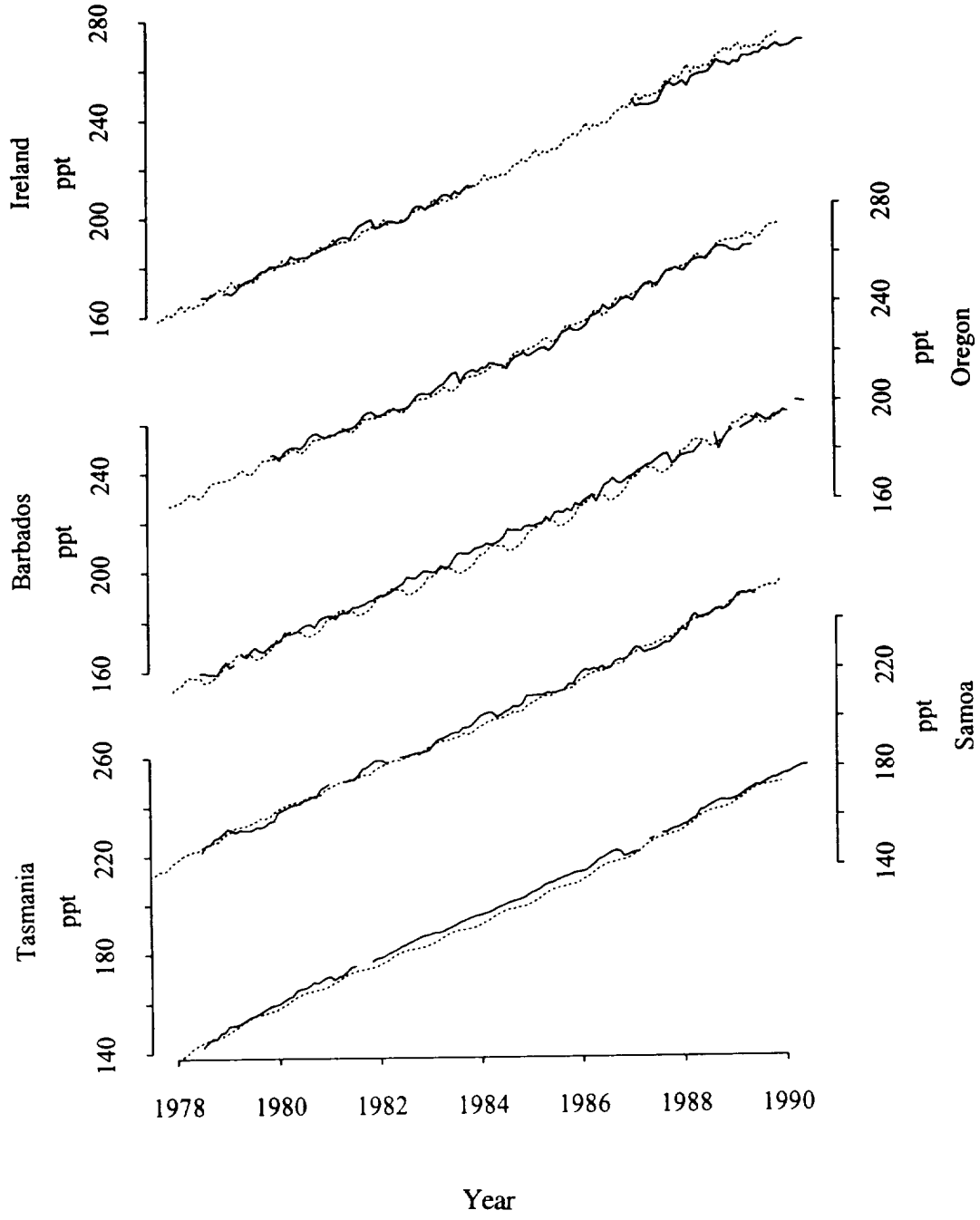

Figure 3.2 Observations (solid lines) and GISS predictions (broken lines) for a CFC-11 lifetime of 39 years and a pseudo-calibration factor of 0.8847.

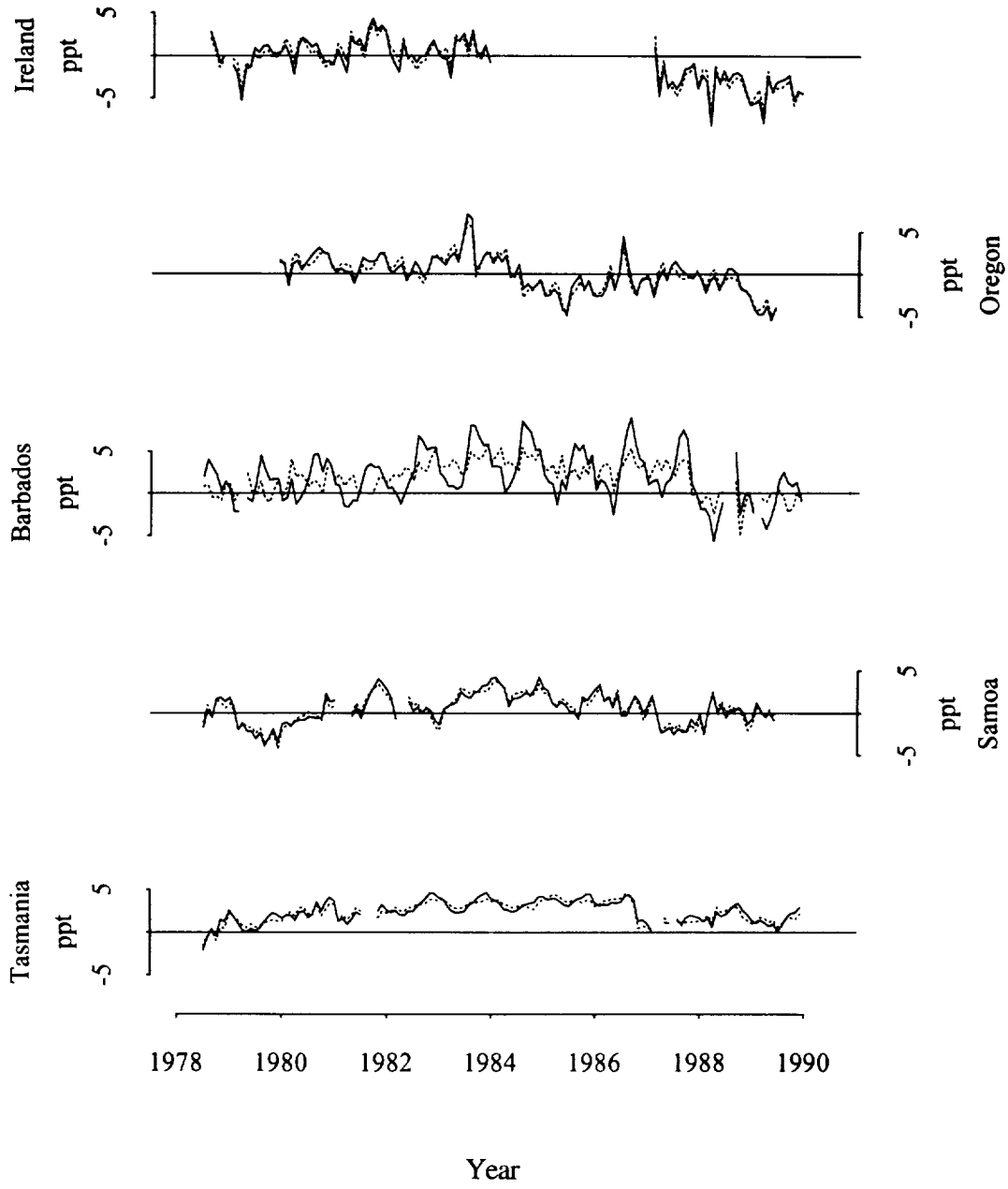

Figure 3.3 Residuals from Figure 3.2, with a CFC-11 lifetime of 39 years and a pseudo-calibration factor of 0.8847. Nonseasonal part of residuals shown by broken line.

3.3.2 Sensitivity to geographical pattern of release

The sensitivity of the inferred lifetime to the geographical distribution of releases was explored by halving the proportion released in the Southern Hemisphere. The perturbed inferred lifetime is also shown in Table 3.3.2 (case "Southern Hemisphere halved"), computed with the pseudo-calibration factor held at 1.0. The shift in the inferred lifetime is trivial in comparison with those caused by changing the statistical error model, indicating that an uncertainty of this magnitude in the hemispheric distribution of release would cause a minor uncertainty in the inferred lifetime. The change is also smaller than the standard errors implied by the confidence intervals shown for base cases in Table 3.3.2.

The separate MPIMet statistical analysis of model output has also been used to explore the issue of changing the geographical pattern of releases, by optimizing the pattern (in the weighted least squares sense) rather than by determining sensitivity to specific changes. In this case the global annual emission numbers are kept fixed, but the spatial emission distribution is adjusted. The limited number of existing observation stations permits only a very coarse emission pattern adjustment. Two adjustments have been explored:

a) Adjustment of the Northern vs. Southern Hemisphere source distribution.

b) Adjustment of the European vs. North American source distribution.

Adjusting the north/south emission distribution results in a virtually unchanged loss rate (and hence lifetime) but a significantly improved fit to the observations: L=957.60 (or 1.25 per data point).

The *a priori* release pattern has 92.6% in the Northern and 7.4% in the Southern Hemisphere. The inferred optimal release pattern has 80.7% in the Northern and 19.3% in the Southern Hemisphere. Such a meridional distribution differs sharply from that presented in Chapter 2. Clearly, if the model underpredicts meridional exchange, a relatively large southern source is required in order to match the observations. This result presumably reflects model limitations, especially in meridional exchange, rather than errors in the emissions inventory.

The change in north/south emission distribution is equivalent to changing the interhemispheric exchange rate. The ALE/GAGE model readjusts most of the transport coefficients to fit this latitudinal gradient in CFCs; the GISS model has one free parameter for north/south diffusion across the tropics that has already been fitted to the early CFC data; but the MPIMet model has no adjustment and thus has the greatest difficulty in matching the latitudinal gradient. There is currently no *a priori* model for atmospheric circulation that would allow for the unique determination of the southern hemispheric component of CFC release from the observations; we must rely on knowledge of CFC usage (see Chapter 2).

If we allow also an adjustment to the relative strengths of the emissions in Europe and North America we obtain a slightly better fit: L=919.87, which we judge, however, not significant. Indeed, the inferred European source would have to be increased by almost 40% at the expense of the North American source. This result primarily depends on the information obtained from the only two Northern Hemisphere stations, ORE and IRE, both lying at the western side of a major continental source region. Clearly, difficulties of the model to resolve accurately the conditions around these stations influence the inferred relative source estimates.

3.3.3 Sensitivity to meridional symmetry of the stratospheric loss process

The MPIMet model output has been used to assess the sensitivity of the results with respect to the assumed meridional symmetry of the stratospheric loss process by performing a series of runs with a meridionally asymmetric loss process. A 10% increase of the loss rate in the Southern Hemisphere and a corresponding 10% decrease in the Northern Hemisphere do not affect the inferred (averaged) optimal loss rate. Also, the inferred optimal north-south source distribution is hardly affected: 80.0% in the Northern, 20.0% in the Southern Hemisphere.

3.3.4 Inferred release history

The MPIMet model output was also used to infer annual emission rates from the observations alone. We considered only the *a priori* spatial emission pattern used here. We find that the loss rate has to be specified *a priori* since otherwise the optimization procedure will be ill-conditioned. Indeed, initial experiments resulted in optimal fits with a loss rate $\lambda = 0$. If the standard loss rate of 0.3074/yr (in the stratospheric layers) is used we obtain a weighted

prediction error of L=1976.8. The inferred annual emission rates are displayed in Figure 3.4 together with the *a priori* estimates of Hartley and Prinn (1990). Quite surprisingly, the procedure reconstructs the temporal evolution of the annual emissions rather closely; only after 1987 somewhat smaller emission rates are inferred. For comparison, the inferred emissions assuming an infinite lifetime of CFC-11 are also shown; these clearly are about 15-20% smaller than the *a priori* estimates.

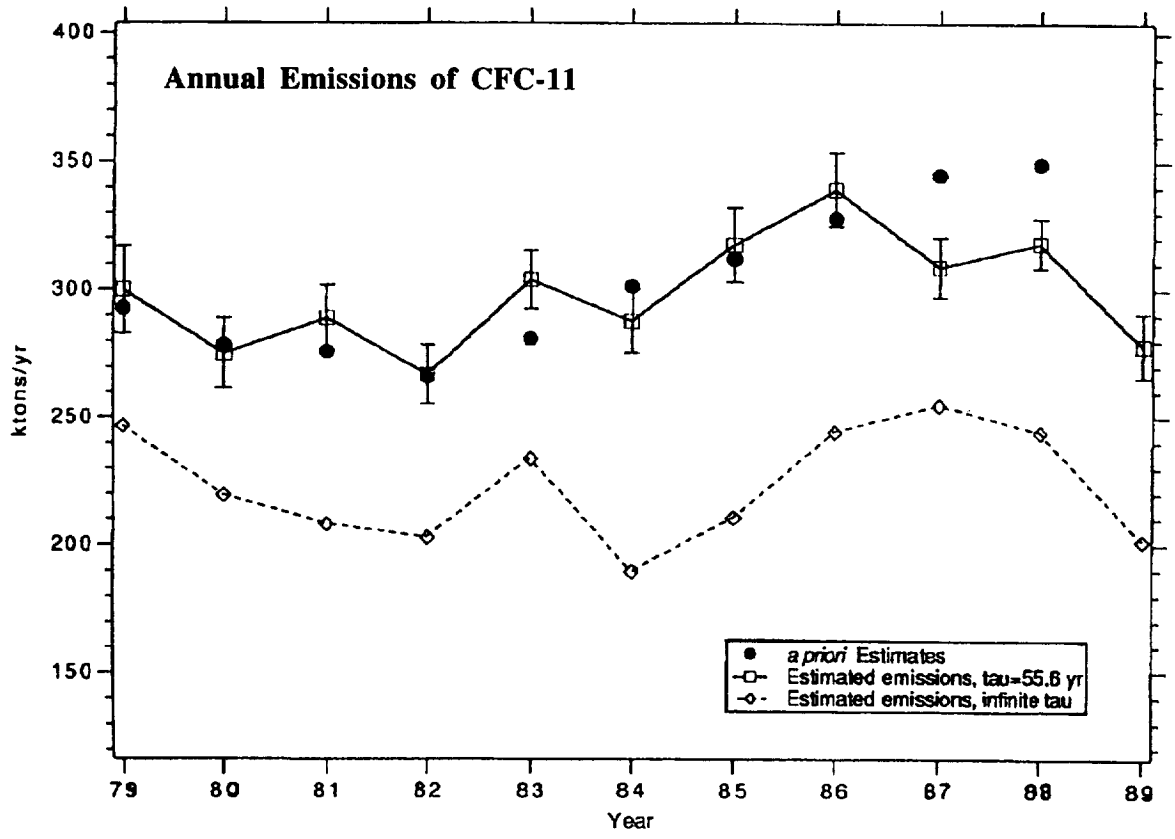

Figure 3.4 MPIMet estimated CFC-11 emissions for lifetimes of 55.6 years and infinity.

3.4. Least Squares Fitting Results: Methyl Chloroform

Various lifetimes inferred for methyl chloroform are shown in Table 3.4.1. All estimates were obtained by ordinary least squares, but 95% confidence intervals were based on 3rd order autoregressive models. Base case calculations use all available data, specified calibration factors, and tabulated emissions. PCF refers to the pseudo-calibration factor, applied as an adjustment to the current GAGE absolute calibration of 0.8. All cases are based on separate emissions for the Far East and the rest of the world. The other cases are used in various sensitivity studies, discussed below.

The results in Table 3.4.1 are grouped as follows. First are lifetimes and pseudo-calibration factors estimated for data from each station in turn. Note that while the pseudo-calibration factors are roughly constant, the lifetimes generally increase from North to South. Thus the harmonic mean lifetimes of 4.18 years for 5 stations is the result of averaging different quantities, and should not be interpreted as good estimate of a single global lifetime. Calculations were also made with the Oregon and Ireland stations combined; the calculated PCF for this case is 0.73 with a lifetime of 3.670 years (not shown in Table 3.4.1). For this case the harmonic mean lifetime of the four stations is 4.22 years, only slightly different from that calculated from the 5 individual stations.

***Table 3.4.1** Inferred lifetimes for methyl chloroform..*

Group	PCF Assumption	Lifetime Assumption	Station	Cal Val	Lifetime	Limits	Comments
a	Station	Station	Ireland	0.74	3.720	(3.418, 4.323)	
			Oregon	0.76	3.968		
			Barbados	0.72	4.111	(3.840, 4.575)	
			Samoa	0.81	4.756	(4.250, 5.479)	
			Tasmania	0.72	3.720	(4.314, 4.699)	
b	Station	Network	Ireland	0.80	4.157		
			Oregon	0.77	4.157		
			Barbados	0.74	4.157		
			Samoa	0.73	4.157		
			Tasmania	0.66	4.157		
c	Network	Network	ALL	0.94	5.771		Base Case
			ALL	0.88	5.171		Double SH Emission
			ALL	0.95	5.826		PCF Drift + 1%/decade
d	Network	Network	ALL	1.0	6.402		Base Case
			ALL	1.0	6.432		Double SH Emission
			ALL	1.0	6.358		PCF Drift + 1%/decade

Legend:
PCF: Pseudo-Calibration Factor relative to ALE/GAGE
Lifetime: Lifetime in years calculated with optimized least squares model
Limits: 95% Confidence Limits to Lifetime calculated with AR(3) model

Next are results for a single lifetime but still with a separate pseudo-calibration factor for each station for the 5 station network. Now the pseudo-calibration factors show a progressive change from North to South, in this case a decrease. These pseudo-calibration factors appear to be adjusting for the larger latitudinal gradient predicted by the model than observed by the network, at the estimated lifetime of 4.157 years. Again, there is no significant difference for the lifetime calculated using the averagte of the Ireland and Oregon stations (4.170 instead of 4.157 years).

In the third group, both the lifetime and the pseudo-calibration are common across the network. These lifetimes are therefore still independent of the absolute calibration of the network, but now incorporate information in the relative latitudinal gradient as well as relative trends in time within observations at each station. The longer lifetime reflects the gradient information, but results in the predicted trends at all stations being higher than observed.

In the final group, the pseudo-calibration factor is set at 1.0 (implying no adjustment to the current ALE/GAGE value). Since this is close to the common pseudo-calibration factors estimated in the previous group, the same comments apply: the latitudinal gradient is moderately well matched, but the time trends are systematically over predicted.

A possible percentage trend in the loss frequency of methyl chloroform was also explored. Table 3.4.2 gives some results. First the pseudo-calibration factor was specified as 1.0, and the 1990 lifetime and loss frequency trend were optimized, giving an estimated loss frequency trend of 1.13% per year. This agrees with the published result derived using optimal inversion (Prinn *et al.*, 1992). In the second case, the pseudo-calibration factor was

***Table 3.4.2:** Inferred loss frequency trend for methyl chloroform.*

Case	Statistical model	1990 lifetime (years)	Loss frequency trend (% per year)	95% Confidence Interval
4 station network, cal = 1.0	AR(3)	5.754	+1.13	0.68, 1.49
Cal = 1.06 (optimized)	OLS	6.020	+1.50	0.93, 2.13*
Cal = 1.00	OLS	5.695	+1.19	
Cal = 0.88	OLS	5.015	+0.48	
Cal = 0.75	OLS	4.378	-0.31	

*This confidence interval was computed for an AR(3) error model. It reflects the uncertainty in the OLS estimates caused by serial correlation.

optimized, together with the 1990 lifetime and loss frequency trend. The estimated pseudo-calibration factor is marginally higher at 1.06, and the 1990 lifetime and loss frequency trend are also marginally higher. The last three rows explore the effect of changing the pseudo-calibration factor from 1.0 to 0.88 or 0.75. The estimated 1990 lifetime and the estimated trend both change systematically. Figure 3.5 shows the dependence of each on the pseudo-calibration factor.

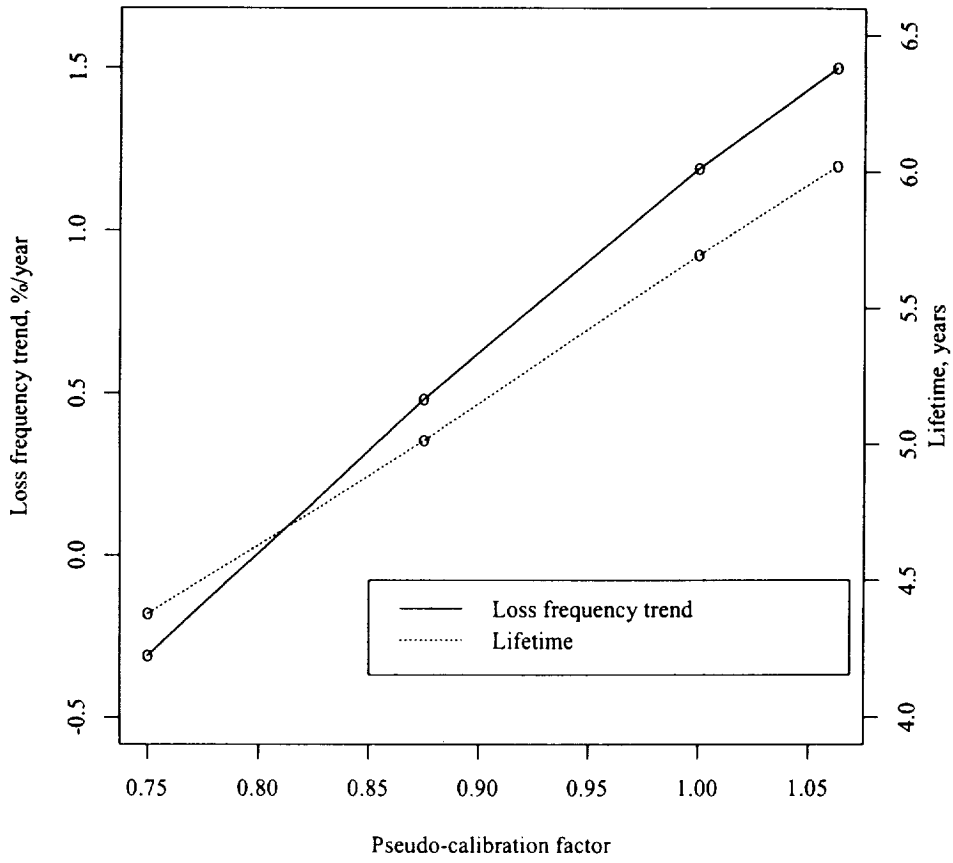

Figure 3.5 CH_3CCl_3 loss rate trend and lifetime *versus* pseudo-calibration factor.

3.5 ALE/GAGE Optimal Inversion Results

The optimal estimation ALE/GAGE inversion technique includes the use of a two-dimensional model of the global atmosphere consisting of eight tropospheric boxes (or grid points) and four upper atmospheric boxes. The four lower tropospheric boxes (or grid points) are intended to provide predictions for comparing with the ALE/GAGE stations in the four semi-hemispheres. Mean inverse advective times and eddy diffusive times in the model vary seasonally and are specified from meteorological observations and an optimal fit to global ALE/GAGE data for $CFCl_3$ (Cunnold *et al.*, 1986; 1992, private communication; Prinn *et al.*, 1990).

The monthly means for the lower tropospheric mixing ratios predicted in this model are used to compare with monthly mean ALE/GAGE observations. As a result of the procedure for choosing transport parameters, this model (unlike the GISS 3-D model) provides excellent simulations of the observed latitudinal gradients and (at most sites) of the observed seasonal cycles also. To account in a statistical way for remaining unsimulated oscillations, the model output is augmented by two empirical statistical models that are designed to describe the spectrum of the differences (residuals) between the observations and the 12-month running mean model predictions (Cunnold *et al.*, 1986).

The optimal inversion procedure uses a modified linear Kalman filter approach as described earlier in Section 3.2.3. The square of the weighted differences between observations and model predictions is minimized where the weighting includes consideration of the measured variances in the monthly means, the accuracy in estimating the trend as defined by the residuals, and the accuracy in estimating lifetimes from each single station.

As discussed by Cunnold *et al.* (1983, 1986), Prinn *et al.* (1987), and Cunnold and Prinn (1991), lifetimes are determined based on three features of the measurements. The first method focuses on optimally fitting the measured fractional trends in CH_3CCl_3 ("trend" method). Estimates of $1/\tau$ using this method are obtained with each station data set alone (Adrigole, Ireland, and Cape Meares, Oregon, data are combined for this purpose) and all data sets simultaneously. The trend method also provides an estimate of the calibration factor ξ. The two other methods focus on optimally fitting the measured global content of the compound of interest ("content" method) and the measured concentrations at individual stations relative to the global average ("gradient" method).

3.5.1 CFC-11 and CFC-12

ALE/GAGE measurements of the chlorofluorocarbons, $CFCl_3$ and CF_2Cl_2, made between July 1978 and June 1991 at the five network stations have recently been analyzed by Cunnold *et al.* (1992, private communication). The measurements have been compared against shipboard measurements south of 30°S by R. Weiss and archived air samples collected at Cape Grim, Tasmania since 1978. The measurements have been placed on the Weiss (SIO 86) calibration scale using $\xi = 0.948$ for $CFCl_3$ and $\xi = 0.959$ for CF_2Cl_2.

Atmospheric lifetimes of $CFCl_3$ and CF_2Cl_2 have been obtained by optimal estimation and are summarized in Tables 3.5.1 and 3.5.2. The releases used in these calculations are of two types. The first are from Chapter 2. The second were developed by Cunnold *et al.* (1992, private communication) and are based on the worldwide release estimates of the Chemical Manufacturers Association, the Alternative Fluorocarbon Environmental Acceptability Study figures on production by reporting companies, and the 1986 consumption figure for Eastern Europe and the former USSR from the United Nations Environment Program. Based on an assumption that releases in Eastern Europe and the former USSR have been constant (at the 1986 rate) since 1982, steady state lifetimes of 42(+7,-5) years for $CFCl_3$ and 122(+91,-37) years for CF_2Cl_2 are obtained by averaging the various approaches. In contrast to all previous calculations, there is now good agreement between the estimates obtained by the trend and content techniques. This results primarily from the new calibration factors and the additional information on world wide releases. Uncertainties remain in the trend estimates because of both nonlinearities in instrument response and release uncertainties. Uncertainties in the inventory lifetime estimates are produced by uncertainties in absolute calibration, in release and in global simulations with the ALE/GAGE two-dimensional model.

Table 3.5.1 *Optimal Inversion ALE/GAGE lifetime estimates (years) for $CFCl_3$ in 1985 and at steady state based on 12.5 years of ALE/GAGE observations and the emissions scenarios from Fisher (Chapter 2) and from Cunnold et al. (1992, private communication). Calibration factors are estimated in trend method and are observed values in inventory method.*

	Lifetime (years)	Steady state lifetime (years)	Calibration factor
Fisher emissions:			
Trend estimate	44 (+10, -7)	40	0.906
Content estimate	56 (+24, -13)	50	0.948
Cunnold *et al.* emissions:			
Trend estimate	41 (+9, -6)	38	0.915
Content estimate	49 (+18, -11)	44	0.948
Average	47 (+9, -7)	42 (+7, -5)	

3.5.2 CH_3CCl_3

Atmospheric ALE/GAGE measurements made between 1978 and 1990 for trichloroethane (CH_3CCl_3) have been used with the optimal inversion method by Prinn *et al.* (1992) to deduce both the lifetime and trend in the lifetime of this compound.

Table 3.5.2 *Optimal Inversion ALE/GAGE lifetime estimates (years) for CF_2Cl_2 in 1985 and at steady state based on 12.5 years of ALE/GAGE observations and the emissions scenarios from Fisher (Chapter 2) and from Cunnold et al., (1992, private communication). Calibration factors are estimated in trend method and are observed values in inventory method.*

	Lifetime (years)	Steady state lifetime (years)	Calibration factor
Fisher emissions:			
Trend estimate	217 (+2300, -103)	192	0.981
Contentestimate	133 (+367, -56)	119	0.959
Cunnold *et al.* emissions:			
Trend estimate	110 (+94, -35)	98	0.951
Content estimate	125 (+275, -51)	111	0.959
Average	137 (+126, -44)	122 (+91, -37)	

Table 3.5.3 summarizes the assumed global emissions used by Prinn *et al.* (1992) in inferring the lifetime of CH_3CCl_3; these data differ in minor ways from those presented in Chapter 2. Table 3.5.4 summarizes the published deduced lifetimes using up to five different approaches: the "trend" method which focuses on optimally fitting the measured percentage trends, the "content" method which focuses on the measured global content, the "gradient" method which focuses on the measured concentrations at individual stations relative to the global average, the "annualized content" method which is similar to the content method but allows the lifetime to change year-by-year, and finally the "variable lifetime" method which allows the lifetime to vary linearly over the observational period. Also given is the recommended best estimate.

***Table 3.5.3** Industrial Emissions (10^9 gm/year) for CH_3CCl_3 assumed in ALE/GAGE inverse model runs.*

Year	ALE/GAGE	Table 2.5.7-2	Percent Difference
1978	518±23	513	+1.0
1979	501±22	511	-2.0
1980	546±24	539	+1.3
1981	544±24	548	-0.7
1982	518±23	521	-0.6
1983	530±23	534	-0.7
1984	579±25	584	-0.9
1985	587±26	591	-0.7
1986	596±26	602	-1.0
1987	617±27	622	-0.8
1988	659±29	666	-1.1
1989	701±31	690	+1.6
1990	743±33	718	+3.5

***Table 3.5.4** Tropospheric lifetime estimates for methyl chloroform derived from trends in ALE/GAGE data at each site and for all sites combined.*

Case	Reciprocal Lifetime, $year^{-1}$	Lifetime, years
Ireland and Oregon	0.222 ± 0.011	4.5
Ragged Point, Barbados	0.219 ± 0.013	4.6
Point Matatula, Samoa	0.191 ± 0.014	5.2
Cape Grim, Tasmania	0.201 ± 0.010	5.0
All sites from trend	0.210 ± 0.006	4.8
All sites from trend, with emission trend uncertainty included	$0.210^{+0.037}_{-0.022}$	4.8
Global atmospheric content, with emission and calibration uncertainty included	0.164 ± 0.031	6.1
Latitudinal gradient	0.166 ± 0.030	6.0
Annualized content	0.167 ± 0.011	6.0
Variable lifetime	0.169 ± 0.025	5.9
Best estimate	0.175 ± 0.020	5.7

The derived tropospheric lifetime for CH_3CCl_3 is 5.7(+0.7,-0.6) years (1σ). As discussed elsewhere in this report (see Chapter 5), this lifetime can be used to deduce a weighted-average OH concentration if OH is the dominant sink. Inclusion of a small loss rate to the ocean for CH_3CCl_3 of 1/85 $year^{-1}$ does not affect the stated lifetime but lowers the derived OH concentration by about 7%. The "variable lifetime" method yields a percentage linear trend in inverse lifetime of 1.0±0.8% $year^{-1}$. The year-to-year lifetimes deduced from the "annualized content" method are given in Table 3.5.5. From these annual numbers a positive linear trend of 1.0±0.6% $year^{-1}$ is obtained for the inverse lifetime in good agreement with the trend deduced using the "variable lifetime" method. This positive trend has major implications for OH, as discussed later.

Table 3.5.5 CH_3CCl_3 lifetimes (years) deduced by ALE/GAGE using the "annualized content" method.

Year	Lifetime
1979	6.7±0.5
1980	6.2±0.4
1981	5.6±0.2
1982	6.2±0.3
1983	6.4±0.3
1984	6.0±0.3
1985	5.9±0.2
1986	5.6±0.2
1987	6.4±0.3
1988	5.8±0.2
1989	5.4±0.3

Prinn *et al.* (1992) caution that the above results assume that current industry estimates of anthropogenic emissions and the absolute calibration are correct. Using an absolute calibration due to Y. Makide which is 0.56/0.80 times the ALE/GAGE value (corresponding to a PCF of 0.7) yields a significantly different average lifetime (3.6 years) and OH trend (-0.7±0.6% $year^{-1}$) using the "variable lifetime" method. In this case however the root-mean-square residual between model and observations is 4.2% compared to 0.8% for the ALE/GAGE calibration. Prinn *et al.* (1991) deduce a best estimate for the calibration using the "trend" method which is 0.77/0.80 times the ALE/GAGE value.

3.5.3 CFC-113

ALE/GAGE CFC-113 measurements for 1982-1990 have been analyzed by Fraser *et al.*, (1992, private communication). Assuming theoretically computed lifetimes, estimated emissions are 19% less than industry estimates. For a calibration factor of 1.47± 0.29 (2σ) it is possible only to deduce from industry emissions and ALE/GAGE data that the CFC-113 lifetime exceeds 20 years. Accuracy of absolute calibration and industry emissions both need improvement to better define the CFC-113 lifetime.

3.6 Comparison of ALE/GAGE and GISS results

The results of optimal inversion and least squares fitting are in some disagreement, particularly for CFC-11, and especially for the case where the absolute calibration is taken to be correct (no pseudo-calibration factor is assumed). Running the two associated atmospheric models (ALE/GAGE 12-box model for optimal inversion, GISS 3-D model for least squares) under the same conditions has given some insight into the reasons for these differences.

Specifically, both models were run first for the case of an atmospheric tracer with the CFC-11 emissions scenario, a stratospheric loss, and a fixed steady-state lifetime of 49.1 years. In the second study, a tropospheric ("OH") sink was added, giving a global mean steady-state lifetime of 4.48 years.

3.6.1 Stratospheric loss

For the case of stratospheric loss, the 12-box model gave 2% higher global mean mixing ratios (specifically, total burden/dry atmospheric mass) than the 3-D model (averaged over the calendar year 1990). This model also has 2% more air mass than the 3-D model, so the atmospheric burden of tracer is actually higher by around 4%. Part of the difference in concentration has been traced to the 3.5 year "lag time" in the 12-box model, between transfer of tracer to a stratospheric box and the beginning of loss. In the 3-D model there is no explicit lag time, but its circulation corresponds to a lag time of around 1 year.

There are even larger differences in calculated concentrations at the ALE/GAGE surface sites, the 12-box model giving around 7% higher mixing ratios than the 3-D model, on average. A simple diagnostic of the atmospheric distribution is the "fill factor", the ratio of the global average mixing ratio to the average over the surface sites: 0.92

for the 12-box model, 0.96 for the 3-D model. The fill factor reflects both tropospheric and stratospheric distributions, including local effects at each surface site.

These differences have been traced to different predictions of vertical profiles: the 12-box model predicts much smaller abundances above 200 mbar than does the 3-D model. However, neither model is capable of making predictions regarding the stratospheric profiles at a resolution that can be verified by observations. Clearly, we must apply models that resolve the stratosphere (see Chapter 5) and have been calibrated against a large suite of tracers in order to resolve this issue.

The inferred lifetimes of long-lived gases are extremely sensitive to the atmospheric model. In this case, a +1% error in the simulated station data leads to a +5% error in the lifetime. Thus, the disagreement in lifetimes between ALE/GAGE and GISS atmospheric models, with a specified calibration factor, should be more than 30%, as found above.

3.6.2 Tropospheric loss

The 1990 average results for the case with tropospheric loss included appear at first to be in much closer agreement: the 3-D model predicts only 1% greater mixing ratios at the surface sites. Such agreement is fortuitous, however, a consequence of canceling factors. The global mean for the 3-D model is 4.4% greater than for the 12-box model, but the difference in fill factors reduces this to 1%. Half of the difference in global means can be explained by the 2% lesser air mass in the 3-D model. The remaining difference can be explained in terms of a different effective tropospheric lifetime due to the different locations of sources and sinks.

The bulk of the loss occurs in the tropical boxes, whence the lag time for stratospheric loss has no impact here. The 3-D model resolves and predicts latitudinal gradients in the tracer for which a significant fraction of the gas spends time at high latitudes, away from the higher loss rates in the tropics. The 12-box model mixes all emissions instantly within the mid-latitude/polar box, and can only predict a gradient at the 30°N boundary. These differences are a possible cause for the remaining 2% difference.

Fortunately, the sensitivity of the inferred CH_3CCl_3 lifetime to these errors is small. For short-lived gases with lifetimes of order 5 years, a +1% error in simulated concentration at surface sites would lead to only a +1% error in the lifetime.

3.6.3 Conclusion

The difference in the empirical derivation of CFC-11 lifetimes using the ALE/GAGE approach (12-box model, optimal inversion) and using the GISS approach (3-D model, least squares) appears to be due in large part to the atmospheric models. It is not obvious which of the two models is more accurate now. The causes outlined above of differences in mixing ratios suggest that errors would be roughly proportional to concentrations, and hence are indistinguishable from calibration errors. Thus lifetimes estimated in conjunction with free-floating pseudo-calibration factors should be relatively insensitive to these problems. This source of error is greatest for the long-lived CFCs and much less important in deriving the lifetime of CH_3CCl_3.

We can make the following recommendations.

- Models should adopt the correct dry air mass of the atmosphere.
- We must understand the stratospheric fill and the time lag in loss from the calibrated 2-D and 3-D stratospheric models.
- Tropospheric 3-D models must be used to understand the redistribution of CFCs within the troposphere relative to the concentrations at the measurement sites.
- We need measurements of halocarbons at other sites and in the middle troposphere in order to calibrate the atmospheric models and to derive the atmospheric burden of CFCs at the percent level.

References

Brost, R. A. and M. Heimann, The effect of the global background on a synoptic scale simulation of tracer concentration, *J. Geophys. Res.*, 96, 15415-15425, 1991.

CMA (1990). "1989 Production and Sales of Chlorofluorocarbons 11 & 12." Chemical Manufacturers Association, Fluorocarbon Program Panel, Washington, DC, 1990.

Cunnold, D., R. Prinn, R. Rasmussen, P. Simmonds, F. Alyea, C. Cardelino, A. Crawford, P. Fraser, and R. Rosen, The atmospheric lifetime experiment, 3, Lifetime methodology and application to three years of $CFCl_3$ data, *J. Geophys. Res.*, 88, 8379-8400, 1983.

Cunnold, D., and R. Prinn, Further comment on "Tropospheric OH in a 3D Chemical Tracer Model: An Assessment based on observations of CH_3CCl_3" by Spivakovsky *et al.*, *J. Geophys. Res.*, 96, 17391-17393, 1991.

Cunnold, D., R. Prinn, R. Rasmussen, P. Simmonds, F. Alyea, C. Cardelino, A. Crawford, P. Fraser, and R. Rosen, The atmospheric lifetime and annual release estimates for $CFCl_3$ and CF_2Cl_2 from 5 years of ALE data, *J. Geophys. Res.*, 91, 10,797-10,817, 1986.

Hansen, J., G. Russell, D. Rind, P. Stone, A. Lacis, S. Lebedeff, R. Ruedy and L. Travis, Efficient 3-D global models for climate studies: models I and II, *Mon. Weather Rev.*, 111, 609-662, 1983.

Hartley, D. and R. Prinn, Proceedings of the World Climate Research Program workshop on global tracer transport modeling, Bermuda, 1990.

Hartley, D. and R. Prinn, Comment on "Tropospheric OH in a 3D Chemical Tracer Model: An Assessment based on observations of CH_3CCl_3" by Spivakovsky *et al.*, *J. Geophys. Res.* 96, 17383-17387, 1991.

Heimann, M. and C. D. Keeling, A three dimensional model of atmospheric CO_2 transport based on observed winds: 2. Model description and simulated tracer experiments, in: Aspects of climate variability in the Pacific and the Western Americas, D. H. Peterson (ed.), Geophysical Monograph 55, AGU, Washington, DC, 237-275, 1989.

Heimann, M., C. D. Keeling, and C. J. Tucker, A three dimensional model of atmospheric CO_2 transport based on observed winds: 3. Seasonal cycle and synoptic time scale variations, in: Aspects of climate variability in the Pacific and the Western Americas, D. H. Peterson (ed.), Geophysical Monograph 55, AGU, Washington, DC, 277-303, 1989.

Jacob, D. J., M. J. Prather, S. C. Wofsy and M. B. McElroy, Atmospheric distribution of ^{85}Kr simulated with a general circulation model, *J. Geophys. Res.*, 92, 6614-6626, 1987.

Jacob, D. J. and M. J. Prather, Radon-222 as a test of the boundary-layer convection in a general circulation model, *Tellus*, 42B, 118-134, 1990.

Prather, M., M. McElroy, S. Wofsy, G. Russell and D. Rind, Chemistry of the global troposphere: fluorocarbons as tracers of air motion, *J. Geophys. Res.* 92, 6579-6613, 1987.

Prinn, R., D. Cunnold, R. Rasmussen, P. Simmonds, F. Alyea, A. Crawford, P. Fraser, and R. Rosen, Atmospheric trends in methyl chloroform and the global average for the hydroxyl radical, *Science*, 238, 945-950, 1987.

Prinn, R., D. Cunnold, R. Rasmussen, P. Simmonds, F. Alyea, A. Crawford, P. Fraser, and R. Rosen, Atmospheric emissions and trends of nitrous oxide deduced from 10 years of ALE/GAGE data, *J. Geophys. Res.*, 95, 18,369-18,385, 1990.

Prinn, R., D. Cunnold, P. Simmonds, F. Alyea, R. Boldi, A. Crawford, P. Fraser, D. Gutzler, D. Hartley, R. Rosen, and R. Rasmussen, Global average concentration and trend for hydroxyl radicals deduced from ALE/GAGE trichloroethane (methyl chloroform) data for 1978-1990, *J. Geophys. Res.*, 97, 2445-2461, 1992.

Simmonds, P., D. Cunnold, F. Alyea, C. Cardelino, A. Crawford, R. Prinn, P. Fraser, R. Rasmussen, and R. Rosen, Carbon tetrachloride lifetimes and emissions determined from daily global measurements during 1978-1985, *J. Atmos. Chem.*, 7, 35-58, 1988.

Spivakovsky, C. M., R. Yevich, J. A. Logan, S. C. Wofsy, M. B. McElroy and M. J. Prather, Tropospheric OH in a 3-D chemical tracer model: an assessment based on observations of CH_3CCl_3, *J. Geophys. Res.*, 95, 18441-18471, 1990.

Spivakovsky, C. M., R. Yevich, J. A. Logan, S. C. Wofsy, and M. B. McElroy, Reply, *J. Geophys. Res.*, 96, 17389-17390.

Tiedtke, M., A comprehensive mass flux scheme for cumulus parameterization in large-scale models, *Mon. Wea. Rev.*, 117, 1179-1800, 1989.

Appendix: Statistical methods

The strategy for inferring the loss frequency λ of an atmospheric constituent, and other quantities such as pseudo-calibration factors, is to match the predicted atmospheric concentration $\chi_{pred}(x, t; \lambda)$ at locations x and times t to the corresponding observed concentrations $\chi_{obs}(x, t)$. In general, loss frequency is both space- and time-dependent. In practice, we use a scalar multiple of a standard local, time-dependent linear chemical loss that is 3-dimensional in the GISS and MPIMet models. Thus λ may be considered to be the unknown scalar multiplier. In general, λ may be a vector containing all the quantities whose values are to be inferred.

The simplest way to carry out the matching is to find λ to minimize the sum of squared residuals

$$S(\lambda) = \Sigma_x \Sigma_t \{\chi_{obs}(x,t) - \chi_{pred}(x,t;\lambda)\}^2.$$

The minimizing λ is called the ordinary least squares (OLS) estimate. Since the reported monthly mean concentrations are based on different numbers of observations and the variability may differ from one month to another, the criterion may be changed to place greater weight on months with more precise means:

$$S(\lambda) = \Sigma_x \Sigma_t w(x,t)\{\chi_{obs}(x,t) - \chi_{pred}(x,t;\lambda)\}^2.$$

The minimizing λ is called the weighted least squares (WLS) estimate. Typically w(x,t) is inversely proportional to the square of the standard error associated with χ_{obs}.

While OLS and WLS estimates are relatively straightforward to obtain and interpret, it is not easy to calculate their standard errors or to provide confidence intervals, except in one special case. This is when the residuals $\chi_{obs} - \chi_{pred}$ are uncorrelated from one time and location to another (and, in principle, have Gaussian distributions). In this case, the set of λs satisfying

$$S(\lambda) \leq S_{min} (1 + F/\nu)$$

comprise a 95% confidence interval, where

- $S_{min} = \min_{\lambda} S()$;
- F = the upper 95% point of the F distribution with 1 and ν degrees of freedom; and
- ν = degrees of freedom for error
  = number of observations - number of estimated parameters.

Since ν is large, F is approximately $1.96^2 = 3.84$.

Another interval that is approximately equivalent for large ν is

$$\nu \ln S(\lambda) \leq \nu \ln S_{min} + 3.84.$$

Taylor's expansion yields a further approximation

$$\lambda = \lambda_{opt} \pm 1.96\{\tfrac{1}{2} d^2/d\lambda^2 \ln S(\lambda_{opt})\}^{\frac{1}{2}}$$

which requires finding only the minimum and second derivative at the minimum of $\ln S(\lambda)$.

When the residuals are serially correlated, these confidence intervals are invalid, in the sense that the probability that they contain the true values of the parameters may be far from 95%. Valid intervals may be constructed by increasing their width by estimated factors, as in the ALE/GAGE procedure, or by introducing a statistical model for the residuals, of the form

$$\chi_{obs}(x,t) = \chi_{pred}(x,t) + n(x,t)$$

where the *noise* n(x,t) has a specified correlated structure. The simplest model for the noise at a given station is the *first order autoregression* AR(1):

$$n(t) = \phi v(t - 1) + \varepsilon(t)$$

where $\varepsilon(t)$ is an error term *uncorrelated* with $\varepsilon(t')$ for $t \neq t'$, called *white noise*. The serial correlations of n(t) are

$$\text{corr}(n(t), n(t')) = \phi^{|t-t'|},$$

which therefore decay strictly exponentially. While there are some geophysical phenomena for which this is a good approximation, the same is not true for many others. In many cases the generalized p'th order model AR(p) defined by

$$n(t) = \phi_1 n(t-1) + \phi_2 n(t-2) + \ldots + \phi_p n(t-p) + \varepsilon(t)$$

provides a better approximation for a reasonably small value of the order p. Other models that are sometimes useful are the *moving average* models MA(q):

$$n(t) = \varepsilon(t) + \theta_1 \varepsilon(t-1) + \theta_2 \varepsilon(t-2) + \ldots + \theta_q \varepsilon(t-q)$$

and mixed autoregressive/moving-average ARMA(p,q) models:

$$n(t) = \phi_1 n(t-1) + \phi_2 n(t-2) + \ldots + \phi_p n(t-p) + \varepsilon(t) + \theta_1 \varepsilon(t-1) + \theta_2 \varepsilon(t-2) + \ldots + \theta_q \varepsilon(t-q)$$

The ARMA models reduce to AR and MA models in the special cases q = 0 and p = 0, respectively, and all reduce to the case of uncorrelated residuals (white noise) when p = q = 0.

When these time series models are used to describe the residuals in a larger model such as those involved in this chapter, the criterion that is commonly used to measure the lack of fit is

$$L(\lambda) = -2 \ln l(\lambda),$$

where $l(\lambda)$ is the *likelihood function* of λ for the given data. Its form is

$$l(\lambda) = (\det 2\pi\Sigma)^{-\frac{1}{2}} \exp(-\tfrac{1}{2} e^T \Sigma^{-1} e),$$

where Σ is the covariance matrix of the error vector $e = \chi_{obs} - \chi_{pred}$, and n is the number of observations. In the present case, the data are time series associated with several locations x, and under the assumption that the noise at one station is uncorrelated with that at any other, the criterion functions may simply be added. Thus the overall criterion is

$$L(\lambda) = \Sigma_x L_x(\lambda),$$

and it may be used in much the same way as the least squares criterion v ln $S(\lambda)$ described above. That is, λ may be estimated by minimizing $L(\lambda)$, the estimate being called a *maximum likelihood* estimate, and a 95% confidence interval for λ may be found from

$$L(\lambda) \leq L_{min} + 3.84.$$

In practice, there are other unknown quantities than simply λ, such as the noise model parameters (θ's and ϕ's), the noise variance (σ^2), and other parameters involved in matching the predictions to the observations. Thus the log likelihood is really of the form $L(\lambda, \theta, \phi, \sigma^2, \ldots)$. The *profile likelihood* $L_{prof}(\lambda)$ is obtained by minimizing with

respect to the other unknowns, and may be used as before to obtain an estimate of λ by minimization, and an associated confidence interval.

The likelihood function is also useful in comparing the goodness of fit of different models. However, adding parameters to a model will always improve the fit, and consequently will give a higher likelihood and a lower value of L_{min}. One technique for adjusting for this effect is to use *Akaike's information criterion*,

$$AIC = L_{min} + 2 \times \text{number of parameters}$$

for comparison, low values indicating a good model.

Chapter 4.

Laboratory Studies of Halocarbon Loss Processes

Lead Author:

S. P. SANDER

Additional Contributors:

D. Gillotay, R. F. Hampson, Jr., H. Magid, O. J. Nielsen, A. R. Ravishankara, and P. C. Simon

Chapter 4
Table of Contents

Chapter 4: Laboratory Studies of Halocarbon Loss Processes

4.0 Summary

- Improved laboratory data have been obtained from reactions of OH with 14 different halocarbons. The most significant changes were those in reactions with HCFC-141b (CH_3CFCl_2), HCFC-142b (CH_3CF_2Cl), HFC-125 (CHF_2CF_3) and HFC-143a (CH_3CF_3). The largest change in rate constant at atmospheric temperatures is a decrease of about 30% for HCFC-141b.

- New evaluations of reaction rates of $O(^1D)$ with 8 different halocarbons were obtained. The branching ratios for the quenching of $O(^1D)$ to $O(^3P)$ were also obtained. In addition, reaction rates of Cl (chlorine) with 18 different halocarbons were measured and the rates of reactions of NO_3 (nitrogen trioxide) with various halocarbons were found to be very slow (room temperature rates slower than 3×10^{-18} cm^3 $molec^{-1}$ sec^{-1}).

- Absorption cross sections (including temperature dependence) were re-evaluated for CFC-11, CFC-12, CFC-113, CFC-114 ($CClF_2CClF_2$), CFC-115 ($CClF_2CF_3$) and the halons. Hydrolysis rates and Henry's Law constants for methyl chloroform and carbon tetrachloride have been reviewed in the context of recent data.

4.1 Introduction

The determination and interpretation of the atmospheric lifetimes of halocarbons both by inference from observed tropospheric trends and by calculation from atmospheric models requires a quantitative understanding of the important chemical and physical loss processes. This chapter contains a critical evaluation of laboratory data relevant to halocarbon loss processes in the atmosphere. The scope of the review includes the gas phase reactions of halocarbons with OH, $O(^1D)$ and Cl, photolysis of selected halocarbons, and heterogeneous loss (dissolution and hydrolysis) of methylchloroform (CH_3CCl_3) and carbon tetrachloride (CCl_4). The specific contents of the review are discussed below.

The predominant loss process for hydrohalocarbons is by reaction with OH radicals in the troposphere. Because of the need to determine the degradation rates of HFCs and HCFCs in the troposphere and to calculate accurately their ozone depletion potentials (ODPs), a large body of new work has appeared on OH reactions with these species. For this review, the data base for the reaction of OH radicals with 14 important HFCs and HCFCs was updated, and temperature dependent rate coefficients were evaluated.

Reactions of $O(^1D)$ with HFCs and HCFCs are unimportant in the troposphere, but may be important in the stratosphere for certain compounds. In this review, new rate constants for $O(^1D)$ with 8 halocarbons as well as the branching ratio for quenching of $O(^1D)$ to $O(^3P)$ by the halocarbon are given. Other possible gas phase chemical destruction mechanisms for CFC substitutes include reaction with Cl and NO_3, although both processes are probably unimportant in the atmosphere compared to the reactions mentioned above. Recommendations for Cl reactions with 18 halocarbons are presented here.

CFCs, HFCs and HCFCs display continuous absorption in the 175-250 nm spectral region making photolysis of the compounds an important destruction process only in the stratosphere. The absorption spectra of halons extend to wavelengths longer than 300 nm, and they can therefore be photodissociated in the troposphere. In this review, UV absorption cross sections and their temperature dependences are given for CFCs 11, 12, 113, 114, 115 and halons 1202, 1211, 1301 and 2402. Lyman-α (121.6 nm) cross sections are given for CFCs 13, 114 and 115.

To assess the heterogeneous loss of CH_3CCl_3 and CCl_4, hydrolysis rates and Henry's Law constants are evaluated.

4.2 Reactions of OH with HFCs and HCFCs

There have been several recent reviews of rate constants for the reactions of OH with HFCs and HCFCs under atmospheric conditions. The most recent include a comprehensive assessment as part of the Alternative Fluorocarbon Environmental Acceptability Study (AFEAS, 1989), and periodic reviews by the NASA Panel for Data Evaluation (DeMore *et al.* [1990, 1992]) and the IUPAC Subcommittee on Gas Kinetic Data Evaluation for Atmospheric Chemistry (Atkinson *et al.* [1989, 1992]). Because of the importance of these reactions in the assessment of the environmental impact of fluorocarbon substitutes, there have been many new studies of OH reaction rates in the last few years and considerable progress has been made in extending the rate constant data base over a wide temperature range. This section updates the work on OH reactions and provides a critical review of a subset of the data base with recommendations for rate constants to be used in atmospheric modelling.

Since the publication of the AFEAS (1989) and DeMore *et al.* (1990) reviews, several new studies have been published or submitted for publication. These include the work of Nelson *et al.* (1990), DeMore (1992), Finlayson-Pitts *et al.* (1992) and Talukdar *et al.* (1992) on methyl chloroform, Talukdar *et al.* (1991) on HFC-32, HFC-125, HCFC-141b and HFC-143a, Zhang *et al.* (1991) on HCFC-225ca and HCFC-225cb, Zhang *et al.* (1992) on HCFC-141b, HCFC-142b and HFC-134a, Nelson *et al.* (1992) on HCFC-225ca, HCFC-225cb and HCFC-243cc, DeMore (1993) on HFC-125, HFC-134a and HFC-152a and Nielsen (1991) on HFC-152a. This new work has significantly enlarged the kinetic data base on OH reactions with CFC replacements. In addition, the first results have been reported on three new C_3 HCFC compounds, namely, HCFC-225ca, HCFC-225cb and HCFC-243cc.

A detailed discussion of the sources of experimental uncertainty in the measurement of rate parameters of the reactions of OH with HFCs and HCFCs is beyond the scope of this review. For this information the reader should consult several of the referenced experimental papers including Gierczak *et al.* (1991), Zhang *et al.* (1992) and Wayne *et al.* (1992). With the exception of the studies of Nelson *et al.* (1990) and DeMore (1992,1993), the reactions considered here were investigated by measuring the first-order loss of OH in the presence of a large excess of the compound of interest. For reactions whose bimolecular rate constants are less than about 10^{-14} cm^3 $molecule^{-1}$ s^{-1}, measurements of the OH decay rate can lead to an overestimation of the rate constant unless extreme care is taken to exclude interferences from faster secondary reactions of OH, such as with impuritites or with reaction products arising from the initial OH attack. While problems associated with interfering reactions are sometimes difficult to detect, they often manifest themselves in one of several ways. For example, the rate constants for such faster reactions generally have smaller temperature dependencies than that of the primary reaction being studied. Hence, appreciable interference due to them can be seen as a non-linearity (upward curvature at low temperatures) in an Arrhenius plot. In addition, the contribution of secondary reaction interferences associated with reaction products is dependent on the initial radical concentration. These contributions can therefore be assessed by measuring changes in the observed rate constant at different initial OH concentrations and can be eliminated by performing experiments at extremely low OH concentrations. Wayne *et al.* (1992) have also highlighted the possible role of bimolecular wall reactions in studies carried out in discharge flow reactors. As discussed in AFEAS (1989), certain early studies such as those of Clyne and Holt (1979a,b) may have suffered from interferences and were therefore not considered in the evaluation.

In the studies by Nelson *et al.* (1990) and DeMore (1992a,b), a relative rate technique was used in which OH is allowed to react with both the compound of interest and a reference compound such as CH_3Cl or CH_4 in a steady-state photolysis reactor. Rate constants are determined relative to the reference compound by measuring the relative disappearance rates of the compound and the reference. This method is insensitive to the presence of impurity hydrocarbons and secondary reactions of OH, provided that the only loss pathway for the compound and the reference is by the initial OH attack. In addition, uncertainties in the absolute rate constant for the reference reaction factor into the final uncertainty for the OH rate constant obtained using this method.

In this review, Arrhenius parameters were derived from plots of ln k vs. 1/T for data below 400 K (Table 4.2-1). It was found that the evaluated data base showed linear Arrhenius behavior for all but three compounds: HFC-32, HCFC-123 and HFC-134a. For these compounds, the preferred Arrhenius parameters were derived by ignoring the data below room temperature. Changes to the data base since the publication of AFEAS (1989) and DeMore *et al.* (1990) have resulted in significant changes to the recommendations for the OH reactions with three compounds: HCFC-141b, HCFC-142b and HFC-143a. Of these, the most significant change is for HCFC-141b where the recommended rate constant at 277 K (the weighted mean tropospheric temperature) has decreased by nearly 30%. Improvements in the purity of the available fluorocarbon samples and in the detection sensitivity of the kinetic apparatus are primarily responsible for these changes. The recommended values for k_{298} that appear in Table 4.2-1 were derived from the temperature dependence expressions in all cases. This approach differs slightly from that used in the AFEAS evaluation in which values of k_{298} were obtained from room temperature rate constant measurements and the value of the Arrhenius pre-exponential factor was adjusted to fit the k_{298} value using the activation energy derived from the recommended studies. Uncertainty estimates (corresponding to approximately one standard deviation) on the rate constants presented in the next three tables (Tables 4.2-1, 4.3-1 and 4.4-1) may be calculated using the uncertainty factor on the rate constant at 298 K, f(298), together with the Arrhenius temperature coefficient uncertainty ($\Delta E/R$) according to the formalism adopted by the NASA Panel for Data Evaluation (DeMore *et al.* [1990,1992]). Thus, the uncertainty ($\approx 1\sigma$) factor at any temperature, T, is given by

$$f(T) = f(298) \exp\{(\Delta E/R)(1/T - 1/298)\}.$$

Table 4.2-1. *Recommended rate constants and uncertainties for reactions of OH with selected HFCs and HCFCs.*

Reactant	Name	$10^{12} \cdot A^1$	$E/R \pm \Delta E/R^2$	$10^{15} \cdot k_{298}{}^1$	f(298)	Note
CHF_2Cl	HCFC-22	1.2	1650 ± 300	4.7	1.3	4.2.1
CH_2F_2	HCFC-32	1.9	1550 ± 300	10	1.3	4.2.2
$CHCl_2CF_3$	HCFC-123	0.77	900 ± 300	38	1.3	4.2.3
$CHFClCF_3$	HCFC-124	0.66	1250 ± 300	10.0	1.3	4.2.4
CHF_2CF_3	HFC-125	0.56	1700 ± 300	1.9	1.3	4.2.5
CH_2FCF_3	HCFC-134a	1.7	1750 ± 300	4.8	1.3	4.2.6
CH_3CCl_3	methyl chloroform	1.8	1550 ± 150	10.0	1.1	4.2.7
CH_3CFCl_2	HCFC-141b	1.3	1600 ± 300	6.0	1.3	4.2.8
CH_3CF_2Cl	HCFC-142b	1.4	1800 ± 200	3.3	1.2	4.2.9
CH_3CF_3	HFC-143a	1.6	2100 ± 300	1.4	1.3	4.2.10
CH_3CHF_2	HFC-152a	1.5	1100 ± 200	37	1.2	4.2.11
$CF_3CF_2CHCl_2$	HCFC-225ca	1.5	1250 ± 200	23	1.3	4.2.12
CF_2ClCF_2CHClF	HCFC-225cb	0.55	1250 ± 200	8.3	1.3	4.2.13
$CH_3CF_2CFCl_2$	HCFC-243cc	0.77	1700 ± 300	2.6	2.0	4.2.14

[1] Units are cm^3 $molecule^{-1}$ s^{-1}

[2] Units are K

Notes

4.2.1 *OH + CHF_2Cl.* The data base for this reaction is well established and there have been no new data recently. The preferred values are derived from a fit to all data below 400 K except the rate constants of Clyne and Holt (1979b), which have a significantly larger temperature dependence than all the other studies. The unpublished data of Orkin *et al.* (private communication), while not considered, agree well with the recommendation. The recommendation for k_{298} is derived from the Arrhenius line.

4.2.2 *OH + CH_2F_2.* The temperature dependence of the preferred rate expression is derived from the data of Jeong and Kaufman (1982a), Talukdar *et al.* (1991) below 400 K and the room temperature data of Howard and Evenson (1976a) and Nip *et al.* (1979). The recommendation for k_{298} is derived from the Arrhenius line. Although the data of Clyne and Holt (1979b) are consistent with the data from the other studies, this study is not included in the least squares fit.

4.2.3 *OH + $CHCl_2CF_3$.* The preferred rate expression is derived from the temperature dependence data below 400 K of Nielsen (1991), Gierczak *et al.* (1991), Liu *et al.* (1990), Watson *et al.* (1979), and the room temperature data of Howard and Evenson (1976b). The recommended value of k_{298} is derived from the temperature dependence expression. The data of Brown *et al.* (1990a) and Clyne and Holt (1979b) were not considered.

4.2.4 *OH + $CHFClCF_3$.* The preferred rate expression is derived from the temperature dependence data of Gierczak *et al.* (1991), Watson *et al.* (1979), and the room temperature data of Howard and Evenson (1976b). The recommended value of k_{298} is derived from the temperature dependence expression.

4.2.5 *OH + CHF_2CF_3.* The preferred rate expression is derived from the temperature dependence data of Talukdar *et al.* (1991) and the room temperature data of Martin and Paraskevopoulos (1983) and DeMore (1993). Due to the large discrepancy between the room temperature rate constant of Clyne and Holt (1979b) and those of Martin and Paraskevopoulos and Talukdar *et al.*, the Clyne and Holt data were ignored. The data from Brown *et al.* (1990a) were not considered due to the likelihood of impurities. The preferred value of k_{298} is taken from the recommended temperature dependence expression.

4.2.6 *OH + CH_2FCF_3.* The preferred rate expression was derived from the data of Gierczak *et al.* (1991) above 243 K, Liu *et al.* (1990), the 270 K data of Zhang *et al.* (1992) and the room temperature data of Martin and Paraskevopoulos (1983), and DeMore (1993). The recommended value of k_{298} is obtained from the temperature dependence expression. The data of Jeong *et al.* (1984), Brown *et al.* (1990a), Clyne and Holt (1979b), and Orkin *et al.* (private communication) were not considered.

4.2.7 *OH + CH_3CCl_3*. The recommendation is based on the absolute rate studies of Talukdar *et al.* (1992) and Finlayson-Pitts *et al.* (1992) and the relative rate study of DeMore (1992) with CH_4 as a reference. The average value of k_{298} from these studies is 35-55% lower than those obtained previously by Watson *et al.* (1977), Chang and Kaufman (1977), and Clyne and Holt (1979a) and 23% lower than the k_{298} value extrapolated from the higher temperature absolute measurements of Nelson *et al.* (1990). The k_{298} values obtained by Jeong and Kaufman (1979) and Kurylo *et al.* (1979) agree reasonably well with the recommended studies but have considerably larger temperature dependences. Talukdar *et al.* (1992) have speculated that the earlier studies may have been affected by impurities, surface decomposition of CH_3CCl_3 and secondary reactions of OH. The relative rate technique used by DeMore (1992) is insensitive to hydrocarbon impurities and yields rate constant ratios which are extremely consistent with those calculated from the absolute values obtained by Talukdar *et al.* (1992) and by Vaghjiani and Ravishankara (1991) for the OH + CH_3CCl_3 and OH + CH_4 reactions, respectively.

4.2.8 *OH + CH_3CFCl_2*. The preferred rate expression is significantly different from that in AFEAS (1989) and DeMore *et al.* (1990) due to the recent data of Talukdar *et al.* (1991) and Zhang *et al.* (1992). The above two reviews were based on the results of Liu *et al.* (1990) and the preliminary data of Talukdar *et al.* which showed noticeable curvature in the Arrhenius plots. The reaction rate at the lowest temperature, being so slow, is most likely to be affected by impurities and/or secondary reactions. The use of higher-purity samples and improved OH detection sensitivity in the studies of Talukdar *et al.* and Zhang *et al.* resolved the problem of Arrhenius curvature. The new results imply an A-factor which is more consistent with similar H-abstractions by OH. The temperature dependence expression is derived from the data of Zhang *et al.* (1992), Liu *et al.* (1990) at 330 K and above, and the data of Talukdar *et al.* above 253 K. The temperature dependence data of Brown *et al.* (1990a) were not considered because the relatively large rate constants and Arrhenius curvature are suggestive of sample impurities. The recommended value of k_{298} is obtained from the temperature dependence expression.

4.2.9 *OH + CH_3CF_2Cl*. The recommended rate expression is derived from a fit to the temperature dependence data of Gierczak *et al.* (1991), Liu *et al.* (1990), Watson *et al.* (1977) and Handwerk and Zellner (1978), the 270 K data of Zhang *et al.* (1992) and the room temperature data of Howard and Evenson (1976b), Paraskevopoulos *et al.* (1981). The value of k_{298} was derived from the rate expression. The data from Brown *et al.* (1990a) and Clyne and Holt (1979b) were not considered.

4.2.10 *OH + CH_3CF_3*. The only temperature dependence data for this reaction are those of Talukdar et al. (1991) and Clyne and Holt (1979b). Due to the large discrepancy between the room temperature rate constant of Clyne and Holt (1979b) and that measured by Martin and Paraskevopoulos (1983), and the generally poor agreement between the Clyne and Holt data and that of other workers for several other halomethanes and haloethanes, the Clyne and Holt data were ignored. The recommended rate expression is derived from a fit to the temperature dependence data of Talukdar *et al.* for $T \geq 261$ K and the room temperature point of Martin and Paraskevopoulos. The recommended value of k_{298} is derived from the rate expression.

4.2.11 *OH + CH_3CHF_2*. The preferred rate expression is derived from the temperature dependence data of Nielsen (1991), Gierczak *et al.* (1991), Liu *et al.* (1990) and the room temperature data of Howard and Evenson (1976b), Handwerk and Zellner (1978), and Nip *et al.* (1979). The data of Brown *et al.* (1990a) and Clyne and Holt (1979b) were not considered. The recommended value of k_{298} is obtained from the temperature dependence expression.

4.2.12 *OH + $CF_3CF_2CHCl_2$*. The preferred rate expression is derived from the temperature dependence data of Nelson *et al.* (1992) and Zhang *et al.* (1991a). The data of Brown *et al.* (1990b) were ignored. The recommended value of k_{298} is obtained from the temperature dependence expression.

4.2.13 *OH + CF_2ClCF_2CHClF*. The preferred rate expression is derived from the temperature dependence data of Nelson *et al.* (1992) and Zhang *et al.* (1991a). The recommended value of k_{298} is obtained from the temperature dependence expression.

4.2.14 *OH + $CH_3CF_2CFCl_2$*. The preferred rate expression is derived from the temperature dependence data of Nelson *et al.* (1992). The recommended value of k_{298} is obtained from the temperature dependence expression.

4.3 Reactions of $O(^1D)$ with CFCs, HFCs and HCFCs

The rate constants for the reactions of $O(^1D)$ with various CFCs, HFCs and HCFCs that were reported before 1989 have been reviewed in DeMore *et al.* (1990). In that review, the total rate constants for the removal of $O(^1D)$ are recommended and the branching ratios for the quenching of $O(^1D)$ to $O(^3P)$ measured by various investigators are listed. Recently, Warren *et al.* (1991) and Ravishankara *et al.* (1993) have studied the reactions of $O(^1D)$ with HCFCs/HFCs and with CFCs, respectively. They directly measured the overall rate constants for the loss of $O(^1D)$,

k[O(^{1}D) loss], and the branching ratio, ϕ, for the production of O(^{3}P) in these reactions. These are the only new data on the O(^{1}D) reactions with CFCs and HCFCs since DeMore *et al.* (1990). The rate coefficients for the loss of the HCFC are calculated from the measured or recommended values of k[O(^{1}D) loss] and ϕ. The recommended values are listed in Table 4.3-1. It is assumed that these rather fast O(^{1}D) reactions will not exhibit any temperature dependence and hence the E/R for the overall reactions is taken to be zero. In addition, the branching ratios for the two channels are also assumed to be independent of temperature.

Table 4.3-1. *Recommended rate constants and uncertainties for reactions of O(^{1}D) with selected CFCs and HCFCs. Rate constants are given for O(^{1}D) loss (k(O(^{1}D)), reaction plus quenching, and fluorocarbon loss (k_X, reaction only).*

Reactant	Name	10^{10}•k(O(^{1}D)) cm^3 s^{-1}	f(298)	10^{10}•k_X	f(298) cm^3 s^{-1}	Notes
$CFCl_3$	CFC-11	2.3	1.2	1.7	1.3	1
CF_2Cl_2	CFC-12	1.4	1.3	1.2	1.4	1
CF_3Cl	CFC-13	0.87	1.3	0.60	1.5	2
CCl_4		3.3	1.2	2.8	1.3	1
CHF_2Cl	HCFC-22	1.0	1.2	0.72	2.0	1
$CFCl_2CF_2Cl$	CFC-113	2.0	2.0	1.5	2.0	2
CF_2ClCF_2Cl	CFC-114	1.3	1.3	1.0	1.8	2
CF_3CF_2Cl	CFC-115	0.50	1.3	0.15	2.0	2
CF_3CHCl_2	HCFC-123	2.0	1.3	1.6	1.5	2
CF_3CHFCl	HCFC-124	0.86	1.3	0.60	1.5	2
CH_3CFCl_2	HCFC-141b	2.6	1.3	1.8	1.5	2
CH_3CF_2Cl	HCFC-142b	2.2	1.3	1.6	1.5	2

Notes

1. Recommendation from DeMore *et al.* (1992).

2. Recommendation based on the work of Warren *et al.* (1991) and Ravishankara *et al.* (1993) who have measured the total rate coefficient for the deactivation of O(^{1}D) by selected CFCs and the branching ratio for the quenching of O(^{1}D) to O(^{3}P).

4.4 Other Loss Processes for HFCs and HCFCs

In addition to photolysis and the reactions with OH and O(^{1}D), the CFC substitutes may be degraded in the atmosphere via reactions with the nitrate free radical (NO_3) and atomic chlorine (Cl). NO_3 reaches its highest concentration at night and is known to be an important oxidizer of many atmospheric species. In the case of the HCFCs and HFCs, which are saturated halocarbons, the reaction with NO_3 is expected to be very slow. A recent relative rate study of NO_3 with several CFC substitutes (CHF_2Cl, CF_3CHCl_2, CH_3CFCl_2, CH_3CF_2Cl and CH_3CHF_2) by Haar *et al.* (1991) showed that these reactions are indeed very slow, all with rate constants less than 3 x 10^{-18} cm^3 molecule^{-1} s^{-1} at 298 K.

The other possible loss process, reaction with Cl, can be evaluated from the available laboratory kinetics data as summarized in Table 4.4-1. Most of the data for the reactions of Cl with HFCs and HCFCs are based on relative rate studies. The 298 K rate constants for the reactions of Cl with HFCs and HCFCs correlate extremely well with the corresponding reactions of OH suggesting that both radicals react with these compounds by hydrogen abstraction at the same sites.

Table 4.4-1 *Recommended rate constants and uncertainties for the reactions of Cl with selected HFCs and HCFCs.*

Reactant	Name	10^{11}•A $cm^3\ s^{-1}$	E/R ± ΔE/R K	k_{298} $cm^3\ s^{-1}$	f(298)	Notes
CH_2Cl_2		3.1	1350 ± 500	$3.3x10^{-13}$	2.0	4.4.1
$CHCl_3$		0.49	1240 ± 500	$7.6x10^{-14}$	3.0	4.4.2
$CHFCl_2$	HCFC-21	---	---	$2.1x10^{-14}$	1.5	4.4.3
CH_2FCl	HCFC-31	2.1	1390 ± 500	$1.9x10^{-13}$	3.0	4.4.4
CH_2F_2	HFC-32	1.7	1630 ± 500	$7.1x10^{-14}$	3.0	4.4.5
CH_3F	HFC-41	0.48	770 ± 500	$3.6x10^{-13}$	1.5	4.4.6
$CHCl_2CF_3$	HCFC-123	---	---	$1.2x10^{-14}$	1.5	4.4.7
$CHFClCF_3$	HCFC-124	---	---	$2.7x10^{-15}$	2.0	4.4.8
CH_2ClCF_3	HCFC-133a	0.18	1710 ± 500	$5.9x10^{-15}$	3.0	4.4.9
CHF_2CHF_2	HCFC-134	0.82	2430 ± 500	$2.4x10^{-15}$	3.0	4.4.10
CH_2FCF_3	HCFC-134a	---	---	$1.4x10^{-15}$	3.0	4.4.11
CH_3CFCl_2	HCFC-141b	---	---	$2.2x10^{-15}$	1.5	4.4.12
CH_3CF_2Cl	HCFC-142b	---	---	$3.9x10^{-16}$	3.0	4.4.13
CH_2FCHF_2	HCFC-143					4.4.14
$\rightarrow CH_2FCF_2$		0.55	1610 ± 500	$2.5x10^{-14}$	3.0	
$\rightarrow CHFCHF_2$		0.77	1720 ± 500	$2.4x10^{-14}$	3.0	
CH_3CF_3	HFC-143a	1.2	3880 ± 500	$2.6x10^{-17}$	5.0	4.4.15
CH_2FCH_2F	HFC-152	2.6	1060 ± 500	$7.5x10^{-13}$	3.0	4.4.16
CH_3CHF_2	HFC-152a					4.4.17
$\rightarrow CH_3CF_2$		0.64	950 ± 500	$2.6x10^{-13}$	1.5	
$\rightarrow CH_2CHF_2$		0.72	2390 ± 500	$2.4x10^{-15}$	3.0	
CH_3CH_2F	HFC-161					4.4.18
$\rightarrow CH_3CHF$		1.8	290 ± 500	$6.8x10^{-12}$	3.0	
$\rightarrow CH_2CH_2F$		1.4	880 ± 500	$7.3x10^{-13}$	3.0	

Notes

4.4.1 Cl + CH_2Cl_2. The recommended value is based on results of the relative rate study of Tschuikow-Roux *et al.* (1988) normalized to the value of the rate constant for the reference reaction (Cl + CH_4) recommended in DeMore *et al.* (1992). The room temperature value is in good agreement with results of the relative rate study of Niki *et al.* (1980). The higher results of Clyne and Walker (1973) were not used.

4.4.2 Cl + $CHCl_3$. The recommended value is based on results of the relative rate study of Knox (1962) normalized to the values of the rate constants for the two reference reactions (Cl + CH_4 and Cl + CH_3Cl) recommended in this evaluation. The higher results of Clyne and Walker (1973) were not used.

4.4.3 Cl + $CHFCl_2$. The recommended values is based on results of the relative rate study of Tuazon *et al.* (1992) normalized to the value of the rate constant for the reference reaction (Cl + CH_4) recommended in DeMore *et al.* (1992). The results of Glavas and Heicklen (1985) were not considered.

4.4.4 Cl + CH_2FCl. The recommended value is based on results of the relative rate study of Tschuikow-Roux *et al.* (1988) normalized to the value of the rate constant for the reference reaction (Cl + CH_4) recommended in DeMore *et al.* (1992). The recent k_{298} value of Tuazon *et al.* (1992) is smaller than the recommendation.

4.4.5 Cl + CH_2F_2. The recommended value is based on results of the relative rate study of Tschuikow-Roux *et al.* (1985) normalized to the value of the rate constant for the reference reaction (Cl + CH_4) recommended in DeMore *et al.* (1992).

4.4.6 Cl + CH_3F. The recommended value is based on results of the direct study of Manning and Kurylo (1977) using the flash photolysis-resonance fluorescence technique. The results of the relative rate study of Tschuikow-Roux *et al.* (1988) are in

good agreement at room temperature but show a stronger temperature dependence, which is encompassed within the error limits. The recommendation for k_{298} is in excellent agreement with the recent value of Tuazon *et al.* (1992).

4.4.7 Cl + $CHCl_2CF_3$. The recommended value is based on results of the direct study of Warren and Ravishankara (private communication) using the pulsed photolysis-resonance fluorescence technique, and the relative rate study of Wallington and Hurley (1992) at room temperature. The recommendation for k_{298} is in excellent agreement with the recent value of Tuazon *et al.* (1992).

4.4.8 Cl + $CHFClCF_3$. The recommended value is based on results of the direct study of Warren and Ravishankara (private communication) using the pulsed photolysis-resonance fluorescence technique. The recommendation for k_{298} is in excellent agreement with the recent value of Tuazon *et al.* (1992).

4.4.9 Cl + CH_2ClCF_3. The recommended value is based on results of the direct study of Jourdain *et al.* (1978) using the discharge flow-mass spectrometric technique to monitor the decay of the HCFC in the presence of a large excess of Cl atoms.

4.4.10 Cl + CHF_2CHF_2. The recommended value is based on results of the relative rate study of Yano and Tschuikow-Roux (1986) normalized to the value of the rate constant for the reference reaction (Cl + C_2H_6) recommended in DeMore *et al.* (1992).

4.4.11 Cl + CH_2FCF_3. The recommended value is based on results of the relative rate study of Wallington and Hurley (1992). The recommendation for k_{298} is in excellent agreement with the recent value of Tuazon *et al.* (1992).

4.4.12 Cl + CH_3CFCl_2. The recommended value is based on results of the direct study of Warren and Ravishankara (private communication) using the pulsed photolysis-resonance fluorescence technique and the relative rate study of Wallington and Hurley (1992) at room temperature.

4.4.13 Cl + CH_3CF_2Cl. The recommended value is based on results of the relative rate study of Wallington and Hurley (1992). The recommendation for k_{298} is in excellent agreement with the recent value of Tuazon *et al.* (1992).

4.4.14 Cl + CH_2FCHF_2. The recommended values for the two reaction channels are based on results of the relative rate study of Tschuikow-Roux *et al.* (1985) normalized to the value of the rate constant for the reference reaction (Cl + CH_4) recommended in DeMore *et al.* (1992).

4.4.15 Cl + CH_3CF_3. The recommended value is based on results of the relative rate study of Tschuikow-Roux *et al.* (1985) normalized to the value of the rate constant for the reference reaction (Cl + CH_4) recommended in DeMore *et al.* (1992).

4.4.16 Cl + CH_2FCH_2F. The recommended value is based on results of the relative rate study of Yano and Tschuikow-Roux (1986) normalized to the value of the rate constant for the reference reaction (Cl + C_2H_6) recommended in DeMore *et al.* (1992).

4.4.17 Cl + CH_3CHF_2. The recommended values for the two reaction channels are based on results of the relative rate study of Yano and Tschuikow-Roux (1986) normalized to the value of the rate constant for the reference reaction (Cl + C_2H_6) recommended in DeMore *et al.* (1992). The overall rate constant value is in good agreement with results of the relative rate study of Wallington and Hurley (1992) at room temperature. The recommendation for k_{298} is in excellent agreement with the recent value of Tuazon *et al.* (1992).

4.4.18 Cl + CH_3CH_2F. The recommended value is based on results of the relative rate study of Tschuikow-Roux *et al.* (1985) normalized to the value of the rate constant for the reference reaction (Cl + CH_4) recommended in DeMore *et al.* (1992).

4.5 Ultraviolet Absorption Cross Sections

Ultraviolet absorption cross sections have been re-evaluated for CFC-11, 12, CFC-113, 114 and 115, and Halon 1301, 1211, 1202 and 2402 in this section based on recent work or new interpretations of older work. Absorption of Lyman-α radiation at 121.6 nm by long-lived CFCs has not been previously considered in lifetime calculations. Ravishankara *et al.* (1993) have recently measured Lyman-α cross sections for several fluorocarbons and have shown that photolysis at this wavelength has an effect on the lifetime calculated for CFC-115. For the purpose of atmospheric modelling, the absorption of a photon leads to the dissociation of the molecule, *i.e.* the quantum yield for dissociation is unity. For molecules that contain more than one Cl atom, the chlorine contained in the photodissociation fragment is assumed to be released fairly rapidly via subsequent reactions.

Evaluated temperature dependent cross sections are given in Tables 4.5-1 through 4.5-6 in the form of power series that are derived from least squares fits to the data. The basis for each of the recommendations is given below.

There have been several recent studies of the temperature dependences of the cross sections for HFCs and HCFCs [Gillotay and Simon (1991a, 1991b), Orlando *et al.* (1991)]. Because photodissociation is only a minor pathway for their removal, absorption spectra of these compounds have not been evaluated here.

Table 4.5-1 *Ultraviolet absorption cross sections vs. temperature (T) and wavelength (λ) for CFC-11 ($CFCl_3$)*

The equation giving the absorption spectrum at 298 K is:

$$\ln(\sigma) = a_0 + \sum_{i=1}^{4} a_i(\lambda - 205)^i$$

where $a_0 = -42.57847$
$a_1 = -0.1463296$
$a_2 = -1.866467 \times 10^{-3}$
$a_3 = 1.648604 \times 10^{-5}$
$a_4 = 4.882447 \times 10^{-8}$

The units for σ are cm^2 molecule^{-1}.

Using these values at different wavelengths as standard, σ_{298}, the absorption spectrum at other temperatures is given by,

$$\frac{\sigma 298}{\sigma T} = (a_0 + \sum_{i=1}^{2} a_i(\lambda - 205)^i) \exp((b_0 + \sum_{i=1}^{4} b_i(\lambda - 205)^i \frac{1}{T})$$

where $a_0 = 0.539095439$ $b_0 = 169.001053$
$a_1 = -0.0190050642$ $b_1 = 12.9541961$
$a_2 = 4.36706795 \times 10^{-5}$ $b_2 = 0.330676979$
$b_3 = 2.37078050 \times 10^{-3}$
$b_4 = -4.2522029 \times 10^{-5}$

The fit is valid only over the temperature range 210-270 K and wavelength range 180-230 nm.

4.5.1 CFC-11 and CFC-12

The absorption cross sections of $CFCl_3$ (CFC-11) and CF_2Cl_2 (CFC-12) as a function of wavelength between 175 and 230 nm at 298 K have been measured by various investigators with reasonably good agreement (± 6% between 175 and 215 nm) being obtained. The recommended 298 K values were obtained by averaging the data from Merienne *et al.* (1990). Simon *et al.* (1988a), Bass and Ledford (1976), Robbins (1976) and Chou *et al.* (1977). The data of Hubrich *et al.* (1977) were not included in the average because they increase the standard deviation of the polynomial fit with respect to the rest of the data. The earlier data of Rowland and Molina (1975) are assumed to be superseded by the results of Chou *et al.* (1977) from the same group. The temperature dependence of the absorption cross sections for CFC-11 was established using the measured values of Simon *et al.* (1988a) at 270, 250, 230 and 210 K, Hubrich and Stuhl (1980) at 208 K, Bass and Ledford (1976) at 223 K, and Chou *et al.* (1977) at 252, 232 and 213 K along with the 298 K values recommended here. The results of Green and Wayne (1976/77) were not included. The derived expressions for CFC-11 are given in Table 4.5-1. The expression for the temperature dependence of the cross sections for CFC-12 was taken from Table 4.5-2 of DeMore *et al.* (1990).

Table 4.5-2 *Ultraviolet absorption cross sections vs. temperature (T) and wavelength (λ) for CFC-12 (CF_2Cl_2)*

The equation giving the absorption spectrum at 298 K is:

$$\ln(\sigma) = a_0 + \sum_{i=1}^{4} a_i(\lambda - 205)^i$$

where $a_0 = -45.07771$
$a_1 = -0.2426733$
$a_2 = -1.184626 \times 10^{-3}$
$a_3 = 5.685441 \times 10^{-5}$
$a_4 = -6.110005 \times 10^{-7}$

The units for σ are cm^2 $molecule^{-1}$.

Using these values at different wavelengths as standard, σ_{298}, the absorption spectrum at other temperatures is given by,

$$\sigma_T = \sigma_{298}\exp[4.1 \times 10^{-4}(\lambda - 184.9)(T - 298)]$$

where σ_{298} = cross section at 298 K
λ = wavelength in nm
T = temperature in K

4.5.2 CFC-113, 114 and 115

The recommended absorption cross sections for these molecules in the 185-230 nm wavelength range as a function of temperature are based on the measurements of Simon *et al.* (1988b). The derived expressions are given in Table 4.5-3. The values measured at 298 K by Chou *et al.* (1978), at 298 and 208 K by Hubrich and Stuhl (1980) and at 298 K by Robbins (1976) are in good agreement with the recommended values. The absorption cross sections at 121.6 nm (Lyman-α) from the measurements of Ravishankara *et al.* (1993) are listed in Table 4.5-4.

Table 4.5-3 *Ultraviolet absorption cross sections vs. temperature (T) and wavelength (λ) for CFC-113, CFC-114 and CFC-115*

$$\log_{10}\sigma(\lambda,T) = \sum_{n=0}^{4} A_n\lambda^n + (T-273)\sum_{n=0}^{4} B_n\lambda^n$$

taken from Simon *et al.* (1988b)

CCl_2FCClF_2

$A_0 = -1087.9$ $B_0 = 12.493$
$A_1 = 20.004$ $B_1 = -2.3937 \times 10^{-1}$
$A_2 = -1.3920 \times 10^{-1}$ $B_2 = 1.7142 \times 10^{-3}$
$A_3 = 4.2828 \times 10^{-4}$ $B_3 = -5.4393 \times 10^{-6}$
$A_4 = -4.9384 \times 10^{-7}$ $B_4 = 6.4548 \times 10^{-9}$

T range: 210-300 K
λ range: 182-230 nm

***Table 4.5-3** Continued*

$CClF_2CClF_2$

$A_0 = -160.50$	$B_0 = -1.5296$
$A_1 = 2.4807$	$B_1 = 3.5248 \times 10^{-2}$
$A_2 = -1.5202 \times 10^{-2}$	$B_2 = -2.9951 \times 10^{-4}$
$A_3 = 3.8412 \times 10^{-5}$	$B_3 = 1.1129 \times 10^{-6}$
$A_4 = -3.4373 \times 10^{-8}$	$B_4 = -1.5259 \times 10^{-9}$

T range: 210-300 K
λ range: 172-220 nm

$CClF_2CF_3$

$A_0 = 5.8281$	$B_0 = 0$
$A_1 = -2.9900 \times 10^{-1}$	$B_1 = 0$
$A_2 = 1.3525 \times 10^{-3}$	$B_2 = 0$
$A_3 = -2.6851 \times 10^{-6}$	$B_3 = 0$

T range: 210-300 K
λ range: 172-204 nm

***Table 4.5-4** Absorption Cross Sections at 121.6 nm, Lyman-α radiation, at 298 K*

Compound	Cross Section 10^{-18} cm^2 molecule^{-1}
CF_3Cl (CFC-13)	8.12 ± 0.54
CF_2ClCF_2Cl (CFC-114)	36.0 ± 2.2
CF_3CF_2Cl (CFC-115)	4.57 ± 0.37

All data from Ravishankara *et al.* (1993)

4.5.3 Halons 1301 (CF_3Br), 1211 (CF_2ClBr), 1202 (CF_2Br_2) and 2402 ($C_2F_4Br_2$)

Absorption cross sections for these compounds have been measured by various investigators. Molina *et al.* (1982) (CF_3Br, CF_2ClBr, CF_2Br_2 and $C_2F_4Br_2$ at 298 K), Giolando *et al.* (1980) (CF_2ClBr at 298 K), and Robbins (1976) ($C_2F_4Br_2$ at 298 K). Gillotay and Simon (1989) and Burkholder *et al.* (1991) have measured the cross sections of all four compounds as a function of temperature. The recommended values were obtained by averaging the results of Burkholder *et al.* and Gillotay and Simon over the wavelength ranges where they overlap. The recommendation is given in Table 4.5-5.

***Table 4.5-5** Ultraviolet absorption cross sections vs. temperature (T) and wavelength (λ) for the Halons*

$$\ln \sigma(\lambda,T) = [A_0 + \sum_{i=1}^{4} A_i(\lambda - \lambda_0)^i] \bullet [1 + (296 - T) \bullet (B_0 + \sum_{i=1}^{4} B_i(\lambda - \lambda_0)^i]$$

Molecule	λ_0(nm)	i	A_i	B_i
	λ range (nm)			
CF_2Br_2 (H-1202)	263.1184	0	-43.61707	1.024236 (-4)
	235-304	1	-0.1392279	5.173454(-6)
		2	-8.847585(-4)	2.582280(-8)
		3	1.423058(-5)	-1.222894(-11)
		4	-6.439138(-8)	6.541614(-12)
CF_2ClBr (H-1211)	253.9698	0	-44.65328	1.05987(-4)
	220-304	1	-0.1205495	5.10452(-6)
		2	-8.133584(-4)	5.367804(-8)
		3	4.626312(-6)	2.196723(-10)
		4	5.079764(-10)-	7.275262(-12)
CF_3Br (H-1301)*	244.8952	0	-47.038912	2039623(-4)
	214-283	1	-0.1629549	8.248259(-6)
		2	-1.155689(-3)	-5.445033(-8)
		3	1.995283(-5)	-3.638785(-9)
		4	2.916192(-9)	-1.39492(-11)
$C_2F_4Br_2$ (H-2402)	229.885	0	-42.49031	9.66205(-6)
	190-279	1	-0.08344399	1.987599(-6)
		2	-1.356491(-3)	5.150506(-8)
		3	3.17866(-6)	5.837533(-10)
		4	7.715186(-8)	6.946091(-13)

* In the wavelength range 190 to 213 nm, the cross sections are temperature independent and are given by σ (in units of 10^{-19} cm^2)= 3.1885074 x 10^3 - 6.0996270 x 10^1 (λ)+ 4.3419069 x 10^{-1} (λ^2) - 1.3618646 x 10^{-3} (λ^3) + 1.5869473 x 10^{-6} (λ^4). *This should be added to the temperature dependent part to get the cross sections in the photolytically active region for this molecule.*

CF_2Br_2 and CF_2ClBr absorb only weakly at wavelengths longer than 300 nm but the calculated photolytic lifetimes are very sensitive to the cross sections in this spectral region. While there are cross section data beyond 300 nm, the agreement between different studies is not particularly good. Therefore, we have extrapolated the recommended cross sections by assuming that log(σ) varies linearly with wavelength beyond 300 nm at each temperature. This assumption, however, introduces considerable uncertainty into the evaluated cross sections in this spectral region. The calculated parameters for these extrapolations are listed in Table 4.5-6.

***Table 4.5-6** Extrapolated ultraviolet absorption cross sections vs. temperature (T) for CF_2Br_2 and CF_2ClBr*

$$\ln \sigma(\lambda,T)) = (A_0 + \sum_{i=1}^{4} A_i(T\text{-}251.2)^i) + (B_0 + \sum_{i=1}^{4} B_i\,(T\text{-}251.2)^i) \bullet (\lambda - 290)$$

Molecule	i	A_i	B_i
CF_2Br_2 (H-1201)	0	-48.31973	-0.1783530
300-340nm	1	1.257516(-2)	4.518468(-4)
	2	3.009917(-7)	5.862273(-6)
	3	8.530738(-10)	1.196068(-8)
	4	-1.468803(-10	-3.751400(-9)
CF_2ClBr (H-1211)	0	-50.63382	-0.1918624
300-340nm	1	1.782180(-2)	7.636243(-4)
	2	4.275152(-7)	1.772590(-5)
	3	3.070216(-10)	-1.847984(-7)
	4	-2.047512(-10)	-6.537606(-9)

4.6 Rate of Hydrolysis and Henry's Law Constant for CH_3CCl_3 and CCl_4

CH_3CCl_3.

In order to assess the possible fate of methylchloroform in the oceans and in fresh water, it is necessary to know the rate of decomposition and the Henry's Law constant in water as a function of temperature. It is also necessary to measure these constants in water approximating the salinity of ocean water in order to determine whether there are any effects due to ionic strength.

The major hydrolysis pathways for methylchloroform in water are shown below:

$$CH_3CCl_3 + 2H_2O \rightarrow CH_3COOH + 3HCl \quad (1)$$

$$CH_3CCl_3 \rightarrow CH_2CCl_2 + HCl \quad (2)$$

Haag and Mill (1988) and Gerkens and Franklin (1989) have shown that at 25° C, the formation of 1,1-dichloroethylene is, respectively, about 22% and 27% of the overall process, whereas Jeffers *et al.* (1989) did not detect any 1,1-dichloroethylene. The pre-exponential factor, A, the activation energy, E_a, the rate constant at 25° C, k, and the lifetime, τ, are given in Table 4.6-1. The data from the three groups are in reasonable agreement, although there is some discrepancy in the activation energy and A-factor. The mean lifetime at 25° C is 1.35 years with a deviation from the mean of about 20%. Trusty *et al.* (1991) repeated the work of Jeffers *et al.* using zero dead-volume ampoules and found that the rate constant at 115° C was within 17% of the Jeffers *et al.* value. Major sources of error include head space correction and the accuracy of the analytical method. Haag *et al.* had about a 33% dead volume in their reaction ampoules, Gerkens *et al.* about 6% and Jeffers *et al*, practically zero.

Table 4.6-1. Rate Constants for the aqueous decomposition of methylchloroform.

A-factor (s^{-1})	E_a (kJ mol^{-1})	k^1, 25°C (s^{-1})	τ (Yr)	Ref.
$1.1x10^{13}$	118	$2.33x10^{-8}$	1.35	Haag and Mill (1988)
$1.26x10^{13}$	117.8	$2.89x10^{-8}$	1.10	Gerkens and Franklin (1989)
$4.93x10^{12}$	116.1	$2.25x10^{-8}$	1.40	Jeffers *et al.* (1989)

[1]The rate constant is determined from: $k = A \exp(-E_a/RT)$

There are very few data available regarding the effect of salinity on the rate of methylchloroform decomposition. A few kinetic runs were carried out by Gerkens *et al.* comparing the rates in distilled and salt water. Any differences observed were small, and it is difficult to determine whether they would be statistically significant.

Gossett (1987), Ashworth (1988) and Leighton and Calo (1981) have determined the values for the Henry's Law constant for methylchloroform as a function of temperature. Henry's Law relates to the solubility of gases in a solvent as shown by equation (3) below,

$$X' = p'/H' \quad (3)$$

where, X' = concentration of the gas in the solvent

p' = partial pressure of the gas above the solvent

H' = Henry's Law constant in units of (pressure/concentration)

The coefficients for the Henry's Law correlation equation are given in Table 4.6-2. Gossett (1987) and Ashworth (1988) used an EPICS (Equilibrium Partitioning In Closed Systems) method where nearly identical amounts of a volatile solute are added to two sealed serum bottles having different water volumes. The concentration of the solute in the vapor phase is determined by gas chromatography, and the Henry's Law constant is calculated from the vapor concentrations in the two bottles. Leighton and Calo used an equilibrium cell, where the concentrations of methylchloroform were determined in the gas and aqueous phases using gas chromatography. Results from the two groups which used the EPICS method are in very good agreement while the results from the equilibrium cell are about 15% higher, which could be due to difficulties in the gas chromatographic measurements.

Table 4.6-2 *Coefficients for the correlation equation of Henry's Law for methylchloroform and carbon tetrachloride (units T, K; H, atm m^3 $mole^{-1}$)*

	ln H = A - B/T			
	Methylchloroform		Carbon tetrachloride	
Investigator	A	B	A	B
Gossett (1987)	9.777	4133	11.29	4411
Ashworth (1988)	7.351	3399	9.739	3951
Leighton and Calo (1981)	10.81	4391	11.09	4381

Ashworth *et al.* (1988) and Dilling (1977) have also measured the Henry's Law constant for methylchloroform in distilled water at 25°C. These results, along with the 25°C results from the temperature dependence investigations, are compared in Table 4.6-3. The value obtained by Ashworth *et al.*, who used a batch air stripping method, agrees within 2% with the value obtained by Ashworth who used the EPICS procedure. There is, however, a 75% discrepancy with the value of Dilling who used a method which required the measurement of the vapor pressure and solubility of methylchloroform. This discrepancy may be due to difficulties in measuring solubilities at low levels.

Table 4.6-3 *Henry's Law constants at 25°C for methyl chloroform and carbon tetrachloride in water.*

	H (atm m^3 $mole^{-1}$)	
Investigator	Methyl chloroform	Carbon tetrachloride
Gossett (1987)	0.0172	0.0304
Ashworth (1988)	0.0174	0.0295
Leighton and Calo (1981)	0.0200	0.0274
Dilling (1977)	0.0302	

The presence of ionic species in the water will lower the solubility of the gas in the solvent (the salting out effect). Gossett (1987) has used the EPICS procedure to determine the activity coefficient, γ, of the solute in the solvent as a function of the ionic strength. A plot of log γ vs. the ionic strength yields a straight line where the slope is the salting out coefficient as shown by equation 4 below.

$$\log \gamma = k\, I \qquad (4)$$

where, k = salting out coefficient (L $mole^{-1}$)

I = ionic strength

His value for the salting out coefficient of methylchloroform is 0.193 (L $mole^{-1}$) at 20°C.

CCl_4.

Jeffers *et al.* (1989) measured the decomposition of carbon tetrachloride dissolved in water as a function of temperature and obtained the following expression for the decomposition rate constant:

$$k\ (s^{-1}) = 6.783 \times 10^{10} \exp(-114.5/RT)$$

where the activation energy is given in kJ mol^{-1}. The resulting decomposition half-lives are 431, 81.8, 37.4 and 17.4 years at temperatures of 10, 20, 25 and 30°C, respectively. Coefficients for the correlation equation determined by Gossett (1987), Ashworth (1988) and Leighton and Calo (1981) are given in Table 4.6-2. The results of Ashworth (1988) at 25°C using a batch stripping method are compared with the results at 25°C from the temperature dependence studies in Table 4.6-3. The results from all these studies are in very good agreement.

References

AFEAS (Alternative Fluorocarbon Environmental Acceptability Study), in *Scientific Assessment of Stratospheric Ozone: 1989*, World Meteorological Organization, Global Ozone Research and Monitoring Project - WMO Report No. 20, Vol. II, 1989.

Ashworth, R. A., Air-water partitioning coefficients of organics in dilute solutions, *J. Hazard. Mat., 18*, 25-38, 1988.

Atkinson, R., D. L. Baulch, R. A. Cox, R. F. Hampson, Jr., J. A. Kerr and J. Troe, Evaluated kinetic and photochemical data for atmospheric chemistry: supplement III, *J. Phys. Chem. Ref. Data, 18*, 881-1097, 1989.

Atkinson, R., D. L. Baulch, R. A. Cox, R. F. Hampson, Jr., J. A. Kerr and J. Troe, Evaluated kinetic and photochemical data for atmospheric chemistry: supplement IV, *Atmos. Environ., 26A*, 1187-1230, 1992.

Bass, A. M. and A. E. Ledford, Jr., Ultraviolet photoabsorption cross-sections of CF_2Cl_2 and $CFCl_3$ as a function of temperature, at the 12th Informal Conference on Photochemistry, Gaithersburg, MD, June 28 - July 1, 1976.

Brown, A. C., C. E. Canosa-Mas, A. D. Parr, and R. P. Wayne, Laboratory studies of some halogenated ethanes and ethers: Measurements of rates of reaction with OH and of infrared absorption cross-sections, *Atmos. Environ., 24A*, 2499-2511, 1990a.

Brown, A. C., C. E. Canosa-Mas, A. D. Parr, K. Rothwell, and R. P. Wayne, 11th Int. Symp. on Gas Kinet., Assisi, 2-7 Sept., 1990b.

Burkholder, J. B., R. R. Wilson, T. Gierczak, R. Talukdar, S. A. McKeen, J. J. Orlando, G. L. Vaghjiani and A. R. Ravishankara, Atmospheric fate of CF_3Br, CF_2ClBr, and CF_2BrCF_2Br, J. *Geophys. Res., 96*, 5025-5043, 1991.

Chang, J. S. and F. Kaufman, Kinetics of the reactions of hydroxyl radicals with some halocarbons: $CHFCl_2$, CHF_2Cl, CH_3CCl_3, CF_2HCl_3, and CCl_4, *J. Phys. Chem., 66*, 4989-4994, 1977.

Chou, C. C., W. S. Smith, J. Vera Ruiz, K. Moe, G. Crescentini, M. J. Molina and F. S. Rowland, The temperature dependences of the ultraviolet absorption cross sections of CCl_2F_2 and CCl_3F, and their stratospheric significance, *J. Phys. Chem., 81*, 286-290, 1977.

Chou, C. C., R. J. Milstein, W. S. Smith, H. Vera Ruiz, M. J .Molina and F. S. Rowland, Stratospheric photodissociation of several saturated chlorofluorocarbon compounds in the current technological use (CFC-13, 113, 114, 115), *J. Phys. Chem., 82*, 1-7, 1978.

Clyne, M. A. A. and P. M. Holt, Reaction kinetics involving ground $X^2\pi$ and excited $A^2\Sigma^+$ hydroxyl radicals. Part 1.-Quenching kinetics of OH $A^2\Sigma^+$ and rate constants for reactions of OH $X^2\pi$ with CH_3CCl_3 and CO, *J. Chem. Soc. Faraday Trans. 2*, 75, 569-581, 1979a.

Clyne, M. A. A. and P. M. Holt, Reaction kinetics involving ground $X^2\pi$ and excited $A^2\Sigma^+$ hydroxyl radicals. Part 2.-Rate constants for reactions of OH $X^2\pi$ with halogenomethanes and halogenoethanes, *J. Chem. Soc. Faraday Trans. 2*, 75, 582-591, 1979b.

Clyne, M. A. A. and R. F. Walker, Absolute rate constants for elementary reactions in the chlorination of CH_4, CD_4, CH_3Cl, CH_2Cl_2, $CHCl_3$, $CDCl_3$ and $CBrCl_3$, *J. Chem. Soc. Faraday Trans. 1, 69*, 1547-1565, 1973.

DeMore, W. B., S. P. Sander, D. M. Golden, M. J. Molina, R. F. Hampson, M. J. Kurylo, C. J. Howard, A. R. Ravishankara, *Chemical kinetics and photochemical data for use in stratospheric modeling, evaluation number 9*, JPL Publication 90-1, Pasadena, CA, 1990.

DeMore, W. B., S. P. Sander, D. M. Golden, C. E. Kolb, M. J. Molina, R. F. Hampson, M. J. Kurylo, C. J. Howard, A. R. Ravishankara, *Chemical kinetics and photochemical data for use in stratospheric modeling, evaluation number 10*, JPL Publication 92-20, Pasadena, CA, 1992.

DeMore, W. B., Relative rate constants for the reactions of OH with methane and methyl chloroform, *Geophys. Res. Lett., 19*, 1367-1370, 1992.

DeMore, W. B., Rates of hydroxyl radical reactions with some HFCs, *Proceedings of the S.P.I.E., 1715*, 1993.

Dilling, W. L., Interphase transfer processes. II. Evaporation rates of chloro methanes, ethanes, ethylenes, propanes, and propylenes from dilute aqueous solutions. Comparisons with theoretical predictions, *Env. Sci. Tech., 11*, 405, 1977.

Finlayson-Pitts, B. J ., M. J. Ezell, T. M. Jayaweera, H. N. Berko and C. C. Lai, Kinetics of the reactions of OH with methyl chloroform and methane: implications for global tropospheric OH and the methane budget, *Geophys. Res. Lett., 19*, 1371-1374, 1992.

Gerkens, R. G. and J. A. Franklin, The rate of degradation of 1,1,1-trichloroethane in water by hydrolysis and dehydrochlorination, *Chemosphere, 19*, 1929-1937, 1989.

Gierczak, T., R. Talukdar, G. L. Vaghjiani, E. R. Lovejoy and A. R. Ravishankara, Atmospheric fate of hydrofluoroethanes and hydrofluorochloroethanes: 1. Rate coefficients for reactions with OH, *J. Geophys.Res., 96*, 5001-5011, 1991.

Gillotay, D. and P. C. Simon, Ultraviolet absorption spectrum of trifluoro-bromo-methane, difluoro-dibromo-methane and difluoro-bromo-chloro-methane in the vapor phase, *J. Atmos. Chem., 8*, 41-62, 1989.

Gillotay, D. and P. C. Simon, Temperature-dependence of ultraviolet-absorption cross-sections of alternative chlorofluoroethanes, *J. Atmos. Chem., 13*, 269-285, 1991a.

Gillotay, D. and P. C. Simon, Temperature-dependence of ultraviolet-absorption cross-sections of alternative chlorofluoroethanes. 2. The 2-chloro-1,1,1,2-tetrafluoroethane - HCFC-124, *J. Atmos. Chem. 13*, 289-299, 1991b.

Giolando, D. M., G. B. Fazekas, W. D. Taylor and G. A. Takacs, Atmospheric photochemistry of CF_2ClBr, *J. Photochem., 14*, 335, 1980.

Glavas, S. and J. Heicklen, Relative reactivity of chlorine atoms with NO, NO_2 and $HCCl_2F$ at room temperature and atmospheric pressure, *J. Photochem., 31*, 21-28, 1985.

Gossett, J. M., Measurement of Henry's Law constants for C1 and C2 chlorinated hydrocarbons, *Env. Sci. Tech., 21*, 202-208,1987.

Green, R. G. and R. P. Wayne, Vacuum ultraviolet absorption spectra of halogenated methanes and ethanes, *J. Photochem., 6*, 375-377, 1976/77.

Haag, W. C. and T. Mill, Effect of a subsurface sediment on hydrolysis of haloalkane and epoxides, *Env. Sci. Tech., 22*, 658-663, 1988.

Haar, N., J. Hjorth, and G. Ottobrini, paper presented at the STEP-HALOCSIDE/AFEAS workshop, Dublin, 14-16 May, 1991.

Handwerk, V., and R. Zellner, Kinetics of the reactions of OH radicals with some halocarbons ($CHClF_2$, CH_2ClF, CH_2ClCF_3, CH_3CClF_2, CH_3CHF_2) in the temperature range 260-370 K, *Ber. Bunsenges Phys. Chem., 82*, 1161-1166, 1978.

Howard, C.J. and K.M. Evenson, Rate constants for the reactions of OH with CH_4 and fluorine, chlorine, and bromine substituted methanes at 296 K, *J. Phys. Chem., 64*, 197-202, 1976a.

Howard, C. J. and K. M. Evenson, Rate constants for the reactions of OH with ethane and some halogen substituted ethanes at 296 K, *J. Phys. Chem., 64*, 4304-4306, 1976b.

Hubrich, C., C. Zetzsch and F. Stuhl, Absorptions spektren von halogenierten methanen in bereich von 275 bis 160 nm bei temperaturen von 298 und 208 K, *Ber. Bunsenges. Phys. Chem., 81*, 437, 1977.

Hubrich, C. and F. Stuhl, The ultraviolet absorption of some halogenated methanes and ethanes of atmospheric interest, *J. Photochem., 12*, 93-107, 1980.

Jeffers, P. M., L. M. Ward, L. M. Woytowitch, and N. L. Wolfe, Homogeneous hydrolysis rate constants for selected chlorinated methanes, ethanes, ethenes and propanes, *Env. Sci. Tech., 23*, 965-969, 1989.

Jeong, K.-M., and F. Kaufman, Rates of the reactions of 1,1,1-trichloroethane (methyl chloroform) and 1,1,2-trichloroethane with OH, *Geophys. Res. Lett., 6*, 757-759, 1979.

Jeong, K.-M., and F. Kaufman, Kinetics of the reaction of hydroxyl radical with methane and with nine Cl- and F-substituted methanes. I. Experimental results, comparisons, and applications, *J. Phys. Chem., 86*, 1808-1815, 1982.

Jeong, K.-M., K.-J. Hsu, J. B. Jeffries, and F. Kaufman, Kinetics of the reactions of OH with C_2H_2, CH_3CCl_3, $CH_2ClCHCl_2$, CH_2ClCCF_2, and CH_2FCF_3, *J. Phys. Chem., 88*, 1222-1226, 1984.

Jourdain J-L., G. LeBras, and J. Combourieu, Etude cinetique des reactions du 1,1,1-trifluoro,2-chloroethane avec les atomes de chlore et d'oxygene, *J. Chim. Physique, 75*, 318-323, 1978.

Knox, J. H., Competitive chlorinations. Part 2.-chloromethanes, *Trans. Faraday Soc., 55*, 275-283, 1962

Kurylo, M. J., P. C. Anderson, and O. Klais, A flash photolysis resonance fluorescence investigation of the reaction OH + $CH_3CCl_3 \rightarrow H_2O + CH_2CCl_3$, *Geophys. Res. Lett., 6*, 760-762, 1979.

Leighton, P. T. and J. M. Calo, Distribution coefficients of chlorinated hydrocarbons in dilute air-water systems for groundwater contamination applications, *J. Chem. Eng. Data, 26*, 382-386, 1981.

Liu, R., R. E. Huie, and M. J. Kurylo, Rate constants for the reactions of the OH radical with some hydrochlorofluorocarbons over the temperature range 270-400 K, *J. Phys. Chem., 94*, 3247-3249, 1990.

Manning, R. and M. J. Kurylo, Flash photolysis resonance fluorescence investigation of the temperature dependencies of the reactions of $Cl(^2P)$ atoms with CH_4, CH_3Cl, CH_3F, CH_3F^+, and C_2H_6, *J. Phys. Chem., 81*, 2609-2614, 1977.

Martin, J.-P., and G. Paraskevopoulos, A kinetic study of the reactions of OH radicals with fluoroethanes. Estimates of C-H bond strengths in fluoroalkanes, *Can. J. Chem., 61*, 861-865, 1983.

Merienne, M. F., B. Coquart, and A. Jenouvrier, Temperature effect on the ultraviolet absorption of $CFCl_3$, CF_2Cl_2, and N_2O, *Planet. Space Sci., 38*, 617-625, 1990.

Molina, L. T., M. J. Molina and F. S. Rowland, Ultraviolet absorption cross-sections of several brominated methanes and ethanes of atmospheric interest., *J. Phys. Chem., 86*, 2672-2676, 1982.

Nelson, D. D., M. S. Zahniser and C. E. Kolb, Chemical kinetics of the reactions of the OH radical with several hydrochlorofluoropropanes, *J. Phys. Chem., 96*, 249-253, 1992.

Nelson, L., I. Shanahan, H. W. Sidebottom, J. Treacy and O. J.Nielsen, Kinetics and mechanism for the oxidation of 1,1,1-Trichloroethane, *Int. J. Chem. Kinet., 22*, 577-590, 1990.

Nielsen, O. J., Rate constants for the gas-phase reactions of OH radicals with CH_3CHF_2 and $CHCl_2CF_3$ over the temperature range 295-388 K, *Chem. Phys. Lett., 187*, 286-290, 1991.

Niki, H., P. D. Maker, C. M. Savage, and L. P. Breitenbach, FTIR studies of the kinetics and mechanism for the reaction of Cl atom with formyl chloride, *Int. J. Chem. Kinet., 12*, 915-920, 1980.

Nip, W. S., D. L. Singleton, R. Overend, and G. Paraskevopoulos, Rates of OH radical reactions. 5. Reactions with CH_3F, CH_2F_2, CHF_3, CH_3CH_2F and CH_3CHF_2 at 297 K, *J. Phys. Chem., 83*, 2440-2443, 1979.

Orlando, J. J., J. B. Burkholder, S. A. McKeen and A. R. Ravishankara, Atmospheric fate of several hydrofluoroethanes and hydrochloroethanes. 2. UV absorption cross-sections and atmospheric lifetimes, *J. Geophys. Res., 96*, 5013-5023, 1991.

Paraskevopoulos, G., D. L. Singleton, and R. S. Irwin, Rates of OH radical reactions. 8. Reactions with CH_2FCl, CHF_2Cl, $CHFCl_2$, CH_3CF_2Cl, CH_3Cl, and C_2H_5Cl at 297 K, *J. Phys. Chem. 85*, 561-564, 1981.

Ravishankara, A. R., S. Solomon, A. A. Turnipseed and R. F. Warren, Atmospheric lifetimes of long-lived halogenated species, *Science, 259*, 194-199, 1993.

Robbins, D. E., paper presented at the International Conference on Problems Related to the Stratosphere, Logan, Utah, 15-17 Sept. 1976.

Rowland, F. S. and M. J. Molina, Chlorofluoromethanes in the environment, *Rev. Geophys. Space Phys., 13*, 1-36, 1975.

Simon, P. C., D. Gillotay, N. Vanlaethem-Meuree and J. Wisemberg, Ultraviolet absorption cross-sections of chloro-and chlorofluoro-methanes at stratospheric temperatures, *J. Atm. Chem., 7*, 107-135, 1988a

Simon, P. C., D. Gillotay, N. Vanlaethem-Meuree and J. Wisemberg, Temperature dependence of ultraviolet absorption cross-sections of chlorofluoro ethanes, *Annales Geophysicae, 6*, 239-248, 1988b.

Talukdar, R., A. Mellouki, T. Gierczak, J. B. Burkholder, S. A. McKeen and A. R. Ravishankara, Atmospheric fate of CF_2H_2, CH_3CF_3, $CHF_2CF_3CFCl_2$: rate coefficients for reactions with OH and UV absorption cross sections of CH_3CFCl_2, *J. Phys. Chem., 95*, 5815-5821, 1991.

Talukdar, R. K., A. Mellouki, A-M. Schmoltner, T. Watson, S. Montzka and A. R. Ravishankara, Kinetics of the OH reaction with methyl chloroform and its atmospheric implications, *Science, 257*, 227-230, 1992.

Trusty, C. D. and J. J. Ellington, Techniques affecting precision and accuracy in hydrolysis rate constant determinations of volatile organic compounds using Jeffers' zero headspace reaction bulbs, *Anal. Lett., 24*, 327-344, 1991.

Tschuikow-Roux, E., T. Yano and J. Niedzielski, Reactions of ground state chlorine atoms with fluorinated methanes and ethanes, *J. Chem. Phys., 82*, 65-74, 1985.

Tschuikow-Roux, E., F. Faraji, S. Paddison, J. Niedzielski, and K. Miyokawa, Kinetics of photochlorination of halogen (F, Cl,Br) substituted methanes, *J. Phys. Chem., 92*, 1488-1495, 1988.

Tuazon, E. C., R. Atkinson and S. B. Corchnoy, Rate constants for the gas-phase reactions of Cl atoms with a series of hydrofluorocarbons and hydrochlorofluorocarbons at 298 ± 2 K, *Int. J. Chem. Kinet., 24*, 639-648, 1992.

Vaghjiani, G. L. and A. R. Ravishankara, New measurement of the rate coefficient for the reaction of OH with methane, *Nature, 350*, 406-409, 1991.

Wallington, T. J. and M. D. Hurley, A kinetic-study of the reaction of chlorine atoms with CF_3CHCl_2, CF_3CH_2F, $CFCl_2CH_3$, CF_2ClCH_3, CH_3D, CH_2D_2, CHD_3, CD_4, and CD_3Cl at 295 ± 2 K, *Chem. Phys. Lett., 189*, 437-442, 1992.

Warren, R. F., T. Gierczak, and A. R. Ravishankara, A study of $O(^1D)$ reactions with CFC substitutes, *Chem. Phys. Lett., 183*, 403-409, 1991.

Watson, R. T., G. Machado, B. Conaway, S. Wagner and D. D. Davis, A temperature dependent kinetics study of the reaction of OH with CH_2ClF, $CHCl_2F$, $CHClF_2$, CH_3CCl_3, CH_3CF_2Cl, and $CF_2ClCFCl_2$, *J. Phys. Chem., 81*, 256-262, 1977.

Watson, R. T., A. R. Ravishankara, G. Machado, S. Wagner and D. D. Davis, A kinetics study of the temperature dependence of the reactions of $OH(^2\pi)$ with CF_3CHCl_2, CF_3CHClF, and CF_2ClCH_2Cl, *Int. J. Chem. Kinet,.11*, 187-197, 1979.

Wayne, R. P., C. E. Canosa-Mas, A. C. Heard and A. D. Parr, On discrepancies between different laboratory measurements of kinetic parameters for the reaction of the hydroxyl radical with halocarbons, *Atmos. Environ., 26A*, 2371-2379, 1992.

Yano, T., and E. Tschuikow-Roux, Competitive photochlorination of the fluoroethanes CH_3CHF_2, CH_2FCH_2F and CHF_2CHF_2, *J. Photochem., 32*, 25-37, 1986.

Zhang, A., R. E. Huie, and M. J. Kurylo, Rate constants for the reactions of OH with CH_3CFCl_2 (HCFC-141b), CH_3CF_2Cl (HCFC-142b), and CH_2FCF_3 (HFC-134a), *J. Phys. Chem., 96*, 1533-1535, 1992.

Zhang Z., R. Liu, R. E. Huie and M. J. Kurylo, Rate constants for the gas-phase reactions of the OH radical with $CF_3CF_2CHCl_2$ (HCFC-225ca) and CF_2ClCF_2CHClF (HCFC-225cb) *Geophys. Res. Lett., 18*, 5-7, 1991.

Chapter 5.

Model Calculations of Atmospheric Lifetime

Lead authors:

M. K. W. KO and C. H. Jackman

Additional Contributors:

B. A. Boville, C. Brüehl, P. Connell, A. Golombek, J. Levy, J. M. Rodriguez, T. Sasaki, and K. K. Tung

Chapter 5
Table of Contents

Chapter 5: Model Calculations of Atmospheric Lifetime

5.0 Summary

- This chapter examines the model-calculated lifetimes of the species discussed in this report. The atmospheric lifetime is defined as the atmospheric burden divided by the atmospheric removal rate. By simulating explicit mechanisms that are responsible for the removal of the trace gases, model calculations can predict how the lifetimes of the species may change as the atmospheric compositions change. They also allow the calculation of lifetimes for species that are not yet emitted to the atmosphere.

- The species discussed in this report can be separated into two groups: those that are removed mainly by UV photolysis in the stratosphere and those that are removed mainly by reaction with OH in the troposphere. Species in each group require different observations for validation of the mechanisms for atmospheric removal.

For species that are mainly removed in the stratosphere by photolysis

- Photochemical removal processes and atmospheric transport are both important and each contribute to the variances in computed lifetimes among the models.

- Differences in computed photolysis loss frequencies for the numerical models are significant and further work is required to totally understand model differences.

- The effects of differences in atmospheric transport on atmospheric lifetimes among the numerical models are at least 30%. There are insufficient observations to allow one to decide whether the 2-D models are correctly simulating the bulk transport of the trace gases in the lower stratosphere. Due to the natural variabilities in the atmosphere, it would be difficult to use stratospheric observations to constrain the lifetimes of these species to better than 30%.

- Current model simulations indicate that the calculated transient lifetimes for the CFCs could be about 10% larger than the calculated steady-state lifetime through the 1980s.

- The calculated atmospheric lifetimes for CFC-11 ($CFCl_3$) are consistent with the values derived in Chapter 3.

- Simultaneous measurements of the stratospheric concentrations of two species can be used to estimate the ratio of their lifetimes if enough is known about their local removal processes and their emission histories.

For species that are removed mainly by reaction with OH in the troposphere

- We determine lifetimes for the HCFCs and HFCs using model calculated stratospheric loss and tropospheric OH loss. The tropospheric OH removal is adjusted using the tropospheric removal rate of methyl chloroform (CH_3CCl_3) derived from the atmospheric lifetime of CH_3CCl_3 from Chapter 3, the estimated ocean removal rate, and the model calculated stratospheric removal.

- Using the methyl chloroform data as a proxy of OH is complicated by uncertainties associated with the statistical methods and with the uncertain role of the ocean sink, not to mention the calibration problems identified in Chapter 1. Thus, it is difficult to be confident about the lifetimes of these species to better than a factor of 1.5.

The following modelling groups provided model results that are used in this chapter.

***Table 5.1** Modelling groups that provided results for this report*

Atmospheric and Environmental Research, Inc.	Malcolm Ko and Debra Weisenstein	AER
NASA/Goddard Space Flight Center	Charles Jackman and Anne Douglass	GSFC
Lawrence Livermore National Laboratory	Don Wuebbles and Peter Connell	LLNL
Max Planck Institute for Chemistry	Christoph Bruehl	MPI
Meteorological Research Institute, Japan	Toru Sasaki	MRI
University of Washington	Ka Kit Tung, Hu Yang, and Eduardo Olaguer	WASH
Massachusetts Institute of Technology*	Amram Golombek and Ronald Prinn	MIT

*3-D model

5.1 Introduction

We examine in this chapter how model-calculated lifetimes of the CFCs compare with the empirically derived lifetimes. In particular, we discuss how observations can help validate the mechanisms that determine the lifetimes in the models. Most of the models whose results are discussed in this chapter are two-dimensional (2-D) representing the longitudinally averaged state of the atmosphere. The model domains are from pole to pole and from the ground to about 60 km. Typical model resolutions are 2 to 3 km in the vertical and 5° to 10° in latitude. A more detailed description of these models is found in Jackman *et al.* (1989). Some results are also included from a low resolution three-dimensional (3-D) model.

The 2-D models used in this report are the simplest forms of the models often used for emission scenario studies. They are purely transport models in which the transporting circulation (vertical and meridional winds) is derived from continuity based on thermodynamic constraints with specified heating rates or heating rates calculated from specified temperatures. The simulated chemical species do not feed back on the circulation through changes in the radiative heating. Similarly, the low resolution 3-D model (Golombek and Prinn, 1986, 1989) used a specified transporting circulation although this was obtained from a simulation using a corresponding simple 3-D dynamical model.

The formulation of 2-D models inherently assumes that the atmosphere is well mixed in the longitudinal direction and is slowly evolving in time. Therefore 2-D models are most useful when the important processes controlling the distribution of a species have seasonal or longer time scales. These assumptions hold reasonably well in much of the stratosphere, so that 2-D models are excellent tools for simulating the behavior of species such as CFCs which are primarily destroyed there. Both of the assumptions are violated in the troposphere where many processes, such as convection and storm systems, affect trace species on relatively short space and time scales. 2-D models are generally not appropriate for simulating species with large tropospheric sinks, such as methyl chloroform. However, the tropospheric processes in 2-D models can be represented to give reasonable transport into the stratosphere to address the stratospheric removal of species whose tropospheric loss is not large enough to prevent significant amounts from reaching the stratosphere.

For the purpose of determining the atmospheric lifetimes of species mainly destroyed in the stratosphere, a fundamental limitation of the 2-D models is that the effects of eddy transports are represented through horizontal and vertical eddy diffusion. Horizontal eddy diffusion is extremely important in 2-D models and primarily represents the effects of transport by planetary scale waves, which are represented explicitly (although crudely) in the low resolution 3-D model. Vertical diffusion is also important and differing treatments of vertical eddy diffusion appear to be responsible for a significant part of the differences in the model results discussed below. The vertical diffusion is largely intended to represent the effects of small scale gravity waves, which are not represented in 3-D models either. Systematic transports by larger scale equatorial waves are also represented by vertical diffusion in the 2-D models. Higher resolution 3-D models can treat these effects explicitly but this is not true of the low resolution model whose results are included in this report. The models included in this report are probably adequate for determining gross properties of chemical species such as the atmospheric lifetimes. They are of more limited use in determining the detailed temporal and spatial evolution of the species.

A different set of problems confront the 2-D and 3-D models when they are used to determine the lifetimes of species mainly destroyed in the troposphere by reaction with OH. The difficulty associated with resolving the spatial scales preclude the calculation of the detailed distribution of OH. However, for species whose lifetimes are of order one to two years, the mixing ratio of the species is sufficiently well-mixed in the troposphere that the model simulated OH distribution may produce a meaningful lifetime. The standard approach is to use the calculated lifetime of CH_3CCl_3 to calibrate the model results. We will discuss this in more detail in this chapter.

We discuss in Section 5.2 the definition of atmospheric lifetime in the context of model results. Section 5.3 summarizes the model results which show relatively large differences among the model predictions. The results from a model intercomparison are discussed in Section 5.4. The discussion is based on a number of model simulations designed to isolate the effects of model-calculated/model-adopted transport and local removal rates on

calculated lifetimes. Section 5.5 concentrates on validation of model calculated lifetimes of species that are removed in the stratosphere and suggests how stratospheric observations can be used to calculate the lifetimes of some of these species. The lifetimes of the HCFCs and HFCs that depend on tropospheric OH for removal are discussed in Section 5.6.

5.2 Derivation of Atmospheric Lifetimes in Modeling Studies

5.2.1 Definitions of lifetimes

The atmospheric abundance of a trace gas which is released at the earth's surface and removed by photochemical reactions in the atmosphere is governed by the equation

$$\frac{dB(t)}{dt} = E(t) - \int LndV \qquad (1)$$

where B(t) is the burden defined by $\int n(x,y,z,t)dV$; n(x,y,z,t) is the local number density, $E(t) = \int E(x,y,z=0,t)dxdy$ is the emission rate at the surface; the *in situ* removal rate is given by Ln where L(x,y,z,t) is the loss frequency; t is the time coordinate; dV=dxdydz; x, y,z are the Cartesian coordinates along the longitudinal, latitudinal and vertical directions respectively. The loss frequency could be generalized to include wash-out and deposition at the ground. In this chapter, we will limit our discussion to *in situ* photochemical removal. However, the role of ocean removal will be discussed in Section 5.6 in conjunction with CH_3CCl_3 and the HCFC species.

Equation (1) can be written in the form

$$\frac{dB(t)}{dt} = E(t) - \frac{B(t)}{\tau(t)} \qquad (2)$$

where τ is the instantaneous lifetime defined by

$$\tau(t) = \frac{B(t)}{\int LndV} \qquad (3)$$

For trace gases with lifetimes of a few years or longer, it is more appropriate to look at the annual averaged version of the equation

$$\frac{d<B>(T)}{dT} = <E>(T) - \frac{<B>(T)}{<\tau>(T)} \qquad (4)$$

and

$$<\tau>(T) = \frac{<B>(T)}{<\int LndV>(T)} \qquad (5)$$

where < > indicates annual averaging, and the parameter T represents time variations in the interannual time scale.

Simulating the state of atmosphere in models requires the use of appropriate boundary conditions. The boundary values could be constant in time to simulate a steady-state or time-dependent condition to simulate the actual evolution of the atmosphere. As part of the model results, L and n for any particular species are computed and equation (5) is used to calculate <τ>(T). If a time-dependent boundary condition is used in the calculation, this lifetime is referred to as the transient lifetime (<τ_{tran}>). It could be different from the steady state lifetime as it depends on the emission history of the gas and the changes in the chemical composition of the atmosphere.

A steady state lifetime ($<\tau_{steady}>$) can be defined as the lifetime computed from equation (5) where n is the steady state distribution calculated assuming E is constant in time and L is calculated assuming fixed (time invariant) boundary conditions for all the trace gases. The steady state lifetime is independent of the choice of initial conditions and the detailed time response of the model.

Finally, it is often convenient to define the local lifetime by

$$\tau_{local} = \frac{1}{L(x,y,z,t)} \tag{6}$$

This definition of a lifetime at a particular location is only mildly dependent on the transport used in the model. The dependence on transport results from two effects: (1) the dependence of the photolysis rate computed from the distribution of ozone which is partly controlled by transport, and (2) transport influences on constituents which can affect chemical removal rates (e.g. OH can be affected by H_2O, O_3, CO and CH_4, which are all affected by transport).

Comparison of equations (5) and (6) indicates that $1/<\tau>$ is the average of $1/\tau$ weighted by $n(x,y,z,t)$. Since the distribution of the concentration depends on both local removal and transport, the lifetime also depends on transport.

5.2.2 Empirical Determination of Lifetimes

For trace gases discussed in the previous chapters, there are certain simplifications :

(1)The mixing in the troposphere is sufficiently rapid that trace gases with lifetimes longer than two years will be uniformly mixed in the vertical direction in the troposphere.

(2)The mixing ratio profile is expected to decrease with height in the stratosphere since there are no *in situ* sources. In this case, at least 90% of the burden resides in the troposphere.

The above two conditions imply that the atmospheric burden is proportional to the surface concentration, f_{surf}. Equation (4) can be used to derive $<\tau>(T)$ from the time series of observed surface concentrations and known emission rates using statistical techniques without referring to specific details about L and n (see Chapter 3). However, the lifetime can also be computed from the distributions of L and n determined either from observations or model computation (Johnston *et al.*, 1979). In this chapter we will restrict the discussion to determination of lifetime by calculating L and n.

5.2.3 Uncertainties and Validation of L and n

It is necessary to discuss the uncertainties in the calculated L and n and how they may be validated against observations. For the purpose of validating the model-calculated lifetimes, one should concentrate on comparisons of L and n in regions where the product Ln contributes to the bulk of the integrated removal rate. It is more convenient for the discussion if we separate the trace gases into two groups: the TR (tropospheric removal) species whose lifetimes are determined by removal in the troposphere and the SR (stratospheric removal) species whose lifetimes are determined by removal in the stratosphere. For both type of compounds considered in this report, their mixing ratios are approximately constant with altitude in the troposphere and decrease with increasing altitude in the stratosphere. The TR and SR species have different removal processes. The SR species are removed mainly by UV photolysis. The photolysis rates of these species decrease rapidly with decreasing altitude because of absorption of solar UV by O_2 and O_3 in the atmosphere. The product Ln attains its maximum in the stratosphere. As a result, the integrated removal is dominated by removal in the stratosphere. The removal of the TR species is dominated by reaction with OH. Since the concentration of OH in the stratosphere increases only slowly with altitude, the removal remains dominated by tropospheric processes within 30° of the equator. The two classes of species require different data and methods for validating the model-calculated lifetimes.

For the SR species, the model-calculated lifetime is sensitive to the spatial distribution of both L and n in the stratosphere. Validation of model-calculated lifetimes would require comparison of both L and n in the stratosphere. Several components that enter into the model calculation of photolysis rates contribute to the model uncertainties. The unattenuated solar flux is uncertain and varies as a function of wavelength with cyclical solar activity. The solar flux at a particular location in the atmosphere is determined by attenuation of the solar flux by absorption of O_2 and

O_3. The optical depth due to absorption by O_2 and O_3 is uncertain at any location in the atmosphere. Finally, uncertainties in the absorption cross-section of the species will also translate into uncertainties for the calculated photolysis rate. The spatial distribution of n depends on both the transport circulation and its local photochemical lifetime (τ_{local}). Both the strength of the circulation (vertical and horizontal winds) and the magnitude of the eddy diffusion (vertical and horizontal) are uncertain. The model transport can be tested to a certain extent by comparing model computed distributions of N_2O and the CFCs with observations. However, this is complicated by the uncertainties both in the emissions and in the removal rates of these gases. An alternative is to use a photochemically inert tracer such as the radioactive tracer ^{14}C which is produced from galactic cosmic rays and nuclear explosions. The uncertainties in L and n will be discussed in Section 5.4 in the context of the model intercomparison. Comparison with observations will be discussed in Section 5.5.

Even for TR (tropospheric removal) species with lifetimes as short as 1 year, the mixing ratio is nearly constant in the troposphere for steady state. Thus validation of lifetime mostly depends on comparison of L, which in most cases depend on the reaction with OH. There are large uncertainties associated with model calculated OH (see Chapter 5, WMO, 1992). The short lifetime of OH implies that it will have large spatial and temporal variabilities as the local concentration is sensitive to the variations of NO_x, O_3, CO and non-methane hydrocarbons. The spatial scales of these variabilities are much smaller than the scale resolved by the models. Since few measurements of tropospheric OH exist, the distribution of the hydroxyl radical calculated by models is calibrated by comparison to measurements of a particular species that is removed by OH. Species used in this comparison must satisfy the following conditions :

1) the magnitude, spatial and temporal distribution of its sources must be well known;
2) fairly continuous measurements must exist at different locations;
3) the main removal mechanism of the species must be reaction with OH and other removal rates must be well known;
4) the rate constant for the reaction with OH is well-known .

Up to the present, only two species have been used in the above context: ^{14}CO (see Volz *et al.*,1981; Derwent and Volz-Thomas, 1990), and CH_3CCl_3 (see Prinn *et al.*, 1987, 1992; Spivakovsky *et al.*, 1990). In practice, the use of CH_3CCl_3 is preferred because the sources can be better quantified although there is some uncertainty in the absolute calibration of the CH_3CCl_3 data. We will discuss this in more detail in Section 5.6.

5.3 Model Calculated Lifetimes

Current estimates indicate that there is a delay of about 2.5 years in transporting material from the troposphere to the stratosphere (see Chapter 8, WMO, 1992). For an SR species whose burden is increasing with time, the concentration in the stratospheric sink region is systematically smaller than would be obtained at steady state, when the emission is balanced by stratospheric removal. Under these conditions, the transient lifetime of the SR species is somewhat longer than the lifetime at steady state. Both steady state and transient lifetimes computed by the models are discussed below.

5.3.1 Steady-state Lifetimes

Seven modeling groups, AER, GSFC, LLNL, MIT, MPI, MRI, and WASH participated in an intercomparison of computed steady-state lifetimes. The acronyms for the modeling groups are given in Table 5.1. The model results discussed in this chapter are mostly from two-dimensional (2-D) zonal-mean models designed to compute the zonal-mean (averaged over longitudes) concentrations of the species as functions of altitude and latitude. The results from a 3-D model (Golombek and Prinn, 1986, 1989) are also included in the discussion.

Steady-state lifetimes were calculated for CFC-11($CFCl_3$), CFC-12(CF_2Cl_2), CFC-113 ($C_2F_3Cl_3$), CFC-114 ($C_2F_4Cl_2$), CFC-115 (C_2F_5Cl), carbon tetrachloride (CCl_4), H-1211 ($CBrClF_2$), H-1301 ($CBrF_3$), N_2O, HCFC-22 (CHF_2Cl), CH_3CCl_3, methyl chloride (CH_3Cl) and methyl bromide (CH_3Br). Note that the six CFCs ($CFCl_3$, CF_2Cl_2, $C_2F_3Cl_3$, CFC-13, CFC-114, CFC-115) and CCl_4, H-1301 and N_2O are SR species removed mainly by UV photolysis while CHF_2Cl , CH_3CCl_3, CH_3Cl and CH_3Br are TR species removed mainly by reaction with OH

in the troposphere. H-1211 is removed by photolysis at visible wavelengths so that the bulk of the removal also occurs in the troposphere. The model lifetimes given in Table 5.2 are calculated using fixed mixing ratio boundary conditions for the major source gas constituents as defined for the 1990 steady state atmosphere (WMO, 1992). The boundary condition used for each of the species is included in Table 5.5 for reference. The range of the lifetimes from the 2-D models is better presented in Table 5.3, where the shortest and longest calculated lifetimes for each species are given as well as the ratio of the longest to the shortest.

***Table 5.2** Steady-state lifetimes from models (in years)*

Constituent	AER	GSFC	LLNL	MIT *	MPI	MRI	WASH
$CFCl_3$	48.9	53.6	53.1	42	40	45.7	60.8
CF_2Cl_2	104.	102	104	107	107	100	123
$C_2F_3Cl_3$	89.0	90.5	84.9	79	76	84.9	95.7
CFC-114	181	225	199				
CFC-115	414	553	520				
CCl_4	40.0	40.6	48.4	30		37.8	53.5
N_2O	121	134	121	124	129	120	139
$CBrClF_2$	20.1	16.1	18.6		9.3	28.2	
$CBrF_3$	68.6	62.8	65.7		58	65.5	
CHF_2Cl	16.5	16.8	13.5	15.8	11.2	26.0	
CH_3CCl_3	6.0	6.0	5.0	5.75	4.3	9.1	
CH_3Cl	1.7	1.54	1.23				
CH_3Br	1.6	1.55	1.22				

* MIT did not use the recommended boundary conditions in the calculations

***Table 5.3** Range of steady-state lifetimes from the 2-D models*

Constituent	Range of lifetimes (years)	High/Low
$CFCl_3$	40-60.8	1.52
CF_2Cl_2	100-123	1.23
$C_2F_3Cl_3$	76-95.7	1.26
CCl_4	30-53.5	1.78
N_2O	120-139	1.16
$CBrClF_2$	9.3-28.2	3.03
$CBrF_3$	58-68.6	1.18
CHF_2Cl	11.2-26.0	2.32
CH_3CCl_3	4.3-9.1	2.12

The SR species ($CFCl_3$, CF_2Cl_2, $C_2F_3Cl_3$, CFC-114, CFC-115, CCl_4, $CBrF_3$, and N_2O) have variations among these five modeling groups of less than about 80%. A correlation between the lifetime of N_2O and the lifetime of the four CFCs calculated from the same model is expected, in that a model that has a relatively weak vertical transport will compute longer lifetimes for N_2O and the CFCs because τ_{local} is shortest in the upper stratosphere. With this lifetime correlation in mind, we have tried to normalize the differences among the models for four of the CFCs by dividing the CFC lifetime by the N_2O lifetime for each model. These results are presented in Table 5.4. The high value for each ratio is divided by the low value and given in the last column of Table 5.4. Since these processes are not linear, some of the differences remain and are particularly noticeable for the species with shorter lifetimes. The differences among the models have now been reduced to about 65% or less. The remaining differences among the models are probably related to the different approaches used in computing the constituent photolysis rates as well as the transport used in the different regions of the atmosphere.

Interpretation of the model range for the TR species is less straightforward as it is more difficult to isolate the parameters that control the model calculated OH in the model for comparison.

***Table 5.4:** Ratio of CFC lifetimes to the N_2O lifetime of each model.*

Constituent	AER	GSFC	LLNL	MIT	MPI	MRI	WASH	High/Low
$CFCl_3$	0.404	0.401	0.439	0.339	0.310	0.382	0.437	1.42
CF_2Cl_2	0.859	0.761	0.860	0.863	0.830	0.839	0.885	1.16
$C_2F_3Cl_3$	0.735	0.676	0.702	0.637	0.589	0.710	0.688	1.25
CCl_4	0.330	0.303	0.400	0.242		0.316	0.385	1.65

5.3.2 Transient Lifetimes

As discussed in Section 5.2, the model-calculated lifetimes can change depending on emission history and the state of the atmosphere. Four modeling groups (AER, GSFC, MRI, and WASH) computed the time-dependent behavior of several CFCs, HCFCs, and halons using the time-dependent boundary conditions presented in Table 5.5. Note the difference between the 1990 time dependent boundary condition and the 1990 steady state boundary condition. The steady state boundary condition is chosen so that the stratospheric distributions calculated in the 1990 steady state atmosphere will approximate those of the time-dependent 1990 atmosphere.

***Table 5.5** Boundary conditions for time-dependent model simulations.*

	1990 SS	1970	1975	1980	1985	1990
CFC-11	253 pptv	60	115	173	222	284
CFC-12	434 pptv	120	205	295	382	485
CFC-113	44 pptv	2	6	15	30	57
CFC-114	7 pptv	1	2	4	5	8
CFC-115	5 pptv	0	1	2	4	6
CCl_4	103 pptv	85	90	95	100	106
HCFC-22	92 pptv	10	27	54	80	104
CH_3CCl_3	145 pptv	40	70	100	130	159
H-1301	2.6 pptv	.1	.2	.6	1.7	3.5
H-1211	2.0 pptv	.1	.2	.5	1.5	2.5
CH_3Cl	600 pptv	600	600	600	600	600
CH_3Br	15 pptv	15	15	15	15	15
N_2O	308 ppbv	295	298	302	306	310
CH_4	1685 ppbv	1420	1495	1570	1650	1715
CO_2	350 ppmv	325	331	337	345	354

Note: CFC-113 and CFC-114 boundary conditions are not the same as what is discussed in Chapter 1.

The time-dependencies of the model calculated lifetimes for CFC-11, CFC-12, and CFC-113 are given in Figures 5.1 (a-c). The models produced lifetime output at 1970, 1975, 1980, 1985, and 1990. The GSFC and WASH models' simulations started in 1960, whereas the AER and MRI models' simulations started in 1970. Therefore, the results for the period before 1975 for AER and MRI are not shown because the results are strongly dependent on the initial conditions chosen to initialize the model.

The model computations clearly show a decrease in the CFC lifetimes from 1975 to 1990. Primary causes include: 1) As a larger portion of the CFC constituent is transported to higher altitudes, its loss rate grows, and its lifetime decreases; and, to a lesser extent, 2) the higher altitude O_3 depletions from the CFC input permit a larger influx of radiation to lower altitudes which provides a larger photodissociative loss for the CFC constituent.

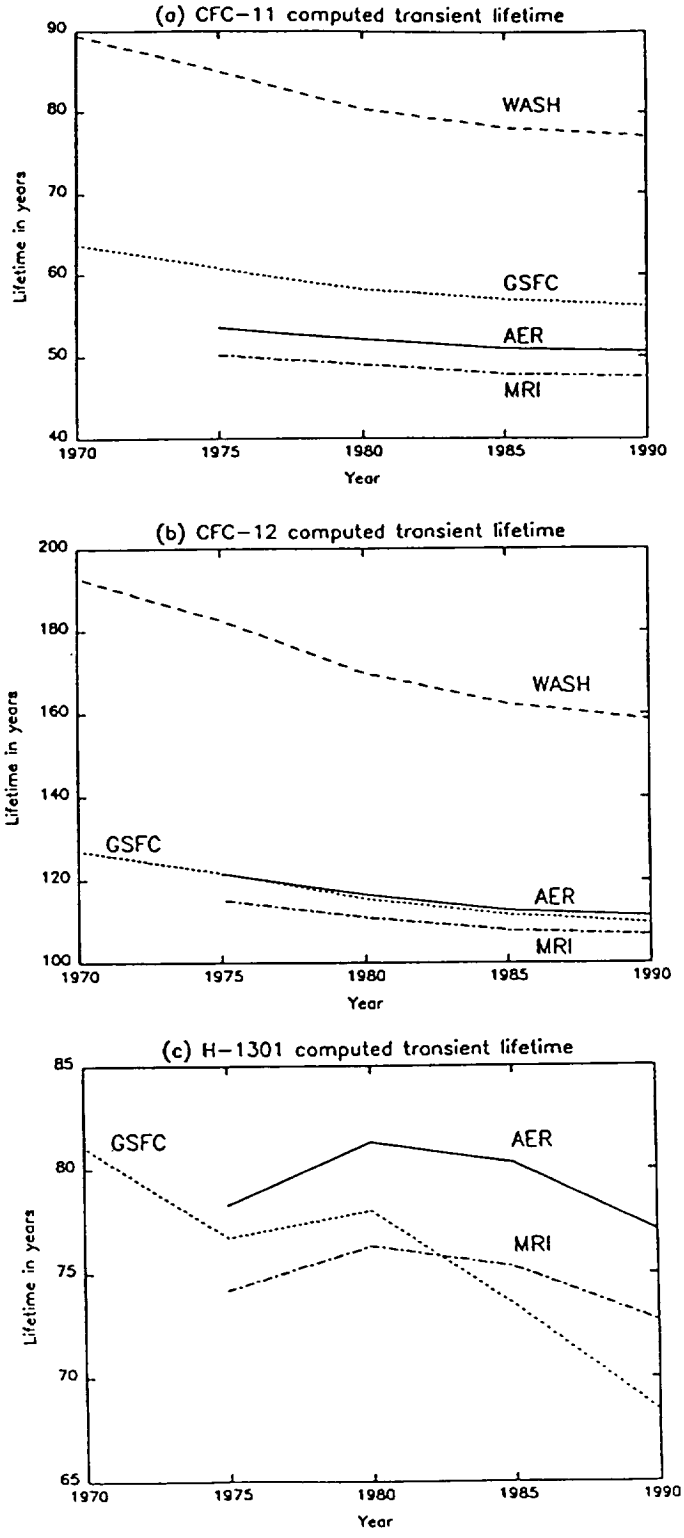

Figure 5.1 Transient lifetimes from 1970-1990 for (a) CFC-11, (b) CFC-12, and (c) H-1301 using input time-dependent boundary conditions from Table 5.5. The results are from AER, GSFC, MRI, and WASH 2-D models.

We compared the transient lifetime to the steady-state lifetime (given in Table 5.2) in Figure 5.2 and Table 5.6. The transient lifetimes are all divided by the corresponding steady-state lifetime. The AER, GSFC, and MRI model results seem to cluster together and show that by 1990 the transient model-computed lifetime is within about 5%, 8%, and 13% of the steady-state lifetime for CFC-11, CFC-12, and H-1301, respectively. The WASH model results, on the other hand, suggest that the transient model-computed lifetime is only within about 27% and 29% of the steady-state lifetime for CFC-11 and CFC-12, respectively. The 3-D results from MIT lie between the two groups. These results are very dependent on the atmospheric transport and mixing incorporated in the individual models.

In the calculation shown for the WASH model, the values for the vertical diffusion coefficient (K_{ZZ}) are taken to be zero. Additional simulations performed using the WASH model indicated that with a non-zero K_{ZZ}, the transient lifetime is within 10% of the steady state lifetime. Unfortunately, the appropriate magnitude of this diffusive mixing term is uncertain.

***Table 5.6** Ratio of transient lifetime for 1990 to steady state lifetime*

Constituent	AER	GSFC	MIT	MRI	WASH
$CFCl_3$	1.03	1.05	1.1	1.04	1.27
CF_2Cl_2	1.07	1.08	1.16	1.06	1.29
$C_2F_3Cl_3$	1.14	1.18	1.39	1.12	1.46
CCl_4	1.01	1.01	1.0	1.01	1.21
N_2O	1.01	1.01	1.07	1.01	1.14
$CBrClF_2$	1.01	1.02		1.05	
$CBrF_3$	1.13	1.14		1.11	
CHF_2Cl	1.01	1.00		1.02	
CH_3CCl_3	1.01	1.00		1.01	

5.3.3 Comparison of Calculated and Inferred Lifetimes

The CFC-11 lifetimes calculated here with the photochemical models are reasonably consistent with those inferred from the concentration and emission data. Using the emissions inventories of Chapter 2 and as the inventory-based inference procedure (which assumes the standard ALE-GAGE calibration factor be correct) a steady-state lifetime for CFC-11 of 50 (+24, -13) years was obtained (see Table 3.5.1). Using the MPI Met model and the standard calibration, a lifetime of 55.6 years was obtained. Using the GISS model, the optimal fit to the data was obtained with a calibration adjustment factor (0.8847), far outside that suggested by experimental measurements; the corresponding lifetime was 39.08 years (see Table 3.3.2). Introduction and a small calibration drift or a decrease in the assumed unreported emissions led to an increase in the lifetime to as much as 56 years (range 50 - 65 years).

These values are very similar to the range of 40 - 60.8 years obtained by the modeling groups. The lifetime of 60.8 years obtained by the Washington group stands apart from those of the other groups. As will be seen below (see Section 5.3.2), the transport in this model differs appreciably from that in the other models. In particular, the assumption of a zero eddy diffusion coefficient has led to vertical transport rates in the lower stratosphere which are lower than in the other models. If one therefore does not consider the Washington result, the range of model-calculated lifetimes is 40 - 53.6 years, which essentially overlaps nearly all the inferred lifetimes (and does so completely once error bars are considered). With the exception of the Washington model, there is little difference between the calculated steady-state and transient lifetimes for 1990 for CFC-11 (see Table 5.6). This suggests that the comparison of the inferred lifetimes with the steady-state ones calculated with the atmospheric models is a reasonable comparison.

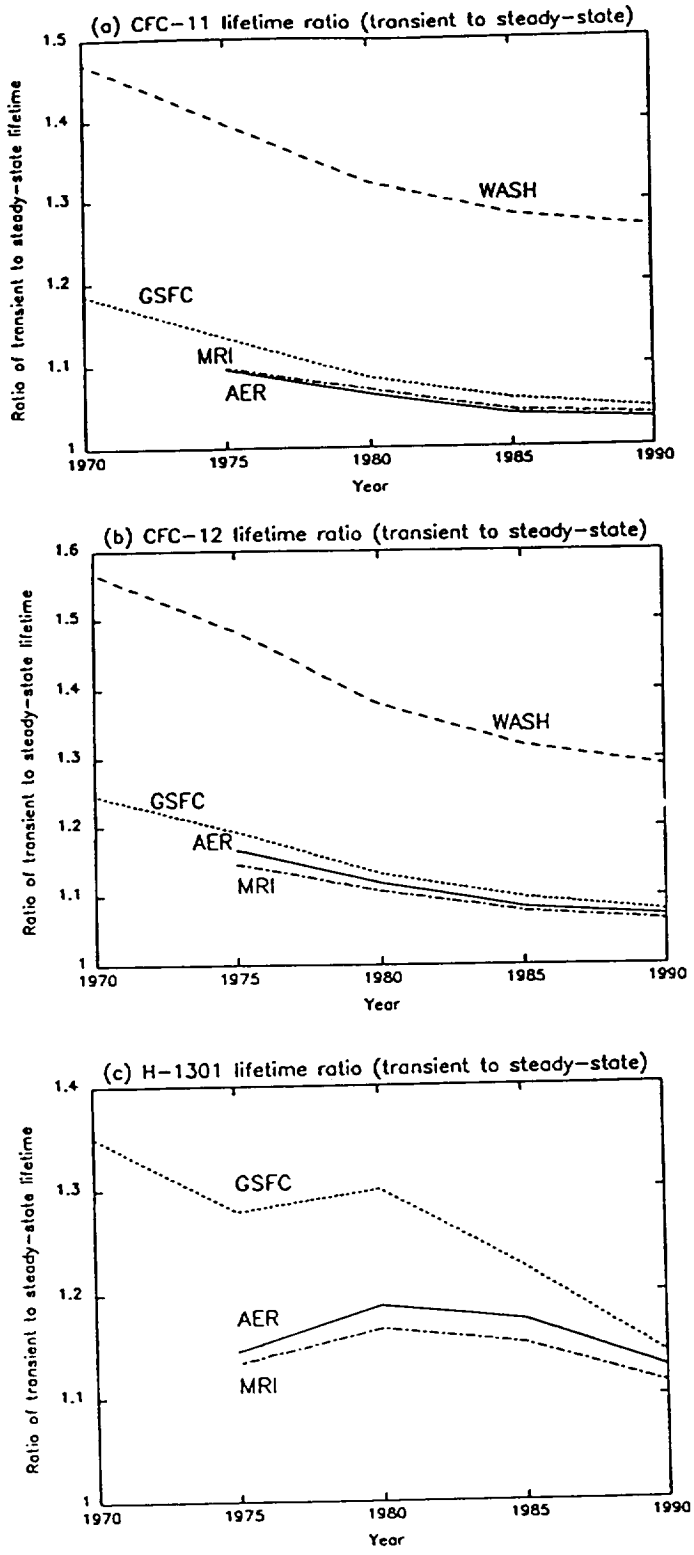

Figure 5.2 Ratio of transient to steady-state lifetime for (a) CFC-11, (b) CFC-12, and (c) H-1301 for the 2-D models AER, GSFC, MRI, and WASH.

For CH_3CCl_3 it is not really proper to do such a detailed comparison. The model OH fields are typically adjusted to provide for a CH_3CCl_3 lifetime consistent with that observed in the ALE-GAGE Network. The inferred lifetimes were approximately 6.4 (GISS model) and 5.7 years (ALE-GAGE analysis) assuming the ALE-GAGE calibration adjustment factor to be correct. If the calibration factor were closer to the lowest values suggested by experimental measurements, lifetimes of 3.5 - 4.0 years are needed to explain the observations.

With the exception of the MRI model value of 9.1 years, all the atmospheric models have obtained lifetimes for CH_3CCl_3 consistent with the inferred values. The MRI model obtained high lifetimes for other species with tropospheric destruction (HCFC-22, Halon-1211), as well as with CH_3CCl_3, suggesting that it differed from the others in its treatment of the troposphere.

5.4 Quantifying the Uncertainties: Model Intercomparison

The differences in the lifetimes calculated by the models can be attributed to differences in both photochemistry and transport. We have undertaken an intercomparison of the photolysis rates and various aspects of the transport with several modeling groups. The five modeling groups which participated in these intercomparisons are AER, GSFC, MPI, MRI and WASH. With the exception of WASH, the circulation in each model is determined by prescribed heating rates and temperatures and is repeated year after year. In the WASH model, the circulation for a four year period is derived from four years of temperature observations. In some of the simulations, (see experiment W), the four year cycle is repeated every four years.

In previous studies, comparison among models has been difficult because 2-D models used different grids in their model formulations. The Upper Atmosphere Data Pilot (UADP) at NASA Langley was established to handle model output using uniform formats. Each modeling group was responsible for interpolating its model result to the standard UADP grid. The UADP is responsible for maintaining the data archive as well as providing graphics from the database.

5.4.1 Photolysis Rates

Photolysis rate constants were intercompared for the constituents $CFCl_3$, CF_2Cl_2, $C_2F_3Cl_3$, CHF_2Cl, CCl_4, CH_3CCl_3, $CBrClF_2$, $CBrF_3$, and N_2O. AER, GSFC, MPI, and WASH models participated and computed the photolysis rate constants in a 24-hour average period for the March 15th condition. The modeling groups used their own standard background atmosphere, computed ozone, and assumed solar flux in computing the rate constants.

Photolysis rate constants are computed from the following relation:

$$J_i(z,\phi) = \int F(\lambda,z,\phi)*\sigma_i(\lambda,T_{local})d\lambda$$

where $J_i(z,\phi)$ is the photolysis rate (in sec^{-1}) for the i^{th} species at altitude z and latitude ϕ; $F(\lambda,z,\phi)$ is the solar flux (in # photons/cm^2/sec/nm) at wavelength λ; and σ_i is the photodissociation cross section (in cm^2) for the i^{th} species at wavelength λ. The cross-section can be a function of local temperature and thus of altitude z and latitude ϕ. The integral goes over all wavelengths for which σ_i is non-zero. $F(\lambda,z,\phi)$ is computed from the unattenuated solar flux after accounting for the absorption by other constituents in the atmosphere above altitude z (primarily O_2 and O_3) and from the impact of Rayleigh (molecular) scattering which is especially important at large solar zenith angles (see, *e.g.*, Luther and Gelinas, 1976; Isaksen *et al.*, 1977; Madronich, 1987).

We compare the photolysis rate (J coefficient) for CFC-11 in Figures 5.3 at the Equator. Figure 5.3a shows J(CFC-11) with a log scale and Figure 5.3b shows J(CFC-11) with a linear scale. The calculations show variations in J(CFC-11) of at least 5 orders of magnitude over the altitude range 12-60 km. The J(CFC-11)'s from AER and GSFC are within 20% of each other (see Figure 5.3b) near 60 km. It is interesting to note that the J(CFC-11)'s from any one model are not consistently larger or smaller than the rest of the model results at all altitudes. For example, the AER J(CFC-11)'s from about 12 km to 34 km are the largest of the models, but at and above 42 km the AER J(CFC-11)'s are the second to the smallest.

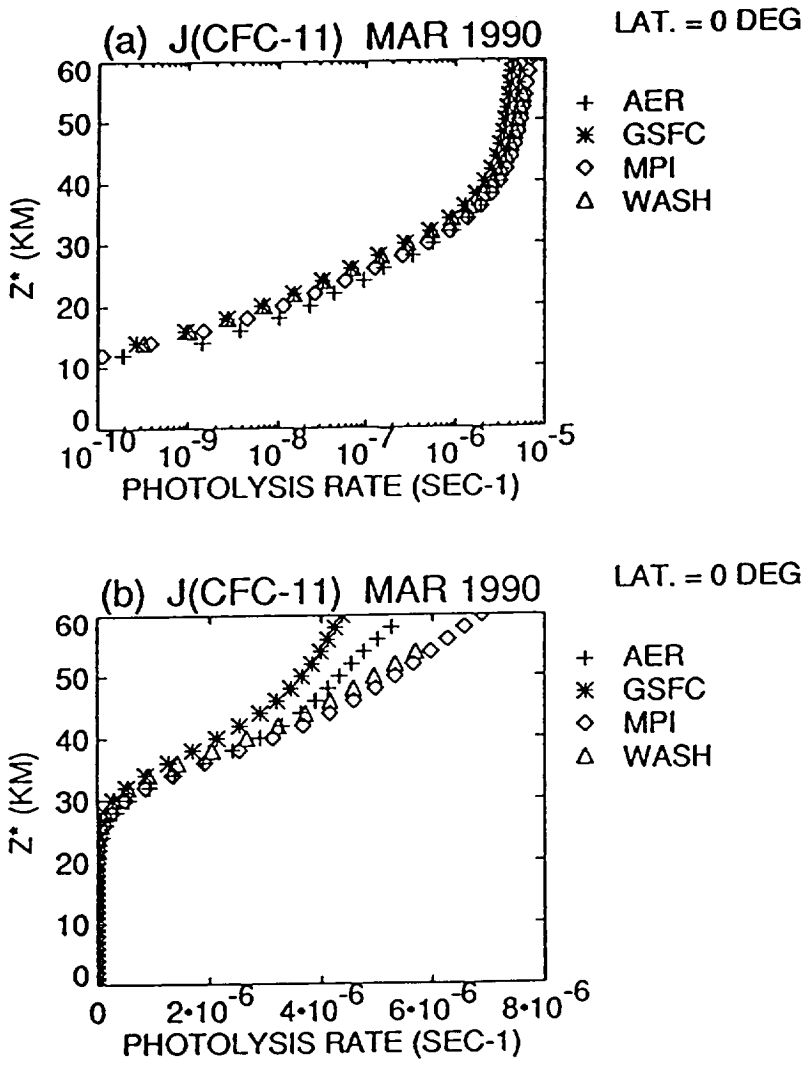

Figure 5.3 Diurnal (24-hour) average photolysis rate for CFC-11 for the Equator on March 15, 1990 for 2-D models AER, GSFC, MPI, and WASH. The altitude dependence of the photolysis rate (J-coefficient) is given in both a logarithm (a) and a linear (b) scale.

The photolysis rate constants calculated for other constituents can vary up to a factor of almost two at 60 km. For example, J(CFC-12) varies from about 7 to 9.5 x 10^{-7} sec^{-1} (see Figure 5.4a); J(CFC-113) varies from about 9.2 to 15 x 10^{-7} sec^{-1} (see Figure 5.4b); and J(H1301) varies from about 2.5 to 4.7 x 10^{-6} sec^{-1} (see Figure 5.4c). These variances reflect the differences in: 1) wavelength resolutions among the models and how the unattenuated solar flux and photolysis cross-sections are interpolated into the adopted wavelength band; 2) the radiative transfer treatment; and 3) the dependence of cross-section on local temperature which may be different in separate models.

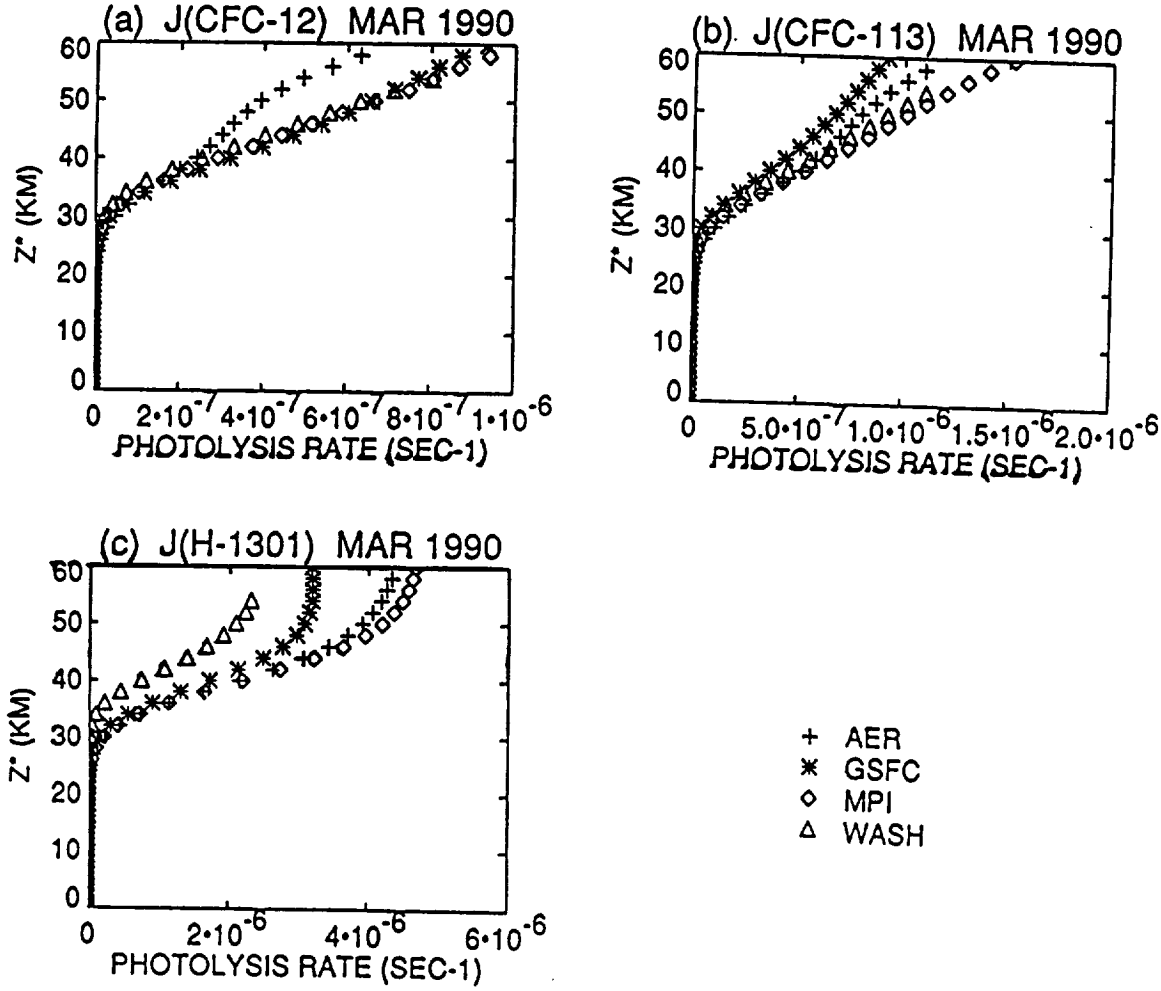

Figure 5.4 Diurnal (24-hour) average photolysis rate for CFC-12, CFC-113, and H-1301 for the Equator on March 15, 1990 for 2-D models AER, GSFC, MPI, and WASH.

5.4.2 Transport of Idealized Tracers

The transport, or movement of constituents vertically and horizontally, can strongly influence the atmospheric lifetime (Jackman *et al.*, 1988; Ko *et al.*, 1991). More rapid transport of CFC molecules from the ground through the tropopause to the stratosphere, where photolysis is faster, can significantly decrease the CFC lifetime. Conversely, slower transport of CFC molecules from the ground to the stratosphere can significantly extend the CFC lifetime. Modeling groups AER, GSFC, MRI, and WASH took part in these studies of model transport.

Three numerical simulations of idealized tracers with prescribed removal frequencies were proposed to help identify model differences. The simplest tracer was Y which had no atmospheric loss, thus corresponding to a tracer with infinite lifetime. The spread of the tracer from near the surface to the stratosphere is examined to see how rapidly the material is transported in the first five years after the material is released. The tracers in the other two experiments (X and W) were assigned a removal frequency that will give them a lifetime of about 100 years. In the X experiment, a continuous surface emission was specified. The steady state lifetimes from the models were compared. In the W experiment, the emission was stopped after 20 years and the transient lifetimes were compared.

Y Experiment

All the mass of Y was confined initially to below 700 mb. At steady state, the mixing ratio of Y is expected to be uniform as a function of latitude and height, with an abundance of approximately 1 ppmv.

Model 2-D distributions of Y were recorded on January 1 and July 1 of each year for a five year simulation. For ease of comparison of the four models, we show results at the Equator for July 1 for each of the five years in Figures 5.5 (a-e). By year 5, all models show a relatively uniform mixing ratio, with the mixing ratio in the lower stratosphere approaching at least 60% of the surface mixing ratio. A large difference in transport among the models is observed early in the simulation. Both the AER and MRI models transport Y vertically much more rapidly in the first six months of the model simulation than do the GSFC and WASH models (see Figure 5.5a). Gradually, over the course of four years, the GSFC model transport of Y catches up to the MRI model's transport of Y in the upper stratosphere (see Figure 5.5e). The transport of Y by the WASH model shows the smallest upward motion for all years (see Figure 5.5). As pointed out in the discussion of transient lifetime, this difference can be attributed to the fact that K_{zz} is zero in the WASH simulation.

W Experiment

The second experiment is for a tracer W which has a removal rate similar to that of N_2O. The adopted loss frequency, L(p), is given below as a function of pressure, p,:

$$L(p) = 0 \text{ for } p > 100 \text{ mbar}$$
$$L(p) = 3.E\text{-}6/p^2 \text{ s}^{-1} \text{ for } 1 \text{ mbar} < p < 100 \text{ mbar}$$
$$L(p) = 3.E\text{-}6 \text{ s}^{-1} \text{ for } p < 1 \text{ mbar}$$

All model simulations of W were for forty years. Tracer W has changing emissions from years 1 to 40, as represented in Figure 5.6. The temporal evolution of tracer W's flux input at the ground is similar to those of the regulated CFCs. The W flux input increases over a course of 10 years, stays constant for a decade, and then is decreased to zero flux by year 30. By the end of the 40 years, the calculated W burden is within 20% of the total input of W. The calculated tracer W lifetimes were appreciably different, however, and are shown in Figure 5.7. GSFC has a smaller computed lifetime than AER, which is reflected in a difference in burden which appears after 15 years of the simulations. The difference remains relatively small (several percent) over the course of the simulation. The WASH model finds a lifetime for tracer W which is considerably smaller than that of the AER or GSFC models.

The time-dependent behavior and tracer W distribution at the Equator is shown in Figures 5.8 (a-c) for selected altitudes. At 20 km, both the AER and GSFC models have a similar transport of W while the WASH model shows

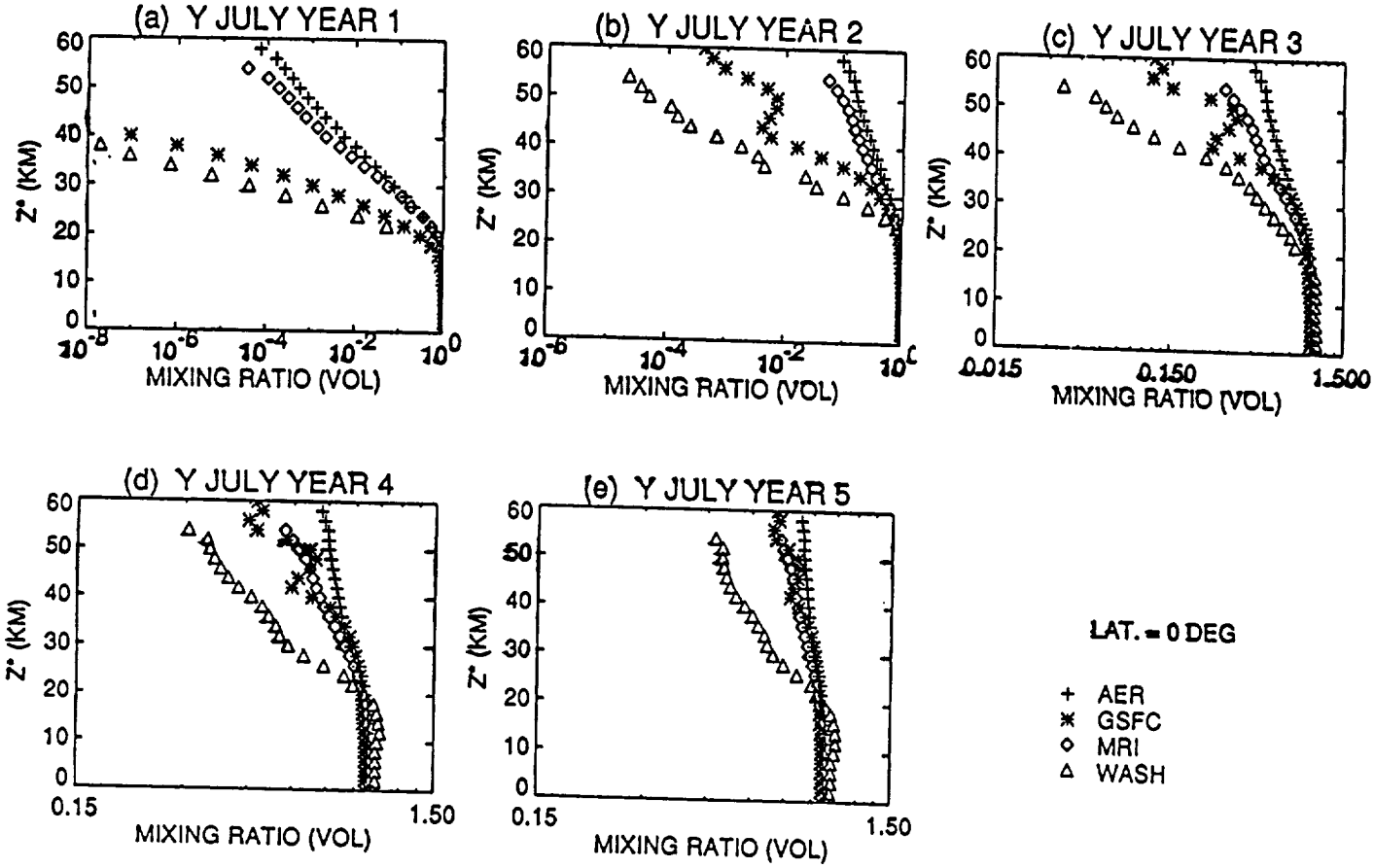

Figure 5.5 Tracer Y at the Equator on July 1 from 2-D models AER, GSFC, MRI, and WASH for years (a) 1, (b) 2, (c) 3, (d) 4, and (e) 5.

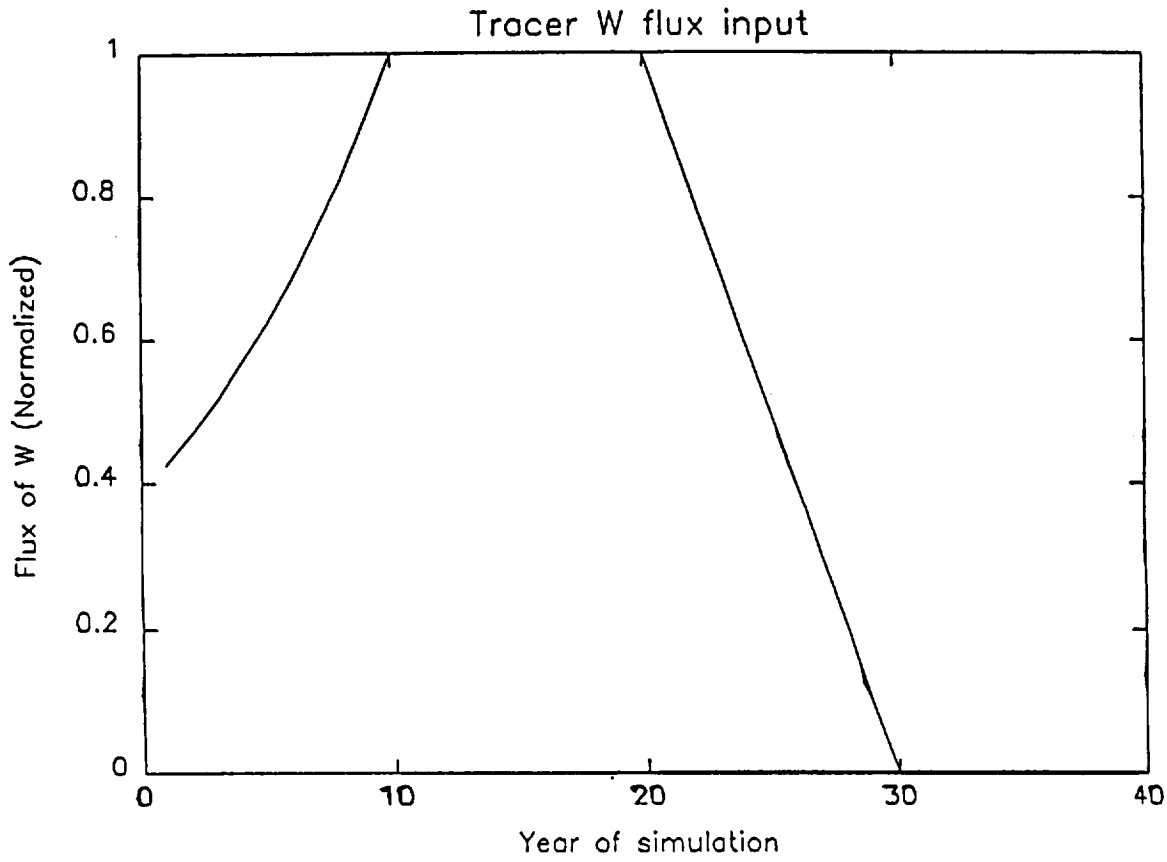

Figure 5.6 Normalized tracer W flux input at the ground as a function of time.

some variation in the overall level of tracer W predicted (see Figure 5.8a). The four year cycle observed in the WASH lifetime data is a consequence of the imposed transport computation. The WASH model has National Meteorological Center (NMC) temperatures for 1979, 1980, 1981, and 1982 used in the formulation of the winds and diffusion. The WASH model results, while not comprehensive in illustrating the interannual changes expected in the atmosphere, do illustrate a transport-driven variation that may be expected. Variations in W of about 15% are possible at 20 and 30 km with variations of nearly a factor of two possible at 40 km (see Figure 5.8). The GSFC model gives a transport of W at 30 km and the Equator which is similar to the upper limit to that obtained in the WASH model. This transport is faster than that in the AER model and the three other years in the four-year cycle associated with the WASH model (see Figure 5.8b). The AER model at 40 km is clearly transporting the most W and the WASH model transporting the least W (see Figure 5.8c).

The calculated tracer W lifetimes (shown in Figure 5.7) illustrate behavior consistent with each individual model's transport. For the WASH model, this four-year cycle of transport is repeated throughout the model simulation and results in 10% changes in the lifetime. The GSFC model, with the fastest transport consistently to 30 km, shows the shortest lifetimes, whereas the WASH model, with the slowest transport for most years at 30 km, shows the longest lifetimes.

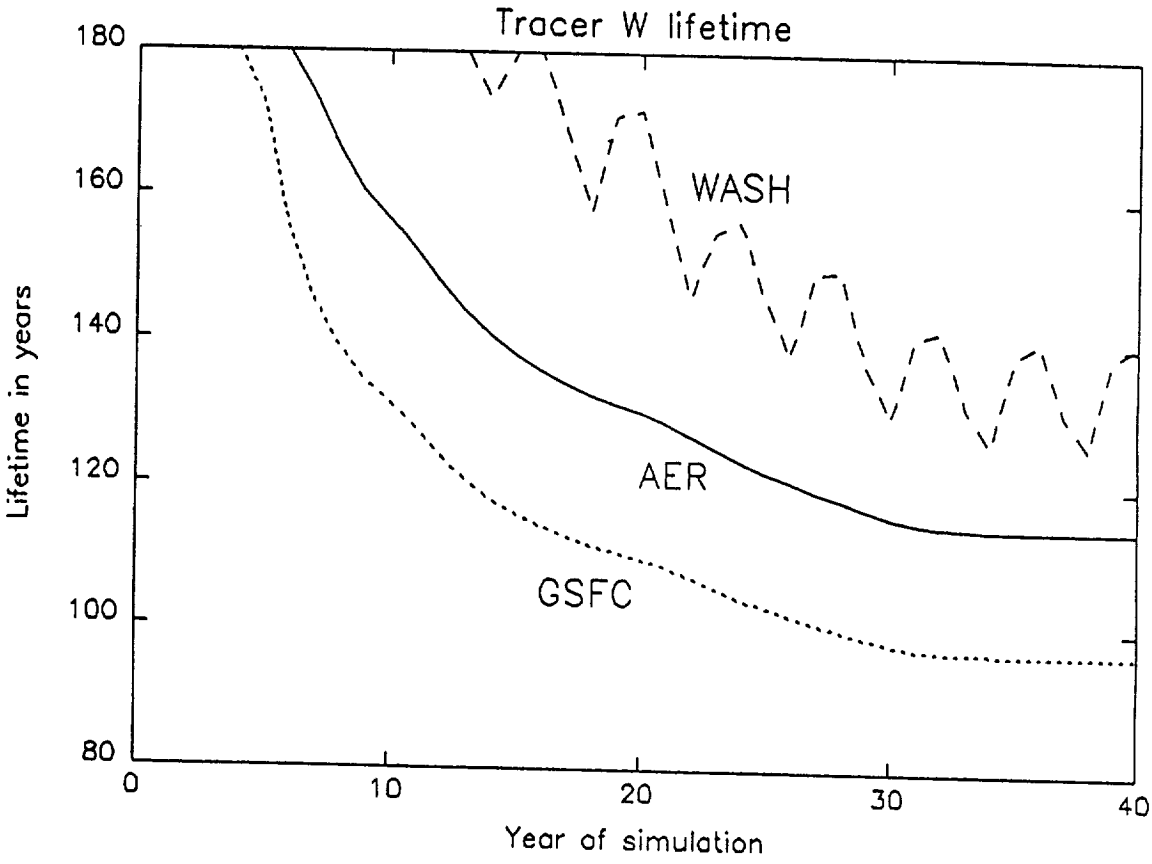

Figure 5.7 Tracer W lifetime as a function of time for AER, GSFC, and WASH 2-D models.

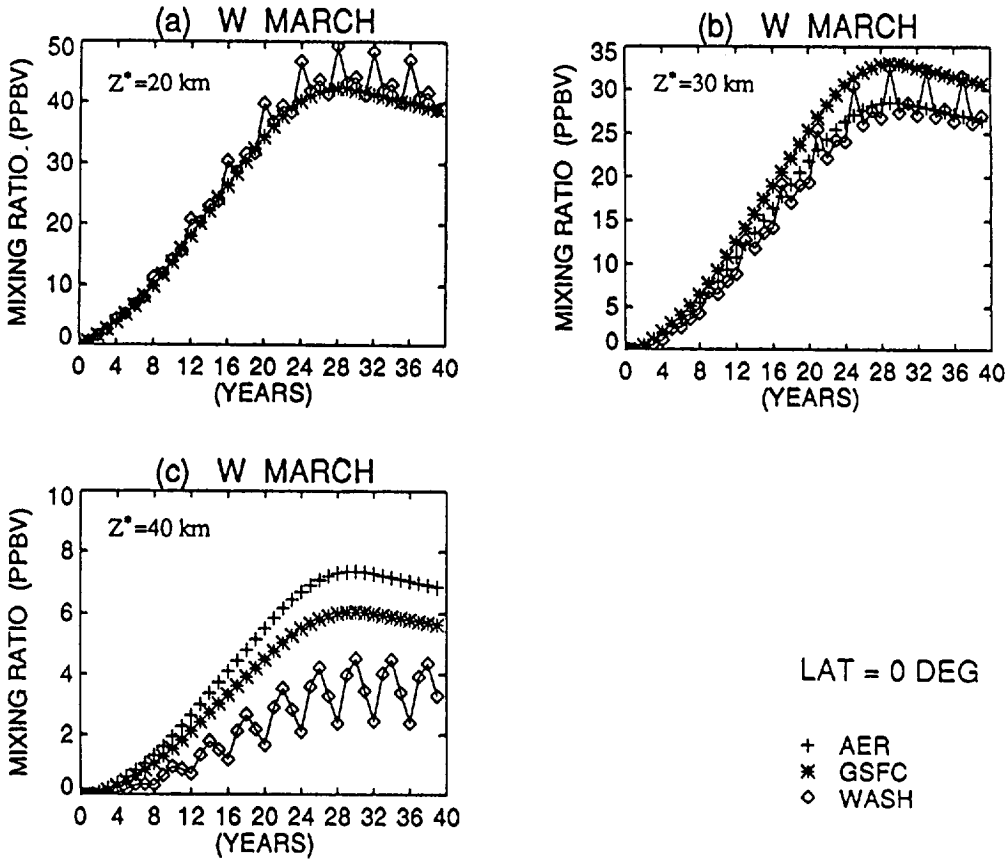

Figure 5.8 Tracer W in March at the Equator form 2-D models AER, GSFC, and WASH for altitudes (a) 20km, (b) 30km, and (c) 40km.

X Experiment

We now examine the steady-state behavior of the tracer in the models in the X simulation. Tracer X has a fixed mixing ratio at 1 ppbv at the ground and a loss frequency, L(p), equivalent to that of tracer W, given above. The four modeling groups AER, GSFC, MRI, and WASH took part in this simulation. Each model was run to steady-state and the March 15th, June 15th, September 15th, and December 15th distributions, as well as the lifetimes, were taken from the final year of the simulation.

The computed lifetime of X from AER was 116.0 years, from GSFC was 98.1 years, and from WASH was 127.9 years. No lifetime is available from MRI. These X lifetime results are compatible with those shown in Figure 5.10 for W. Both the AER and GSFC models computed lifetimes for the last year of the W simulation are less than those computed for X, even though the imposed loss rate is the same for both W and X. The lifetimes for W at year 40 from AER and GSFC were 114.2 and 96.8 years, respectively. The WASH model computed lifetime for W cannot be easily compared with the steady-state lifetime of X because the WASH model simulation of W used four different years of transport whereas the WASH model simulation of X used the same one year of transport throughout.

The relationship between a steady-state lifetime (X) and a transient lifetime (W) after several years of zero mass injection of W is important, because tracer W is very similar to the CFCs and halons which are currently being phased-out. After emissions of these gases have gone to zero, the burdens of the gases will be expected to e-fold in approximately their computed steady-state lifetime.

The percentage differences between each of the three other modeling groups and AER are illustrated in Figures 5.9 (a-c) for the March 15th distributions. These results are similar to those obtained from analyses of tracer W. The GSFC model transports slightly less X than predicted by the AER model in the troposphere. Between about 15 and 35-45 km (depending on latitude), the GSFC model transports more X than the AER model, whereas above 35-45 km (depending on latitude) the AER model transports more X than does the GSFC model (see Figure 5.9a).

The MRI and AER models have reasonably similar transport with large differences (greater than 50%) between the models only apparent at the highest altitudes and at northern polar latitudes (see Figure 5.9b). The WASH model generally transports more X to middle and high latitudes in the 25 to 40 km than does the AER model, whereas the AER model transports more X above about 30 km in the tropics and above 45 km at all latitudes than does the WASH model (see Figure 5.9c).

The tracer experiments discussed above show that the differences in the efficiency of transport among the models are variable with altitudes. Thus, a specific model may calculate a longer or shorter lifetime for a species with prescribed removal, depending on the spatial distribution of the imposed local removal frequency.

5.5. Problems Associated with Comparison of Model Results with Stratospheric Measurements

In this section, we discuss how to use observations to test the model calculated removal frequencies, concentrations and lifetimes for the SR species.

5.5.1 Stratospheric J-rates

One could, in principle, use *in situ* measurements of solar UV flux to validate the solar flux, $F(\lambda,z,\phi)$, used in calculating the J-rates. However, small uncertainties in the O_2 and O_3 columns can translate into large changes in the J-rate for large optical depth. Even if the overhead O_2 and O_3 columns are known accurately, direct comparison of model-calculated attenuated flux and observed flux is still subject to uncertainties, e.g. whether the unattenuated flux assumed in the model is the same as the actual flux at time of the observation and how the O_2 Schumann-Runge band absorption is treated. Further coordination with the measurement program such as those reported in Herman and Mentall (1982), Anderson and Hall (1986), and Schurath *et al. (1987)* is needed for future validation.

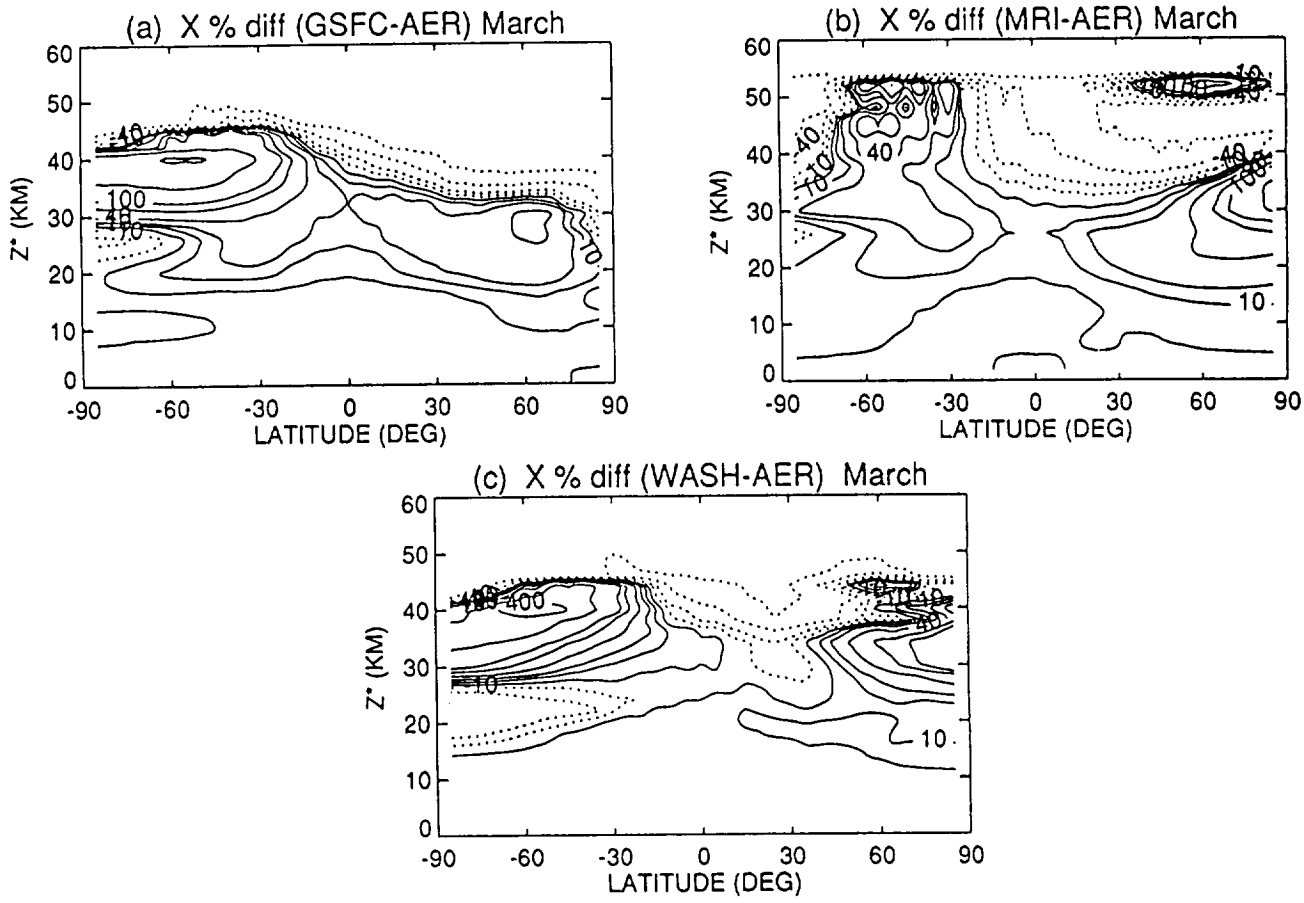

Figure 5.9 Tracer X percentage difference in March between models (a) GSFC and AER; (b) MRI and AER; and (c) WASH and AER.

5.5.2 Species Concentration in the Lower Stratosphere

A standard check of the model-simulated concentration has been a comparison of the calculated vertical profile with available observations. The spatial and temporal coverage was limited to balloon profiles and to data taken mainly either at the tropics or at 40°N. When only 1-D model results were available, there was a preference to compare the 1-D model calculated profiles with the data at mid-latitudes, as it was felt that the conditions at mid-latitudes may be more representative of the global averaged conditions than at the tropics. Ko and Sze (1982) pointed out that the global removal rate, $\int LndV$, obtained from average of the product Ln is larger than the product of globally averaged L and n because both n and L attain larger values at the tropics than mid-latitudes at the same pressure levels. The larger L in the 2-D models is related to the sun angle while the higher n is obtained because of the upwelling motion in the tropics resulting in the downward sloping of the isolines towards the pole. As a result, the model calculated lifetimes in 2-D models are shorter than 1-D model calculated lifetimes (see also Holton, 1986). Thus, a calculated profile representative of the global averaged profiles may not provide the best test for lifetime.

Figures 5.10(b) and 5.11(b) show mid-latitude balloon profiles and comparable calculated profiles from AER, GSFC, LLNL, MRI and WASH models for N_2O and CFC-11 respectively. The same group of model-calculated profiles in the tropics are shown without balloon data in Figures 5.10(a) and 5.11(a). There are substantial differences between the models but they all fall within the uncertainties of the balloon data. The differences in the simulated profiles contribute to the differences in computed lifetimes (see Table 5.2). Figure 5.12 shows the comparison of the observed N_2O balloon data with two versions of the AER model. The old model refers to results from Ko *et al.* (1984) with a calculated lifetime of 160 years while the new model results are from Ko *et al.* (1991) with a calculated lifetime of 120 years. Despite the difference in lifetime, results from both models can be considered to be consistent with observations. The work of Ko *et al.* (1991) showed that differences in the lower stratosphere translate almost directly into changes in lifetime of 20-30%. Thus, it is difficult to validate lifetimes to better than 30% by direct comparison with *in situ* data.

The measurement of N_2O from SAMS on Nimbus 7 provided the first global measurement of N_2O. However, the uncertainties in the middle stratosphere are quite large in the tropics. Figure 5.13 shows the comparison of the model-calculated N_2O distributions with the SAMS observations. The differences in the middle stratosphere are quite large. Furthermore, there are interannual variabilities in the data as well. Figure 5.14 shows the differences between the 1980 data and the 1979 data. The difference in the middle stratosphere would imply a difference in removal rate of about 15% if one uses the same photolysis rate in the calculation (see Ko *et al.*, 1991).

There is no clear answer to the question, "What is the correct transport for the atmosphere?" The utility of long-lived constituents such as N_2O and the CFCs in determining atmospheric transport is somewhat limited, since they are removed by photolysis in the stratosphere and the uncertainties in the model calculated photolysis rates tend to complicate the interpretation of the results. It may be possible to use inert tracers such as CF_4 and C_2F_6 however. An alternative tracer is ^{14}C, which is a radioactive tracer produced continuously in the background atmosphere by galactic cosmic rays and also produced by nuclear explosions. Carbon-14 has no photochemical loss and its half-life through loss by radioactive decay is very long (5730 years). The major loss of ^{14}C is at the surface. Thus, its stratospheric content is controlled by stratospheric-tropospheric exchange rate in the model. For a discussion of transport validation using ^{14}C data, see Johnston (1989), Shia *et al.* (1989), Jackman *et al.* (1991) and Kinnison *et al.* (1991).

5.5.3 Lifetimes

In addition to balloon data, there are data obtained from limited locations on a space platform (ATMOS) and a number of aircraft campaigns. In the case of balloon and aircraft campaigns, the information on vertical profiles is usually limited. However, several species are measured simultaneously in the same air-mass. The question arises whether such simultaneous measurements can help to validate the calculated lifetimes.

Large variability in the observed concentration at any location is expected because the concentration will fluctuate in response to the vertical and horizontal displacements of air during passage of meteorological disturbances. Thus, one can never be certain whether any particular measurement is representative of the climatological mean condition

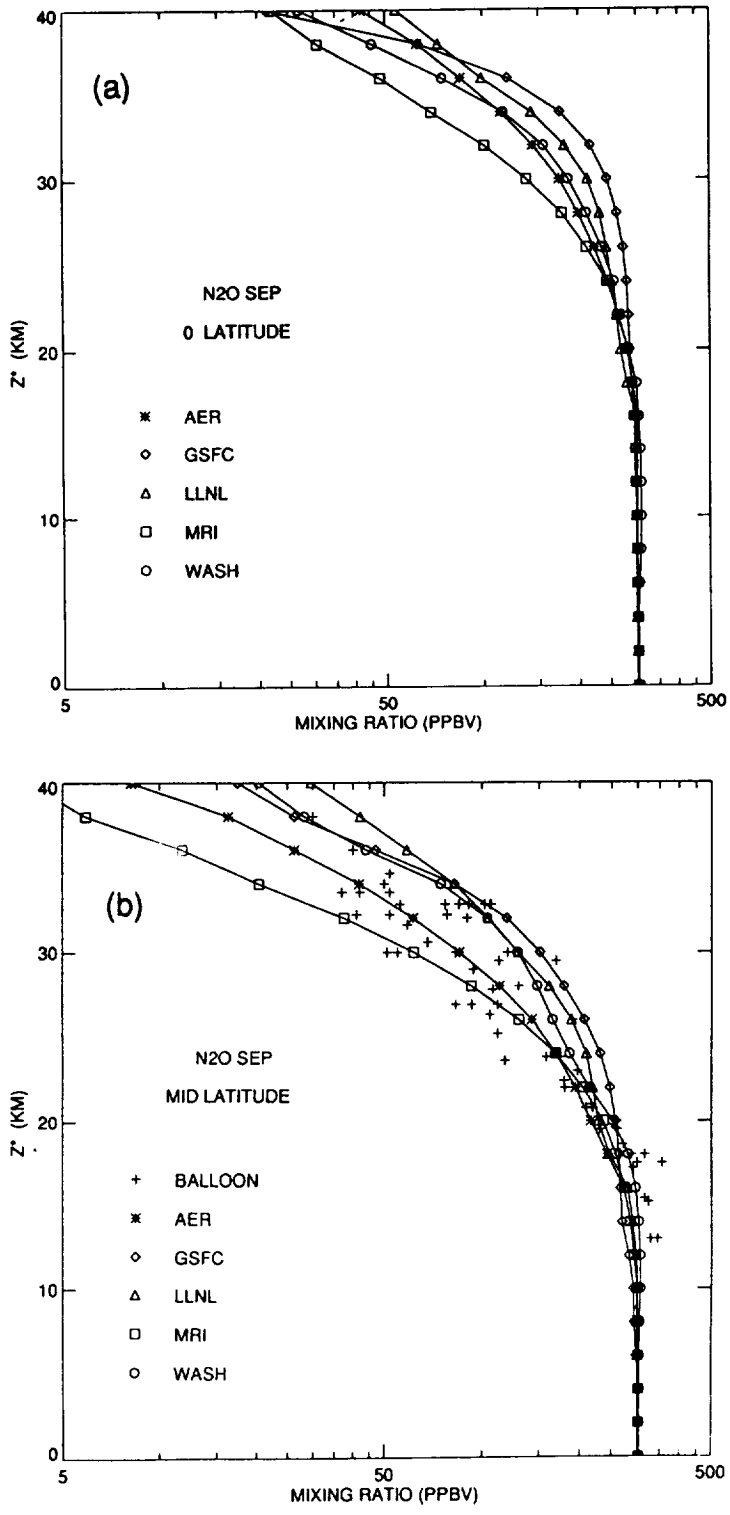

Figure 5.10 Comparison of model calculated vertical profiles of the mixing ratio of N_2O at (a) the equator and (b) 40°N for September condition. A sample of the balloon data is included for comparison.

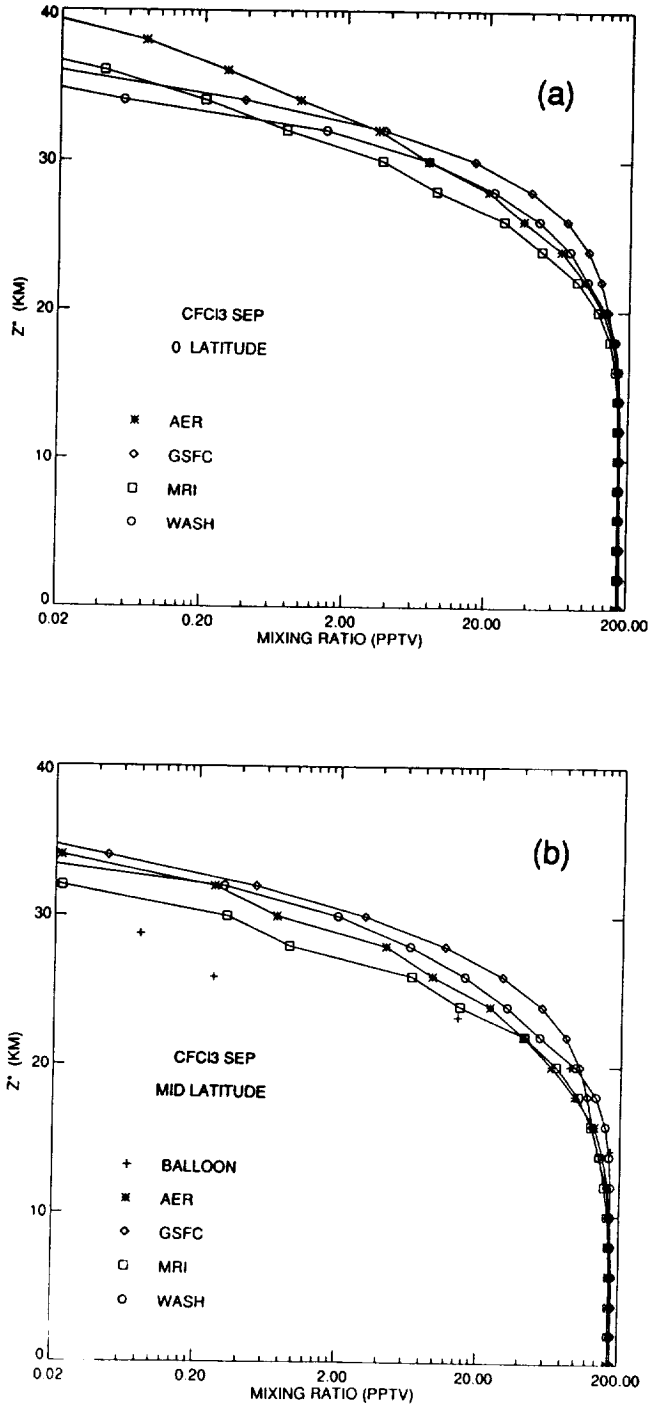

Figure 5.11 Comparison of model calculated vertical profiles of the mixing ratio of CFC-11 at (a) the equator and (b) 40°N for September condition. A sample of the balloon data is included for comparison.

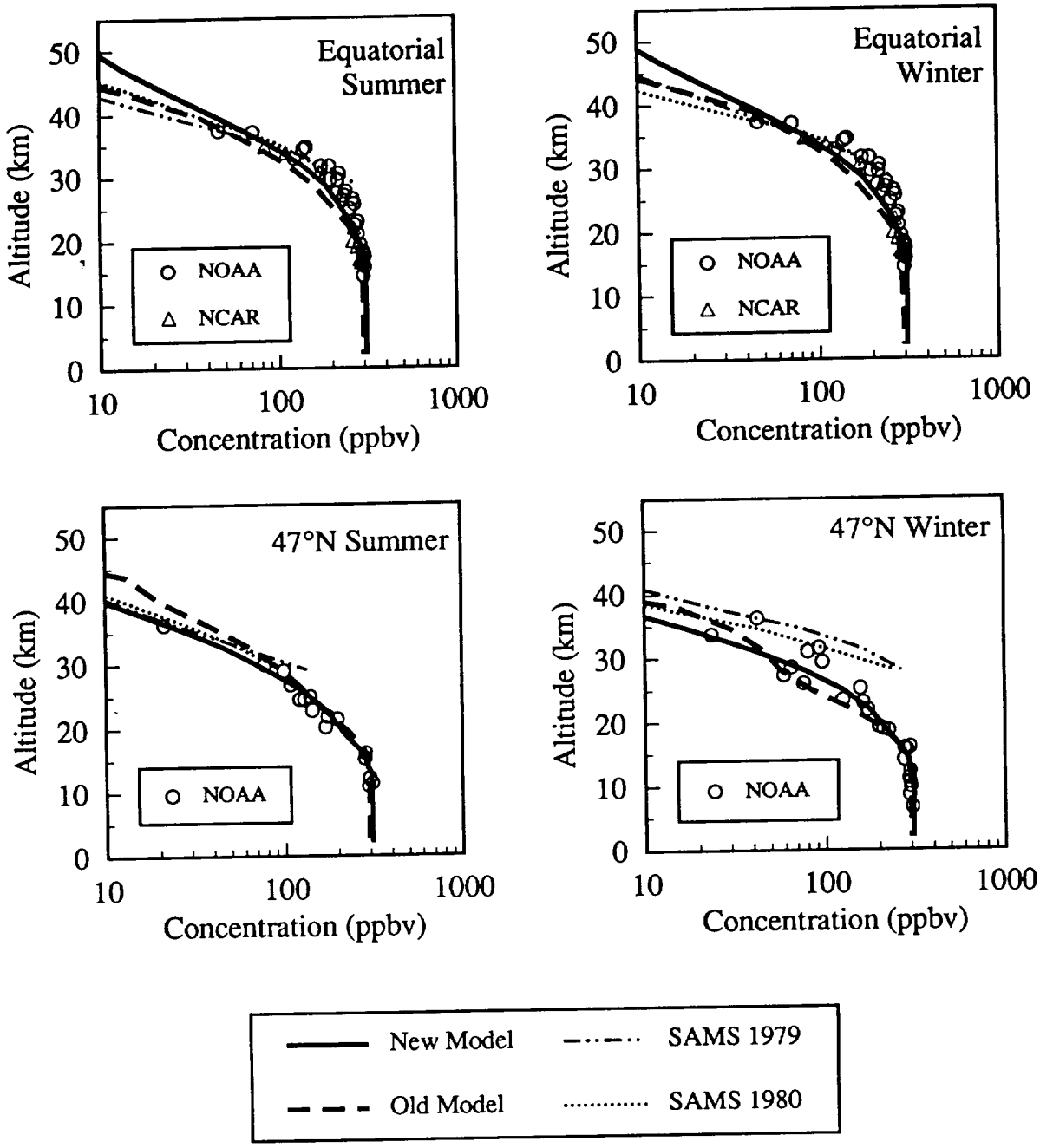

Figure 5.12 Comparison of the calculated vertical profiles of the mixing ratio of N_2O with balloon data from two AER models. The results labelled old model and new model are from Ko *et al* (1984) and Ko *et al* (1991) respectively. Note that the model calculated mixing ratio from the 1984 model is smaller than the observations at 25 km in the tropics while the agreement is better in the 1991 model. The differences in the model calculated profiles translate into a lifetime of difference of 160 versus 120 years.

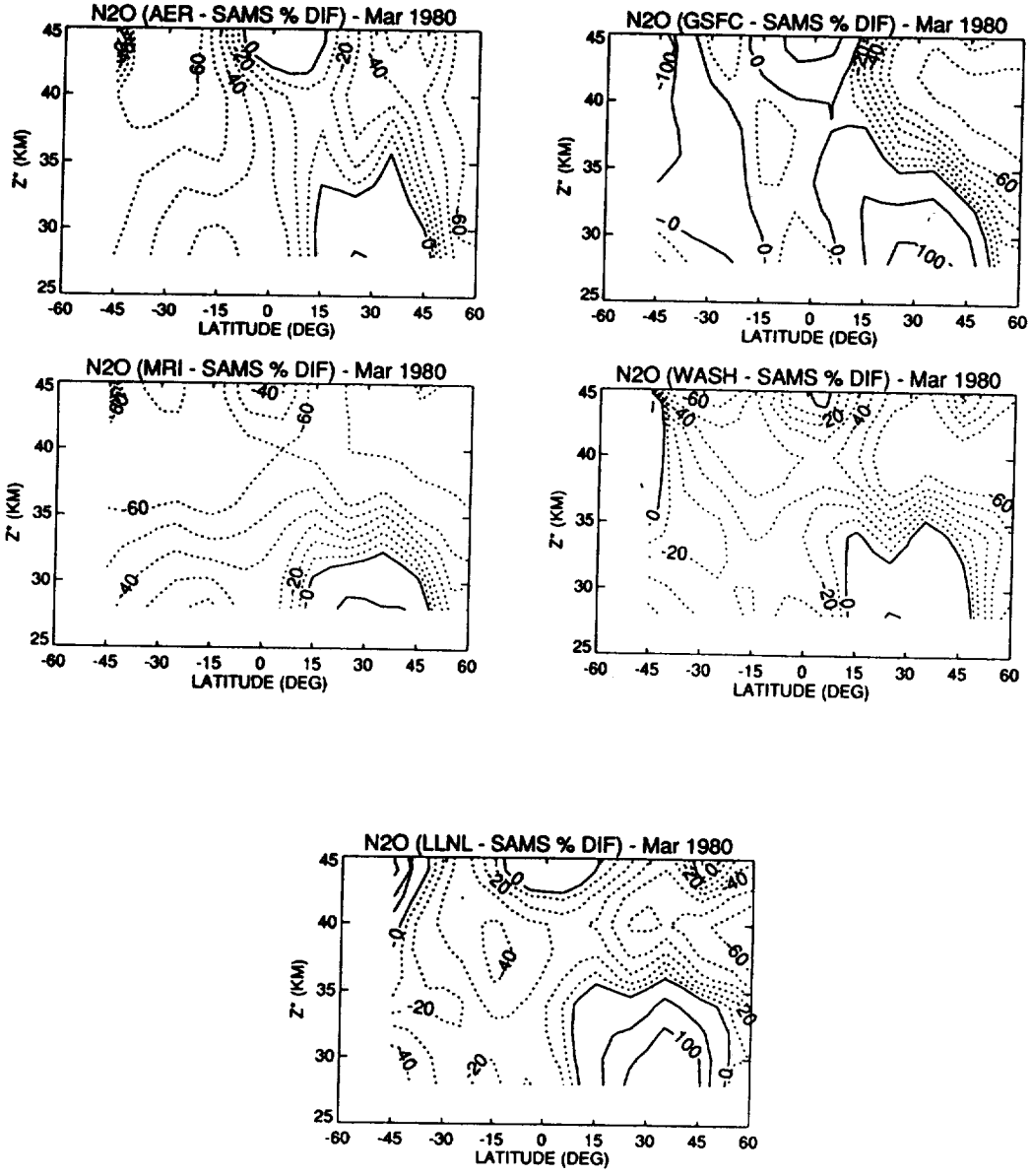

Figure 5.13 Comparison of model calculated mixing ratio of N_2O with SAMS observation for March of 1980. Plotted in each panel is the percentage differences of each model relative to the 1980 SAMS data.

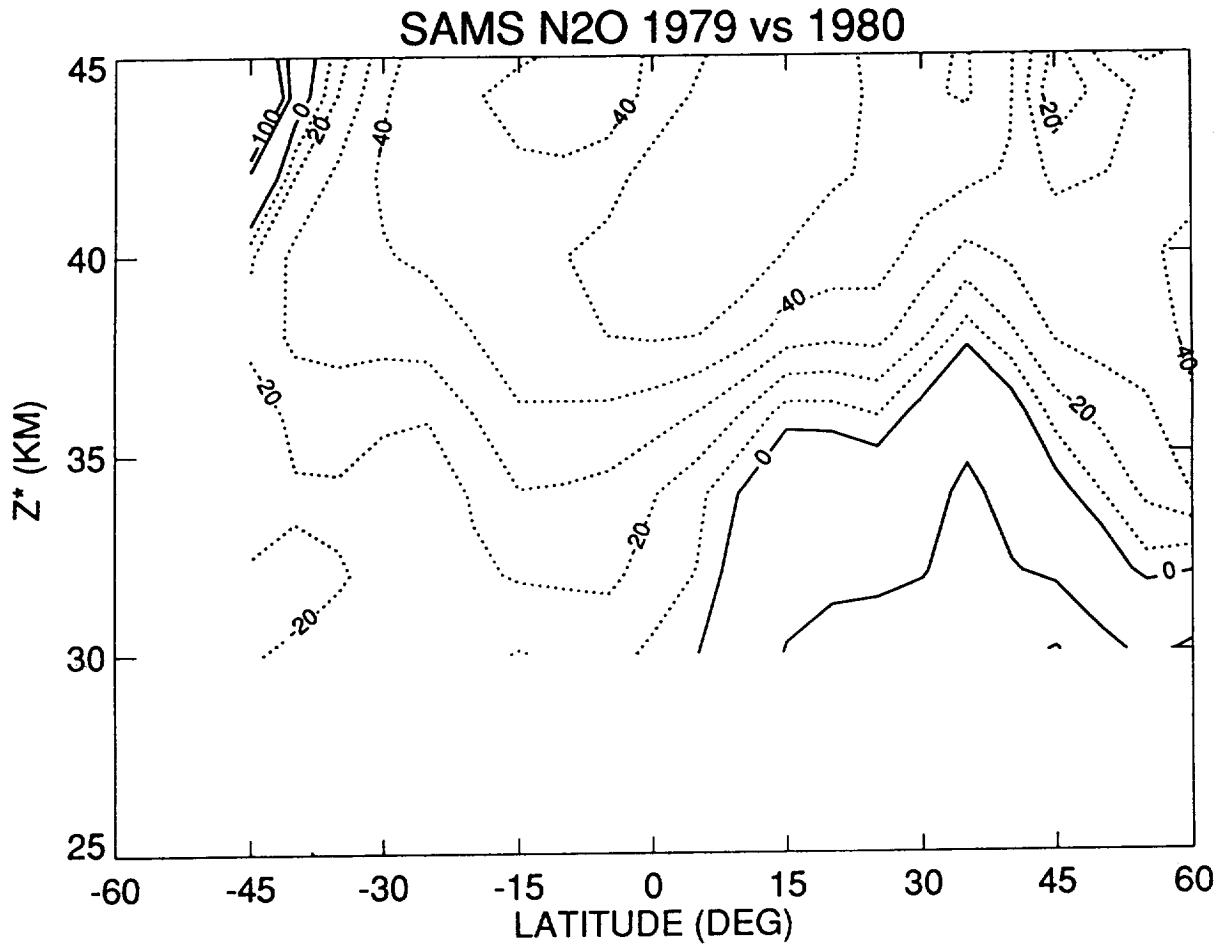

Figure 5.14 Percent difference of the 1979 SAMS observation of N_2O relative to the 1980 SAMS observation for March.

at that location. Recent studies (Schoeberl *et al*, 1989; Lait *et al*, 1990) showed that observations taken at different locations and times can be compared more readily if they are collated using potential temperature and potential vorticity instead of altitude and latitude. Hartmann *et al* (1989) pointed out that if one displays the observed species concentrations against the concentration of N_2O of the same air-mass in a correlation diagram, results from different locations show an almost linear correlation with N_2O.

The work of Plumb and Ko (1992) argued that the surfaces of constant mixing ratio of the species with sufficiently long lifetimes coincide with each other in the lower stratosphere. As a result, all measurements from the same mixing ratio surface will show up as a point in the correlation diagram (see Chapter 1). When a meteorological disturbance passes through, it will distort the mixing surface. However, the mixing ratios of the species on the surface are unchanged if their lifetimes are sufficiently long. In these cases, the points on the correlation diagram will show up as a compact curve. Plumb and Ko (1992) also showed that, for species that are in steady state, the local gradient at any point along the compact curve in the correlation diagram is related to the ratio of the integrated removal rates of the species above the common mixing ratio surface. One can then deduce a relative lifetime as follows

$$\tau'_y = \frac{\tau'_x}{N} = \frac{\tau'_x}{\frac{fx}{fy}\frac{dy}{dx}} \qquad (7)$$

where N is the normalized gradient, fx and fy are the mixing ratios and $\frac{dy}{dx}$ is the local gradient on the correlation diagram at point (fx,fy); τ' is the lifetime defined from equation (5) with the burden and removal rate calculated by integrating over the region above the common surface of constant mixing ratio. If the common mixing ratio surface is chosen so that the integrated removal rate above that surface is approximately equal to the global removal rate, then the mixing ratio is also approximately equal to the surface mixing ratio. In this case, τ' corresponds to the atmospheric lifetime. Thus, if one can find enough observations for two species to form a correlation diagram to obtain the gradient around such a mixing ratio surface, equation (7) provides a way to evaluate the ratio of the lifetimes. If the lifetime for one of the species is known, this will give the lifetime of the other species. Finally, it should be noted that the relative lifetime depends on dx/f_x and dy/f_y and is therefore independent of absolute calibrations.

If the species y is not in steady state, i.e. the concentration in the stratosphere is changing with time, τ'_x and τ'_y is related by

$$\frac{1}{\tau'_y} + \frac{1}{By}\frac{dFy}{dt} = \frac{N}{\tau'_x} \qquad (8)$$

where Fy is the burden of y above the mixing ratio surface, and By is the global burden. When $\frac{1}{\tau y'} << \frac{1}{By}\frac{dFy}{dt}$, equation (8) is not very useful for deriving τ'_y as small uncertainty in $\frac{1}{By}\frac{dFy}{dt}$ would lead to large error in τ'_y. For illustration purposes, we assume $\frac{dFy}{dt} = 0$ even though we know this is not true for the CFCs. For species with positive $\frac{dFy}{dt}$, ignoring the term will underestimate the lifetime.

Table 5.7 gives values for estimated lifetimes of several species from equation (7) using the gradients of the correlation diagrams in Chapter 1 (Table 1.3.1). We assume a range of 110 years to 168 years for the N_2O lifetime (Chapter 8, WMO, 1992) in the calculations. It should be noted that since we ignore the $\frac{dF}{dt}$ term in equation (8), the values should be considered as lower limits, in which case the experimental values point to a minimum lifetime for CFC-11 of 54 years (see Chapter 3).

Table 5.7 Estimated lifetimes τ' from stratospheric data with assumed lifetime for N_2O

Species	Normalized Gradient x10^3	Estimated lifetimes assuming N_2O lifetime is 110 years	Estimated lifetimes assuming N_2O lifetime is 168 years
CFC-11	2.1	54	82
CFC-12	1.3	84	130
CCl_4	2.0	56	85
CFC-113	1.6	70	110
CFC-114	1.0	110	170
CFC-115	0.40	280	420
CFC-13	0.36	310	470
H-1301	2.2	50	77
H-1211	3.1	35	54
CH_3CCl_3	3.5	31	48
CH_3Cl	2.6	4.2	64

Given the uncertainties associated with the derivation of the gradient, this method will not replace the methods discussed in Chapter 3. However, for species that have only a recent release history and whose lifetimes are sufficiently long, the above method may provide first estimates for lifetimes. Equation (7) can only provide an estimate of the lifetime due to stratospheric removal. This is why that for species such as CH_3Cl, CH_3CCl_3 and H-1211 that have tropospheric removal, the estimated τ' is significantly different from the model calculated atmospheric lifetime.

5.6 HCFC/HFC Lifetimes and OH

Given the difficulty in calculating and validating the model OH, an alternative is to use the lifetime of CH_3CCl_3 to derive an empirical scaling factor for the OH removal of each of the HCFCs in the troposphere.

5.6.1 Lifetime of CH_3CCl_3 as Proxy for Tropospheric OH

Analysis of methyl chloroform data from the ALE/GAGE experiment (Prinn *et al.*, 1987; 1992) determined a lifetime of 5.7 (+0.9, -0.7) years in the atmosphere. Some previous analyses have assumed that reaction with tropospheric OH is the only significant removal mechanism of CH_3CCl_3 and have therefore scaled the calculated lifetimes of the HCFCs by the lifetime of methyl chloroform. If other removal mechanisms are important, the value of the scaling factor deduced from the ALE/GAGE data would be decreased.

Two other removal mechanisms have been identified for CH_3CCl_3, photolysis in the stratosphere and removal by hydrolysis in the ocean. The total atmospheric lifetime τ_{atm} of CH_3CCl_3 is given by

$$\frac{1}{\tau_{OH}} + \frac{1}{\tau_{strat}} + \frac{1}{\tau_{ocean}} = \frac{1}{\tau_{atm}} \qquad (9)$$

where τ_{OH}, τ_{strat}, and τ_{hydr} denote the lifetimes for reaction with tropospheric OH, stratospheric removal, and ocean removal, respectively. Removal by photolysis in the stratosphere is well known and is estimated to correspond to a lifetime of 40-50 years. The lifetime for removal of methyl chloroform by processes in the oceans is more uncertain. Measurements of methyl chloroform concentrations in tropical ocean waters (Butler *et al.*, 1991) determined an under-saturation of about 12-15%. If this undersaturation were typical of the oceans on a global scale, these measurements would imply a lifetime of about 62 years for uptake of CH_3CCl_3 by the oceans (Butler *et al.*, 1991). At the same time, Wine and Chameides (AFEAS report, 1990) estimated a lifetime of about 40 years against hydrolysis in the oceans, with at least a factor of two uncertainty. Combined uncertainties in the derivation

of fluxes from saturation anomalies, and in the extrapolation of local measurements to the whole ocean, yield a fairly large range for ocean uptake (31-254 years).

Estimates and uncertainties for the different time constants in Equation (9) are given in Table 5.8. The total atmospheric time constant is derived from the ALE/GAGE data (Prinn *et al.*, 1992) and the estimated range reflects the statistical uncertainty in the data analysis. Averages and the estimated range for τ_{tot}, τ_{strat}, and τ_{ocean} are used in Equation (9) to estimate values and ranges for τ_{OH}.

***Table 5.8** Time constants and Uncertainties for Removal Processes of Methyl Chloroform*

	Lifetimes (years)	Estimated Range (years)
τ_{atm} (ALE-GAGE)	5.7	4.2-6.4
τ_{strat} (model results)	45	40-50
τ_{ocean} (Butler *et al.*, 1991)	62	31-254
τ_{OH} (derived from eq (9))	7.3	4.7-10.1

Estimates for HCFC/HFC Lifetimes due to OH

Estimated values and uncertainties in average tropospheric OH have been combined with model calculations of tropospheric and stratospheric removal to produce estimated lifetimes and ranges for different HCFC/HFCs. These are listed in Table 5.9. The first entry in the table summarizes the information on CH_3CCl_3. The values for τ_{atm} and its range are taken from Chapter 3; the values for τ_{strat} are from the AER 2-D model; the values for τ_{OH} and its range is taken from Table 5.8.

***Table 5.9** Estimated Lifetimes*

Compound	τ_{OH} (yrs.)	range for τ_{OH} (years)	τ_{strat} (years.)	τ_{atm} (years)	range for τ_{atm} (years)
CH_3CCl_3	7.3	4.7-10	45	5.7	4.2-6.4*
HCFC-22	16	10-22	210	15	9.7-20
HCFC-123	1.6	1.1-2.3	47	1.6	1.0-2.2
HCFC-124	6.7	4.3-9.3	130	6.4	4.2-8.7
HCFC-141b	12	7.8-17	76	10	7.1-14
HCFC-142b	23	15-32	220	21	14-28
HCFC-225ca	3.0	1.9-4.1	60	2.8	1.9-3.8
HCFC-225cb	8.1	5.2-11	130	7.6	5.0-10
HFC-125	40	26-56	400	37	24-49
HFC-134A	16	10-22	210	15.8	9.8-20
HFC-152A	1.7	1.1-2.4	61	1.7	1.1-2.3

*Includes ocean removal

The value for τ_{OH} for each species is obtained from τ_{OH} for CH_3CCl_3 using the scaling argument of Prather and Spivakosky (1990). Specifically,

$$\tau_X = \tau CH_3CCl_3 \frac{kCH_3CCl_3\ (277°K)}{k_X\ (277°K)}$$

where k_X and kCH_3CCl_3 are the reaction rate constants of OH with X and CH_3CCl_3 respectively. The scaling calculations use the rate recommendation from JPL (1992). Equation (9) is then used to calculate τ_{atm} from τ_{OH} and τ_{strat}. Please note that the range of values for the OH removal (Table 5.8) induce uncertainties in the HCFC/HFCs lifetimes of order 20-30%. The total atmospheric lifetimes in Table 5.9 do not include the possibility of additional removal in the ocean. This is discussed in the next section.

5.6.2 Estimates of Lifetime for HCFC/HFC due to Ocean Removal

Due to the lack of data, particularly on hydrolysis rate constants and other oceanic removal processes, we carried out a study of the sensitivity of the calculated atmospheric time constants to different assumed values of hydrolysis (or other removal rates) in the ocean. We use a simple two box diffusion model and assume that removal by hydrolysis occurs at different rates in the two layers. The top layer is the well-mixed layer of the ocean (depth of about 100 m) and is characterized by a one-dimensional eddy diffusion coefficient of about 40 $cm^2\ s^{-1}$ (Wine and Chameides, 1990). The average temperature is taken to be about 22°C. The second layer is the deep ocean layer (depths of 100 - 2000 m). Because of the slower mixing, transport in this layer is a multi-dimensional process and therefore harder to characterize in a one dimensional model. However, a canonical value of 1.7 $cm^2\ s^{-1}$ for the eddy diffusion coefficient is used as an approximation (Li *et al.*, 1984), with an average temperature of 10°C. We assume that removal rates in the second layer are a factor of 5 lower than in the mixed layer, to account for possible slowing down of hydrolysis or other removal processes with lower temperatures. In the calculation, the values of the Henry's constants were taken from AFEAS (1990).

Our calculation shows that an assumed removal rate of $10^{-7}\ s^{-1}$ in the mixed-layer will reduce the lifetime of short-lived HCFCs (123, 152a and 124) by 2-6%. Removal rates of $3 \times 10^{-8}\ s^{-1}$ or faster (half-lives less than 0.7 years) will reduce the calculated lifetimes of HCFC-141b, 134a, 142b and 125 by 10% or more.

Available data on HCFC/HFCs or similar compounds seems to indicate that hydrolysis rates are slower than the values required by the above analysis. Other processes, such as reaction with hydrated electrons, or biodegradation could accelerate oceanic removal. Little or no data are available on these processes. It would also be important to map their spatial and temporal variability in order to arrive at a realistic estimate of their global impact.

5.7 Concluding Remarks

In this chapter, we addressed the issue of validation of model calculated lifetimes. Clearly, the lifetimes derived in Chapter 3 provide the most reliable data for validation once the emission data are verified. We used a model intercomparison approach to identify the sensitivity of the calculated lifetimes to the inputs in the model. We would like to point out that such comparisons only constitute a partial validation of the mechanisms. It is possible that constituent distributions or lifetimes could appear similar between model and measurement, but that the modeled transport and photochemistry could be different from that in the atmosphere. In the case of the constituent distributions, the modeled transport and photochemistry could compensate for each other. In the case of the lifetime computation, the integral over space and time glosses over localized disagreements between model and measurements.

We also discussed how observed concentrations in the stratosphere can be used to provide first order estimates for lifetimes of SR species.

Acknowledgment

We would like to thank Karen Sage and Linda Hunt of NASA Langley for help in producing the graphics from the UADP database.

References

AFEAS, *Scientific Assessment of Stratospheric Ozone: 1989*, World Meteorological Organization, Global Ozone Research and Monitoring Project, Report No. 20, WMO, Geneva, 1990.

Anderson, G. P, and L. A. Hall, Stratospheric determination of O_2 cross sections and photodissociation rate coefficients: 1991-215 nm, *J. Geophys. Res., 91*, 14,509-14,514, 1986.

Butler, J. H., J. W. Elkins, T. M. Thompson, B. D. Hall, T. H. Swanson, and V. Koropalov, Oceanic consumption of CH_3CCl_3: Implications for tropospheric OH, *J. Geophys. Res., 96,* 22347-22355, 1991.

Derwent, R.G. and A. Volz-Thomas, *The tropospheric lifetimes of halocarbons and their reactions with OH radicals: An assessment based on the concentration of ^{14}CO*, AFEAS Report, World Meteorological Organization, Geneva, 1990.

Golombek, A. and R. G. Prinn, A global three-dimensional model of the circulation and chemistry of $CFCl_3$, CF_2Cl_2, CH_3CCl_3, CCl_4 and N_2O, *J. Geophys. Res., 91*, 3985-4001, 1986

Golombek, A. and R. G. Prinn, Global three-dimensional model calculations of the budgets and present-day atmospheric lifetimes of $CF_2ClCFCl_2$ (CFC-113) and $CHClF_2$ (CFC-22), *Geophys. Res. Lett., 16*, 1153-1156, 1989.

Hartmann, D. L., K. R. Chan, B. L. Gary, M. R. Schoeberl, P. A. Newman, R. L. Martin, M. Loewenstein, J. R. Podolske and S. E. Strahan, Potential vorticity and mixing in the south polar vortex during spring, *J. Geophys. Res., 94*, 11625-11640, 1989.

Herman, J. R., and J. E. Mentall, O_2 absorption cross sections (187-225 nm) from stratospheric solar flux measurements, *J. Geophys. Res., 87*, 8967-8975, 1982.

Holton, J. R., A dynamically based transport parameterization for one-dimensional photochemical models of the stratosphere, *J. Geophys. Res., 91*, 2681-2686, 1986.

Isaksen, I. S. A., K. Helge, M. Sunde, J. Sunde, and P. J. Crutzen, A simplified method to include molecular scattering and reflection in calculations of photon fluxes and photo-dissociation rates, *Geophysica Norvegica, 31*, 11-26, 1977.

Jackman, C. H., P. A. Newman, P. D. Guthrie, and M. R. Schoeberl, Effect of computed horizontal diffusion coefficients on two-dimensional N_2O model distributions, *J. Geophys. Res., 93*, 5213-5219, 1988.

Jackman, C. H., R. K. Seals and M. J. Prather, Editors, *Two-Dimensional Intercomparison of Stratospheric Models*. NASA Conference Publication 3042, Proceedings of a workshop (Virginia Beach, VA Sept. 11-16, 1988) sponsored by the National Aeronautics and Space Administration, Washington, D.C., Upper Atmosphere Theory and Data Analysis, 1989.

Jackman, C. H., A. R. Douglass, K. S. Brueske and S. A. Klein, The influence of dynamics on two-dimensional model results: Simulation of ^{14}C and stratospheric aircraft NO_X injection, *J. Geophys. Res., 96*, 22,559-22,572, 1991.

Jet Propulsion Laboratory, *Chemical Kinetics and Photochemical Data for Use in Stratospheric Modeling, Evaluation Number 10.* JPL Publication 92-20, National Aeronautics and Space Administration, Jet Propulsion Laboratory, California Institute of Technology, Pasadena, CA, 1992.

Johnston, H. S., Evaluation of excess carbon-14 and strontium-90 data for suitability to test two-dimensional stratospheric models, *J. Geophys. Res., 94*, 18485-18493, 1989.

Johnston, H. S., O. Serang, and J. Podolske, Instantaneous global nitrous oxide photochemical rates, *J. Geophys. Res., 84*, 5077-5082, 1979.

Kinnison, D. E., D. J. Wuebbles and H. S. Johnston, *Two-dimensional model study of atmospheric transport using Carbon-14 and Strontium-90 as inert tracers*, Lawrence Livermore National Laboratory Report, Livermore, CA 1991.

Ko, M. K. W. and N. D. Sze, A 2-D model calculation of atmospheric lifetimes for N_2O, CFC-22 and CFC-12, *Nature, 297*, 317-319, 1982.

Ko, M. K. W., N. D. Sze, M. Livshits, M. B. McElroy and J. A. Pyle, The seasonal and latitudinal behavior of trace gases of O_3 as simulated by a two-dimensional model of the atmosphere, *J. Atmos. Sci., 41*, 2381-2408, 1984.

Ko, M. K. W., N. D. Sze, and D. K. Weisenstein, Use of satellite data to constrain the model-calculated atmospheric lifetime for N_2O: Implications for other trace gases, *J. Geophys. Res., 96*, 7547-7552, 1991.

Jones, R. L. and J. A. Pyle, Observations of CH_4 and N_2O by the Nimbus 7 SAMS: A comparison with *in situ* data and two-dimensional numerical model calculations, *J. Geophys. Res., 89*, 5263-5279, 1984.

Lait, L. R., M. R. Schoeberl, P. A. Newman, M. H. Proffitt, M. Loewenstein, J. R. Podolske, S. E. Strahan, K. R. Chan, B. Gary, J. J. Margitan, E. Browell, M. P. McCormick and A. Torres, Reconstruction of O_3 and N_2O fields from ER-2, DC-8 and balloon observations, *Geophys. Res. Lett., 17*, 521-524, 1990.

Li, Y. H., T. H. Peng, W. Broecker, and H. G. Ostlund, The average vertical mixing coefficient for the oceanic thermocline, *Tellus, 36B*, 212-217, 1984.

Luther, F. M., and R. J. Gelinas, Effect of molecular multiple scattering and surface albedo on atmospheric photodissociation rates, *J. Geophys. Res., 81*, 1125-1132, 1976.

Madronich, S., Photodissociation in the atmosphere: 1. Arctic flux and the effects of ground albedo and clouds, *J. Geophys. Res.*, *92*, 9740-9752, 1987.

Plumb, R. A. and M. K. W. Ko, Interrelationships between mixing ratios of long-lived stratospheric constituents, *J. Geophys. Res.*, *97*, 10,145-10,156, 1992.

Prather, M. J. and C. M. Spivakovsky, Tropospheric OH and the lifetimes of hydrochlorofluorocarbons, *J. Geophys. Res.*, *95*, 18,723-18,729, 1990.

Prinn, R. G., D. Cunnold, R. Rasmussen, P. Simmonds, F. Alyea A. Crawford, P. Fraser, R. Rosen, Atmospheric trends in methyl chloroform and the global average for the hydroxyl radical, *Science*, *238*, 945-950, 1987.

Prinn, R. G., D. Cunnold, P. Simmonds, F. Alyea, R. Boldi, A. Crawford, P. Fraser, D. Gutzler, D. Hartley, R. Rosen, and R. Rasmussen, Global average concentration and trend for hydroxyl radicals deduced from ALE/GAGE trichloroethane (methyl chloroform) data for 1978-1990, *J. Geophys. Res.*, *97*, 2445-2461, 1992.

Schoeberl, M. R., L. R. Lait, P. A. Newman, R. L. Martin, M. H. Proffitt, D. L. Hartmann, M. Loewenstein, J. Podolske, S. E. Strahan, J. Anderson, K. R. Chan, and B. Gary, Reconstruction of the constituent distribution and trends in the Antarctic polar vortex from ER-2 flight observations, *J. Geophys. Res.*, *94*, 16815-16845, 1989.

Shia, R. L., Y. L. Yung, M. Allen, R. W. Zurek, and D. Crisp, Sensitivity study of advection and diffusion coefficients in a two-dimensional stratospheric model using excess carbon 14 data, *J. Geophys. Res.*, *94*, 18,467-18,484, 1989.

Spivakovsky, C. M., R. Yevich, J. A. Logan, S. C. Wofsy, and M. B. McElroy, Tropospheric OH in a three-dimensional chemical tracer model: An Assessment based on observations of CH_3CCl_3, *J. Geophys. Res.*, *95*, 18,441-18,471, 1990

Tans, P. A., Computation of bomb C-14 data for use in global carbon model calculations, in Carbon Cycle Modeling, edited by B. Bolin, *SCOPE 16*, 131-157, 1981.

Volz, A., D. H. Ehhalt, and R.G. Derwent, seasonal and latitudinal variation in ^{14}CO and the tropospheric concentration of OH radicals, *J. Geophys. Res.*, *86*, 4163-5171, 1981.

Wine, P. H. and Chameides, W. L., *Possible atmospheric lifetimes and chemical reaction mechanisms for selected HCFCs, HFCs, CH_3CCl_3, and their degradation products against dissolution and/or degradation in seawater and cloudwater,* AFEAS Report, World Meteorological Organization, Geneva, 1990.

World Meteorological Organization, *Scientific Assessment of ozone depletion: 1991*, Global Ozone Research and Monitoring Project, Report No. 25, United Nations Environment Program, World Meteorological Organization, 1992.

LIST OF INTERNATIONAL CONTRIBUTORS AND REVIEWERS

CO-CHAIRS

Jack Kaye	National Aeronautics and Space Administration	USA
Stuart Penkett	University of East Anglia	UK

CFC PEER-REVIEW MEETING
BLAKENEY, U.K.
January 20-24, 1992

Peter Bloomfield	North Carolina State University	USA
Byron Boville	National Center for Atmospheric Research	USA
Peter Connell	Lawrence Livermore National Laboratory	USA
Tom Duafala	TRICAL	USA
Donald Fisher	E.I. DuPont de Nemours and Company	USA
Paul Fraser	CSIRO	Australia
Amram Golombek	Israel Institute for Biological Research	Israel
Michael Gunson	Jet Propulsion Laboratory	USA
Charles Jackman	NASA Goddard Space Flight Center	USA
Jack Kaye	National Aeronautics and Space Administration	USA
Malcolm Ko	Atmospheric and Environmental Research, Inc.	USA
Joel Levy	National Oceanic and Atmospheric Administration	USA
Hillel Magid	Allied-Signal Corporation	USA
Arjun Makhijani	Institute for Energy and Environmental Research	USA
Pauline Midgley	ICI, Inc.	UK
Ole-John Nielsen	Forskningscenter Riso	Denmark
Carol Niemi	Dow Chemical Company	USA
Stuart Penkett	University of East Anglia	UK
Michael Prather	University of California - Irvine	USA
Ronald Prinn	Massachusetts Institute of Technology	USA
Sherwood Rowland	University of California - Irvine	USA
Ulrich Schmidt	KFA Jülich	Germany
Paul Simon	Institut d'Aeronomie Spatiale	Belgium
Hanwant Singh	NASA Ames Research Center	USA
Ray Weiss	Scripps Institution of Oceanography	USA

Chapter 1 Measurements

Chapter Coordinator

Paul Fraser	CSIRO	Australia

Lead Authors

Michael Gunson	Jet Propulsion Laboratory	USA
Stuart Penkett	University of East Anglia	UK
Sherwood Rowland	University of California - Irvine	USA
Ulrich Schmidt	KFA Jülich	Germany
Ray Weiss	Scripps Institution of Oceanography	USA

Additional Contributors

Fred Alyea	Georgia Institute of Technology	USA
Don Blake	University of California - Irvine	USA
E. Brunke	CSIR	Rep. S. Africa
James Butler	National Oceanic and Atmospheric Administration/CMDL	USA
Derek Cunnold	Georgia Institute of Technology	USA
James Elkins	National Oceanic and Atmospheric Administration/CMDL	USA
Michio Hirota	Japan Meteorological Agency	Japan

F. Irion	California Institute for Technology	USA
Yoshino Makide	University of Tokyo	Japan
Ronald Prinn	Massachusetts Institute of Technology	USA
Rei Rasmussen	Oregon Graduate Institute for Science & Technology	USA
Toru Sasaki	Meteorological Research Institute	Japan
H. Scheel	Fraunhofer Institute for Atmos. Env. Research	Germany
Wolfgang Seiler	Fraunhofer Institute for Atmos. Env. Research	Germany
P. Simmonds	University of Bristol	UK
Hanwant Singh	NASA Ames Research Center	USA

Mail Reviewers

Shyam Lal	Physical Research Laboratory	India
Curtis Rinsland	NASA Langley Research Center	USA
Jochen Rudolph	KFA Jülich	Germany

Chapter 2 Production and Emission of CFCs, Halons, and Related Molecules

Chapter Coordinator

Donald Fisher	E.I. DuPont de Nemours and Company	USA

Lead Authors

Tom Duafala	TRICAL	USA
Pauline Midgley	ICI, Inc.	UK
Carol Niemi	Dow Chemical Company	USA

Additional Contributors

Steven Seidel	Environmental Protection Agency	USA
Arjun Makhijani	Institute for Energy and Environmental Research	USA

Mail Reviewers

Stuart Gaffin	Environmental Defense Fund	USA
Dana Hartley	Georgia Institute of Technology	USA
Archie McCullogh	ICI Chemicals and Polymers, Ltd.	UK

Chapter 3 Inferred Lifetimes

Chapter Coordinator and Lead Author

Peter Bloomfield	North Carolina State University	USA

Additional Contributors

Martin Heimann	Max-Planck Institut für Meteorologie	Germany
Michael Prather	University of California - Irvine	USA
Ronald Prinn	Massachusetts Institute of Technology	USA

Mail Reviewers

Lane Bishop	Allied-Signal, Inc.	USA
Margaret Brown	University of Washington	USA
Ian Enting	CSIRO	Australia
J. Mulquiney	Australian National University	Australia
Xufeng Niu	Florida State University	USA
Greg Reinsel	University of Wisconsin	USA

Chapter 4 Laboratory Studies of Halocarbon Loss Processes

Chapter Coordinator and Lead Author

Stanley Sander	Jet Propulsion Laboratory	USA

Additional Contributors

D. Gillotay	Institut d'Aeronomie Spatiale	Belgium
Robert Hampson, Jr.	National Institute for Standards and Technology	USA
Hillel Magid	Allied-Signal Corporation	USA
Ole-John Nielsen	Forskningscenter Riso	Denmark
A. Ravishankara	NOAA Aeronomy Laboratory	USA
Paul Simon	Institute d'Aeronomie Spatiale	Belgium

Mail Reviewers

Roger Atkinson	University of California - Riverside	USA
R. Anthony Cox	National Environment Research Council	UK
William DeMore	Jet Propulsion Laboratory	USA
J. A. Kerr	EAWAG	Switzerland
Michael Kurylo	National Institute for Standards and Technology	USA
Robert LesClaux	Universite de Bordeaux	France
V. Orkin	Russian Academy of Sciences	Russia
Andreas Wahner	KFA Jülich	Germany
Paul Wine	Georgia Institute of Technology	USA

Chapter 5 Model Calculations of Atmospheric Lifetime

Chapter Coordinator

Malcolm Ko	Atmospheric and Environmental Research, Inc.	USA

Lead Author

Charles Jackman	NASA Goddard Space Flight Center	USA

Additional Contributors

Byron Boville	National Center for Atmospheric Research	USA
C. Bruehl	Max Planck Institut für Chemie	Germany
Peter Connell	Lawrence Livermore National Laboratory	USA
Amram Golombek	Israel Institute for Biological Research	Israel
Joel Levy	National Oceanic and Atmospheric Administration	USA
Jose Rodriguez	Atmospheric and Environmental Research, Inc.	USA
Toru Sasaki	Meteorological Research Institute	Japan
Ka Kit Tung	University of Washington	USA

Mail Reviewers

Richard Derwent	UK Department of the Environment	UK
Lesley Gray	Rutherford Appleton Laboratory	UK
Evgeny Jadin	Central Aerological Observatory	Russia
Hans Schneider	CSIRO	Australia
Susan Solomon	NOAA Aeronomy Laboratory	USA

• • • • •

ADDITIONAL CONTRIBUTORS

William Hill	Allied-Signal, Inc.	USA
Helene LeTexier	Service d'Aeronomie du CNRS	France
Nien-Dak Sze	Atmospheric and Environmental Research, Inc.	USA
Robert Watson	National Aeronautics and Space Administration Office of Science and Technology Policy	USA

EDITORS

Jack Kaye	Co-Chair, NASA	USA
Stuart A. Penkett	Co-Chair, University of East Anglia	UK
Flo Ormond	Birch & Davis Associates, Inc.	USA

UK Coordination and Documentation

Marigold Penkett	University of East Anglia	UK

ACKNOWLEDGEMENTS

AFEAS	Alternative Fluorocarbon Environmental Acceptability Study
Linda Hunt	NASA Langley Research Center
Karen Sage	NASA Langley Research Center

GLOSSARY

AAOE	Airborne Antarctic Ozone Experiment
AASE	Airborne Arctic Stratospheric Expedition
AER	Atmospheric and Enviornmental Research, Inc.
AERE	Atomic Energy Research Establishment (UK)
AFEAS	Alternative Fluorocarbon Environmental Acceptability Study
ALE	Atmospheric Lifetime Experiment
ALE/GAGE	Atmospheric Lifetime Experiment/Global Atmospheric Gases Experiment
ATMOS	Atmospheric Trace Molecule Spectroscopy Experiment
BLP	Bromine Loading Potential
BOIC	Balloon Ozone Intgercomparison Campaign
CFC	Chlorofluorocarbon
CLP	Chlorine Loading Potential
CMA	Chemical Manufacturers Association
CMDL	Climate Monitoring and Diagnostics Laboratory (NOAA) (United States)
CNRS	Centre National de la Recherche Scientifique (France)
CSIRO	Commonwealth Scientific and Industrial Research Organization (Australia)
DU	Dobson Unit
EASOE	European Arctic Stratospheric Ozone Expedition
ENSO	El Niño/Southern Oscillation
EPICS	Equilibrium Partitioning in Closed Systems
FIAER	Fraunhofer Institute for Atmospheric Environmental Research (Germany)
GAGE	Global Atmospheric Gases Experiment
GISS	Goddard Institute for Space Studies
GIT	Georgia Institute of Technology (United States)
IPCC	Intergovernmental Panel on Climate Change
KFA	Institut für Chemie der Kernforschungsanlage Jülich
MPAE	Max Planck Institut für Aeronomie
MRI	Meteorological Research Institute (Japan)
NASA	National Aeronautics and Space Administration
NBS	National Bureau of Standards (now NIST) (United States)
NIST	National Institute of Standards and Technology (formerly NBS) (United States)
NOAA	National Oceanic and Atmospheric Administration (United States)
OGC	Oregon Graduate Center (now OGIST) (United States)
OGIST	Oregon Graduate Institute for Science and Technology (formerly OGC)
PNW	Pacific North West region of the United States
ppbv	parts per billion by volume
ppmv	parts per million by volume
pptv	parts per trillion by volume
PSCs	Polar Stratospheric Clouds
QBO	Quasi-Biennial Oscillation
SAGE	Stratospheric Aerosol and Gas Experiment
SIO	Scripps Institution for Oceanography (United States)
TOMS	Total Ozone Mapping Spectrometer
UADP	Upper Atmosphere Data Pilot (NASA Langley)
UARS	Upper Atmosphere Research Satellite
UCI	University of California at Irvine (United States)
UEA	University of East Anglia (United Kingdom)
UNEP	United Nations Environment Programme
UT	University of Tokyo (Japan)
UV	Ultraviolet
WMO	World Meteorological Organization

NASA

Report Documentation Page

1. Report No.	2. Government Accession No.	3. Recipient's Catalog No.
NASA RP-1339		

4. Title and Subtitle	5. Report Date
Report on Concentrations, Lifetimes, and Trends of CFC, Halons, and Related Species	April '94
	6. Performing Organization Code

7. Author(s)	8. Performing Organization Report No.
J.A. Kaye, S.A. Penkett, and F.M. Ormond	
	10. Work Unit No.

9. Performing Organization Name and Address	11. Contract or Grant No.
NASA Office of Mission to Planet Earth Science Division	
	13. Type of Report and Period Covered
12. Sponsoring Agency Name and Address	Reference Publication
National Aeronautics & Space Administration	14. Sponsoring Agency Code

15. Supplementary Notes

16. Abstract

The atmospheric lifetimes of molecules containing chlorine and bromine are the dominant parameters influencing their ability to promote enhanced ozone destruction in the stratosphere. The purpose of this report is to assess the present state of knowledge of the lifetimes of halocarbons using two complementary approaches. First, a time series of measurements of gas concentrations is used together with information on their emissions histories and a computational model of atmospheric circulation and chemistry to infer lifetimes through a mass balance approach. Second, an atmospheric chemical-dynamical model is used with detailed information on the chemistry and spectroscopy of the molecules of interest to calculate lifetimes. The lifetimes determined by these two methods are then compared. Attention is focused most closely on fully halogenated chlorine- and bromine-containing molecules, primarily the chlorofluorocarbons, and the halons, because of their ability to deliver chlorine and bromine to the stratosphere. Some attention will be given to those molecules containing hydrogen, which are subject to removal in the troposphere primarily by reaction with OH and by other processes.

17. Key Words (Suggested by Author(s))	18. Distribution Statement
Ozone, Chloro-fluorocarbons, CFCs, halons, stratos-phere, photochemistry, chemical kinetics, atmosphericlifetimes	UNCLASSIFIED - UNLIMITED Subject Category 46

19. Security Classif. (of this report)	20. Security Classif. (of this page)	21. No. of pages	22. Price
UNCLASSIFIED	UNCLASSIFIED	247	A07